DISS. ETH NO. 21583

Simulating tree species dynamics in a changing climate: requirements, problems and implementation of model upscaling when tree species migration is simulated explicitly

A dissertation submitted to

ETH ZURICH

for the degree of

Doctor of Sciences

presented by

JULIA ESTHER MARLENE SOPHIA NABEL

Diplom-Informatikerin (Dipl.-Inf.), Universität Hamburg

born 03.05.1981

citizen of Germany

accepted on the recommendation of

Prof. Dr. Felix Kienast, examiner
Dr. Heike Lischke, co-examiner
Prof. Dr. James W. Kirchner, co-examiner
Prof. Dr. Robert M. Scheller, co-examiner

2013

"Well we know what makes the flowers grow – but we don't know why
And we all have the knowledge of DNA – but we still die
We perch so thin and fragile here upon the land
And the earth that moves beneath us, we don't understand"

– (Sullivan/Heaton/Harris) *1987*

"This is a jigsaw puzzle."
"It's broken."
"That's the object. You are supposed to put it together."
"Why? I didn't break it."

– Alf, Strangers In The Night *1986*
(die Nacht in der die Pizza kam)

"soll ich jetzt den knaller zünden?"
"zünd den knaller!"
pöff
"irre!"

– Die Ärzte, 13 – Angeber *1998*

"Après la pluie viendra le beau temps."

– le devin, *Asterix 1972*

Contents

Summary

Changes in the climate can threaten important ecosystem services, for example by entailing changes in forest compositions or in the distribution of forested areas. To be able to mitigate or adapt to such changes, it is important to understand the dynamics of forests. Forest dynamics are often studied with dynamic vegetation models (DVMs). DVMs simulate vegetation dynamics (and particularly tree species dynamics) over time and generally contain representations of those processes considered to be most important for this purpose, namely establishment, growth and mortality, driven by climatic influences and competitive interactions. In addition to these processes, different DVMs include representations of several further aspects. Which aspects are represented, and on which scales a DVM can be applied (e.g. with which cell size, i.e. spatial grain, and with how many cells, i.e. spatial extent), is not only connected with the research question of a study, but also strongly connected with the associated computational costs. Studies with a large spatial extent, for example, are mostly conducted with a coarse spatial grain and with the assumption of a general availability of seeds of all simulated species, instead of simulating the dispersal of seeds (see Chapter 1).

In a changing climate, however, the assumption of a general availability of seeds is not adequate, because different species react in different ways and with different paces to climatic changes. Particularly, the geographic adaptation of different species will neither be immediate nor synchronous, but will depend on the different species traits, as well as on various small scale processes and environmental influences. It would therefore be desirable to simulate tree species migration explicitly, thus, to represent those small scale processes and environmental influences in a DVM, which have an important influence on migration. For simulations with large spatial extents, however, such an explicit representation creates the need to reduce computational cost. Reductions in computational costs are often accomplished with upscaling methods that are used to coarsen the spatial, temporal or thematic resolution of a model or to simplify single aspects represented in a model. Upscaling methods are used in the construction and in the application of DVMs, and in Chapter 1 I suggest that it might not have been sufficiently tested whether previously applied, well-established upscaling methods influence simulated migration outcomes. Furthermore, I argue that upscaling methods which replace a fine spatial resolution with a coarse spatial resolution can cause problems when simulating migration explicitly, due to the reduced possibility to represent important small scale processes and environmental influences. Therefore, the aims of my studies were: (1) to test influences of previously applied upscaling methods on simulated migration outcomes and, if required, to suggest improvements, and (2) to develop and apply a new upscaling method which allows reducing computational costs, but nevertheless maintains the fine spatial resolution of the model it is applied to.

As a base model for my studies I selected the forest-landscape model TreeMig, which already allows for an explicit simulation of migration, since it contains representations of several underlying processes, namely seed dispersal, establishment, maturation and seed production. In order to test the influence of upscaling methods on simulated migration outcomes, I developed a test application with a realistic migration situation (Chapter 2). This test application describes the northwards migration of *Ostrya carpinifolia* Scop. (European Hop Hornbeam) through a 210 km x 70 km sized transect, which encloses parts of the climatically heterogeneous and spatially fragmented Swiss Alps. I selected this migration situation because I assumed that approximation errors, resulting from the application of upscaling methods, would particularly become apparent in a critical heterogeneous situation. With this test application I investigated effects on simulated migration outcomes of two upscaling methods, previously applied in the construction and application of TreeMig, as well as effects on migration outcomes of the new method that I developed and implemented with TreeMig. The first upscaling method I examined (Chapter 3) was a change in the representation of local populations in the simulated grid cells. TreeMig has been derived from a forest gap model, i.e. from a single-stand model. To reduce the com-

putational costs associated with a spatially explicit representation, formerly separately simulated individuals in a grid cell, were aggregated to population densities, which is a commonly applied upscaling method. Subsequently, test simulations were conducted to investigate the effect of this aggregation on locally simulated species compositions, but not on simulated migration outcomes. In order to investigate potential influences on simulated migration outcomes, I implemented a minimum population density threshold in TreeMig and compared simulation results of the test application with different thresholds and without a threshold. I was able to demonstrate that, if simulated without a threshold, *O. carpinifolia* unrealistically crossed the Alps with infinitesimal population densities (less than one thousandth individual per grid cell). I concluded that minimum population density thresholds are appropriate and required to correct this side-effect of the upscaling by aggregating individuals to population densities, when migration is simulated explicitly (Chapter 3).

In the subsequent study I investigated whether simplifications in the spatial or temporal representation of interannual climate fluctuations influence simulated migration outcomes (Chapters 3 and 4). Such simplifications are commonly applied when climate time series are interpolated or extrapolated for simulations with DVMs and can be regarded as upscalings because they, for example, reduce computational costs by avoiding the simulation of stochastic replicates. In Chapter 3 I compared outcomes of the test application from simulations with common simplifications of the temporal representation of climate fluctuations, namely the steady application of mean values, cyclic repetitions of a given base climate and the application of single stochastically generated climate time series. With this comparison, I was able to show that different simplifications can lead to notably differing migration outcomes, which means that the actual chronology of climatic fluctuations can influence migration outcomes. I concluded that multiple simulations with stochastically generated climate time series are recommendable when migration is simulated explicitly (Chapter 3). In Chapter 4 I investigated how simulation outcomes are influenced, when spatial correlations in the climate fluctuations are neglected, which is what has been done in extrapolations of climate time series in previous studies with TreeMig. For this investigation I implemented a simple extrapolation method in TreeMig, which conserves spatial correlations in climatic fluctuations, and I compared outcomes of simulations of the test application with and without conservation of the spatial correlations. This comparison demonstrated that spatial correlations in climatic fluctuations can entail spatial correlations in the simulated biomass, which cannot be generated when the spatial correlations in the climatic fluctuations are neglected. I furthermore showed that neglecting spatial correlations causes an unrealistic invariance of the simulated biomass over time and among simulations with stochastically generated climate time series. To be able to systematically investigate how migration outcomes are influenced, I developed a cellular automaton with a simplified representation of migration processes. Simulations with this cellular automaton revealed that spatial correlations in climatic fluctuations can have strong influences on simulated migration outcomes (Chapter 4).

In Chapters 5 and 6 I introduced a new upscaling method which I developed in the course of my studies, described its implementation in TreeMig and presented the results of different test applications, which I conducted to investigate the performance of the method. The underlying idea of the proposed upscaling method is to conduct simulations on two different layers. The first layer consists of the grid of the original model and the second layer is a new layer used to aggregate grid cells with similar climate conditions and similar species abundances for calculations of certain processes. Which cells are aggregated is thereby dynamically determined during runtime to be able to account for changes in the species abundances caused by processes that are simulated on the first layer. Due to the underlying idea I named the method the dynamic two-layer classification (D2C) concept. In order to apply the D2C concept to a model, the processes represented in the model are divided into *spatial* and *non-spatial* processes. Spatial processes are those processes which require information on the position of a grid cell relative to other grid cells. Such spatial processes are simulated on the first layer, i.e. for all grid cells, while non-spatial processes are simulated on the second layer, i.e. collectively for similar grid cells. In TreeMig, the dispersal of seeds amongst different grid cells is the only spatial process. Other processes were therefore assigned to the second layer in the implementation of the D2C concept in TreeMig (TreeMig-2L). Thus, in simulations with TreeMig-2L grid cells with similar climate conditions and species abundances are aggregated for calculations of non-spatial processes, whereby changes in the species abundances resulting from seed dispersal amongst grid cells are dynamically accounted for. To investigate the performance

of TreeMig-2L, I compared outcomes of and the CPU-time required for simulations with the original TreeMig implementation and TreeMig-2L. These comparisons showed that TreeMig-2L can lead to a notable reduction in CPU-times (up to 85% in the conducted studies) with small to moderate approximation errors (80-90% similarity to simulations with the original TreeMig implementation). Furthermore, simulations of the main test application demonstrated that the migration of *O. carpinifolia* was accurately reproduced in simulations with TreeMig-2L (Chapter 6). I concluded that the D2C concept is an appropriate method to maintain small scale representations of processes and climatic influences in essential situations but nevertheless allows reducing computational costs.

In summary, my studies highlighted important requirements for the application of upscaling methods, when tree species migration is simulated explicitly. I showed that the aggregation of individuals to population densities creates the need to apply minimum density thresholds and I demonstrated the importance for an accurate representation of the spatiotemporal heterogeneity in the driving climate time series. These results underlined the need for studies, such as the presented ones, that investigate how applied upscaling methods influence simulated migration outcomes. Furthermore, the results also underlined that an upscaling method should maintain small scale representations of processes and climatic influences in a migration situation. With the D2C concept I presented such a method which maintains small scale representations but nevertheless allows reducing computational costs by aggregating calculations in situations which either cause no or at least less influential differences in the simulation outcomes. I demonstrated the applicability of the D2C concept with the implementation of TreeMig-2L, and I am convinced that the D2C concept has potential for further model development beyond the presented TreeMig-2L implementation (see Chapter 1).

Zusammenfassung

Klimaänderungen können wichtige Ökosystemleistungen bedrohen, beispielsweise dadurch, dass sie zu Änderungen von Waldzusammensetzungen oder dem Vorkommen von bewaldeten Flächen führen. Um solchen Änderungen entgegenwirken zu können oder sich ihnen anzupassen, ist es wichtig, die Dynamik in Wäldern zu verstehen. Um die Dynamik von Wäldern zu studieren, werden oft dynamische Vegetationsmodelle (DVMs) verwendet. DVMs simulieren Vegetationsdynamiken über die Zeit und beziehen generell die hierzu als am wichtigsten angesehenen Prozesse mit ein, nämlich Wachstum, Etablierung und Mortalität, unter Einfluss von Konkurrenz und klimatischen Bedingungen. Zusätzlich zu diesen Prozessen werden in unterschiedlichen DVMs verschiedene weitere Aspekte abgebildet. Welche Aspekte abgebildet werden und für welche Anwendungsskala ein DVM verwendet wird (z.B. Größe der Gitterzellen, also die räumliche Auflösung, und Anzahl der Gitterzellen, also die räumliche Ausdehnung) ist nicht nur von der Forschungsfrage abhängig, sondern hängt unter anderem auch stark vom den entstehenden Berechnungskosten ab. So wird aufgrund der Berechnungskosten in Modellstudien mit großer räumlicher Ausdehnung in der Regel mit einer groben räumlichen Auflösung gerechnet und von einer allgemeinen Verfügbarkeit von Samen jeder simulierten Art ausgegangen, anstatt die Verbreitung von Samen explizit zu simulieren (siehe Kapitel 1).

Die Annahme der allgemeinen Samenverfügbarkeit ist allerdings unzureichend, da nicht alle Arten auf die gleiche Weise auf Klimaänderungen reagieren. Im Besonderen wird auch die geographische Adaption einzelner Arten auf unterschiedliche Weise und mit unterschiedlichen Geschwindigkeiten vonstatten gehen, abhängig von den Artmerkmalen und unter Einwirkung vieler kleinräumiger Prozesse und Umwelteinflüsse. Daher ist es wünschenswert, Migration explizit zu simulieren, d.h. die für Migration grundlegenden kleinräumigen Prozesse und Umwelteinflüsse direkt im Modell dazustellen. Für großräumige Anwendungen ist hierfür allerdings eine Reduktion der Berechnungskosten notwendig. Reduktionen in den Berechnungskosten werden häufig dadurch erreicht, dass die zeitliche, räumliche oder thematische Darstellung von Aspekten der Realität im Modell mit Hilfe sogenannten Upscaling-Verfahren vereinfacht oder vergröbert wird. Upscaling-Verfahren werden in der Konstruktion und auch in der Anwendung von DVMs eingesetzt und in Kapitel 1 argumentiere ich, dass für bereits in DVMs eingesetzte, etablierte Verfahren häufig nicht hinreichend getestet wurde, wie sie sich auf simulierte Migration auswirken. Des Weiteren führe ich aus, dass Verfahren, welche die kleinskalige räumliche Auflösung durch eine gröbere räumliche Auflösung ersetzen, für die Simulation von Migration problematisch sein können, da sie wichtige kleinräumige Prozesse und Umwelteinflüsse nicht hinreichend abbilden können. Die Ziele meiner Arbeit waren daher, etablierte Upscaling-Verfahren auf ihre Auswirkung auf simulierte Migration hin zu untersuchen und gegebenenfalls zu verbessern, sowie ein neues Upscaling-Verfahren zu entwickeln, das eine Reduktion der Berechnungskosten erlaubt, ohne die kleinskalige räumliche Auflösung mit einer gröberen räumlichen Auflösung zu ersetzen.

Als Ausgangspunkt für meine Studien habe ich das Wald-Landschaftsmodell TreeMig gewählt, welches die explizite Simulation von Migration von Baumarten gestattet, da es grundlegende Prozesse beinhaltet, nämlich Samenausbreitung, Etablierung, Reife und Samenproduktion. Um die Auswirkung von Upscaling-Verfahren auf simulierte Migration hin zu untersuchen, habe ich in einer Vorstudie eine reale Migrationssituation herausgearbeitet (Kapitel 2). Diese Migrationssituation beschreibt die nordwärts gerichtete Migration von *Ostrya carpinifolia* Scop. (europäische Hopfenbuche) durch ein 210 km x 70 km großes Gebiet welches einen Teil der Schweizer Alpen umschließt. Dieses Gebiet ist klimatisch sehr heterogen und räumlich stark fragmentiert. Ich habe diese Migrationssituation gewählt, da ich annahm, dass sich durch die Anwendung von Upscaling-Verfahren bedingte Approximationsfehler besonders in einer entsprechend kritischen Migrationssituation zeigen würden. Anhand von Simulationen dieser Migrationssituation habe ich sowohl zwei Upscaling-Verfahren, welche bei der Konstruktion und Anwendung von TreeMig verwendet wurden, als auch das von mir

im Rahmen dieser Arbeit entwickelte und in TreeMig implementierte Upscaling-Verfahren untersucht.

Das erste untersuchte Upscaling-Verfahren (Kapitel 3) betraf eine Modifikation der Darstellung der lokalen Population in den simulierten Gitterzellen. Ursprünglich wurde TreeMig aus einem Forest-Gap-Model, d.h. einem Einzelstandortmodell, abgeleitet. Um die mit der räumlichen Darstellung verbundenen Berechnungskosten zu reduzieren, wurden Individuen, die im Gap-Model einzeln simuliert wurden, in TreeMig zu Populationsdichten aggregiert, was ein oft verwendetes Upscaling-Verfahren darstellt. Anschließend wurde zwar getestet, wie sich diese Aggregation auf die lokal simulierte Artzusammensetzung auswirkt, nicht aber, ob die simulierte Migration beeinflusst wird. Um einen möglichen Einfluss auf die simulierte Migration zu testen, habe ich einen Schwellwert in TreeMig implementiert, welcher eine Mindestgröße für die lokalen Populationsdichten fordert. Anhand eines Vergleichs von Ergebnissen von Simulationen der Migrationssituation mit unterschiedlichen großen Schwellwerten und ohne einen Schwellwert konnte ich zeigen, dass *O. carpinifolia* die Alpen in vielen der Simulationen ohne Schwellwert mit unrealistisch kleinen Populationsdichten durchquerte (weniger als ein-Tausendstel Individuum pro Gitterzelle). Daraus habe ich gefolgert, dass die im Test verwendeten Schwellwerte geeignet und notwendig sind, um diesen Nachteil der Aggregation von Individuen zu Populationsdichten zu beheben, wenn Migration explizit simuliert wird (Kapitel 3).

In der anschließenden Studie habe ich untersucht, wie sich Vereinfachungen der zeitlichen oder räumlichen Darstellung von jährlichen Klimafluktuationen auf simulierte Migration auswirken können (Kapitel 3 und 4). Solche Vereinfachungen werden häufig in der Interpolation und der Extrapolation von Klimazeitreihen für Simulationen mit DVMs verwendet und können insofern als Upscaling angesehen werden, als dass sie beispielsweise erhöhte Berechnungskosten durch stochastische Wiederholungen vermeiden. In Kapitel 3 habe ich Simulationsergebnisse der Migrationssituation für verschiedene, häufig verwendete Vereinfachungen der Darstellung zeitlicher Abfolgen von jährlichen Klimafluktuationen verglichen, und zwar die ausschließliche Verwendung eines Mittelwertes, die zyklische Wiederholung einer bestimmten Klimazeitreihe und die Verwendung einer einzelnen stochastisch erzeugten Klimazeitreihe. Dieser Vergleich ergab, dass diese unterschiedlichen Vereinfachungen von jährlichen Klimafluktuationen zu großen Unterschieden in den Simulationsergebnissen führen können, und somit, dass die zeitliche Abfolge von Klimafluktuationen einen Einfluss auf Migration haben kann. Daraus habe ich geschlossen, dass bei der expliziten Simulation von Migration mehrfache Wiederholungen mit stochastisch erzeugten Klimazeitreihen durchgeführt werden sollten (Kapitel 3). In Kapitel 4 habe ich untersucht, wie sich die Vernachlässigung von räumlichen Korrelationen von Klimafluktuationen, welche in vorherigen TreeMig Simulationen bei der Extrapolation von Klimazeitreihen angewendet wurde, auf die Simulationsergebnisse auswirken kann. Hierfür habe ich ein einfaches Extrapolationsverfahren in TreeMig implementiert, welches die räumlichen Korrelationen von Klimafluktuationen berücksichtigt und habe die Ergebnisse von Simulationen der Migrationssituation mit und ohne räumliche Korrelationen verglichen. Ich konnte zeigen, dass räumliche Korrelationen in den Klimafluktuationen zu räumlichen Korrelationen der simulierten Biomasse führen, welche nicht erzeugt werden können, wenn die räumlichen Korrelationen in den Klimafluktuationen vernachlässigt werden. Im Besonderen habe ich gezeigt, dass eine Vernachlässigung von räumlichen Korrelationen zu einer unrealistischen Invarianz der simulierten Biomasse über die Zeit und zwischen Wiederholungen mit stochastisch erzeugten Klimazeitreihen führt. Durch eine vereinfachende Darstellung von Migrationsprozessen mit Hilfe eines von mir entwickelten Zellulären Automaten konnte ich zudem zeigen, dass räumliche Korrelationen in den Klimafluktuationen eine starke Auswirkung auf simulierte Migration haben können (Kapitel 4).

In Kapitel 5 und 6 habe ich das von mir im Rahmen dieser Arbeit entwickelte Upscaling-Verfahren vorgestellt, beschrieben wie ich es in TreeMig implementiert habe und unterschiedliche Testsituationen präsentiert, welche ich durchführte, um die Performanz des Verfahrens zu untersuchen. Die zugrundeliegende Idee des vorgeschlagenen Upscaling-Verfahrens ist, Simulationen auf zwei Ebenen durchzuführen, wobei die Gitterzellen des ursprünglichen Modells die erste Ebene bilden und eine zweite zusätzliche Ebene genutzt wird, um Gitterzellen mit ähnlichen Klimabedingungen und ähnlicher Artenzusammensetzung für Berechnungen bestimmter Prozesse zusammenzufassen. Welche Gitterzellen zusammengefasst werden, soll dabei dynamisch zur Laufzeit bestimmt werden, um Änderungen in der Artenzusammensetzung durch solche Prozesse berücksichtigen zu können, die auf der ersten Ebene berechnet werden. Daher auch der Name des Verfahrens: dy-

namic two-layer classification (D2C) Verfahren. Um das D2C Verfahren anzuwenden, werden die Prozesse des Ausgangsmodells in *räumliche* und *nicht räumliche* Prozesse aufgeteilt. Räumliche Prozesse sind solche, welche Informationen über die räumliche Position einer Gitterzelle relativ zu anderen Gitterzellen benötigen. Diese räumlichen Prozesse werden nach wie vor auf der ersten Ebene, also für alle Gitterzellen simuliert, während nicht räumlichen Prozesse auf der zweiten Ebene simuliert werden, also gemeinsam für ähnliche Gitterzellen. Der einzige räumliche Prozess in TreeMig ist die Verbreitung von Samen von Gitterzelle zu Gitterzelle, so dass andere Prozesse in der Implementierung mit dem D2C Verfahren (TreeMig-2L) entsprechend der zweiten Ebene zugeordnet wurden. In TreeMig-2L werden also solche Gitterzellen für die Berechnung von nicht räumlichen Prozessen zusammengefasst, welche ähnliche Klimabedingungen und eine ähnliche Artzusammensetzung haben, wobei Änderungen in der Artzusammensetzung durch die Samenverbreitung dynamisch berücksichtigt werden. Um die Effizienz von TreeMig-2L zu untersuchen habe ich Simulationsergebnisse und die benötigte CPU-Zeit von Simulationen mit der ursprünglichen TreeMig Implementierung und von Simulationen mit TreeMig-2L verglichen. Ich konnte zeigen, dass TreeMig-2L zu einer deutlichen Reduktion der CPU-Zeit führen kann (bis zu 85% in den durchgeführten Studien) und es dabei nur zu geringen bis moderaten Approximationsfehlern kommt (80-90% Ähnlichkeit zu den Simulationen mit der ursprünglichen TreeMig Implementierung). Im Besonderen wurde die Migration von *O. carpinifolia* in Simulationen der Migrationssituation sehr akkurat dargestellt (Kapitel 6). Aus diesen Studien habe ich gefolgert dass das D2C Verfahren eine geeignete Methode ist, kleinräumige Prozesse und Umwelteinflüsse in entscheidenden Situationen zu bewahren und trotzdem die Berechnungskosten zu senken.

Zusammenfassend haben meine Studien wichtige Anforderungen für die Verwendung von Upscaling-Verfahren für Modelle aufgezeigt, welche Migration explizit simulieren. Ich habe demonstriert, dass bei einer Aggregation von Individuen zu Populationsdichten eine Mindestgröße vorgeschrieben werden muss, und dass eine akkurate Darstellung der zeitlich räumlichen Heterogenität im Klima wichtig ist. Diese Resultate verdeutlichten, wie wichtig Studien wie die vorliegende sind, welche testen, wie sich verwendete Upscaling-Verfahren auf die Simulation von Migration auswirken. Zudem unterstreichen die Resultate, das ein Upscaling-Verfahren kleinräumige Prozesse und Umwelteinflüsse in Migrationssituationen bewahren sollte. Mit dem D2C Verfahren habe ich eine solche Methode vorgestellt, die kleinräumige Prozesse und Umwelteinflüsse in Migrationssituationen bewahrt und trotzdem die Berechnungskosten senken kann, indem sie Berechnungen nur für solche Situationen zusammenfasst, aus denen keine oder für die Simulationsergebnisse weniger entscheidende Abweichungen resultieren. Mit der Implementierung von TreeMig-2L habe ich die Anwendbarkeit des D2C Verfahrens demonstriert und ich bin davon überzeugt, dass das D2C Verfahren über die vorgestellte TreeMig-2L Implementierung hinaus Potential für zukünftige Modellentwicklung bietet (siehe Kapitel 1).

Chapter 1

Introduction and Synthesis

My Ph.D. thesis is a cumulative thesis comprising five manuscripts in its core. These manuscripts build upon each other to study requirements and problems of model upscaling when simulating tree species migration explicitly, and to develop and implement an adaptive upscaling method. The five manuscripts constitute Chapters 2 to 6. The current chapter, Chapter 1, presents the motivation of the study, the interrelationship and a summary of the different chapters, as well as summaries of further studies I contributed to. This chapter is closed with a synthesis of the overall findings, further research recommendations and conclusions.

1.1 General introduction, challenges and aims

Humans are strongly dependent on the ecological environment they live in. This dependency is often expressed in terms of ecosystem services, which range from those which are life-enhancing to those which are essential for survival (Millennium Ecosystem Assessment, 2005b; Fischlin et al., 2007; Carpenter et al., 2009). In particular, forests, which cover about 31% of the global land cover and store more than 290 gigatonnes of carbon in their biomass alone (FAO, 2010), provide many ecosystem services ranging from recreational use to the regulation of water and carbon cycles (Millennium Ecosystem Assessment, 2005a; Bonan, 2008; Helfenstein and Kienast, 2014). Changes in the climate entail changes of ecosystems (Walther et al., 2002; Rosenzweig et al., 2007) and both observed and projected climatic changes – driven by anthropogenic changes in the earth's atmosphere – can entail changes in ecosystems that jeopardise their services (Millennium Ecosystem Assessment, 2005a; Elkin et al., 2013). Ecosystem services provided by forests can be threatened by changes in forest composition and by loss of forested areas. In other places, however, the spread of trees into previously non-forested areas could also have negative impacts, for example, by reducing surface albedo (Bonan, 2008). For adaptation to as well as the mitigation of such changes, it is important to study the dynamics of forests, including possible changes of forest composition and future forest ranges.

An important and often applied method to study vegetation dynamics in general, and forest dynamics in particular, is the use of dynamic vegetation models (DVMs – Snell et al., accepted[1]). DVMs generally contain representations of the processes considered to be most important in their influence on dynamic changes of vegetation, namely birth, growth and death, mediated by competitive interactions and climatic influences (Snell et al., accepted; attached as Appendix A). However, one problem for the development and application of models to study forest dynamics is the complexity of forest ecosystems. Processes governing the dynamics of forests are highly interactive and often non-linear (Burkett et al., 2005). Furthermore, their influences act on different temporal and spatial scales, ranging from photosynthesis on small scales and competition for light on intermediate scales up to species migration on large scales (see e.g. Fig. 1.1).

A single model cannot cover all aspects that influence forest dynamics, and different DVMs focus on different aspects. In Section 1.1.1 I will present the main DVM types. Common to all modelling efforts is the discussion about which process and process drivers need to be covered by a model and with which spatial, temporal and thematic resolution they need to be represented. This discussion in turn is strongly connected to the trade-off between computational feasibility and represented realism (Urban, 2005; Lischke et al., 2007; Huntley et al., 2010).

[1] I contributed as a co-author to this paper. The paper is summarised in Section 1.2.4.1 and attached as Appendix A.

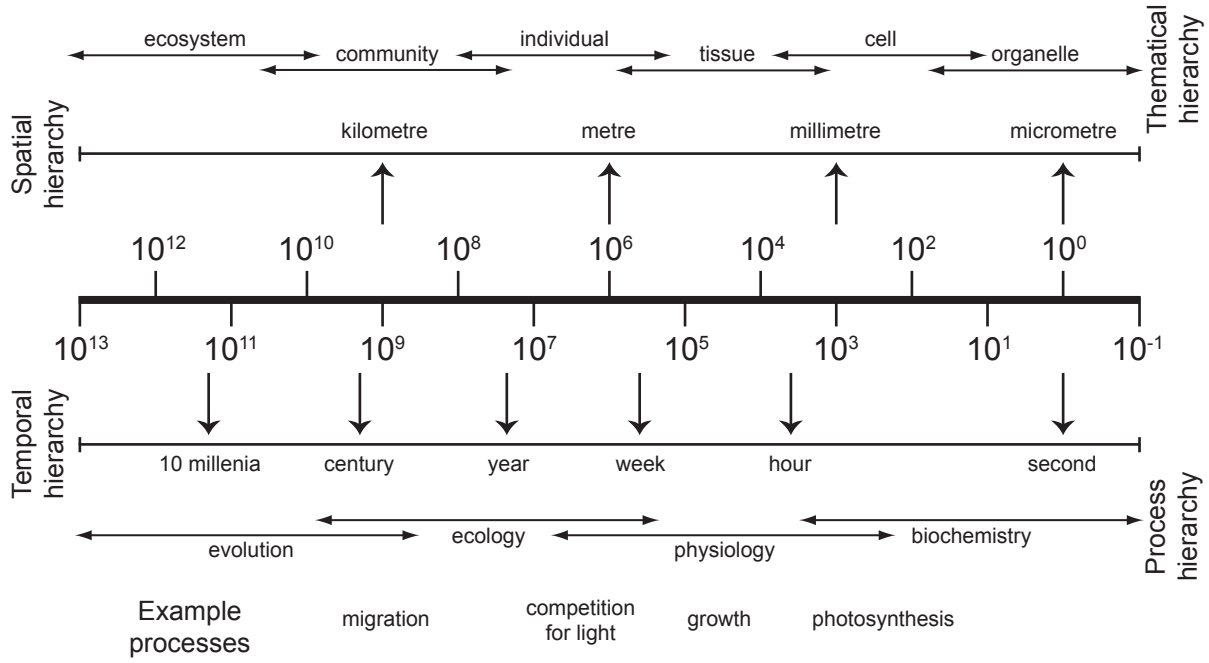

Figure 1.1 : Visualisation of different hierarchies and one possible division into different scales (adapted from Osmond et al., 1980 after Delcourt et al., 1982 and Bugmann et al., 2000). Most dynamic vegetation models (DVMs) conduct all calculations on one specific resolution, thus, all processes which are directly expressed as model formulas are framed on a predetermined spatial, temporal and thematic resolution. Processes acting on a smaller resolution can be included via upscaling (e.g. aggregated from smaller scales, see Section 1.1.2). Processes which are not directly expressed as model formulas but act on the model resolution or on larger scales can emerge, i.e. they can be simulated explicitly with the model, provided that they can be generated by the processes which are represented in the model. There are first attempts to enable different resolutions in DVMs in order to represent processes on the scales on which they actually act, for example, LANDIS-II (Scheller et al., 2007) includes variable time steps for different processes.

But what are the important aspects, i.e. processes and process drivers, influencing forest distributions and forest compositions? On broad geographical scales, climate is regarded as the main determinant of species ranges (Pearson and Dawson, 2003; Normand et al., 2011; Araújo and Peterson, 2012), thus, strongly climate-driven processes, such as establishment, growth and mortality, are represented in all DVMs, albeit differing in the degree of detail (Snell et al., accepted; see Appendix A). However, climatic changes do not necessarily entail immediate changes, and depending on their traits, different species respond in different ways and at different rates to climatic changes (Brubaker, 1986; McLeod and MacDonald, 1997; Rosenzweig et al., 2007; Thomas, 2010). Particularly range shifts of species with limited dispersal distances and long generation times, such as many tree species, can lag behind rapid climatic changes (Bertrand et al., 2011; Chen et al., 2011; Hof et al., 2011; Svenning and Sandel, 2013). Time lags can, on the one hand, entail remnant trees in areas where changes in the climatic conditions prevent new establishment and, on the other hand, lead to a lack of propagules in climatically inhabitable areas (Davis, 1989; Svenning and Skov, 2004; Zhu et al., 2011; Matías and Jump, 2012). Such time lags can therefore influence large-scale tree species distributions and forest compositions and lead to no-analogue communities with unknown population dynamics (Williams and Jackson, 2007; Bertrand et al., 2011). As opposed to other model types, most DVMs have the advantage that they can account for effects on forest dynamics caused by remnant trees, because they simulate dynamics over time and contain a representation of competition (Snell et al., accepted; see Appendix A). Accounting for migration lags, however, is more difficult. Migration lags can be caused by constrained dispersal distances (Corlett and Westcott, 2013; Svenning and Sandel, 2013), aggravated by landscape fragmentation (Pitelka et al., 1997; Collingham and Huntley, 2000; Rosenzweig et al., 2007; Hof et al., 2011), and by competition from resident species (McLeod and MacDonald, 1997; Leithead et al., 2010; Sato and Ise, 2012). To be able to account for the different influences causing migration lags and for their interactions, migration needs to be simulated as an emergent process, i.e. in an explicit

way, generated by the processes that are hypothesised to be most important: seed dispersal, establishment, maturation and seed production (Neilson et al., 2005; Keel, 2007). I argue that from this perspective there is a gap in what can be studied with the different DVM types (see Section 1.1.1). DVMs that simulate forest dynamics on larger spatial extents neglect migration lags, while DVMs that simulate tree species migration explicitly operate only on smaller spatial extents. An important research area is thus how to facilitate the explicit simulation of tree species migration for larger spatial extents.

A collective term for the activity of transferring or extrapolating ecological information represented on one scale to a larger scale is upscaling (King, 1991; Jarvis, 1995). Besides other purposes, a frequent aim of upscaling is to simplify the spatial, temporal or thematic representation of certain aspects of a model to reduce computational expenses of simulations and to thereby, for example, enable model applications on larger scales. Upscaling is ubiquitous in dynamic vegetation modelling, and in Section 1.1.2 I will give some examples of upscaling methods and discuss challenges for model upscaling in more detail. One of the main challenges of upscaling is to decide which aspects of a model can be simplified, aggregated or neglected (King, 1991). With regards to the explicit simulation of migration, it is still not well understood which aspects need to be represented in a DVM in full detail and which could be simplified, aggregated or even neglected. A recent study from a neighbouring discipline can serve as a good example: Bocedi et al. (2012) simulated the migration of animal populations, and studied how the migration of the target species would be influenced, when coarsening the spatial resolution by averaging, which is a simple upscaling method ('extrapolation by lumping' sensu King, 1991; Bugmann et al., 2000). Bocedi et al. (2012) found that population size and migration speed were severely overestimated with decreasing resolution, and concluded that there is a need for better-informed upscaling methods that maintain important fine scale patterns and processes. The study by Bocedi et al. (2012) furthermore demonstrated that there is a need to reassess previously applied upscalings.

After presenting the main DVM types in Section 1.1.1 and some of the challenges linked to upscaling in Section 1.1.2, I will derive my research aims in Section 1.1.3. In Section 1.1.4 I list the requirements that a base model must fulfil in order to facilitate the study of my research aims and I describe important properties of the selected model. In the last part of this section I formulate specific research questions related to the previously derived aims (Section 1.1.5).

In addition to DVMs other model types are used to develop hypotheses about (1) future species distributions or (2) influences on species spread across landscapes. Examples for (1) are, amongst others, species distribution models (SDMs –Thuiller et al., 2008; Araújo and Peterson, 2012), SDMs coupled to simple process-based models and SDMs informed with rates derived from process-based models (e.g. Engler and Guisan, 2009; Dullinger et al., 2012; Meier et al., 2011; Iverson and McKenzie, 2013). Such modelling approaches are important to complement results of DVMs, in particular because they are less complex, can be calculated for far more species, and often incorporate more information on abiotic factors than DVMs (Thuiller et al., 2008; Kearney and Porter, 2009; Dormann et al., 2012). However, due to the lack or only reduced representation of dynamic aspects emergent effects, such as competition by remnant species, can – if at all – only be included in a very abstract way (e.g. Leathwick and Austin, 2001; Kearney and Porter, 2009; Meier et al., 2010; Kissling et al., 2012). Examples for (2), i.e. models studying species spread across landscapes, range from reaction diffusion models and integro-differential equations to cellular automatons (see e.g. reviews in Higgins and Richardson, 1996; Hastings et al., 2005; Hui et al., 2011). Such models are often developed for analytical or theoretical investigations and rely on many simplifications. They, for example, often assume a spatially or temporally homogeneous environment (e.g. Dewhirst and Lutscher, 2009; Caswell et al., 2011). Furthermore, like SDMs, they often do not account for biotic influences (Svenning et al., accepted[2], but see e.g. Hastings et al., 2005). Due to the reduced possibilities to study forest dynamics, other model types than DVMs were not in the focus of this dissertation and an in-depth discussion of these models was considered to be beyond the scope. However, where aspects of other model types were considered to be useful, they were picked up in discussions. Moreover, for one analysis (see Chapter 4) a cellular automaton was implemented to simplify a migration situation and to enable a more detailed analysis.

[2]I contributed as a co-author to this paper. The paper is summarised in Section 1.2.4.2.

1.1.1 Dynamic vegetation models (DVMs)

DVMs are usually time- and space-discrete models, often with a focus on forests. Common to DVMs is a process-based representation of birth, growth and death, mediated by competitive interactions and climatic influences (Snell et al., accepted; see Appendix A). DVMs can be roughly divided into three to four different main types (see also Box 1 in Snell et al., accepted; see Appendix A), namely (1) single-stand models, particularly forest gap models (e.g. reviewed in Bugmann, 2001; Lischke, 2001), (2) regional (forest-) landscape models (e.g. Scheller and Mladenoff, 2004; Schumacher et al., 2004; Lischke et al., 2006) and (3) continental to global models, referred to as dynamic global vegetation models (DGVMs), which are mostly so called one-dimensional DGVMs (sensu Fisher et al., 2010), i.e. DGVMs without spatial linkages. DGVMs can further be divided into (a) DGVMs without representations of local heterogeneity (see e.g. Prentice et al., 2007; Sitch et al., 2008) and (b) DGVMs with some kind of representation of local heterogeneity (e.g. Moorcroft et al., 2001; Smith et al., 2001; Sato et al., 2007; Scheiter and Higgins, 2009). The latter are often referred to as second generation DGVMs (sensu Fisher et al., 2010) or hybrid DGVMs (sensu Snell et al., accepted; see Appendix A). This rough division already indicates that the different models concentrate on different aspects of vegetation (or forest) dynamics. In particular they differ in the applied spatial and temporal resolution, in simulated spatial and temporal extents, and also in the processes represented in the models (see e.g. Table 1 in Snell et al., accepted; see Appendix A). Although there are distinguishable main types of DVMs, there is a broad overlap (see e.g. Table 1 and 2 in Snell et al., accepted; see Appendix A). Moreover, aspects represented in one DVM are frequently used to enhance or develop another DVM, in particular also across the different main types, often by means of upscaling methods (see Section 1.1.2). Stand models, for example, are often used to enhance DGVMs (e.g. Smith et al., 2001) or forest-landscape models (e.g. Schumacher et al., 2004) and also to derive forest-landscape models in the first place (e.g. Lischke et al., 2006).

Despite the overlap and the ongoing enhancements there is still a gap in what can be studied with the different model types, in particular regarding the effects of migration on vegetation dynamics and on large-scale vegetation changes. Single-stand models and most DGVMs assume a general availability of propagules for all simulated species and do not simulate migration as an emergent process. This is mainly due to the modelling context of single-stand models and DGVMs. In their paper on uncertainties in a second-generation DGVM, Fisher et al. (2010) wrote: "DGVMs are spatially one-dimensional, as they consider single points in space that do not interact with one-another". The conceptual spatial one-dimensionality arises for different reasons, and I would like to highlight two, which both are connected to the trade-off between computational feasibility and represented detail. Firstly, the spatial resolution used in most DGVMs is quite coarse (e.g. Table 1 in Snell et al., accepted; see Appendix A), which is largely due to the computational trade-off between spatial resolution and the spatial extent (e.g. King, 1991; He et al., 2011). A coarse resolution hampers the communications between different grid cells due to the increased cell size, raising questions about the within-cell heterogeneity (in the context of migration, for example, how far a species has already migrated within the cell, i.e. the within-cell spread). A second reason for spatial one-dimensionality is that calculations of different grid cells do not have to be conducted synchronously, when different grid cells of a simulation area do not communicate. When synchrony in the calculations is not required, calculations are called 'embarrassingly parallel', i.e. they can be conducted independently, concurrently and in an arbitrary order which can save huge amounts of computational memory and computation time. A first study which included spatial linkage via seed dispersal in a DGVM, by Snell (2013), highlighted these challenges. Inspired by epidemiology, where the spread of diseases in populations is often described using logistics growth functions (Berger, 1981), Snell (2013) used a logistic growth formula to upscale the within-cell spread to the coarse spatial resolution used in her simulations (18 km cell side length). She then calibrated the growth rate such that the overall simulation results fitted historical migration rates (Snell, 2013). However, migration rates in the new model were highly sensitive to the fitted growth rates and the author concluded that a careful parameterisation and further investigations are required (Snell, 2013). This study thus highlighted the difficulties involved with the upscaling of the within-cell spread. Additionally, computational expenses of the new model substantially increased, because the single grid cells had to be simulated synchronously (Snell, personal communication). Therefore, the test transect for the first

applications was restricted to 80 grid cells.

The named challenges for the inclusion of an explicit representation of migration into DGVMs are connected to the reasons why the spatial extent for forest-landscape models is constrained. Forest-landscape models are able to simulate migration explicitly because they include representations of important processes, such as seed dispersal, establishment, maturation and seed production (e.g. Scheller and Mladenoff, 2004; Lischke et al., 2006). However, the computational expenses associated with spatial linkage and with the fine spatial resolution required to represent the important processes strongly constrain possible application extents, demonstrating the need for future developments of upscaling methods.

1.1.2 Upscaling methods

Upscaling is defined as the activity of translating or extrapolating ecological information from one scale to a larger scale (King, 1991; Jarvis, 1995). A scale is thereby a more-or-less arbitrarily defined order of magnitude along a hierarchy, which can be a (discretised) spatial, temporal or thematical hierarchy (see Fig. 1.1). When ecological information from one scale is required on a larger scale it would be straightforward to represent all the required information from the smaller scale explicitly on the larger scale, however, this is often not possible due to computational constraints (King, 1991). Thus, many upscaling methods have been developed that simplify, aggregate or completely neglect aspects of the small-scale information to reduce the computational expenses compared to an explicit upscaling. One example is the method of simple upscaling by averaging mentioned above ('extrapolation by lumping' – King, 1991; Bugmann et al., 2000), which could be done on a regular grid or, for example, with an adaptive grid method where time and space discretisations are dynamically refined or coarsened according to local gradients (Berger and Oliger, 1984; Zumbusch, 2003). Upscaling methods include, amongst others, complex analytical aggregations based on the separation of scales (Weinan and Engquist, 2003; Auger et al., 2012); so-called equation free approaches, where only selected small-scale experiments are evaluated to determine the state on the large scale at a certain point in time (Erban et al., 2006; Kevrekidis and Samaey, 2009); and purely technical solutions, such as the aggregation of identical items to only conduct calculations once (e.g. the often applied cohort method, see e.g. He et al., 1999; Bugmann, 2001; Hickler et al., 2012).

The use of upscaling methods is ubiquitous in ecological modelling (see e.g. examples in Jarvis, 1995; Urban, 2005; Lischke et al., 2007; Auger et al., 2012) and they also find broad application in the development and enhancement of DVMs (see e.g. examples in Bugmann et al., 2000 and Snell et al., accepted; for the latter see Appendix A). As mentioned above, upscaling methods are often applied with the aim to reduce the computational expenses of a DVM. A decrease in computational complexity could not only facilitate a broader spatial or temporal application, but could, for example, also facilitate multiple repetitions in case of stochastic models to better assess uncertainties, allow for the introduction or enhancement of other processes, or enable spatially linked simulations in the first place.

Jarvis (1995) stated that "non-linearity between processes and variables, and heterogeneity in properties that determine rates of processes" are the key challenges for upscaling methods (which are to be understood apart from explicit upscaling or purely technical solutions). Key questions in an upscaling attempt are therefore how non-linear processes and the spatiotemporal heterogeneity need to be dealt with. It needs to be assessed what parts of the small scale do have an important influence on the larger scale or can presumably be neglected or simplified or where patterns occur which can be used to simplify the heterogeneity and could be aggregated for considerations on the larger scale. These questions in turn depend on the ecological information to be translated or extrapolated, and on the objectives of the investigation (King, 1991).

1.1.3 Challenges and research aims

As described above, the migration of species with limited dispersal distances and long generation times – traits which many tree species have – can cause lag effects in the adaptation to rapid climatic changes and can hence influence long-term changes in large-scale forest distributions and species compositions. In order to represent

tree species migration explicitly in simulations with a DVM, several presumably important and interdependent processes need to be included, in particular seed dispersal, establishment, growth to reproductive maturity, and production of viable seeds. Section 1.1.1 highlighted that simulating tree species migration explicitly in large-scale applications of dynamic vegetation models is a challenge that has not yet been overcome. High computational costs caused by the need to represent the interdependent processes at a sufficiently accurate spatial and temporal resolution were identified as a key problem. The development of new upscaling methods which have a low impact on simulated migration is thus an important research gap. One of my research aims was therefore to develop, implement and test a new upscaling method with low impact on simulated migration.

As a starting point for new implementations, an already existing forest-landscape model was selected. Section 1.1.4 describes the selection process and the requirements that I imposed on the model.

Pre-studies that I conducted with the selected model indicated that well-established upscaling methods, which enabled the explicit simulation of migration in the first place, themselves, could markedly influence migration outcomes. This in turn underlines that the key challenge generally associated with upscaling – namely to decide what to simplify or to neglect – is still a research gap for models that explicitly simulate migration. Testing, and if necessary revising, previously applied upscalings was therefore regarded as an important research aim. Revising previously applied upscalings can lead to a more accurate representation of migration and the knowledge gained in testing them can, furthermore, be used to inform the development of a new upscaling method. For this reason, the latter research aim was approached first. Thus, my research aims were:

- ***Aim 1: Analyse effects of previously applied upscalings on migration outcomes in a well-established DVM which simulates tree species migration explicitly.***
- ***Aim 2: Develop, implement, and test a novel upscaling method which maintains fine-scale processes required for an accurate representation of tree species migration.***

In summary, the aims of this study are important because (1) testing well-established upscalings can increase the knowledge about important but not well represented aspects of tree species migration and (2) developing new and enhancing already applied upscalings leads to a more accurate representation of migration in DVMs and, therefore, allows for more sophisticated hypotheses about future tree species distributions and forest compositions.

1.1.4 Model requirements and selection of a base model

As a starting point for the implementation of the new upscaling method a base model needed to be selected. The first requirement imposed was that the model be a time- and space-discrete DVM, thus that the model included a process-based representation of birth, death and growth, mediated by competitive interactions and climatic influences (Section 1.1.1; Snell et al., accepted; see Appendix A). Further requirements for an efficient implementation were to select a well-established model which, in the ideal case, already simulated tree species migration explicitly. Alternatively, I could have used a stand model to derive a spatially explicit and linked model with the help of commonly applied upscalings, or I could have attempted to include an explicit representation of tree species migration in a DGVM. However, since well-established forest-landscape models are available, I regarded a start from a forest-landscape model as more efficient in the scope of this thesis. The requirements that I imposed on the forest-landscape model were, that it should contain processes regarded as important for the explicit simulation of tree species migration, i.e. seed dispersal, establishment, maturation and seed production (Neilson et al., 2005; Keel, 2007).

The base model selected for this thesis was the intermediate-complexity forest-landscape model TreeMig (Lischke et al., 2006), which was named to be one of the models with the most detailed representation of seed dispersal and subsequent regeneration processes in Thuiller et al. (2008). TreeMig has already been used to investigate the relative impact of migration in comparison to succession in a study of tree migration in the Alps during the Holocene (Lischke, 2005) as well as in a study of the northward migration of trees into the arctic tundra (Epstein et al., 2007). Other forest-landscape models fulfilling the above mentioned requirements

would, for example, have been LANDIS derivatives, such as LANDIS, LANDCLIM or LANDIS-II. Studies conducted with these models, however, have often had less focus on migration than the studies conducted with TreeMig (e.g. LANDIS: Franklin et al., 2001; Gustafson et al., 2004 – LANDCLIM: Schumacher and Bugmann, 2006; Schumacher et al., 2006 – LANDIS-II: Ravenscroft et al., 2010; Scheller et al., 2011; but see Scheller and Mladenoff, 2008).

TreeMig can be described as follows (Nabel et al., 2013): "TreeMig is a multi-species, spatially linked and dynamic intermediate-complexity model which was developed with the aim to simulate spatiotemporal patterns of tree species distributions with emphasis on endogenous dynamics, such as competition and migration (Lischke et al., 2006). TreeMig includes many processes required to simulate migration explicitly, for example, seed production, seed dispersal and seed bank dynamics. TreeMig simulations are driven by three bioclimate variables per year and per cell (default cell size: 1 km^2): the annual sum of daily mean temperatures above 5.5 °C ($DDsum_{>5.5\,°C}$), the minimum winter temperature and an index describing the severity of drought events. These bioclimate variables directly influence various processes such as simulated tree species growth, establishment and mortality (Lischke et al., 2006). When developing TreeMig, the trade-off between computational efficiency and accuracy has been approached by employing a distribution-based representation of the local spatial forest heterogeneity per simulated grid cell (Lischke et al., 1998, 2006). The forest in each cell is described by a density of seeds per species in the seed bank and by tree densities per species in a constant number of distinct height classes. These state variables are real-valued and represent mean densities, each determining a Poisson distribution of the density on a given unit area, so called patch area (cf. Bugmann, 1994). The resulting vertical and horizontal structure can be regarded as a deterministic representation of multiple patch repetitions – as used in ForClim (Bugmann, 1994), the forest gap model preceding TreeMig – retaining the small-scale variability originally resulting from stochastic establishment and mortality. This deterministic representation counterbalances the increase in computational complexity (memory and time) accompanying the increased spatial extent – compared to simulating single stands – and the spatial linkage through seed dispersal."

1.1.5 Research questions

1.1.5.1 Research aim 1: Analyse effects of previously applied upscalings on migration outcomes in a well-established DVM which simulates tree species migration explicitly

As described in Section 1.1.4 TreeMig is a spatially explicit and linked implementation of a model upscaled from a forest gap model. Stand models are often very complex individual-based models, and reductions in complexity were necessary for the spatial implementation. In the development of TreeMig, Lischke et al. (1998) therefore conducted an upscaling by aggregating the individual trees and patches to densities in discrete height classes. Shifting the argumentation from individuals to populations is a commonly applied upscaling method to reduce the complexity involved with the representation of local stands (see e.g. Fulton, 1991; Picard and Franc, 2004; Gómez-Mourelo and Ginovart, 2013). Whilst the representation of the simulated local forest composition was tested by Lischke et al. (1998) against the composition simulated with the upscaled forest gap model and against real forest stands for different forest sites, possible influences on simulated tree species migration have so far not been tested. For migration, population dynamics on the range limits are more important than population fluctuations in parts of the simulation area far from the front (Melbourne et al., 2006), and previous simulation studies found that species abundances at the external range boundaries can be an important factor influencing their migration rates (e.g. Iverson et al., 2004). I therefore suspected that the possibility to disperse subinteger fractions of seeds could be a critical aspect of a continuous representation when explicitly simulating migration. Thus, my first research question was:

- ***RQ 1: Does a continuous representation of tree species populations affect simulated tree species migration by allowing for the spread of infinitesimal seed densities?***

Despite the aggregation of individuals and patches to population densities, TreeMig still has a high computational complexity. To reduce computational expenses, previous TreeMig studies often only used single runs, although climatic conditions were interpolated or extrapolated by stochastically sampling from available climate data for time points for which data was not directly available (e.g. in Lischke, 2005; Lischke et al., 2006; Epstein et al., 2007; Lischke et al., 2012). A comparable simplification, the cyclic repetition of the climate of a certain base period, is quite commonly applied to interpolate or extrapolate climate time series for studies with other DVMs (e.g. Hickler et al., 2012; Sato and Ise, 2012). In both cases – stochastic sampling and cyclic repetition – only a single realisation is applied, out of a multitude of possible climate time series with the same temporal mean and variability. Such simplifications could be justifiable if influences of climatic fluctuations would be negligible compared to the influence of the mean climate, or if the timing of the fluctuations would have a negligible influence on simulation outcomes. However, when simulating migration explicitly, recruitment will only happen where and when environmental conditions are favourable and when seeds are available. I therefore raised the question of whether the applied simplification of the temporal variability could influence simulated migration outcomes. While studying the effects of temporal variability, a further associated simplification was identified, namely that the stochastic method used to interpolate and extrapolate climate time series in TreeMig neglects spatial correlations of climatic fluctuations. Thus, my research questions were:

- ***RQ 2: How do climate fluctuations need to be represented when migration is simulated explicitly?***
  - *RQ 2a: Does interannual climate variability influence simulated migration outcomes?*
  - *RQ 2b: Do spatial correlations in climatic fluctuations influence simulated migration outcomes?*

The presented research questions emerged from pre-studies that I conducted with TreeMig, and the selection of another model possibly would have led to other research questions concerning other previously applied upscalings. Although these research questions are motivated by TreeMig's implementation and previous TreeMig applications, I expect them to lead to more general insights for future model upscalings. Assessing whether climatic fluctuations influence explicit simulations of tree species migration, in particular, might allow for general conclusions about how climatic fluctuations need to be represented in simulation studies.

1.1.5.2 Research aim 2: Develop, implement and test a novel upscaling method which maintains fine-scale processes required for an accurate representation of tree species migration

The issues I reviewed when developing the core idea of the new upscaling method were (1) how migration is currently represented in DVMs, and (2) what problems I found with the upscalings I previously investigated regarding their influence on simulated migration. Due to the approximation errors involved when coarsening the spatial resolution (e.g. He et al., 2011; Bocedi et al., 2012) and due to the importance of the spatiotemporal fluctuations of the climate drivers for simulated migration which resulted in my preceding studies (see Section 1.2.2), I decided to develop a method that preserves the spatial and temporal resolution of the model it is applied to. When the objective is to maintain the spatial and temporal resolution, remaining possibilities for cost reductions are thus thematical (see e.g. Fig. 1.1). Cost reductions exploiting thematical similarities are a very common idea behind many upscaling methods. Examples applied in DVMs range from perfect solutions, such as aggregations of identical individuals into cohorts (e.g. He et al., 1999; Bugmann, 2001; Hickler et al., 2012) to solutions introducing approximation errors, for example, by grouping similar species into plant functional types (e.g. Smith et al., 1997; Sato et al., 2007) or by grouping landscape patches with similar environmental conditions to landscape elements (King, 1991; Bugmann et al., 2000). This last upscaling method has often been applied to extrapolate stand models to larger scales (King, 1991 and references therein). The underlying idea is the observation that, when a landscape is divided on a space-discrete grid with assumed homogeneous environmental inner cell conditions, several cells will be subject to similar environmental conditions. Simulations of grid cells with similar environmental conditions in turn will lead to similar state variables, if their simulations start with the same species compositions and no spatial interactions among grid cells are

simulated. This, however, directly highlights the problem of such an upscaling method when migration is simulated explicitly. One of the processes important for the explicit simulation of migration is seed dispersal. Seed dispersal from one grid cell to the next grid cell, and subsequent establishment, can introduce changes to previously identical grid cells, namely when a new species establishes in one of the grid cells but not in the other. Despite the spatial linkage due to seed dispersal, simulations with TreeMig showed that often simulation cells share similar values in their state variables and drivers for long periods of time. One of my questions regarding the second research aim was therefore, whether such similarities could be exploited without precluding the explicit simulation of migration and without strong impacts on migration outcomes. I therefore developed an upscaling method based on dynamic pooling of grid cells with the aim to simultaneously allow to exploit the similarities and to explicitly simulate migration. A dynamic upscaling method based on similarity presumably entails several key challenges for its implementation and application, whose possible solutions in turn are expected to influence the performance of the method. My research questions regarding the second research aim were therefore:

- ***RQ 3: Can similarities in climate drivers and in tree species compositions among grid cells be exploited in form of an upscaling when migration is simulated explicitly?***
  - *RQ 3a: How can similar grid cells be pooled for some calculations without precluding the explicit simulation of migration?*
  - *RQ 3b: What are the challenges when implementing a dynamic upscaling method based on grid cell similarity? How can these challenges be dealt with, and how do they influence the performance of the method?*

1.2 Summary of the findings and interrelationship of the chapters

To study influences of previous upscalings on the simulation of tree species migration with TreeMig an adequate test application was required. This test application needed to describe a migration situation that was presumably sensitive to approximation errors introduced by the studied upscalings. I therefore selected a migration situation in which the migrating species was close to its climatic boundaries in a fragmented landscape and in a competitive situation to other species. I deemed such critical conditions to be appropriate for spotting influences of upscalings, because more favourable conditions could potentially have concealed such influences. The test application used in this thesis was developed in a pre-study in which I investigated the influence of species parameter uncertainties in simulations of tree species migration with TreeMig (Nabel et al., 2012; see Chapter 2). I selected a realistic migration situation, namely the northwards migration of the tree species *Ostrya carpinifolia* Scop. (European Hop Hornbeam) through the fragmented and climatically heterogeneous landscape of the Swiss Alps. *O. carpinifolia* is a submediterranean tree species currently limited to the southern side of the Swiss Alps (Swiss National Forest Inventory, 2004/06; European Forest Data Center, 2012).

Besides other test applications, I used this migration situation and different sets of species parameters for *O. carpinifolia* to test all of the upscalings considered in this thesis. The simulation setting was developed in Chapter 2, but further refined in Chapter 3, mainly by reducing the simulated extent to the part of the simulation area where most changes regarding the simulated biomass of *O. carpinifolia* occurred. The simulation setup is described in detail in the Appendix of Chapter 3 (Section 3.A). The simulation setup evolved during the thesis due to enhancements in the TreeMig implementation and due to the different upscaling assumptions tested in the different chapters.

In the papers contained as Chapters 2 to 6 summarised below (Sections 1.2.1 to 1.2.3), I, as the main author, tackled all research questions mentioned in Section 1.1.5. Furthermore, I also participated in several publications as a co-author, summarised in Section 1.2.4. One of these co-authored papers is particularly relevant for the thesis and I therefore also included it as Appendix A.

1.2.1 RQ 1: Does a continuous representation of tree species populations affect simulated tree species migration by allowing for the spread of infinitesimal seed densities? (Nabel et al., 2013; see Chapter 3)

To investigate the first research question, I implemented a minimum density threshold for TreeMig's state variables, i.e. a threshold below which a species is treated as absent in a simulated cell. This threshold in particular also prevents the germination of infinitesimally small seed fractions into TreeMig's lowest height class. By comparing simulation outcomes of the test application, i.e. the northwards migration of *O. carpinifolia*, conducted with different thresholds and without a threshold, it was possible to test the impact of infinitesimal seed densities. The default minimum density threshold applied was one occurrence per km^2. To test the sensitivity of the simulation outcomes to this threshold, I additionally used minimum density thresholds of 0.11, 0.04 and 0.02 occurrences per km^2, which correspond approximately to one expected individual per 9 km^2, 25 km^2 and 49 km^2, respectively (Nabel et al., 2013; see Chapter 3). Whilst simulations with and without threshold showed only very small differences in simulated biomass when comparing the biomass of all simulated species, considerable differences were found comparing the simulation outcomes for the migration of *O. carpinifolia*. In simulations without a threshold, *O. carpinifolia* always successfully migrated through the critical region of the transect – namely a pass with spatial fragmentation and severe climate influences – irrespective of the simulated species parameters. For simulations with thresholds, in contrast, *O. carpinifolia* was not able to migrate for most species parameter sets, or the migration was much slower. The magnitude of the thresholds had minor relevance for migration success and even the smallest threshold applied inhibited the migration of *O. carpinifolia* for most simulated species parameter sets. The inhibition of migration in simulations with the smallest threshold suggests that some subarea of the pass must have been crossed in form of even smaller population densities in simulations without thresholds, i.e. that allowing for the spread of infinitesimal seed densities had an impact on simulated tree species migration in the test application. The findings for the first research question confirm that the discrete nature of seeds (cf. Higgins et al., 2003; Nathan et al., 2011) needs to be recognised. Due to my findings I recommend that models upscaled by replacing discrete individuals with real-valued densities should be improved with minimum density thresholds to prevent unrealistic migration by means of infinitesimal population densities (Nabel et al., 2013; Chapter 3).

1.2.2 RQ 2: How do climate fluctuations need to be represented when migration is simulated explicitly?

To investigate this question, I studied the effects of different simplifications in the temporal and spatiotemporal fluctuations of the climate drivers on simulated migration. In these studies, I compared migration outcomes for the test application, i.e. the northwards migration of *O. carpinifolia*, resulting from simulations using different methods to extrapolate the climate drivers after the simulation year 2100.

1.2.2.1 RQ 2a: Does interannual climate variability influence simulated migration outcomes? (Nabel et al., 2013; see Chapter 3)

To test if interannual climate variability influences migration outcomes, I compared results from simulations with climate extrapolations using different simplifications of the temporal fluctuations which were applied in previous studies, namely: statically applying mean values (e.g. Scheller and Mladenoff, 2005, 2008), cyclically repeating a base period (e.g. Hickler et al., 2012; Sato and Ise, 2012), and applying a single realisation of a stochastic extrapolation method (e.g. Epstein et al., 2007; Lischke et al., 2012). For my comparisons all extrapolation methods used the last 30 years of the available climate time series as base period and the generated climate time series therefore shared the same mean value. The stochastic realisations of the driving climate were sampled from probability distributions derived from the base period (see Section 3.B.2.3 in the Appendix of Chapter 3), which is the method used in previous TreeMig applications (e.g. in Lischke, 2005; Lischke et al., 2006; Epstein et al., 2007; Lischke et al., 2012).

I conducted these comparisons for different sets of species parameters for *O. carpinifolia*. Simulation runs with different stochastic realisations of annual climatic influences led to notable differences in migration outcomes for some of the simulated species parameter sets. Simulations with the deterministic representations – i.e. cyclic repetition of the base period and steadily applied mean values – often led to migration outcomes at the slower end of the range spanned by the stochastic realisations or even below that range (Nabel et al., 2013; see Chapter 3). These results are consistent with previous studies, which found that changes in the interannual climate variability can influence tree species range limits (Miller et al., 2008; Notaro, 2008; Giesecke et al., 2010). Additionally, I showed that even different realisations with the same interannual climate variability can lead to notably differing results. My simulations thus demonstrated that the actual sequence of annual climate influences can affect simulated tree species migration. This result is reasonable, since several of the processes involved, for example establishment, growth and mortality, are climatically driven (in nature and in TreeMig). Thus, for example, single extremely unfavourable years or sequences of favourable years can have a large influence on establishment and maturation, which was also described in other simulation studies and in historical data records (Brubaker, 1986; Camarero and Gutiérrez, 2004; Jackson et al., 2009; Mendoza et al., 2009; Matías and Jump, 2012). I concluded that interannual climate variability can influence simulated migration outcomes when tree species migration is simulated explicitly and that simulation studies should thus explore the effects of different stochastic realisations when interpolating or extrapolating driving climate time series (Chapter 3).

1.2.2.2 RQ 2b: Do spatial correlations in climatic fluctuations influence simulated migration outcomes? (Nabel et al., submitted; see Chapter 4)

This second question arose because the stochastic approach to interpolate and extrapolate the climate drivers used in Chapter 3 and in previous TreeMig applications (e.g. in Lischke, 2005; Lischke et al., 2006; Epstein et al., 2007; Lischke et al., 2012) generates random climate time series for single cells based on independent probability distributions. Applying this method can be regarded as a simplification, because, in contrast to other interpolation and extrapolation methods, it neither requires the storage of information on the correlation among cells, nor a communication between cells in the interpolation or extrapolation step. This method is common in single-stand models and was recommended in Bugmann (2001) for the application with forest gap models. Whilst this method might be suitable for single-stand models, I raised the question whether it has an impact on explicitly simulated tree species migration, in particular, because a model explicitly simulating migration will necessarily be a spatially linked model. In a single-stand model, only the processes and drivers within the single stand are important. In a spatially linked model, however, different grid cells interact. I hypothesised that neglecting the spatial synchronism in the climate drivers could possibly affect the spatial synchronism in species abundances and thereby influence interactions among cells, which in turn could also affect simulated tree species migration (Nabel et al., submitted; see Chapter 4).

To investigate this hypothesis I implemented and compared two methods for the interpolation and extrapolation of the climate driver, one conserving and one neglecting spatial correlations (Chapter 4). The method which neglects the spatial correlation is closely related to the stochastic extrapolation method used in previous TreeMig studies (e.g. in Lischke, 2005; Lischke et al., 2006; Epstein et al., 2007; Lischke et al., 2012). However, instead of deriving a probability distribution, it draws directly from the empirical distribution found in the base period. This was done to ensure comparability to the new method which conserves spatial correlations and which also samples from empirical distributions. Sampling from probability distributions could have entailed effects of extreme climate conditions that could have interfered with the effects of spatial correlations (see Chapter 4). Furthermore, the stochastic extrapolation method used in Chapter 3 and in previous TreeMig studies not only neglected the spatial autocorrelation for the three bioclimate variables used as climate drivers in TreeMig (see Section 1.1.4), but also neglected covariance between these variables. Neglecting covariance between bioclimate variables is obviously incorrect, since all three bioclimate variables used in TreeMig are influenced by the average monthly temperatures (see e.g. Lischke et al., 2006). The extrapolation methods used in Chapter 4 both account for the covariance in the bioclimate variables and I did not further consider effects on migration caused by neglecting covariance between variables but concentrated on the spatial correlations.

I used the two methods accounting for and neglecting the spatial correlation of climatic fluctuations to extrapolate the climate drivers for simulations of the test application described above and examined whether the simulations resulted in different tree species abundances and migration outcomes. I found that the spatial correlation in the resulting simulated tree species abundances is influenced by the spatial correlation in the fluctuations of the climate driver. While I expected this result, it was not certain because many biological processes are non-linear (Laakso et al., 2001), and so is their representation in TreeMig (Lischke et al., 2006). Due to this non-linearity, spatially correlated climatic fluctuations in a spatially heterogeneous environment do not automatically translate to spatially correlated biotic responses (Grenfell et al., 2000; Greenman and Benton, 2001; Currie, 2007). Nevertheless, my simulations showed synchronised fluctuations in tree species abundances for simulations with spatially correlated climatic fluctuations which were lost in simulations in which spatial correlations in the climatic fluctuations were neglected (Nabel et al., submitted; see Chapter 4). Moreover, when the spatial correlations in the climate drivers were neglected, the resulting biomass sum over the simulation transect was invariant over time and repetitions. In Chapter 4 I discussed how this lack of variability can be explained with the central limit theorem (Spanos, 1999), and I concluded that spatial correlations in the fluctuations of the climate drivers must not be neglected when biomass fluctuations over areas larger than a single grid cell are of interest (Chapter 4). With regards to the simulation of migration, the comparisons of simulations with the test application indicated that neglecting the spatial correlation in the fluctuations of the climate drivers can introduce a bias towards faster migration and reduces differences among simulations with different realisations of the stochastically extrapolated climate drivers (Chapter 4). To be able to study potential biases more systematically I developed a simplified cellular automaton (Chapter 4). With this cellular automaton, I demonstrated that tree species migration outcomes can be markedly different in simulations with and without spatially correlated fluctuations of the model driver. Particularly, I found that simulations with spatially uncorrelated fluctuations always led to faster migrations than simulations with correlated fluctuations, provided that establishment was not simulated to be positively density dependent, i.e. dependent on the number of mature neighbouring individuals. However, when there was a positive density dependence, migration was faster in simulations with spatially correlated fluctuations, which is in agreement with the simulation results by McInerny et al. (2007).

Overall, I concluded that spatial correlations in climatic fluctuations can influence simulated migration outcomes and should not be neglected in spatially explicit simulations of tree species dynamics (Chapter 4).

1.2.3 RQ 3: Can similarities in climate drivers and in tree species compositions among grid cells be exploited in form of an upscaling when migration is simulated explicitly?

Grouping of landscape patches with similar environmental conditions to landscape elements has often been applied to extrapolate stand models to larger scales (King, 1991 and references therein). However, this method is not applicable as soon as spatial processes can alter the aggregated landscape patches (Bugmann et al., 2000). I therefore expected the spatial linkage between grid cells via seed dispersal – which is a precondition for an explicit simulation of migration – to be the key challenge for the upscaling method. Particularly, I regarded the following two points as the main challenges: (1) spatial linkage requires that the spatially explicit positions of dispersing source and associated sink cells are preserved in the upscaling, and (2) seed dispersal and subsequent establishment of new species can introduce changes to previously identical grid cells. The suggested upscaling method therefore (1) aimed to only pool similar grid cells for some calculations (Section 1.2.3.1) and (2) aimed to conduct this pooling in a dynamic manner (Section 1.2.3.2).

1.2.3.1 RQ 3a: How can similar grid cells be pooled for some calculations without precluding the explicit simulation of migration? (Nabel and Lischke, 2013; see Chapter 5)

To resolve this question the proposed upscaling method strives to disentangle calculations which require explicit spatial positions of cells relative to other cells, i.e. calculations for spatially linking processes, from those calculations which do not require such information. I named the proposed upscaling method the dynamic

two-layer classification (D2C) concept, because it divides the processes of the original model to two layers. The first layer is a two-dimensional grid whose resolution and extent equals the resolution and extent of the original model. Processes requiring explicit spatial positions in the grid, for example seed dispersal, are calculated on this first layer. Processes which do not require explicit spatial grid positions, such as growth and seed production, are calculated on a new, associated layer with a variable size. This new 'non-spatial' layer is used to pool similar grid cells for calculations not requiring explicit spatial positions. Each cell on the two-dimensional layer is associated with one element on the non-spatial layer and the two layers exchange status information. A cell on the two-dimensional layer, for example, receives information on seeds available for dispersal from its associated element and an element on the non-spatial layer receives information on newly established individuals. To account for changes in the similarity among grid cells induced by processes simulated on the two-dimensional layer, associations between the two layers need to be dynamic. A first outline of the concept is given in (Chapter 5) and a detailed description of the concept is given in (Chapter 6).

To assess if associations between the two layers actually are required to be dynamic and to obtain a first assessment of possible gains of a D2C implementation, I conducted a preliminary study with TreeMig, in which I introduced two layers with a static association according to a stratification of the climate drivers (Nabel and Lischke, 2013; see Chapter 5). The stratification of landscape patches with similar environmental conditions for joint simulations is a common upscaling method when working with single-stand models (see e.g. King, 1991; Bugmann et al., 2000). Here I used three different stratifications of the climate drivers with a coarse, medium and fine subdivision to pool similar cells into elements of the non-spatial layer. To test the performance of these first preliminary and static upscalings I conducted simulations on three nested simulation areas: a small transect embedded in a larger transect, which itself is embedded in Switzerland (see Fig. 5.2a). I then compared computational expenses (CPU-time and peak heap memory) and simulated species biomass resulting from simulations with the original TreeMig version and simulations with the statically associated layers. Both reductions in the computational expenses and the differences in the simulated species biomass were strongly dependent on the applied stratification of the climate drivers (Chapter 5). Nevertheless, all stratifications led to notable reductions of the computational expenses (Table 5.1) and to relatively similar simulation outcomes (see Figs. 5.3 and 5.4). These results indicated that implementations of the D2C concept can strongly reduce computational expenses in exchange for small to intermediate approximation errors. These first preliminary tests with a static association between the layers were conducted for simulations with and without seed dispersal. Simulations with seed dispersal generally led to smaller reductions in computational expenses and to larger differences in the simulated species biomass compared to original TreeMig simulations than simulations without seed dispersal. Due to the increased differences in the simulated species biomass I concluded that the spatial dynamics resulting from the seed dispersal have to be taken into consideration and thus that associations between the layers are actually required to be dynamic (Chapter 5).

In summary, the first preliminary study described in Chapter 5 demonstrated that the D2C concept enables the pooling of grid cells for some calculations and that this pooling is required to be dynamic to allow for an explicit simulation of migration.

1.2.3.2 RQ 3b: What are the challenges when implementing a dynamic upscaling method based on grid cell similarity? How can these challenges be dealt with, and how do they influence the performance of the method? (Nabel, manuscript; see Chapter 6)

In order to be efficient, an upscaling method needs to maintain a good trade-off between reductions of computational expenses and introduced approximation errors. For the implementation and the application of the D2C method this trade-off manifests in the number of elements on the non-spatial layer over time. The reductions in computational expenses will be higher for lower numbers of elements, and the target therefore was to only have as many elements on the non-spatial layer as necessary to achieve an acceptable approximation of the base model (for details see Nabel, manuscript; Chapter 6). The number of elements on the non-spatial layer will certainly be influenced by the criteria specified for the similarity of the climate driver. When allowing dynamic changes in the associations between the layers, and therefore in the number of elements, it gets addi-

tionally important how and when elements on the non-spatial layer are split or merged. Splitting is important to account for deviations among grid cells associated with the same element due to processes simulated on the two-dimensional layer. Merging, on the other hand, is important to identify similar elements and to combine them for future calculations. These two processes therefore have different impacts on the performance. Splitting is required to preserve accuracy, but the addition of new elements increases the computational expenses. Merging reduces the number of elements and therefore the computational expenses, but can in turn also reduce the accuracy. Furthermore, both operations entail an organisational overhead. In the implementation of the D2C concept with TreeMig as well as in the applications, I regarded merging, splitting and the organisational overhead entailed by these processes as key challenges.

The new two-layer implementation of TreeMig – TreeMig-2L – is based on TreeMig versions developed in the preceding studies of this dissertation and therefore includes the minimum density threshold implementation (Chapter 3; see summary in Section 1.2.1) and the simple extrapolation method which conserves spatial correlations in the climatic fluctuations (Chapter 4; see summary in Section 1.2.2). When implementing TreeMig-2L, I considered the organisation of the non-spatial layer and its linkage to the two-dimensional layer as the most important aspects, in particular in order to achieve an efficient implementation of the splitting and merging processes and a small organisational overhead. I identified the following two issues as key problems: (1) that the number of elements on the non-spatial layer is not known in advance and, furthermore, variable over time due to splitting and merging processes, and (2) that a comparison for similarity of all elements with all elements would lead to an inefficient merging process. A fundamental step in the implementation of TreeMig-2L was therefore the development of an architecture (i.e. employed data types and their connections) which at the same time had to (1) permit a dynamic and variable sized non-spatial layer and (2) enable a pre-structuring of the elements for similarity comparisons. In the development of TreeMig-2L's architecture I took advantage of the fact that climate is used as a driver in TreeMig and is therefore known in advance. Therefore, I was able to use the climate drivers, i.e. TreeMig's bioclimate variables, to implement pre-processing functions which pre-structure a given simulation area according to similarities in the temporal development of these variables among grid cells. The static structure derived in the pre-processing step is then used for the efficient organisation of the dynamic non-spatial layer in TreeMig-2L simulations. A detailed description of the implementation of TreeMig-2L is given in Chapter 6.

A further goal in the development of TreeMig-2L was to obtain an adaptive model implementation, meaning that the similarity criteria were not to be hardcoded in the implementation but to be adjustable, i.e. that the similarity criteria were kept as input parameters to TreeMig-2L. For an application of TreeMig-2L different similarity criteria need to be specified. The first set of similarity criteria deals with the climate drivers. TreeMig-2L's pre-processing functions require a specification about how to bin different grid cells according to their temporal development in TreeMig's bioclimate variables. In the TreeMig-2L version described in the following and used in my studies, the temporal development in the bioclimate variables of a bin is calculated as the average of all grid cells associated with the same bin. This averaged temporal development is then used to drive the associated cells during the simulation (for more details on the implementation see Sections 6.3.1.3 and 6.A.2). This approach is comparable to the ecoregions used in the forest-landscape model LANDIS, where cells associated with the same ecoregion share important process rates (Scheller and Mladenoff, 2004). TreeMig-2L requires further similarity criteria to organise the merging and splitting of elements on the non-spatial layer. Merging requires the specification of similarity thresholds which determine when two elements are similar enough to be merged. Thus, these similarity thresholds specify allowed deviations in the abundances of the simulated species. Splitting requires the specification of criteria defining when changes induced by processes simulated on the two-dimensional layer disturb the similarity of two grid cells associated with the same element, i.e. when deviations in newly established species among the grid cells require a split of their element. In the implementation of TreeMig-2L, I regarded these splitting criteria as particularly critical for the performance. Since TreeMig is a multi-species model (Lischke et al., 2006), seed dispersal is simulated for multiple species. Depending on the specified similarity criteria it can therefore be possible that cells associated with the same element diverge in multiple different ways with regards to newly established species. This in turn entails the requirement for multiple similarity tests at runtime and can possibly entail large numbers of splits per element. TreeMig-2L's im-

plementation therefore allows to constrain the number of tree species for which similarity tests are conducted and therefore to focus on selected so-called 'tracked' species.

To test the performance of the TreeMig-2L implementation and in particular to also investigate the influence of the adjustable similarity criteria on the performance of TreeMig-2L, I conducted simulations with two different test applications. One of these was the test application already used in the previously described upscaling studies, i.e. the northwards migration of *O. carpinifolia*. As a second test application I selected the medium transects used in Chapter 5. I considered these two test applications to be complementary and well suited for the performance tests, because they had different specifications, in particular regarding grid resolution and extent (see Table 3.1). Amongst others, I conducted test simulations to disentangle performance influences of the averaging of the climate drivers and of the dynamic associations. Additionally, I conducted several simulations investigating the sensitivity of the performance to changes in the adjustable similarity criteria. I tested different sets of bins for the bioclimate variables used to pre-structure the simulation area, different similarity thresholds on the species abundances used for merging, as well as the number of species tracked for splitting decisions and the similarity requirements imposed on these tracked species (for details see Section 6.C.3). These tests confirmed the preliminary findings of Chapter 5 (see also Section 1.2.3.1) that the D2C concept can enable large reductions in computational expenses in exchange for small to intermediate approximation errors (Table 6.4). Comparing the resulting performance with a previous upscaling applied in the construction of TreeMig, presented in Lischke et al. (1998), the simulations conducted with TreeMig-2L led to smaller CPU-time reductions, but also entailed smaller accuracy losses.

Tests disentangling performance influences demonstrated that simulations with dynamic associations between the layers led to notable reductions in the approximation errors, and attributed the main share of resulting approximation errors to the averaging of the climate drivers. The sensitivity tests on the similarity criteria identified the different sets of bins for the bioclimate variables used to pre-structure the simulation area as most important for the performance, accuracy as well as computational expenses. The performance was also influenced by the number of tracked species. A reduction of the number of tracked species led to an increase of approximation errors and a larger reduction in computational expenses. An increase in the number of tracked species led to a decrease of the approximation error and smaller reductions in computational expenses. Applied merging and splitting thresholds were least influential in the conducted sensitivity tests (see Chapter 6, in particular Section 6.C.3). Simulations of the test application with the migration situation demonstrated that the method is applicable when simulating migration explicitly because migration outcomes for the tracked species, in this test application *O. carpinifolia*, were well approximated (see Sections 6.4.2.1 and 6.C.2 and in particular Fig. 6.C.9). This is an important advantage compared to decreasing the resolution by a simple averaging, which can lead to a large overestimation of migration speed as demonstrated in Bocedi et al. (2012).

In summary, I regarded the development of an efficient architecture, the implementation of splitting and merging as well as the specification of appropriate similarity criteria as the key challenges when using a dynamic upscaling method based on cell similarity. The simulations conducted with the test applications demonstrated that the organisational overhead required for splitting and merging was very small in TreeMig-2L applications (see Table 6.5), which can be attributed to the efficient architecture and implementation of TreeMig-2L. Furthermore, because the similarity criteria were kept adjustable in the TreeMig-2L implementation, they can be used directly in a simulation study to mediate the trade-off between accuracy and computational expenses according to the requirements of the application.

1.2.4 Additional contributions and required preparatory steps

In addition to the core work described in the five main manuscripts (Chapters 2 to 6), I contributed to further related studies. Firstly, I contributed to two papers (Snell et al., accepted; see Appendix A) and (Svenning et al., accepted) which arose from two workshops entitled 'Advancing concepts and models of species range dynamics: understanding and disentangling processes across scales'. I summarise the main findings of these papers in Sections 1.2.4.1 and 1.2.4.2. Secondly, I contributed to a study in which a coupled avalanche-forest model was developed based on TreeMig, i.e. on the model I also used as the base model in my thesis. Findings of

this study were documented in two manuscripts (Zurbriggen et al., in press and Zurbriggen et al., manuscript) and in Sections 1.2.4.3 and 1.2.4.4 I summarise particularly those aspects of these manuscripts that relate to my studies.

At the end of this section I address preparatory steps which were required for the investigations and implementations conducted in this thesis with regards to the original TreeMig implementation (Section 1.2.4.5).

1.2.4.1 Using dynamic vegetation models to simulate plant range shifts (Snell et al., accepted; see Appendix A)

Rebecca S. Snell, Andreas Huth, Julia E. M. S. Nabel, Greta Bocedi, Justin M. J. Travis, Dominique Gravel, Harald Bugmann, Alvaro G. Gutiérrez, Thomas Hickler, Steven I. Higgins, Marc Scherstjanoi, Björn Reineking, Natalie Zurbriggen, Heike Lischke
Ecography, accepted

The aim of this study was to discuss the potential and methodological challenges for simulating range dynamics using dynamic vegetation models (DVMs), and to present recommendations on, as well as promising tools for future required model development.

In this paper, we gave an overview of the main types of DVMs and of the processes and process representations commonly contained in models of each type (see also Section 1.1.1). For each type we presented example models and listed the typical setup (e.g. spatial resolution and extent) used in simulations with these models. We emphasised that DVMs can improve our understanding of the factors that influence species ranges and are particularly suitable for studying species range shifts due to their capacity to simulate population dynamics at both the leading and the trailing edge (see e.g. Sato and Ise, 2012). Subsequently we highlighted that, despite their suitability, DVMs only have seldom been used in studies on range shifts so far (e.g. Lischke et al., 2006; Scheller and Mladenoff, 2008), and we discussed potential reasons for the lack of such studies and related methodological challenges for simulations of species range dynamics with DVMs. We identified that not all DVMs include the processes deemed to be most important for explicit simulations of species range shifts (e.g. that seed dispersal is missing in DVMs applied on large scales), and that there is a strong trade-off between the spatial resolution and the spatial extent of the study region simulated with a DVM.

To enhance the capability of DVMs for species range shift simulations, we recommended that model development should focus on four aspects: reproduction, dispersal, establishment, and trait variability. For each of these aspects we discussed how they are currently represented in DVMs and why we deem future development to be important. We then gave examples on how models could be improved regarding these aspects, and identified challenges and requirements with regard to future model development. For example, current representations of reproduction in DVMs only account for indirect, long-term climatic influences on reproductive effort (e.g. through growth), although it is known that environmental conditions can have strong direct influences on reproductive effort (e.g. Kelly and Sork, 2002; Ladeau and Clark, 2006; Pérez-Ramos et al., 2010; Bykova et al., 2012). We suggested that direct climatic effects on reproductive efforts can be important for species range shifts but concluded that the data required for parameterisations of more detailed process functions is not yet available.

To mediate the trade-off between spatial resolution and spatial extent and to enable the inclusion of further processes, we presented upscaling techniques that have been used to reduce model complexity and computational expenses in DVMs. Presented upscaling techniques were, for example, the aggregation of species to plant functional types (e.g. Smith et al., 1997; Sato et al., 2007), the D2C concept developed in this thesis (Chapters 5 and 6) or the aggregation of individual trees and patches to densities in height classes (Lischke et al., 1998; see also Section 1.1.5.1).

In summary, we highlighted gaps between different DVM types regarding the simulation of species range shifts, recommended further steps in the development of DVMs and presented upscaling methods used to reduce model complexity and involved computational expenses. As this paper is particularly relevant for my thesis it is attached as an appendix (Appendix A).

1.2.4.2 The influence of interspecific interactions on species range expansion rates (Svenning et al., accepted)

Jens-Christian Svenning, Dominique Gravel, Robert D. Holt, Frank M. Schurr, Wilfried Thuiller, Tamara Münkemüller, Katja H. Schiffers, Stefan Dullinger, Thomas C. Edwards, Jr., Thomas Hickler, Stephen Higgins, Julia E.M.S. Nabel, Jörg Pagel and Signe Normand
Ecography, accepted

In this paper, we consolidated available knowledge on the influence of interspecific interactions (such as competition, facilitation, mutualism and predation) on species range expansion rates from theory, empirical studies of invasive species and natural range expansions, as well as from simulation studies with process-based models. Based on this knowledge we derived recommendations about when interspecific interactions need to be explicitly represented in studies forecasting range expansions.

Starting with the appreciation that interspecific interactions are often neglected in analyses of species ranges, we used the simple equation for the asymptotic rate of spread $\sqrt{4rD}$ following from the Skellam-Fisher model (Skellam, 1951; Okubo and Levin, 2001) to discuss how interspecific interactions could theoretically modulate range expansion rates, by influencing the population growth at low densities (r) and the diffusion coefficient (D). For example, a closed forest could reduce D for a spreading wind dispersed tree species by altering wind-driven dispersal distances (Schurr et al., 2008) and reduce r for this species via competition for light.

To complement the theoretical considerations, we reviewed findings on effects of interspecific interactions on species ranges from empirical studies of invasive species and natural range expansions, as well as from simulations conducted with process-based models. While we reviewed studies investigating animal as well as plant taxa, I concentrate on examples from studies dealing with tree species in the following. Examples from studies on invasive tree species were (1) limited invasion rates of exotic Pinaceae (pine species) in areas where neither the trees nor their associated fungi are native (Nũnez et al., 2009; Dickie et al., 2010), i.e. a reduction in r due to missing but required belowground mutualists; and (2) varying invasion rates of *Ficus microcarpa* (a strangler fig) in Florida depending on the abundances of fig-eating birds (Caughlin et al., 2012), i.e. influences on D due to mutualism by means of dispersing agents. Most of the reviewed studies on natural range shifts concerned tree species, such as (1) slowed range expansions explained by interspecific competition (van der Knaap et al., 2005), i.e. reductions in r; (2) spatially variable range expansions explained by multiple interactions between dependence on fire disturbances and competitive ability (McLeod and MacDonald, 1997), i.e. variations in r; and (3) reductions in D for various endo- or epizoochorously dispersed trees due to megafaunal losses (Janzen and Martin, 1982; Campos-Arceiz and Blake, 2011). Regarding simulations with process-based models, we found only few studies which considered effects of interspecific interactions on expansion rates, namely studies with DVMs on the effects of light competition, such as (1) the study by Scheller and Mladenoff (2008) using LANDIS-II (Scheller et al., 2007) and (2) the study by Meier et al. (2011) using TreeMig (Lischke et al., 2006) which both found that interspecific light competition can reduce tree species expansion rates, i.e. via a reduction in r.

From these findings we conclude that there is emerging evidence that interspecific interactions can influence large-scale species distributions via their influence on range expansion rates. We then discuss in which situations interspecific interactions need to be represented explicitly in a forecasting study, and when the use of an 'abiotic shortcut' could be sufficient, i.e. linking r and D to abiotic variables (Svenning et al., accepted). We stress that by using an abiotic shortcut, interspecific interactions which are explained by abiotic variables that are included in a study are only implicitly and incompletely accounted for, which again can be regarded as an upscaling. We conclude that interspecific interactions should be explicitly accounted for when their influence is strong and varies in time or space, because in such cases neglecting or simplifying the interspecific interaction could cause biases. We close the paper with a list of situations in which we expect large influences and strong spatiotemporal variations, for example, when the interspecific interaction only includes a few species as opposed to many species and therefore a higher chance for functional equivalence (Svenning et al., accepted).

In summary, this paper stressed that there can be a need for explicit representations of interspecific interactions in studies of species range shifts and that the implicit upscaling by means of an abiotic shortcut, which is often used in studies for the forecasting of species range shifts, might need to be revisited in certain situations.

The findings of this study can furthermore be seen as a motivation to more strongly investigate the effects of competition on species range shift simulations with DVMs (see also the discussion on the representation of disturbances in Section 1.3.2).

1.2.4.3 Explicit avalanche-forest feedback simulations improve the performance of a coupled avalanche-forest model (Zurbriggen et al., in press)

Natalie Zurbriggen, Julia E.M.S. Nabel, Michaela Teich, Peter Bebi, Heike Lischke
Ecological Complexity, in press

This paper is the first of two manuscripts in which we presented simulations with a new coupled avalanche-forest model called TreeMig-Aval (Zurbriggen, 2013). In the development of TreeMig-Aval, we coupled an avalanche release module to the forest-landscape model TreeMig (Lischke et al., 2006), the model that was also the base model for my thesis. The aim of this model coupling was to enhance the representation of disturbances in TreeMig for simulations of mountain forests under climate change.

In this manuscript, we described the implementation of the new avalanche release module and its coupling to TreeMig. One benefit of the explicit representation of avalanches in TreeMig-Aval is the possibility to study the positive feedback between forests and avalanche disturbances in a spatially-explicit forested mountain landscape. Avalanches change forest compositions and decrease forest density leading to increased avalanche release probabilities (Kulakowski et al., 2006). Increases in forest density, on the other hand, can decrease avalanche release probabilities (Bebi et al., 2009). The avalanche protection function of forests depends on many influences, such as climatic and topographic conditions (Schneebeli and Meyer-Grass, 1992) and further factors which affect forest densities and forest compositions, such as anthropogenic or natural disturbances. Avalanche release probabilities used in the simulations with TreeMig-Aval were based on a statistical analysis of historical avalanche release data sets (Schneebeli and Meyer-Grass, 1992; Maggioni and Gruber, 2003). Based on this analysis, the avalanche release probability in TreeMig-Aval was implemented to depend on forest density and composition, slope, curvature and aspect of the terrain, and winter length as a proxy for snow amounts (Zurbriggen et al., in press).

In the studies described in this manuscript, we used an artificial transect (representing an elevational temperature gradient) to investigate how the feedback between forests and avalanches is mediated by temperature, slope steepness and additional mortality which, for example, could be caused by anthropogenic or natural disturbances (Zurbriggen et al., in press). Additionally, we conducted a model simplification study (cf. the simplifying phase in Van Nes and Scheffer, 2005), investigating if the fully coupled TreeMig-Aval model could be replaced by a reduced complexity model; either by omitting the feedback of avalanches on forests or by replacing forest dynamics with an average forest. We found strong effects of temperature, slope and additional mortality on the simulated forest-avalanche feedback, including non-linear effects and interactions between these environmental influences. Effects of environmental influences on feedback strength have also been reported in other simulation studies investigating positive feedbacks (e.g. Bekker and Malanson, 2009). Regarding the simplification study, simulations showed that particularly treelines are sensitive to the explicit representation of the forest-avalanche feedback and the simplified model versions led to an overestimation of the simulated treeline elevation and an underestimation of avalanche release probabilities. From this simplification study we conclude that the forest-avalanche feedback needs to be explicitly simulated, which was also recommended in simulation studies investigating other vegetation-disturbance feedbacks (e.g. Seidl et al., 2007; Vorpahl et al., 2013).

While we did not investigate the effects of the representation of forest-avalanche feedbacks on explicitly simulated tree species migration, the detected sensitivity of the treelines to the model simplifications suggests that if and how forest-avalanche feedbacks are represented in a model could at least affect the simulation of altitudinal migration. Furthermore, the findings of the study on the effects of environmental influences, here temperature, slope and additional mortality, suggest that the spatiotemporal influences resulting from simulations with explicitly simulated disturbances could generally strongly influence simulated forest dynamics (see

also Section 1.2.4.4). Together with the findings presented in the study on the effects of interspecific interactions on species range expansion rates (Svenning et al., accepted; see Section 1.2.4.2) one could thus expect a strong influence on simulated migration outcomes (see discussion in Section 1.3.1.1).

1.2.4.4 Performance of alternative disturbance formulations in a spatially explicit avalanche-forest model (Zurbriggen et al., manuscript – to this date published in Zurbriggen, 2013, Ph.D. Thesis)

Natalie Zurbriggen, Michaela Teich, Julia E.M.S. Nabel, Peter Bebi, Heike Lischke
Manuscript intended for submission to Ecological Modelling; published in Zurbriggen, 2013

While the simulation studies with TreeMig-Aval presented in Section 1.2.4.3 (Zurbriggen et al., in press) used an artificial elevational transect of 3 rows with 30 cells each, the simulation studies presented in this second manuscript were conducted on a landscape, representing the area of the Dischma Valley in Davos, in the eastern Swiss Alps (Zurbriggen et al., manuscript). Simulations on a real landscape, spatially heterogeneous in topography and with spatiotemporal climatic influences, enabled us to study the spatiotemporal effects of the forest-avalanche feedback on forest density and forest composition, as well as the simulation of avalanche flow. In TreeMig-Aval, avalanche flow is simulated with a probabilistic flow direction and a probabilistic flow stop, influenced by topography, forest structure and forest type (Zurbriggen, 2013).

In this manuscript, we investigated if the spatially explicit and spatially linked representation of avalanches is required or could be simplified by means of stochastic disturbances or could even be neglected. As already discussed in Section 1.1.2, such simplifications are often motivated by computational expenses. Furthermore, previous TreeMig versions only contained spatially non-explicit stochastic disturbances, adaptable by means of parameters for disturbance intensity and disturbance probability (see Lischke et al., 2006, supplementary material), and this test allowed us to revisit this simplified representation of disturbances. Similar to the approach taken in Section 1.2.4.3 (Zurbriggen et al., in press) we conducted a simplification study, this time with regards to the spatial representation of avalanches. We compared model versions (1) with spatially explicit and linked avalanches, (2) with simplified stochastic disturbances with the same intensity as the avalanches disturbances and an occurrence probability spatially and temporally averaged from a run with avalanches, and (3) without disturbances. Besides comparisons between model versions, we also compared simulated forest densities and compositions with observed forest densities (LiDAR vegetation height data – 2003 ALS data) and compositions (Wildi and Ewald, 1986).

The comparisons between the different model versions and between simulation results and observed data demonstrated that realistic spatial patterns of forest density and forest type only resulted for simulations with avalanches, i.e. with spatially explicit and linked disturbances. For example, forest densities resulting from simulations with avalanches showed a strong spatial aggregation with large clusters of high density forests in undisturbed areas and large clusters with no forest cover in frequently disturbed areas, which matched the observed forest densities relatively well (Zurbriggen, 2013). Simulations with stochastic disturbances, in contrast, resulted in an unrealistic spatially random mosaic of high and mid density forest regularly interspersed with cells without forest cover. In simulations without disturbances, finally, the whole simulation area was covered by high density forests. In most of the conducted comparisons the performance of the model version with avalanches led to significant improvements compared to the model version with random disturbances, representing previous TreeMig version. We concluded that the effect of avalanches on forests should be represented in a spatially explicit and spatially linked manner.

Based on the findings presented in this manuscript and the findings in Chapter 4, I expect that simulations with forest-avalanche feedback and avalanche flow could change simulated migration outcomes compared to simulations which neglect disturbances or simulate spatially random disturbances when simulating migration explicitly (see discussion in Section 1.3.1.1).

1.2.4.5 Required preparatory steps for this thesis

For the investigations conducted in my Ph.D. studies, different preparatory steps reviewing, enhancing and refactoring the previously available TreeMig implementation were performed (as e.g. recommended in Kelly et al., 2009; Wilson et al., 2012).

Firstly, the previous TreeMig implementation worked with a platform dependent pseudo-random number generator (PRNG) leading to different results with different compilers and it was not possible to set a seed for this PRNG, and thus to replicate simulation runs. However, replicability is a fundamental demand of scientific software (Plesser et al., 2009). Furthermore, when effects of different model versions are tested, it is important to compare runs with identical pseudo-random number streams (PRNSs), i.e. with the same seed for the PRNG, in order to actually compare differences in the model versions as opposed to stochastic effects. Such comparisons were conducted in all chapters of this thesis, as well as in the studies described in Sections 1.2.4.3 and 1.2.4.4. Therefore, I replaced the platform-dependent PRNG, which was used in the previously available TreeMig implementation to generate one PRNS for all stochastic processes, with a platform-independent PRNG (the Mersenne Twister, see Matsumoto and Nishimura, 1998) now generating an individual PRNS for each of the stochastic processes. Using individual PRNSs was required in the studies described in Sections 1.2.4.3 and 1.2.4.4. In these studies we used different processes with stochastic representations, namely the extrapolation of climate sequences, avalanche release and flow, and additional mortality. For the conducted sensitivity studies, for example comparisons of simulations with and without additional mortality or with and without avalanche release, it was important that the remaining stochastic processes were always simulated with the same PRNS, in order to actually compare differences in the simulation setup as opposed to stochastic effects.

Further enhancements and refactorings were:

1. The introduction of dynamic memory allocations (e.g. to prevent that the code needed to be recompiled for executions with a differently sized simulation area).
2. Code optimisations, for example vectorisation of loops and extraction of expensive repetitive calculations detected with callgrind (Weidendorfer, 2008) to lookup tables.
3. A transfer of the input and output interface to a standard format (as recommended by Baxter et al., 2006), namely from formatted ASCII to NetCDF (see Rew and Davis, 1990).
4. Various corrections of erroneous code detected with memcheck (Seward and Nethercote, 2005) or gfortran compiler options (http://gcc.gnu.org/onlinedocs/gfortran/), for example buffer overflows overwriting other memory locations and implicit conversions from real to integer with subsequent errors due to the entailed rounding.
5. Various code enhancements (as e.g. recommended in Wilson et al., 2012), such as introduction of assertions, code documentation, removal of non-functional legacy code, and self explaining error messages, method names and variable names.

1.3 Synthesis

While I presented and briefly discussed the main findings of Chapters 2 to 6 as they related to the specific research questions derived in Section 1.1.5 in the previous sections (Sections 1.2.1 to 1.2.3) I will return to my more general research aims (as stated in Section 1.1.3) in this synthesis. I will subsume my findings and their limitations in a general discussion including the findings of the studies I additionally contributed to (as described in Section 1.2.4). Subsequently I will derive recommendations for further research and future model development.

1.3.1 General discussion

1.3.1.1 Research aim 1: Analyse effects of previously applied upscalings

The studies conducted in conjunction with the first research aim showed notable influences of well-established upscalings applied in the development and application of TreeMig on simulated migration outcomes and, within these studies, I proposed measures to overcome the identified problems. Specifically, I demonstrated that the representation of tree species populations by means of population densities in TreeMig can influence simulated tree species migration, because it allowed for the spread of infinitesimal seed densities. I showed that the implementation of a minimum population density threshold can prevent the spread of infinitesimal seed densities, which therefore led to a more realistic representation of migration in TreeMig (Nabel et al., 2013; see Chapter 3). In the subsequent studies I demonstrated that the spatiotemporal representation of climate fluctuations can influence simulated migration outcomes and that interpolations and extrapolations of climate time series should account for spatial correlations of climatic fluctuations and that simulations of tree species migration should be conducted with multiple stochastic repetitions to account for interannual climate variability (Nabel et al., 2013; see Chapter 3 and Nabel, manuscript; see Chapter 4). Most of my studies were conducted with an illustrative and realistic test application (Section 1.2), namely the northwards migration of the thermophile tree species *Ostrya carpinifolia* through a transect in the Alps. In this test application *O. carpinifolia* was close to its climatic boundaries and migrated in a fragmented landscape and, due to the simulation of multiple species, in a competitive context. This test application was selected because it was deemed to be sensitive to approximation errors introduced by the studied upscalings. Some of the conducted simulations indicated that the influence of interannual variability on migration might be less influential in another simulation setup (Nabel et al., 2013; see Chapter 3). However, I suggest that the findings of this study are nevertheless relevant beyond the presented test application, because changes in the climatic suitability in current species ranges are observed and projected for many species (Svenning and Skov, 2004; Rosenzweig et al., 2007), and most species are particularly sensitive to climate fluctuations on their external range boundaries (Camarero and Gutiérrez, 2004; Zimmermann et al., 2009). Similarly, competition with resident species is assumed to generally influence range shifts (McLeod and MacDonald, 1997; Leithead et al., 2010; Svenning et al., accepted), and strong spatial fragmentation, as in the test application, is common in our anthropogenically modified landscape (Pitelka et al., 1997; Hof et al., 2011).

The presented studies were motivated by TreeMig's implementation and previous TreeMig applications. Nevertheless, they can contribute to a better understanding of how certain influences generally need to be represented in a model when explicitly simulating migration. This is particularly the case for the findings of the second research question, investigating how climate fluctuations need to be represented in a simulation when migration is simulated explicitly. Studies with mathematical models already demonstrated the importance of climatic fluctuations and of static spatial heterogeneity for the migration of invasive species (see e.g. reviews by With, 2002; Hui et al., 2011), however, the influence of spatiotemporal fluctuations has so far not been studied in such models (With, 2002; Melbourne et al., 2006; Hui et al., 2011). Furthermore, although the importance of interannual climate variability has also already been discussed in studies with DVMs (Bugmann and Pfister, 2000; Miller et al., 2008; Giesecke et al., 2010), the current practice for climate interpolations and extrapolations in DVM studies is to apply simplifications of spatiotemporal climate fluctuations. As already mentioned in Section 1.2 this is done by statically applying mean values (e.g. Scheller and Mladenoff, 2005, 2008), cyclically repeating base periods (e.g. Hickler et al., 2012; Sato and Ise, 2012), or applying stochastic extrapolation methods that neglect spatial autocorrelations (e.g. Lischke et al., 2006; Epstein et al., 2007; Lischke et al., 2012). Overall, my studies thus demonstrated that commonly applied upscalings can influence migration outcomes, which in turn also underlines the need to conduct studies like the presented studies which investigate previously applied upscalings when a certain process is targeted.

Studies with another model than TreeMig would possibly have led to other research questions concerning other previously applied upscalings than the ones I presented above. Furthermore, during my studies and the additionally studies I contributed to, it became apparent that commonly applied upscalings of various other

aspects could also influence migration outcomes strongly. In the following I will discuss one such upscaling that is closely intertwined with my studies and studies I contributed to, namely the representation of disturbances. Other upscalings that I consider as important will be listed in the outlook (Section 1.3.2).

Small-scale disturbances leading to single tree mortality are accounted for indirectly in TreeMig by means of the distribution-based representation of the local spatial forest heterogeneity in TreeMig's height classes (Lischke et al., 1998, 2006). Additionally, TreeMig optionally allows for spatially non-explicit stochastic disturbances on the cell level, increasing the mortality in all height classes of an affected cell (Lischke et al., 2006, electronic supplementary material). In the studies presented in Chapters 2 to 6 I neglected such cell level disturbances in order to exclude stochasticity additional to the climatic fluctuations in the simulations. However, the studies conducted with TreeMig-Aval (Zurbriggen et al., in press; see Section 1.2.4.3 and Zurbriggen et al., manuscript; see Section 1.2.4.4) demonstrated that the representation of disturbances in a model can strongly influence spatial patterns of forest density and forest type. The effects of spatially independent random disturbances on forest densities that resulted in the study described in Section 1.2.4.4 compare well to the effect of spatially independent climatic fluctuations shown in Chapter 4. In both cases spatially randomised influences, via disturbances by avalanches or via interannual climatic fluctuations, lead to unrealistic spatial patterns in the forest cover, represented as forest densities in Zurbriggen et al. (manuscript) and represented as biomass in Chapter 4. The spatial mosaic of low and high forest cover resulting from the simulations with spatially randomised influences could entail other competitive interactions and a different distribution of local seed sources, compared to large patches of low and high forest cover in simulations with spatially connected influences. Both aspects, competitive interactions and the distribution of local seed sources, might in turn influence tree species migration (Scheller and Mladenoff, 2005; Leithead et al., 2010; Svenning et al., accepted; for the latter see also Section 1.2.4.2) Effects on competitive interactions could particularly be important because competition from resident species is often considered to cause lags in tree species migration (McLeod and MacDonald, 1997; Leithead et al., 2010; Sato and Ise, 2012). I therefore suggest that a simulation study investigating the effects of different representations of disturbances on explicitly simulated migration would be an important further analysis (see Section 1.3.2).

1.3.1.2 Research aim 2: Develop, implement an test a novel upscaling method

In the course of my thesis I developed an adaptive dynamic upscaling method, the dynamic two-layer classification (D2C) method, and presented its implementation in TreeMig (Chapters 5 and 6). In subsequent simulations with the new TreeMig-2L model I demonstrated its applicability and tested its performance in two different simulation setups and with various sensitivity tests of the adaptable parameters (Chapter 6). The realised reductions of computational expenses were strongly dependent on the spatial resolution of the simulation area, which is discussed below. For TreeMig's default spatial resolution of 1 km^2 (Lischke et al., 2006; Epstein et al., 2007) TreeMig-2L simulations performed very well (Chapter 6). Simulations in which a migrating species was tracked explicitly demonstrated that migration outcomes can be very well approximated with TreeMig-2L, which is an important advantage compared to decreasing the resolution by a simple averaging, which can lead to a large overestimation of migration speeds as demonstrated in Bocedi et al. (2012). In comparison to a previous upscaling applied in the construction of TreeMig, which was presented in Lischke et al. (1998), the exemplary simulations conducted with TreeMig-2L led to smaller CPU-time reductions, however, they also entailed smaller losses of accuracy. Specifically, in TreeMig-2L simulations with the coarsest stratification of the bioclimate variables applied, computational expenses were reduced by 80% with a smaller approximation error than reported by Lischke et al. (1998).

The development of the D2C concept incorporated the findings of my previously conducted studies (Chapters 3 and 4) in that it aimed to maintain large parts of the spatiotemporal climate heterogeneity. This was enabled by keeping the original spatial resolution for both layers, the two-dimensional and the non-spatial layer (see summary in Section 1.2.3.1), and by only associating grid cells with comparable driving climate time series to the same element of the non-spatial layer (see summary in Section 1.2.3.2). In TreeMig-2L, similarity criteria on the climate time series of the single grid cells are used in a pre-processing step to derive a static base

structure of cells which can theoretically be associated with the same element. In the current TreeMig-2L version, the climate drivers of all cells which can be associated with the same element are then averaged and the averaged driver is used for the simulations no matter if the cells are actually associated with the same element or not. Comparison among simulation outcomes with different similarity criteria regarding the driving climate time series demonstrated that the simulated species abundances were particularly sensitive to these similarity criteria. In contrast, simulation outcomes were less sensitive to variations of similarity criteria regarding the species abundances and germinated seeds, which are used to control dynamic associations between the layers of TreeMig-2L (Chapter 6). These experiments demonstrated that the main share of the approximation error in TreeMig-2L simulations was caused by the aggregation of the climate time series, which again underlines the importance of the climate driver. Whilst the static base structure derived in the pre-processing step is fundamental for the performance of TreeMig-2L (see summary in Section 1.2.3.2), the averaging of climate time series does not have to be conducted in the pre-processing step. Parts of this approximation error could therefore possibly be reduced if the averaging in the pre-processing would be replaced by an averaging per iteration in which only climate time series of those grid cells are averaged that are actually currently associated with the same element. Even though this might reduce parts of the approximation error, it might also reduce the reductions in computational expenses and should therefore be subject of a thorough test study.

One of the main goals in the development of the D2C concept was to keep all processes which are simulated by the base model and to maintain their spatial resolution. Instead of changing the spatial resolution or reducing the number of processes, the D2C concept reduces the computational expenses by only aggregating similar grid cell calculations for certain processes (Chapters 5 and 6). The conservation of the spatial resolution for all simulated processes is an important advantage of the D2C concept compared to upscaling methods that change the spatial resolution. Firstly, approximation errors are prevented that would result when simply coarsening the spatial resolution by averaging ('extrapolation by lumping' sensu King, 1991; Bugmann et al., 2000 and 'naïve upscaling' sensu Bocedi et al., 2012). Secondly, no new formulas have to be derived, which is often necessary for more complex upscaling methods and usually requires restrictive assumptions about the behaviour of the base model (see e.g. reviews by Lischke et al., 2007; Auger et al., 2012). Another advantage of the D2C concept is that the grid cells aggregated for calculations of non-spatial processes can be arbitrarily distributed in space and in particular do not need to be spatially contiguous. Other methods that coarsen the resolution usually can only aggregate spatially contiguous grid cells with predetermined spatial arrangements. Finally, the D2C concept allows for an explicit simulation of migration because seed dispersal is still simulated on the original two-dimensional layer and associations between this two-dimensional layer and the non-spatial layer are dynamic (Chapter 6). This is an important advantage over previously applied static stratifications (e.g. King, 1991; Bugmann, 2001), because a static aggregation of grid cells precludes the explicit simulation of migration. Still, the D2C concept exploits recurring patterns in a manner similar to previous stratifications, which is an important underlying idea of upscaling (e.g. Lischke et al., 2007).

The example applications with TreeMig-2L demonstrated that the D2C concept is well applicable to aggregate local processes (non-spatial processes) that have a deterministic process description, or are stochastically conditional on previously known drivers. Moreover, when a model is upscaled with the D2C concept, the inclusion of new non-spatial processes with deterministic process descriptions can come with lower costs, given that they do not have to be simulated for the whole simulation area but only for the elements on the non-spatial layer. If a local process has a stochastic representation (stochastically conditional on other than previously known drivers, e.g. purely random establishment) and if the results of such stochastic processes are linked among grid cells through spatially linking processes (e.g. seed dispersal), the D2C concept might be less applicable. Other limitations of the applicability of the D2C concept are the cost ratio between spatially linking processes and non-spatial processes. The limitation caused by the cost ratio between spatially linking processes and non-spatial processes got apparent in the simulations conducted with TreeMig-2L: the obtained reductions in computational expenses were much lower with a fine spatial resolution due to an increase of the percentage of computation time spent with seed dispersal (see Section 6.4.2.2). The dependence on the spatial resolution in TreeMig-2L is due to the employed dispersal algorithm and it should be possible to mitigate this by applying a more efficient dispersal algorithm, which is what I suggest as one of the next step in the devel-

opment of TreeMig-2L (see Section 1.3.2). These experiments indicated that the D2C concept might be less applicable for a model with several and expensive spatially linking processes. Furthermore, multiple spatially linking processes can potentially increase the spatial heterogeneity among cells and therefore decrease the number of similar cells and thus reduce the benefit of applying the D2C concept.

The three aspects listed above, i.e. the influence of the cost ratio between non-spatial and spatially linking processes, as well as the spatial heterogeneity caused be the spatially linking processes and the influence of the representation (i.e. stochastic vs. deterministic) of non-spatial processes, can be used to assess the applicability of the D2C concept for other DVMs. Regarding the representation of non-spatial processes the D2C concept, as stated above, will not be applicable when the local stochastic processes are linked among grid cells through spatially linking processes as for example in LANDCLIM (Schumacher et al., 2004). However, it should be applicable for models in which the stochasticity only stems from previously known drivers, as the bioclimate variables in TreeMig-2L, or models in which the local stochasticity is realised in form of patch replicates and averaged on the cell level, as for example done in LPJ-Guess (Smith et al., 2001). With regards to the costs and the number of spatially linking processes, the D2C concept might be less applicable for models which contain many and complex interacting spatially linked processes such as LANDIS-II (Scheller et al., 2007), particularly when used with several extensions including spatially linking processes (e.g. interactions between seed dispersal, spruce budworm disturbances and fire disturbances, as in Sturtevant et al., 2012). The D2C concept should be applicable for models with few and simple spatially linked processes, such as TreeMig (provided the default spatial resolution or a more efficient dispersal algorithm is used) and trivially also for spatially independent one-dimensional DVMs (sensu Fisher et al., 2010), such as ED (Fisher et al., 2010) and most implementations of LPJ-Guess (e.g. Smith et al., 2001; Hickler et al., 2012). In the ideal case, reductions with the D2C concept could be used to decrease the spatial resolution and to implement a simple dispersal kernel in one of the latter mentioned models (see Section 1.3.2).

1.3.2 Outlook

In my studies and in the studies I contributed to, the representation of further aspects in DVMs was identified to potentially influence simulated migration outcomes, i.e. further previously applied upscalings were put into question. In the following I will highlight several aspects that I consider particularly important for further research. Subsequently I will give some recommendations about future improvements of TreeMig-2L and further applications of the D2C concept.

In the general discussion of the findings to my first research aim, I suggested that effects of different **representations of disturbances** on explicitly simulated migration should be subject to future studies, particularly also in the light of the assumed importance of competition for species range shifts (Svenning et al., accepted; see Section 1.2.4.3). First steps in this direction were carried out in a study by Scheller and Mladenoff (2005), in which the authors studied interactive effects of climate change, disturbances and tree species migration in simulations with LANDIS-II. Comparing results from simulations with and without windthrow and harvesting, Scheller and Mladenoff (2005) found that the negative effect of disturbances on seed dispersal due to removed local seed sources was stronger than the positive effect due to gaps with reduced competition. Disturbances can thus affect tree species migration in different ways. A systematic study of such effects and of the influence of different representations, such as spatially stochastic disturbances compared to spatially explicit and spatially linked disturbances (see Section 1.3.1.1), could contribute to a better understanding of how disturbances should be represented when simulating migration explicitly.

In the study on the potential and methodological challenges for simulating range dynamics using DVMs we evaluated key processes which we recommended to be improved to enhance the simulation of species range dynamics with DVMs. One of the highlighted aspects was the lack of a **representation of trait variability** (Snell et al., accepted; see Appendix A). The potential importance of trait variability was also demonstrated in my studies, where different species parameter sets, selected within the plausible parameter range of the migrating species, led to strong differences in migration outcomes (Nabel et al., 2012; see Chapter 2 and Nabel et al., 2013; see Chapter 3). Migration outcomes particularly differed much more among simulations with dif-

ferent species parameter sets than among runs with different stochastically extrapolated climate time series (Nabel et al., 2013; see Chapter 3). Similar to neglecting the variability between different species when conducting simulations with plant functional types (see e.g. Smith et al., 1997; Sato et al., 2007) neglecting the intra-species variability between different proveniences, but also between single individuals, is one form of a thematic upscaling. In Snell et al. (accepted) we suggest several approaches to better represent trait variability in DVMs, for example, by including several randomly selected subtypes (Snell et al., accepted; Appendix A). I recommend comparing outcomes of simulations that include more detailed representations to simulations with the original representation in a model, to test in how far simulated migration outcomes are affected and how large the resulting increases in computational expenses are.

In the context of trait variability, I consider another aspect as very important, which we also highlighted in Snell et al. (accepted), namely the **representation of dispersal kernels** in DVMs. The dispersal traits of a species are regarded to be one of the main factors determining if a species can track climatic changes (e.g. Bullock et al., 2012). The few DVMs that include an explicit representation of seed dispersal usually contain a predefined, stochastically or deterministically applied dispersal kernel, which is adapted with species-specific parameters (see e.g. TreeMig – Lischke et al., 2006 or LANDIS-II – Ward et al., 2004), which again is a thematic upscaling. Similar to other species parameters, dispersal traits can vary between individuals and are subject to adaptations (Davis and Shaw, 2001; Wright et al., 2008; Burton et al., 2010). Moreover, dispersal is not only determined by characteristics of the dispersing species, but also by biotic and abiotic environmental influences (Damschen et al., 2008; Schurr et al., 2008; Tackenberg and Stöcklin, 2008). Furthermore, a species can have more than one dispersing agent (Jongejans et al., 2008; Wichmann et al., 2009). Thus, the current representation of strongly simplified single dispersal kernels per species for all environmental situations might be insufficient to accurately represent dispersal and I recommend that the influence of the representation of dispersal kernels in DVMs on migration outcomes should be subject to future studies. One starting point could be to derive a larger set of representative dispersal kernels from mechanistic models (e.g. Katul et al., 2005; Nathan, 2008; Nathan et al., 2011; Bullock et al., 2012) for different dispersal agents and different environmental conditions, such as closed canopy vs. open ground or lowland vs. alpine conditions, and to compare migration outcomes from simulations with one comprehensive kernel against simulations with several specific kernels.

Finally, I found a high sensitivity of the simulated population dynamics to the bioclimate variables used as drivers in all studies I conducted with TreeMig (Chapters 2 to 6). Furthermore, migration outcomes were strongly influenced by the species parameter 'minimum required $DDsum_{>5.5\,^{\circ}C}$' [3](see Chapter 2), which governs growth and mortality in TreeMig and constitutes a threshold on germination (Table 3.1). Most forest-landscape models, including TreeMig, use bioclimate variables to govern empirically derived process descriptions, for example for growth and mortality (e.g. TreeMig – Lischke et al., 2006 and LANDCLIM – Schumacher et al., 2004). However, these bioclimate variables are only proxies and the empirical process descriptions are derived under current conditions and are probably not valid for future environmental conditions, for example under changed atmospheric CO_2 concentrations (Williams and Jackson, 2007; Jackson et al., 2009). Therefore I suggest that a combination of explicit simulation of physiology and migration in a DVM would be an important future contribution and the work by Snell (2013) is an important first step in this direction. One of the challenges entailed with the simulation of physiology and migration in the same model is the increase in computational expenses and the proposed D2C concept could improve this situation because it enables to increase the detail of non-spatial dynamics, as long as they are represented in a deterministic way (see discussion in Section 1.3.1.2).

TreeMig-2L could thus be extended with a more processed-based, though deterministic, description of the local population dynamics, and could then be used to test how such a more detailed representation affects migration outcomes under different environmental conditions. Another extension of TreeMig-2L could be the integration of spatially explicit and spatially linked disturbances, such as the avalanches described in Zurbriggen (2013), see Sections 1.2.4.3 and 1.2.4.4. Similar to the dispersal of seeds, such disturbances would need to be simulated on the two-dimensional layer and similarity criteria would need to be defined for when two cells associated with the same element differ due to experienced disturbances. Thus, besides the newly

[3] $DDsum_{>5.5\,^{\circ}C}$ is the sum of daily mean temperatures above 5.5 °C.

germinated seeds of tracked species, which are currently used to assess if an element needs to be split (see Chapter 6), also a criterion for the experienced disturbances would be required, for example, the disturbance intensity. The performance of simulations on two layers compared to simulations on one layer would thereby probably depend on the disturbance frequency and the spatial pattern of disturbances. The performance of two layer simulations of disturbances with reoccurring spatially correlated patterns, such as avalanches (Zurbriggen, 2013; see Section 1.2.4.4), would presumably be much better than for disturbances tending to be spatially random. Besides extending TreeMig-2L with further processes, it would be beneficial to replace the expensive simulation of seed dispersal with a more efficient seed dispersal algorithm. Recent studies which proposed efficient seed dispersal algorithms suggested learning from image processing techniques, for example solving the dispersal algorithm with Fast Fourier Transforms (Prasad et al., 2013) or using Graphic Processor Units (Tang et al., 2011; van de Koppel et al., 2011; Fan et al., 2012).

In Section 1.3.1.2 I highlighted that the **D2C concept** could be implemented in a one-dimensional DVM. In the ideal case, reductions in the computational expenses could be used to decrease the spatial resolution of such a DVM, which is a precondition for an explicit simulation of migration, due to the problems of within-cell heterogeneity and the uncertainty about within-cell spread, which are associated with a coarse spatial resolution (see Section 1.1.1). Provided that a reduction in the spatial resolution is possible, the next step would be to implement an efficient dispersal kernel. Such a study would furthermore be a good test of the applicability of the D2C concept for other models.

1.3.3 Conclusions

The studies presented in my thesis and the additional studies that I contributed to highlighted that upscalings used in the implementation and application of DVMs need to be revisited when migration is simulated explicitly. I demonstrated this need on the example of the continuous representation of within-cell populations in TreeMig and the representation of spatiotemporal climate fluctuations in extrapolations of climate time series, and I showed how current shortcomings can be dealt with (Chapters 3 and 4). My studies thus revealed important requirements for the application of upscaling methods, when tree species migration is simulated explicitly. Furthermore, the findings of the study on the influence of spatially correlated climatic fluctuations (Chapter 4) together with the findings of the study on spatially explicit and linked disturbances (Sections 1.2.4.3 and 1.2.4.4) demonstrated that revisiting formerly applied upscalings is not only required for the simulation of tree species migration but generally for a more accurate representation of the spatiotemporal arrangement of forests.

In the outlook (Section 1.3.2) I identified several upscalings which should be tested on their influence on simulated migration and species range shifts in future studies. However, adding further detailed process descriptions that interact with the processes already contained in a model is not only problematic with regards to computational expenses. Additional problems, which I did not discuss in my thesis, are the parameterisation and the validation of new processes (but see Snell et al., accepted; see Appendix A), and particularly also the handling of model implementations with growing complexity. The addition of further processes, if conducted without a rigorous and systematic development and testing protocol, can lead to incomprehensible model implementations (see e.g. Section 1.2.4.5). A promising approach is the implementation of modular model architectures, with clearly defined interfaces (see e.g. Scheller et al., 2007). A modular architecture allows implementing new or refined process descriptions which can be coupled via predefined interfaces without interfering with the core implementation of the model, which particularly facilitates comparisons of simulations with and without an investigated process.

Provided a rigorous and systematic development and testing protocol is applied, I consider the possibility to conduct such process-based studies as one of the main advantages of DVMs. Due to their dynamic and process-based approach, DVMs facilitate studies on the influence of refined or new process descriptions and their interaction with other processes on simulation outcomes (as e.g. demonstrated in Section 1.2.4.3). Such process-based studies can increase the understanding of forest dynamics (see also Snell et al., accepted; see Appendix A) and can also be used to inform other model types (Svenning et al., accepted; see Section 1.2.4.2),

or at least to highlight which of the aspects neglected in forecasting studies (e.g. on species range shifts) need to be considered when interpreting their results.

One of the main problems when conducting studies with DVMs on larger scales is the trade-off between spatial resolution and spatial extent. As highlighted in the introduction to my thesis, coarse spatial resolutions and the entailed loss of small scale heterogeneity can lead to biases in the simulation outcomes (see e.g. He et al., 2011; Bocedi et al., 2012). Furthermore, my studies on the effect of simplifications of the spatiotemporal representation of climate fluctuations confirmed the importance of small scale heterogeneity and underlined that an upscaling method should maintain small scale representations of climatic influences in a migration situation. With the D2C concept, I presented an upscaling method which can conserve the spatiotemporal resolution and the processes of the model it is applied to, and can nevertheless notably reduce computational costs. Instead of decreasing the spatial resolution, aggregations are conducted dynamically and only in situations which either cause no or at least less differences in the simulation outcomes. I believe that the D2C concept bears potential for future model development, however, its implementation needs to be customised to the model it is applied to. With TreeMig-2L, I demonstrated the applicability of the D2C concept and provided one further step to enable studies of tree species migration on larger scales.

References

Araújo, M.B., Peterson, A.T., 2012. Uses and misuses of bioclimatic envelope modeling. Ecology 93, 1527–1539.

Auger, P., Poggiale, J., Sánchez, E., 2012. A review on spatial aggregation methods involving several time scales. Ecological Complexity 10, 12–25.

Baxter, S.M., Day, S.W., Fetrow, J.S., Reisinger, S.J., 2006. Scientific Software Development Is Not an Oxymoron. PLoS Computational Biology 2, 0975–0978.

Bebi, P., Kulakowski, D., Rixen, C., 2009. Snow avalanche disturbances in forest ecosystems – State of research and implications for management. Forest Ecology and Management 257, 1883–1892.

Bekker, M.F., Malanson, G.P., 2009. Modeling feedback effects on linear patterns of subalpine forest advancement. Developments in Earth Surface Processes 12, 167–190.

Berger, M.J., Oliger, J., 1984. Adaptive mesh refinement for hyperbolic partial differential equations. Journal of Computational Physics 53, 484–512.

Berger, R., 1981. Comparison of the Gompertz and Logistic Equations to Describe Plant Disease Progress. Phytopathology 71, 716–719.

Bertrand, R., Lenoir, J., Piedallu, C., Riofrío-Dillon, G., de Ruffray, P., Vidal, C., Pierrat, J.C., Gégout, J.C., 2011. Changes in plant community composition lag behind climate warming in lowland forests. Nature 479, 517–520.

Bocedi, G., Pe'er, G., Heikkinen, R.K., Matsinos, Y., Travis, J.M., 2012. Projecting species' range expansion dynamics: sources of systematic biases when scaling up patterns and processes. Methods in Ecology and Evolution 3, 1008–1018.

Bonan, G.B., 2008. Forests and climate change: forcings, feedbacks, and the climate benefits of forests. Science 320, 1444–1449.

Brubaker, L.B., 1986. Responses of Tree Populations to Climatic-change. Vegetatio 67, 119–130.

Bugmann, H., 1994. On the Ecology of Mountainous Forests in a Changing Climate: A Simulation Study. Ph.D. thesis. Swiss Federal Institute of Technology Zurich.

Bugmann, H., 2001. A Review of Forest Gap Models. Climatic Change 51, 259–305.

Bugmann, H., Lindner, M., Lasch, P., Flechsig, M., Ebert, B., Cramer, W., 2000. Scaling Issues in Forest Succession Modelling. Climatic Change 44, 265–289.

Bugmann, H., Pfister, C., 2000. Impacts of interannual climate variability on past and future forest composition. Regional Environmental Change 1, 112–125.

Bullock, J.M., White, S.M., Prudhomme, C., Tansey, C., Perea, R., Hooftman, D.A., 2012. Modelling spread of British wind-dispersed plants under future wind speeds in a changing climate. Journal of Ecology 100, 104–115.

Burkett, V.R., Wilcox, D.A., Stottlemyer, R., Barrow, W., Fagre, D., Baron, J., Price, J., Nielsen, J.L., Allen, C.D., Peterson, D.L., et al., 2005. Nonlinear dynamics in ecosystem response to climatic change: case studies and policy implications. Ecological Complexity 2, 357–394.

Burton, O.J., Phillips, B.L., Travis, J.M.J., 2010. Trade-offs and the evolution of life-histories during range expansion. Ecology Letters 13, 1210–1220.

Bykova, O., Chuine, I., Morin, X., Higgins, S.I., 2012. Temperature dependence of the reproduction niche and its relevance for plant species distributions. Journal of Biogeography 39, 2191–2200.

Camarero, J.J., Gutiérrez, E., 2004. Pace and Pattern of Recent Treeline Dynamics: Response of Ecotones to Climatic Variability in the Spanish Pyrenees. Climatic Change 63, 181–200.

Campos-Arceiz, A., Blake, S., 2011. Megagardeners of the forest – the role of elephants in seed dispersal. Acta Oecologica 37, 542–553.

Carpenter, S.R., Mooney, H.A., Agard, J., Capistrano, D., DeFries, R.S., Diaz, S., Dietz, T., Duraiappah, A.K., Oteng-Yeboah, A., Pereira, H.M., et al., 2009. Science for managing ecosystem services: Beyond the Millennium Ecosystem Assessment. Proceedings of the National Academy of Sciences 106, 1305–1312.

Caswell, H., Neubert, M.G., Hunter, C.M., 2011. Demography and dispersal: invasion speeds and sensitivity analysis in periodic and stochastic environments. Theoretical Ecology 4, 407–421.

Caughlin, T., Wheeler, J.H., Jankowski, J., Lichstein, J.W., 2012. Urbanized landscapes favored by fig-eating birds increase invasive but not native juvenile strangler fig abundance. Ecology 93, 1571–1580.

Chen, I.C., Hill, J.K., Ohlemüller, R., Roy, D.B., Thomas, C.D., 2011. Rapid range shifts of species associated with high levels of climate warming. Science 333, 1024–1026.

Collingham, Y.C., Huntley, B., 2000. Impacts of Habitat Fragmentation and Patch Size upon Migration Rates. Ecological Applications 10, 131–144.

Corlett, R.T., Westcott, D.A., 2013. Will plant movements keep up with climate change? Trends in ecology & evolution 28, 482–488.

Currie, D.J., 2007. Disentangling the roles of environment and space in ecology. Journal of Biogeography 34, 2009–2011.

Damschen, E.I., Brudvig, L.A., Haddad, N.M., Levey, D.J., Orrock, J.L., Tewksbury, J.J., 2008. The movement ecology and dynamics of plant communities in fragmented landscapes. Proceedings of the National Academy of Sciences of the United States of America 105, 19078–19083.

Davis, M.B., 1989. Lags in vegetation response to greenhouse warming. Climatic Change 15, 75–82. 10.1007/BF00138846.

Davis, M.B., Shaw, R.G., 2001. Range Shifts and Adaptive Responses to Quaternary Climate Change. Science 292, 673–679.

Delcourt, H.R., Delcourt, P.A., Webb III, T., 1982. Dynamic plant ecology: the spectrum of vegetational change in space and time. Quaternary Science Reviews 1, 153–175.

Dewhirst, S., Lutscher, F., 2009. Dispersal in heterogeneous habitats: thresholds, spatial scales, and approximate rates of spread. Ecology 90, 1338–1345.

Dickie, I.A., Bolstridge, N., Cooper, J.A., Peltzer, D.A., 2010. Co-invasion by Pinus and its mycorrhizal fungi. New Phytologist 187, 475–484.

Dormann, C.F., Schymanski, S.J., Cabral, J., Chuine, I., Graham, C., Hartig, F., Kearney, M., Morin, X., Römermann, C., Schröder, B., Singer, A., 2012. Correlation and process in species distribution models: bridging a dichotomy. Journal of Biogeography 39, 2119–2131.

Dullinger, S., Gattringer, A., Thuiller, W., Moser, D., Zimmermann, N.E., Guisan, A., Willner, W., Plutzar, C., Leitner, M., Mang, T., Caccianiga, M., Dirnbock, T., Ertl, S., Fischer, A., Lenoir, J., Svenning, J.C., Psomas, A., Schmatz, D.R., Silc, U., Vittoz, P., Hulber, K., 2012. Extinction debt of high-mountain plants under twenty-first-century climate change. Nature Clim. Change advance online publication, 1–4.

Elkin, C., Gutiérrez, A.G., Leuzinger, S., Manusch, C., Temperli, C., Rasche, L., Bugmann, H., 2013. A 2°C warmer world is not safe for ecosystem services in the European Alps. Global Change Biology 19, 1827–1840.

Engler, R., Guisan, A., 2009. MigClim: Predicting plant distribution and dispersal in a changing climate. Diversity and Distributions 15, 590–601.

Epstein, H., Yu, Q., Kaplan, J., Lischke, H., 2007. Simulating Future Changes in Arctic and Subarctic Vegetation. Computing in Science Engineering 9, 12–23.

Erban, R., Kevrekidis, I.G., Othmer, H.G., 2006. An equation-free computational approach for extracting population-level behavior from individual-based models of biological dispersal. Physica D: Nonlinear Phenomena 215, 1–24.

European Forest Data Center, 2012. Distribution of *Ostrya carpinifolia*. Accessed from http://efdac.jrc.ec.europa.eu/index.php/climate, on 28.01.2012.

Fan, J., Ji, H.f., Guan, X.x., Tang, Y., 2012. A GPU-based multi-resolution algorithm for simulation of seed dispersal. Journal of Zhejiang University SCIENCE C 13, 816–827.

FAO, 2010. Global forest resources assessment 2010. Food and Agriculture Organization of the United Nations (FAO), Rome, http://www.fao.org/docrep/013/i1757e/i1757e.pdf. Latest access date: 20.12.10.

Fischlin, A., Midgley, G.F., Price, J.T., Leemans, R., Gopal, B., Turley, C., Rounsevell, M.D.A., Dube, O.P., Tarazona, J., Velichko, A.A., 2007. Ecosystems, their properties, goods, and services. Climate Change 2007: Impacts, Adaptation and Vulnerability. Contribution of Working Group II to the Fourth Assessment Report of the Intergovernmental Panel on Climate Change. M.L. Parry, O.F. Canziani, J.P. Palutikof, P.J. van der Linden and C.E. Hanson, Eds., Cambridge University Press, Cambridge, UK, 211-272.

Fisher, R., McDowell, N., Purves, D., Moorcroft, P., Sitch, S., Cox, P., Huntingford, C., Meir, P., Woodward, F.I., 2010. Assessing uncertainties in a second-generation dynamic vegetation model caused by ecological scale limitations. New Phytologist 187, 666–681.

Franklin, J., Syphard, A.D., Mladenoff, D.J., He, H.S., Simons, D.K., Martin, R.P., Deutschman, D., O'Leary, J.F., 2001. Simulating the effects of different fire regimes on plant functional groups in Southern California. Ecological Modelling 142, 261–283.

Fulton, M.R., 1991. A computationally efficient forest succession model: Design and initial tests. Forest Ecology and Management 42, 23–34.

Giesecke, T., Miller, P.A., Sykes, M.T., Ojala, A.E.K., Seppä, H., Bradshaw, R.H.W., 2010. The effect of past changes in inter-annual temperature variability on tree distribution limits. Journal of Biogeography 37, 1394–1405.

Gómez-Mourelo, P., Ginovart, M., 2013. A connection between discrete individual-based and continuous population-based models: A forest modelling case study. Artificial Intelligence Research 2, p28.

Greenman, J.V., Benton, T.G., 2001. The impact of stochasticity on the behaviour of nonlinear population models: synchrony and the Moran effect. Oikos 93, 343–351.

Grenfell, B.T., Finkenstadt, B.F., Wilson, K., Coulson, T.N., Crawley, M., 2000. Reply: Nonlinearity and the Moran effect. Nature 406, 847–847.

Gustafson, E.J., Zollner, P.A., Sturtevant, B.R., He, H.S., Mladenoff, D.J., 2004. Influence of forest management alternatives and land type on susceptibility to fire in northern Wisconsin, USA. Landscape Ecology 19, 327–341.

Hastings, A., Cuddington, K., Davies, K.F., Dugaw, C.J., Elmendorf, S., Freestone, A., Harrison, S., Holland, M., Lambrinos, J., Malvadkar, U., Melbourne, B.A., Moore, K., Taylor, C., Thomson, D., 2005. The spatial spread of invasions: new developments in theory and evidence. Ecology Letters 8, 91–101.

He, H.S., Mladenoff, D.J., Boeder, J., 1999. An object-oriented forest landscape model and its representation of tree species. Ecological Modelling 119, 1–19.

He, H.S., Yang, J., Shifley, S.R., Thompson, F.R., 2011. Challenges of forest landscape modeling – Simulating large landscapes and validating results. Landscape and Urban Planning 100, 400–402.

Helfenstein, J., Kienast, F., 2014. Ecosystem service state and trends at the regional to national level: A rapid assessment . Ecological Indicators 36, 11 – 18.

Hickler, T., Vohland, K., Feehan, J., Miller, P.A., Smith, B., Costa, L., Giesecke, T., Fronzek, S., Carter, T.R., Cramer, W., Kühn, I., Sykes, M.T., 2012. Projecting the future distribution of European potential natural vegetation zones with a generalized, tree species-based dynamic vegetation model. Global Ecology and Biogeography 21, 50–63.

Higgins, S., Clark, J., Nathan, R., Hovestadt, T., Schurr, F., Fragoso, J., Aguiar, M., Ribbens, E., Lavorel, S., 2003. Forecasting plant migration rates: managing uncertainty for risk assessment. Journal of Ecology 91, 341–347.

Higgins, S., Richardson, D., 1996. A review of models of alien plant spread. Ecological Modelling 87, 249–265.

Hof, C., Levinsky, I., Araújo, M.B., Rahbek, C., 2011. Rethinking species' ability to cope with rapid climate change. Global Change Biology 17, 2987–2990.

Hui, C., Krug, R.M., Richardson, D.M., 2011. Modelling spread in invasion ecology: a synthesis. Fifty years of invasion ecology. Wiley-Blackwell, UK. chapter 25. pp. 329–343.

Huntley, B., Barnard, P., Altwegg, R., Chambers, L., Coetzee, B.W.T., Gibson, L., Hockey, P.A.R., Hole, D.G., Midgley, G.F., Underhill, L.G., Willis, S.G., 2010. Beyond bioclimatic envelopes: dynamic species' range and abundance modelling in the context of climatic change. Ecography 33, 621–626.

Iverson, L.R., McKenzie, D., 2013. Tree-species range shifts in a changing climate: detecting, modeling, assisting. Landscape Ecology 28, 879–889.

Iverson, L.R., Schwartz, M.W., Prasad, A.M., 2004. How fast and far might tree species migrate in the eastern United States due to climate change? Global Ecology and Biogeography 13, 209–219.

Jackson, S.T., Betancourt, J.L., Booth, R.K., Gray, S.T., 2009. Ecology and the ratchet of events: Climate variability, niche dimensions, and species distributions. Proceedings of the National Academy of Sciences of the United States of America 106, 19685–19692.

Janzen, D.H., Martin, P.S., 1982. Neotropical anachronisms: the fruits the gomphotheres ate. Science 215, 19–27.

Jarvis, P.G., 1995. Scaling processes and problems. Plant, Cell & Environment 18, 1079–1089.

Jongejans, E., Skarpaas, O., Shea, K., 2008. Dispersal, demography and spatial population models for conservation and control management. Perspectives in Plant Ecology, Evolution and Systematics 9, 153–170.

Katul, G.G., Porporato, A., Nathan, R., Siqueira, M., Soons, M.B., Poggi, D., Horn, H.S., Levin, S.A., 2005. Mechanistic analytical models for long-distance seed dispersal by wind. American Naturalist 166, 368–381.

Kearney, M., Porter, W., 2009. Mechanistic niche modelling: combining physiological and spatial data to predict species' ranges. Ecology letters 12, 334–350.

Keel, B., 2007. Assisted Migration as a Conservation Strategy for Rapid Climate Change: Investigating Extended Photoperiod and Mycobiont Distributions for Habenaria repens Nuttall (Orchidaceae) as a Case Study. Ph.D. thesis. Antioch University New England.

Kelly, D., Hook, D., Sanders, R., 2009. Five Recommended Practices for Computational Scientists Who Write Software. Computing In Science & Engineering 11, 48–52.

Kelly, D., Sork, V.L., 2002. Mast seeding in perennial plants: why, how, where? Annual Review of Ecology and Systematics 33, 427–447.

Kevrekidis, I.G., Samaey, G., 2009. Equation-Free Multiscale Computation: Algorithms and Applications. Annual Review of Physical Chemistry 60, 321–344.

King, A.W., 1991. Translating models across scales in the landscape, in: Turner, M.G., Gardner, R.H. (Eds.), Quantitative Methods in Landscape Ecology. Springer. volume 82 of *Ecological Studies*, pp. 479–517.

Kissling, W.D., Dormann, C.F., Groeneveld, J., Hickler, T., Kühn, I., McInerny, G.J., Montoya, J.M., Römermann, C., Schiffers, K., Schurr, F.M., et al., 2012. Towards novel approaches to modelling biotic interactions in multispecies assemblages at large spatial extents. Journal of Biogeography 39, 2163–2178.

Kulakowski, D., Rixen, C., Bebi, P., 2006. Changes in forest structure and in the relative importance of climatic stress as a result of suppression of avalanche disturbances. Forest Ecology and Management 223, 66–74.

Laakso, J., Kaitala, V., Ranta, E., 2001. How does environmental variation translate into biological processes? Oikos 92, 119–122.

Ladeau, S.L., Clark, J.S., 2006. Elevated CO2 and tree fecundity: the role of tree size, interannual variability, and population heterogeneity. Global Change Biology 12, 822–833.

Leathwick, J., Austin, M., 2001. Competitive interactions between tree species in New Zealand's old-growth indigenous forests. Ecology 82, 2560–2573.

Leithead, M.D., Anand, M., Silva, L.C.R., 2010. Northward migrating trees establish in treefall gaps at the northern limit of the temperate-boreal ecotone, Ontario, Canada. Oecologia 164, 1095–1106.

Lischke, H., 2001. New developments in forest modeling: convergence between applied and theoretical approaches. Natural Resource modeling 14, 71–102.

Lischke, H., 2005. Modeling tree species migration in the Alps during the Holocene: What creates complexity? Ecological Complexity 2, 159–174.

Lischke, H., von Grafenstein, U., Ammann, B., 2012. Forest dynamics during the transition from the Oldest Dryas to the Bølling-Allerød at Gerzensee – a simulation study. Palaeogeography, Palaeoclimatology, Palaeoecology in press, –.

Lischke, H., Löffler, T.J., Fischlin, A., 1998. Aggregation of Individual Trees and Patches in Forest Succession Models: Capturing Variability with Height Structured, Random, Spatial Distributions. Theoretical Population Biology 54, 213–226.

Lischke, H., Löffler, T.J., Thornton, P.E., Zimmermann, N.E., 2007. Model Up-scaling in Landscape Research. A Changing World. Challenges for Landscape Research. Springer. chapter 16. pp. 249–272.

Lischke, H., Zimmermann, N.E., Bolliger, J., Rickebusch, S., Löffler, T.J., 2006. TreeMig: A forest-landscape model for simulating spatio-temporal patterns from stand to landscape scale. Ecological Modelling 199, 409–420.

Maggioni, M., Gruber, U., 2003. The influence of topographic parameters on avalanche release dimension and frequency. Cold Regions Science and Technology 37, 407–419.

Matías, L., Jump, A.S., 2012. Interactions between growth, demography and biotic interactions in determining species range limits in a warming world: The case of *Pinus sylvestris*. Forest Ecology and Management 282, 10–22.

Matsumoto, M., Nishimura, T., 1998. Mersenne twister: A 623-dimensionally equidistributed uniform pseudo-random number generator. ACM Transactions on Modeling and Computer Simulation 8, 3–30.

McInerny, G., Travis, J., Dytham, C., 2007. Range shifting on a fragmented landscape. Ecological Informatics 2, 1–8.

McLeod, T., MacDonald, G., 1997. Postglacial range expansion and population growth of *Picea mariana*, *Picea glauca* and *Pinus banksiana* in the western interior of Canada. Journal of Biogeography 24, 865–881.

Meier, E.S., Kienast, F., Pearman, P.B., Svenning, J.C., Thuiller, W., Araújo, M.B., Guisan, A., Zimmermann, N.E., 2010. Biotic and abiotic variables show little redundancy in explaining tree species distributions. Ecography 33, 1038–1048.

Meier, E.S., Lischke, H., Schmatz, D.R., Zimmermann, N.E., 2011. Climate, competition and connectivity affect future migration and ranges of European trees. Global Ecology and Biogeography 21, 164–178.

Melbourne, B.A., Cornell, H.V., Davies, K.F., Dugaw, C.J., Elmendorf, S., Freestone, A.L., Hall, R.J., Harrison, S., Hastings, A., Holland, M., et al., 2006. Invasion in a heterogeneous world: resistance, coexistence or hostile takeover? Ecology Letters 10, 77–94.

Mendoza, I., Zamora, R., Castro, J., 2009. A seeding experiment for testing tree-community recruitment under variable environments: Implications for forest regeneration and conservation in Mediterranean habitats. Biological Conservation 142, 1491–1499.

Millennium Ecosystem Assessment, 2005a. Ecosystems and Human Well-being: Current State and Trends. Chapter 21: Forest and Woodland Systems. (Island Press, Washington, DC).

Millennium Ecosystem Assessment, 2005b. Ecosystems and Human Well-Being: Synthesis. (Island Press, Washington, DC).

Miller, P.A., Giesecke, T., Hickler, T., Bradshaw, R.H.W., Smith, B., Seppä, H., Valdes, P.J., Sykes, M.T., 2008. Exploring climatic and biotic controls on Holocene vegetation change in Fennoscandia. Journal of Ecology 96, 247–259.

Moorcroft, P.R., Hurtt, G.C., Pacala, S.W., 2001. A Method for Scaling Vegetation Dynamics: The Ecosystem Demography Model (ED). Ecological Monographs 71, 557–586.

Nũnez, M.A., Horton, T.R., Simberloff, D., 2009. Lack of belowground mutualisms hinders Pinaceae invasions. Ecology 90, 2352–2359.

Nabel, J.E.M.S., manuscript. The dynamic two-layer classification concept: a dynamic upscaling method to reduce computational expenses in spatial simulations of vegetation dynamics.

Nabel, J.E.M.S., Kirchner, J.W., Zurbriggen, N., Kienast, F., Lischke, H., submitted. Extrapolation methods for climate time series revisited – spatial correlations in climatic fluctuations influence simulated tree species abundance and migration.

Nabel, J.E.M.S., Lischke, H., 2013. Upscaling of spatially explicit and linked time and space discrete models studying vegetation dynamics under climate change. In: B. Page, A.G. Fleischer, J. Göbel, V. Wohlgemuth (Eds.) (2013): Environmental Informatics and Renewable Energies - 27th International Conference on Informatics for Environmental Protection. Shaker Verlag, pp. 842-850, ISBN 978-3-8440-1676-5.

Nabel, J.E.M.S., Zurbriggen, N., Lischke, H., 2012. Impact of species parameter uncertainty in simulations of tree species migration with a spatially linked dynamic model. In: R. Seppelt, A.A. Voinov, S. Lange, D. Bankamp (Eds.) (2012): International Environmental Modelling and Software Society (iEMSs) 2012. Managing Resources of a Limited Planet: Pathways and Visions under Uncertainty, Sixth Biennial Meeting, Leipzig, Germany. p.909-916. ISBN: 978-88-9035-742-8, http://www.iemss.org/society/index.php/iemss-2012-proceedings.

Nabel, J.E.M.S., Zurbriggen, N., Lischke, H., 2013. Interannual climate variability and population density thresholds can have a substantial impact on simulated tree species' migration. Ecological Modelling 257, 88–100.

Nathan, R., 2008. An emerging movement ecology paradigm. Proceedings of the National Academy of Sciences of the United States of America 105, 19050–19051.

Nathan, R., Horvitz, N., He, Y., Kuparinen, A., Schurr, F.M., Katul, G.G., 2011. Spread of North American wind-dispersed trees in future environments. Ecology Letters 14, 211–219.

Neilson, R., Pitelka, L., Solomon, A., Nathan, R., Midgley, G., Fragoso, J., Lischke, H., Thompson, K., 2005. Forecasting Regional to Global Plant Migration in Response to Climate Change. BioScience 55, 749–759.

Normand, S., Ricklefs, R.E., Skov, F., Bladt, J., Tackenberg, O., Svenning, J.C., 2011. Postglacial migration supplements climate in determining plant species ranges in Europe. Proceedings of the Royal Society B: Biological Sciences 278, 3644–3653.

Notaro, M., 2008. Response of the mean global vegetation distribution to interannual climate variability. Climate Dynamics 30, 845–854. 10.1007/s00382-007-0329-7.

Okubo, A., Levin, S.A., 2001. Diffusion and ecological problems: modern perspectives. volume 14. Springer.

Osmond, C.B., Björkman, O., Anderson, D.J., et al., 1980. Physiological processes in plant ecology. Toward a synthesis with Atriplex. Springer Verlag.

Pearson, R.G., Dawson, T.P., 2003. Predicting the impacts of climate change on the distribution of species: are bioclimate envelope models useful? Global Ecology and Biogeography 12, 361–371.

Pérez-Ramos, I., Ourcival, J., Limousin, J., Rambal, S., 2010. Mast seeding under increasing drought: results from a long-term data set and from a rainfall exclusion experiment. Ecology 91, 3057–3068.

Picard, N., Franc, A., 2004. Approximating spatial interactions in a model of forest dynamics. Forest Biometry, Modelling and Information Sciences 1, 91–103.

Pitelka, L.F., Gardner, R.H., Ash, J., Berry, S., Gitay, H., Noble, I.R., Saunders, A., Bradshaw, R.H.W., Brubaker, L., Clark, J.S., Davis, M.B., Sugita, S., Dyer, J.M., Hengeveld, R., Hope, G., Huntley, B., King, G.A., Lavorel, S., Mack, R.N., Malanson, G.P., McGlone, M., Prentice, I.C., Rejmanek, M., 1997. Plant migration and climate change. American Scientist 85, 464–473.

Plesser, H., Nordlie, E., Gewaltig, M., 2009. Is computational biology a reliable science? Lecture, PSBio2009: Biological Explanation: Systems, Levels, and Causes, Oslo. http://arken.umb.no/~plesser/publications/Ples_PSBio2009.pdf. Latest access date: 20.12.2010.

Prasad, A.M., Gardiner, J.D., Iverson, L.R., Matthews, S.M., Peters, M., 2013. Exploring tree species colonization potentials using a spatially explicit simulation model: implications for four oaks under climate change. Global change biology 19, 2196–2208.

Prentice, I.C., Bondeau, A., Cramer, W., Harrison, S.P., Hickler, T., Lucht, W., Sitch, S., Smith, B., Sykes, M.T., 2007. Dynamic Global Vegetation Modeling: Quantifying Terrestrial Ecosystem Responses to Large-Scale Environmental Change. Terrestrial Ecosystems in a Changing World. Springer-Verlag, Berlin. chapter 15. pp. 175–192.

Ravenscroft, C., Scheller, R.M., Mladenoff, D.J., White, M.A., 2010. Forest restoration in a mixed-ownership landscape under climate change. Ecological Applications 20, 327–346.

Rew, R., Davis, G., 1990. NetCDF: an interface for scientific data access. Computer Graphics and Applications, IEEE 10, 76–82.

Rosenzweig, C., Casassa, G., Karoly, D., Imeson, A., Liu, C., Menzel, A., Rawlins, S., Root, T., Seguin, B., Tryjanowski, P., 2007. Assessment of observed changes and responses in natural and managed systems. In: Impacts, Adaptation and Vulnerability. Contribution of Working Group II to the Fourth Assessment Report of the Intergovernmental Panel on Climate Change, M.L. Parry, O.F. Canziani, J.P. Palutikof, P.J. van der Linden and C.E. Hanson, Eds., Cambridge University Press, Cambridge, UK, 79-131.

Sato, H., Ise, T., 2012. Effect of plant dynamic processes on African vegetation responses to climate change: Analysis using the spatially explicit individual-based dynamic global vegetation model (SEIB-DGVM). Journal of Geophysical Research-biogeosciences 117, G03017.

Sato, H., Itoh, A., Kohyama, T., 2007. SEIB–DGVM: A new Dynamic Global Vegetation Model using a spatially explicit individual-based approach. Ecological Modelling 200, 279–307.

Scheiter, S., Higgins, S., 2009. Impacts of climate change on the vegetation of Africa: an adaptive dynamic vegetation modelling approach. Global Change Biology 15, 2224–2246.

Scheller, R., Mladenoff, D., 2008. Simulated effects of climate change, fragmentation, and inter-specific competition on tree species migration in northern Wisconsin, USA. Clim Res 36, 191–202.

Scheller, R.M., Domingo, J.B., Sturtevant, B.R., Williams, J.S., Rudy, A., Gustafson, E.J., Mladenoff, D.J., 2007. Design, development, and application of LANDIS-II, a spatial landscape simulation model with flexible temporal and spatial resolution. Ecological Modelling 201, 409–419.

Scheller, R.M., Hua, D., Bolstad, P.V., Birdsey, R.A., Mladenoff, D.J., 2011. The effects of forest harvest intensity in combination with wind disturbance on carbon dynamics in Lake States Mesic Forests. Ecological Modelling 222, 144 – 153.

Scheller, R.M., Mladenoff, D.J., 2004. A forest growth and biomass module for a landscape simulation model, LANDIS: design, validation, and application. Ecological Modelling 180, 211–229.

Scheller, R.M., Mladenoff, D.J., 2005. A spatially interactive simulation of climate change, harvesting, wind, and tree species migration and projected changes to forest composition and biomass in northern Wisconsin, USA. Global Change Biology 11, 307–321.

Schneebeli, M., Meyer-Grass, M., 1992. Avalanche starting zones below the timber line–structure of forest, in: Proceedings International Snow Science Workshop. Breckenridge, Colorado, pp. 4–8.

Schumacher, S., Bugmann, H., 2006. The relative importance of climatic effects, wildfires and management for future forest landscape dynamics in the Swiss Alps. Global Change Biology 12, 1435–1450.

Schumacher, S., Bugmann, H., Mladenoff, D.J., 2004. Improving the formulation of tree growth and succession in a spatially explicit landscape model. Ecological Modelling 180, 175–194.

Schumacher, S., Reineking, B., Sibold, J., Bugmann, H., 2006. Modeling the impact of climate and vegetation on fire regimes in mountain landscapes. Landscape Ecology 21, 539–554.

Schurr, F.M., Steinitz, O., Nathan, R., 2008. Plant fecundity and seed dispersal in spatially heterogeneous environments: models, mechanisms and estimation. Journal of Ecology 96, 628–641.

Seidl, R., Baier, P., Rammer, W., Schopf, A., Lexer, M.J., 2007. Modelling tree mortality by bark beetle infestation in Norway spruce forests. Ecological modelling 206, 383–399.

Seward, J., Nethercote, N., 2005. Using Valgrind to Detect Undefined Value Errors with Bit-Precision, in: USENIX Annual Technical Conference, General Track, pp. 17–30.

Sitch, S., Huntingford, C., Gedney, N., Levy, P., Lomas, M., Piao, S., Betts, R., Ciais, P., Cox, P., Friedlingstein, P., et al., 2008. Evaluation of the terrestrial carbon cycle, future plant geography and climate-carbon cycle feedbacks using five Dynamic Global Vegetation Models (DGVMs). Global Change Biology 14, 2015–2039.

Skellam, J.G., 1951. Random Dispersal In Theoretical Populations. Biometrika 38, 196–218.

Smith, B., Prentice, I.C., Sykes, M.T., 2001. Representation of vegetation dynamics in the modelling of terrestrial ecosystems: comparing two contrasting approaches within European climate space. Global Ecology and Biogeography 10, 621–637.

Smith, T.T.M., Shugart, H.H., Woodward, F.I., 1997. Plant functional types: their relevance to ecosystem properties and global change. Cambridge University Press.

Snell, R.S., 2013. Simulating long-distance seed dispersal in a dynamic vegetation model. Global Ecology and Biogeography .

Snell, R.S., Huth, A., Nabel, J.E.M.S., Bocedi, G., Travis, J.M.J., Gravel, D., Bugmann, H., Gutiérrez, A.G., Hickler, T., Higgins, S.I., Scherstjanoi, M., Reineking, B., Zurbriggen, N., Lischke, H., accepted. Using individual based forest models to simulate species range shifts. Ecography .

Spanos, A., 1999. Probability theory and statistical inference: econometric modeling with observational data. Cambridge University Press.

Sturtevant, B.R., Miranda, B.R., Shinneman, D.J., Gustafson, E.J., Wolter, P.T., 2012. Comparing modern and presettlement forest dynamics of a subboreal wilderness: Does spruce budworm enhance fire risk? Ecological Applications 22, 1278–1296.

Svenning, J.C., Gravel, D., Holt, R.D., Schurr, F.M., Thuiller, W., Münkemüller, T., Schiffers, K.H., Dullinger, S., Edwards, T.C.J., Hickler, T., Higgins, S., Nabel, J.E., Pagel, J., Normand, S., accepted. The influence of interspecific interactions on species range expansion rates. Ecography .

Svenning, J.C., Sandel, B., 2013. Disequilibrium vegetation dynamics under future climate change. American Journal of Botany 100.

Svenning, J.C., Skov, F., 2004. Limited filling of the potential range in European tree species. Ecology Letters 7, 565–573.

Swiss National Forest Inventory, 2004/06. Stem numbers of observed tree species (woody species, 56 classes) in the different biogeographical regions of Switzerland according to the NFI3 grid. Accessed from http://www.lfi.ch/resultate/regionen-en.php, on 28.01.2012.

Tackenberg, O., Stöcklin, J., 2008. Wind dispersal of alpine plant species: A comparison with lowland species. Journal of Vegetation Science 19, 109–118.

Tang, Y., Guan, X., Fan, J., 2011. Design and implementation of seeds dispersion on graphic processor unit, in: Proceedings of the 10th International Conference on Virtual Reality Continuum and Its Applications in Industry, ACM. pp. 403–406.

Thomas, C.D., 2010. Climate, climate change and range boundaries. Diversity and Distributions 16, 488–495.

Thuiller, W., Albert, C., Araújo, M.B., Berry, P.M., Cabeza, M., Guisan, A., Hickler, T., Midgley, G.F., Paterson, J., Schurr, F.M., Sykes, M.T., Zimmermann, N.E., 2008. Predicting global change impacts on plant species' distributions: Future challenges. Perspectives in Plant Ecology, Evolution and Systematics 9, 137–152.

Urban, D.L., 2005. Modeling Ecological Processes Across Scales. Ecology 86, 1996–2006.

van de Koppel, J., Gupta, R., Vuik, C., 2011. Scaling-up spatially-explicit ecological models using graphics processors. Ecological Modelling 222, 3011–3019.

van der Knaap, W., van Leeuwen, J.F., Finsinger, W., Gobet, E., Pini, R., Schweizer, A., Valsecchi, V., Ammann, B., 2005. Migration and population expansion of *Abies*, *Fagus*, *Picea*, and *Quercus* since 15000 years in and across the Alps, based on pollen-percentage threshold values. Quaternary Science Reviews 24, 645–680.

Van Nes, E.H., Scheffer, M., 2005. A strategy to improve the contribution of complex simulation models to ecological theory. Ecological Modelling 185, 153–164.

Vorpahl, P., Dislich, C., Elsenbeer, H., Märker, M., Schröder, B., 2013. Biotic controls on shallow translational landslides. Earth Surface Processes and Landforms 38, 198–212.

Walther, G.R., Post, E., Convey, P., Menzel, A., Parmesan, C., Beebee, T.J.C., Fromentin, J.M., Hoegh-Guldberg, O., Bairlein, F., 2002. Ecological responses to recent climate change. Nature 416, 389–395.

Ward, B.C., Scheller, R.M., Mladenoff, D.J., 2004. Technical report: LANDIS-II double exponential seed dispersal algorithm. Univ. of Wisconsin-Madison, WI, http://www.landis-ii.org/documentation/DoubleExpSeed.pdf.

Weidendorfer, J., 2008. Sequential performance analysis with callgrind and kcachegrind, in: Tools for High Performance Computing. Springer, pp. 93–113.

Weinan, E., Engquist, B., 2003. Multiscale modeling and computation. Notices of the AMS 50, 1062–1070.

Wichmann, M.C., Alexander, M.J., Soons, M.B., Galsworthy, S., Dunne, L., Gould, R., Fairfax, C., Niggemann, M., Hails, R.S., Bullock, J.M., 2009. Human-mediated dispersal of seeds over long distances. Proceedings of the Royal Society B: Biological Sciences 276, 523–532.

Wildi, O., Ewald, K., 1986. Der Naturraum und dessen Nutzung im alpinen Tourismusgebiet von Davos. Ergebnisse des MAB-Projektes Davos. Technical Report. Birmensdorf.

Williams, J.W., Jackson, S.T., 2007. Novel climates, no-analog communities, and ecological surprises. Frontiers in Ecology and the Environment 5, 475–482.

Wilson, G., Aruliah, D., Brown, C.T., Hong, N.P.C., Davis, M., Guy, R.T., Haddock, S.H., Huff, K., Mitchell, I., Plumbley, M., Waugh, B., White, E.P., Wilson, P., 2012. Best practices for scientific computing. CoRR abs/1210.0530.

With, K.A., 2002. The Landscape Ecology of Invasive Spread. Conservation Biology 16, 1192–1203.

Wright, S.J., Trakhtenbrot, A., Bohrer, G., Detto, M., Katul, G.G., Horvitz, N., Muller-Landau, H.C., Jones, F.A., Nathan, R., 2008. Understanding strategies for seed dispersal by wind under contrasting atmospheric conditions. Proceedings of the National Academy of Sciences of the United States of America 105, 19084–19089.

Zhu, K., Woodall, C.W., Clark, J.S., 2011. Failure to migrate: lack of tree range expansion in response to climate change. Glob Change Biol 18, 1042–1052.

Zimmermann, N.E., Yoccoz, N.G., Edwards, T.C., Meier, E.S., Thuiller, W., Guisan, A., Schmatz, D.R., Pearman, P.B., 2009. Climatic extremes improve predictions of spatial patterns of tree species. Proceedings of the National Academy of Sciences 106, 19723–19728.

Zumbusch, G., 2003. Parallel Multilevel Methods. Adaptive Mesh Refinement and Loadbalancing. Teubner.

Zurbriggen, N., 2013. Avalanche disturbance and regeneration in mountain forests under climate change: experimental and modeling approaches. Ph.D. thesis. Swiss Federal Institute of Technology Zurich.

Zurbriggen, N., Nabel, J.E.M.S., Teich, M., Bebi, P., Lischke, H., in press. Explicit avalanche-forest feedback simulations improve the performance of a coupled avalanche-forest model. Ecological Complexity .

Zurbriggen, N., Teich, M., Nabel, J.E.M.S., Bebi, P., Lischke, H., manuscript. Performance of alternative disturbance formulations in a spatially explicit avalanche-forest model. To this date published in Zurbriggen (2013), Ph.D. Thesis.

Chapter 2

Impact of species parameter uncertainty in simulations of tree species migration with a spatially linked dynamic model

Published in Proceedings of the sixth biannual meeting of the International Environmental Modelling and Software Society, Leipzig, Germany, 2012; available at http://www.iemss.org/sites/iemss2012/proceedings.html

Julia E. M. S. Nabel[a], *Natalie Zurbriggen*[a,b], *Heike Lischke*[a]

[a]*Landscape Dynamics, Swiss Federal Institute for Forest, Snow and Landscape Research WSL, Zürcherstrasse 111, 8903 Birmensdorf, Switzerland*
[b]*Forest Ecology, Institute of Terrestrial Ecosystems, Swiss Federal Institute of Technology ETH, Universitätstr. 22, 8092 Zurich, Switzerland*

Abstract

The simulation of tree species migration suffers from many sources of uncertainty. In our study we examined the influence of species parameter uncertainty on simulated tree species migration, using the spatially linked dynamic forest landscape model TreeMig. The impact of uncertainty becomes especially apparent under critical situations arising from the interaction of species limitations, competition and spatial fragmentation. Therefore we examined the differences in migration success and speed in a realistic scenario including these critical conditions. The south-north migration of the submediterranean tree species *Ostrya carpinifolia* through the highly fragmented and climatically heterogeneous landscape of the Swiss Alps was simulated for 27 different species parameter sets covering the plausible range of species parameters for *O. carpinifolia*. To account for the additional uncertainty introduced by the stochastic representation of future climate variability, each species parameter set was simulated with multiple repetitions. We found that migration success and speed resulting from simulations with the different sets varied highly. The current situation of rapid climate change and high landscape fragmentation due to human land use could create critical conditions comparable to the simulated scenario for various species. We therefore recommend testing for species parameter sensitivities and – if indicated – to repeat simulations with different parameter sets when projecting future tree species distributions with explicit simulation of migration.

2.1 Introduction

The capabilities of plants to track climate changes are crucially influencing future plant species distributions. In particular the migration of tree species can lag behind rapid climate changes, because of their long generation times (FAO, 2010). Despite the acknowledged importance of migration, many modelling studies projecting future plant distribution do not explicitly model migration (Thuiller et al., 2008). One reason is the requirement for sufficiently accurate spatial and temporal representations of several processes and interactions involved,

for example, maturation, seed dispersal and establishment in competitive situations driven by environmental influences. In contrast to other model types, spatially linked dynamic models can fulfil this requirement, if they make a successful trade-off between accuracy and computational efficiency (time and memory). One such model is TreeMig (Lischke et al., 2006), the model used for the present study. TreeMig approaches the trade-off between accuracy and computational efficiency by employing a distribution-based representation of the local spatial forest heterogeneity and by applying empirically derived formulations of important processes and species parameters characterising species traits. Empirically derived species parameters, however, are associated with uncertainties. Bugmann (1994) has shown that such uncertainties have small influences on the overall species composition, but can impact single species abundances in simulations with the forest gap model ForClim, the predecessor model of TreeMig. The influence of species parameter uncertainties on tree species migration simulated with TreeMig has not been examined so far and is considered in the present study. Additional sources of uncertainty include assumptions about model drivers, such as climatic influences, which are particularly important for tree species migration because of the long time-spans involved. One approach generating climatic influences, for time-spans exceeding measured data or predictions of climate models, is the sampling from distributions based on available data, as proposed in Bugmann (2001) and applied in TreeMig (Lischke et al., 2006). The present study explored potential influences of species parameter uncertainty on tree species migration, taking into account this stochastic sampling from distributions. The impact of uncertainties presumably becomes most obvious where a species is not abundant, hence in critical situations, which for example can arise from the interaction of species limitations, presence of competitors and spatial fragmentation. Therefore we examined the differences in migration success and speed among different species parameter sets within the plausible parameter range of an example species under realistic and critical conditions. The simulation scenario was a south-north migration of the submediterranean tree species *Ostrya carpinifolia* in a transect through the Swiss Alps, a highly fragmented and climatically heterogeneous landscape.

2.2 Methods

2.2.1 Model

The applied TreeMig version is described in Lischke et al. (2006) with amendments described in Rickebusch et al. (2007). TreeMig is a grid-based, spatially linked dynamic forest landscape model with a spatial resolution of 1km^2 and yearly time steps. It is designed for use at regional to subcontinental extent. The local dynamics are calculated on height-structured distributions which can be regarded as aggregations of single patches with individual trees (Lischke et al., 1998). This aggregation covers the small scale stochasticity representing local processes in gap models, such as establishment and mortality. It was introduced to replace multiple single patch repetitions with a deterministic representation and thereby to counterbalance the increase in computational complexity accompanying the spatial linkage and the increased spatial extent compared to single site simulations in forest gap models. However, the model still has a high computational complexity and the approximate computation time for each 1km^2 cell and each year amounts to 0.001 seconds on a 2.8GHz CPU of an AMD Opteron cluster.

The driving variables of the model are three bioclimate variables per year and cell: degree-day sum (sum of daily mean temperatures above 5.5 °C), minimum winter temperature (average temperature of the coldest winter month) and an index describing the severity of drought events. These variables can be derived from monthly mean temperatures, monthly precipitation sums and constant site data (slope, aspect and water storage capacity) with the model ForClim-E (Bugmann and Cramer, 1998). In addition to the bioclimate variables, a zero-one mask is required, which indicates for each cell if it is stockable, i.e. if something can grow in this cell. Cells with a stockability of zero can, for example, represent big water bodies, solid rock surfaces or different kinds of human land use. The mask is constant over time and is the main representation of fragmentation.

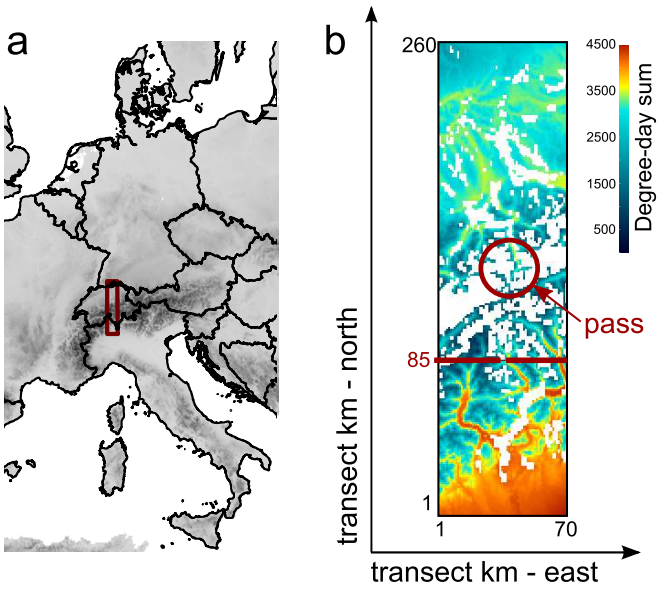

Figure 2.1 : The 260km x 70km simulation transect (1km^2 cells). Panel a shows the location in central Europe. In panel b the mean degree-day sum (sum of daily mean temperatures above 5.5 °C) of the distributions used for bioclimatic influences after 2100 is depicted. White areas represent non-stockable cells, i.e. cells where trees can not grow. The circle marks the pass through the Swiss Alps and the dashed line at km 85 the starting point for the migration of *Ostrya carpinifolia* in the year 1800.

2.2.2 Simulation setup

The simulated scenario was a south-north migration of the submediterranean tree species *Ostrya carpinifolia* in a 260km x 70km transect (see Fig. 2.1). Most of the cells in the area of the Swiss Alps, in the centre of the transect, are bare rock surfaces, regarded as not stockable for trees in TreeMig. Therefore the only possibility to cross the Swiss Alps in the simulations is through one pass with several bottlenecks (see Fig. 2.1, panel b). *O. carpinifolia* is currently limited to the southern side of the Swiss Alps, according to the Swiss National Forest Inventory (NFI) (2004/06) and to the European Forest Data Center (2000). In addition to *O. carpinifolia*, 21 other species (*Abies alba, Larix decidua, Picea abies, Pinus cembra, P. sylvestris, Taxus baccata, Acer platanoides, A. pseudoplatanus, Alnus incana, Betula pendula, Carpinus betulus, Castanea sativa, Fagus sylvatica, Fraxinus excelsior, Populus tremula, Quercus petraea, Q. pubescens, Sorbus aucuparia, Tilia cordata, T. platyphyllos, Ulmus scabra*) were included as competitors in the simulations. All species besides *Quercus pubescens*, which was added because of its importance at dry sites, are in the list of the 30 species identified as most abundant in Switzerland in the first Swiss NFI (Brändli, 1998).
The TreeMig simulations were computed for 1600 years (1400-3000). The bioclimate variables were derived from past climate (1901-2000 – CRU data (Mitchell et al., 2003)) and from SRESA1B (Nakicenovic, N. et al., 2000) projections calculated with the regional climate model CLM (2001-2100 – (Lautenschlager et al., 2009). Both data sets were first downscaled to 30" using WorldClim data (Hijmans et al., 2005) and then projected with FIMEX-0.28 (Klein, 2012) to an Albers equal area projection of 1km^2 resolution.
The first 400 years (1400-1800) of the simulation were used as an initial spin-up phase with a general availability of propagules instead of simulating seed production and dispersal (cf. Lischke et al., 2006). In congruence with its approximate current distribution, *O. carpinifolia* was restricted to the lower 85km of the transect (Fig. 2.1, panel b) until the end of the spin-up phase. The bioclimate was stochastically drawn from distributions based on the years 1901-1931. After the 400 spin-up years, seed production and dispersal were enabled and the restriction of *O. carpinifolia* was removed. The bioclimate was drawn for another 100 years (1801-1900) from the 1901-1931 distributions. The subsequent 200 years represent the near past and the future up to 2100 for which yearly bioclimate values were available. After 2100 the bioclimate was stochastically drawn for another 900 years (2101-3000) from distributions based on the years 2071-2100.

Table 2.1 : Listed are original, most optimistic and most pessimistic values – for max. height, max. age, min. height required for maturity, max. number of seeds, indices for sapling and adult shade tolerance, max. height growth rate, low nitrogen tolerance index and browsing susceptibility index – according to the parameter plausibility ranges found in [1] Bugmann (1994) or to the values found in the other references: [2] Noack (1979), [3] Korkut and Guller (2008), [4] Hecker (1998) and [5] Franz (2002). The parameters marked with H* were estimated according to the uncertainty for species height (43.75 %).

	Species parameters influencing fertility and competitiveness								
parameter	Max. h. [m]	Max. age [a]	Min. maturity h. [m]	Max. seeds	Sapl. shade tol.	Adult shade tol.	Max. growth [cm/a]	N tol. index	Browse sus. index
original	16	150	3.4	91259	5	3	134	2	3
optimistic	23	200	1.94	131185	3	1	161	1	2
pessimistic	9	100	4.9	51333	7	5	107	3	3
uncertainty	± 7	± 50	± 1.5	± 39926	± 2	± 2	± 30 %	± 1	± 1
reference	[2,3]	[4,5]	H*	H*	[1]	[1]	[1]	[1]	[1]

Table 2.2 : Listed are original, most optimistic and most pessimistic values – for min. degree-day sum (sum of daily mean temperatures above 5.5 °C), min. wintertemp. (mean temperature of the coldest winter month) and an index describing the drought tolerance – according to the parameter plausibility ranges found in Bugmann (1994).

	Species parameters influencing the sensitivity to bioclimate		
parameter	Min. Degree-day sum	Min. wintertemp. [°C]	Drought index
original	1200	-10	0.33
optimistic	960	-12	0.43
pessimistic	1440	-8	0.23
uncertainty	± 20 %	± 2 °C	± 0.1

2.2.3 Species parameters and species parameter plausibility ranges

The original parameter values for *Ostrya carpinifolia*, as well as the uncertainty in these parameters, are listed in Table 2.1 (parameters influencing fertility and competitiveness of *O. carpinifolia*) and Table 2.2 (parameters influencing the sensitivity to bioclimate). Most of the original values were taken from the Mediterranean mountain forest gap model GREFOS (Fyllas and Troumbis, 2009), which was possible, because GREFOS and TreeMig are both descendants of the forest gap model ForClim (Bugmann, 1994; Bugmann and Cramer, 1998) and therefore share important similarities in the calculations of local dynamics. Two parameters had to be transformed according to known relationships with regard to differences between ForClim and TreeMig (indices for sapling and adult shade tolerance). Another two parameters were scaled according to empirical relationships observed in other TreeMig species (max. number of seeds; max. growth rate). The remaining unknown parameter values (min. maturity height; low nitrogen tolerance index; browsing susceptibility index) and the probability kernel used for seed dispersal in TreeMig (see (Lischke et al., 2006) for more details) were taken from *Carpinus betulus*, which was already parametrised in TreeMig and – like *O. carpinifolia* – belongs to the *Coryloideae* subfamily.

2.2.4 Simulations

The number of possible simulations was constrained due to the computational complexity of TreeMig. One single run of the simulation setup (1600 years and 260 x 70 cells) took approximately 21'840 seconds, i.e. around 6 hours, of computation time on a 2.8GHz CPU of an AMD Opteron cluster. Moreover, it was necessary to make multiple runs with different pseudo-random number (prn) streams, to account for the stochastic representation of future climatic influences. Each of the different species parameter sets was thus simulated 20 times with varying prn streams.

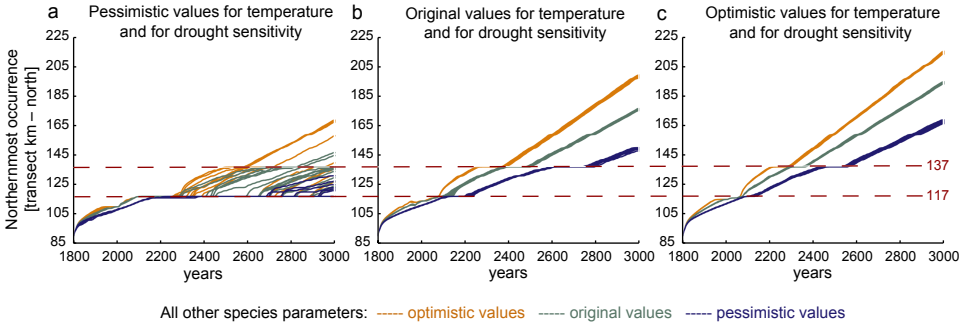

Figure 2.2 : Northernmost occurrence (transect km - north – smoothed over 20 year periods) for the years 1800-3000, starting at km 85, to which *Ostrya carpinifolia* was restricted until 1800. Depicted are the results of simulations with different species parameter sets used for *O. carpinifolia*. The panels show the results for three out of nine combinations of parameter values for temperature and drought sensitivities: both pessimistic (panel a), both original (panel b) and both optimistic (panel c). The different colours represent scenarios of parameter values for all other parameters (see Table 2.1). In each panel, series of lines with the same colour depict the results of 20 repetitions with the according parameter set. The dashed horizontal lines mark the two main stagnation points at km 117 and km 137.

Since *O. carpinifolia* is known to be limited to warm temperatures and is suspected of being able to grow under conditions which are too dry for *Fagus sylvatica* (e.g. (Brändli, 1998; Noack, 1979)), the uncertainties in the bioclimate sensitivities listed in Table 2.2 are of special interest and were therefore in the focus when selecting species parameters for the simulations. However, the min. winter temperature sensitivity is only used as a threshold in TreeMig to determine if establishment is possible at all. Therefore, it was possible to exclude its uncertainties based on the fact that the most pessimistic value for *O. carpinifolia* (-8 °C) was already significantly lower than the mean min. winter temperature (-4 °C± -2 °C) found in the distributions used to draw future bioclimatic influences.
We simulated 27 species parameter sets, resulting from all combinations of the most optimistic, the original and the most pessimistic parameters for (1) the minimum required degree-day sum, (2) the drought tolerance index and (3) all other parameters (Table 2.1).

2.3 Results

Table 2.3 shows the results for several measures calculated from the 20 repetitions for each of the 27 simulated species parameter sets. Migration success – defined as successfully crossing the two main stagnation points[1] at km 117 and km 137 (see Fig. 2.2 dashed lines for a visualisation) – thereby depended most on the temperature sensitivity. A complete inhibition of migration within the simulated timespan only occurred for the three most pessimistic parameter sets, with either all parameters at the pessimistic end of the plausibility range, or with drought or temperature having its original value (for the most pessimistic runs see Fig. 2.2, panel a). The variability between the 20 repetitions – measured as the standard deviation of the year in which the first stagnation point at km 117 was passed – is very low for all scenarios, except for the ones with pessimistic values for the temperature sensitivity. In contrast to the differing influences on migration success, all parameter changes for temperature and drought sensitivity, as well as for the group of all other parameters comparably affected migration speed of the furthest run. Parameter changes from optimistic to original or from original to pessimistic values led to a slowdown of 3 – 22 m/a (see Table 2.3 '(3) avg. speed of the furthest run' and Fig. 2.2).

[1]Since the Alps lie diagonally in the transect (see Fig. 2.1), the two stagnation points are not the actual bottlenecks of the pass but the furthest reachable dead ends east of the bottlenecks.

Table 2.3 : Measures calculated from the 20 repetitions of each of the 27 simulated species parameter sets. The symbols in the first two columns denote the parameter values used for the temperature sensitivity (T) and the drought sensitivity (D), respectively, where '+' denotes optimistic, 'o' original and '-' pessimistic values. The main columns show the measures: (1) mean year in which the first stagnation point at km 117 (for a visualisation see Fig. 2.2) was passed in the 20 runs, together with the standard deviation (in years) and, if not all runs passed km 117, the number of runs which did so; (2) the number of runs which passed the second stagnation point at km 137 and (3) the average speed found for the run with the furthest migration distance. All three main columns are subdivided, with one sub-column for each scenario for all other parameters (see Table 2.1). The symbols have the same denotation as for temperature and drought sensitivity.

		(1) mean year passed km 117 ± std (#of runs if not all passed)			(2) # passed km 137			(3) avg. speed furthest run [m/a]		
		other paras.			other paras.			other paras.		
T	D	+	o	-	+	o	-	+	o	-
+	+	2072±0	2083±9	2123±9	20	20	20	109	90	68
+	o	2072±0	2083±12	2134±12	20	20	20	101	83	61
+	-	2072±0	2085±15	2165±15	20	20	20	90	73	51
o	+	2089±0	2120±10	2201±10	20	20	20	101	83	61
o	o	2089±0	2124±9	2234±9	20	20	20	94	76	54
o	-	2089±0	2147±19	2348±19	20	20	0	82	62	–
-	+	2442±237(19)	2522±262(17)	2621±235(11)	8	5	2	83	61	49
-	o	2443±237(19)	2604±219(17)	2720±208(12)	8	3	0	78	58	–
-	-	2528±250(19)	2627±205(17)	2806±107(6)	6	2	0	61	51	–

2.4 Discussion

Migration speeds resulting from simulations with different parameter sets (50 – 110 m/a) were in the expected ranges (Svenning and Skov, 2007). However, we found that species migration can be highly sensitive to species parametrisation, which is in agreement with the findings of Bugmann (1994) for single species abundances. Migration outside of the pass situation was not influenced to the same degree (see Fig. 2.2) as inside the pass, despite the similar temperature influence on the cells in the near neighbourhood of the pass (see Fig. 2.1, panel b). This simulation result indicates that the high fragmentation and the 'pass situation' are the main triggers for changes in the migration success. In the bottleneck situation of the pass, the temperature sensitivity appeared to be particularly important for the migration success, which agrees with the fact that temperature is the limiting factor for submediterranean species in the Swiss Alps. Although the selected scenario is a specific critical situation, the current global conditions of rapid climate change and high fragmentation of the landscape due to human land use could create comparably critical situations for various other species.
The variance in the results for repetitions of the same scenario indicates that the stochasticity in the climate driver can have an important impact. This impact might even be higher if spatial autocorrelation in the climatic influences was taken into account which is not the case in the current approach, where sampling from independent distributions is applied for each cell. This will be subject of future studies.

2.5 Conclusions and Recommendations

The present study illustrates the necessity of sensitivity and uncertainty analyses in spatially linked dynamic modelling of tree species migration. The results emphasise that simulations with different parameter sets and multiple repetitions can be essential in estimating migration speed and migration success when simulating single species migration. The study also underlines the key role of the trade-off between computational efficiency and model specificity, and shows the need for further investigations into reducing computational costs in order to facilitate comprehensive simulation studies.

Acknowledgements

We like to thank Thomas Wüst for the support with the cluster, Dirk Schmatz for assistance with the data preparation and Heiko Klein from the IT Department of the Norwegian Meteorological Institute for the help in applying FIMEX. We further thank James Kirchner for his comments on the use of the English language. JN was supported by the Swiss National Science Foundation Grant 315230-122434, NZ was supported by the research project MOUNTLAND funded by the Competence Center Environment and Sustainability of the ETH Domain (CCES).

References

Brändli, U.B., 1998. Die häufigsten Waldbäume der Schweiz. Ergebnisse aus dem Landesforstinventar 1983-85: Verbreitung, Standort und Häufigkeit von 30 Baumarten. Berichte der Eidgenöss. Forschungsanstalt für Wald, Schnee und Landschaft.

Bugmann, H., 1994. On the Ecology of Mountainous Forests in a Changing Climate: A Simulation Study. Ph.D. thesis. Swiss Federal Institute of Technology Zurich.

Bugmann, H., 2001. A Review of Forest Gap Models. Climatic Change 51, 259–305.

Bugmann, H., Cramer, W., 1998. Improving the behaviour of forest gap models along drought gradients. Forest Ecology and Management 103, 247–263.

European Forest Data Center, 2000. Distribution of *Ostrya Carpinifolia*. Accessed from http://efdac.jrc.ec.europa.eu/index.php/climate, on 28.01.2012.

FAO, 2010. Global forest resources assessment 2010. Food and Agriculture Organization of the United Nations (FAO), Rome, http://www.fao.org/docrep/013/i1757e/i1757e.pdf. Latest access date: 20.12.11.

Franz, W.R., 2002. Die Hopfenbuche (Ostrya carpinifolia Scop.) in Österreich und Nordslowenien. Carinthia II. Naturwissenschaftliche Beiträge zur Heimatkunde Kärntens, Klagenfurt, 58. Sonderheft: 256 S.

Fyllas, N.M., Troumbis, A.Y., 2009. Simulating vegetation shifts in north-eastern Mediterranean mountain forests under climatic change scenarios. Global Ecology and Biogeography 18, 64–77.

Hecker, U., 1998. Handbuch Bäume und Sträucher. Einbändige Neuausgabe der BLV Intensivführer Laubgehölze und Nadelgehölze - 2., durchges. Aufl. - München; Wien; Zürich: BLV, ISBN 3-405-14738-7.

Hijmans, R.J., Cameron, S.E., Parra, J.L., Jones, P.G., Jarvis, A., 2005. Very high resolution interpolated climate surfaces for global land areas. International Journal of Climatology 25, 1965–1978.

Klein, H., 2012. FIMEX-0.28. https://wiki.met.no/fimex/start. Last access date: 09.01.12.

Korkut, S., Guller, B., 2008. Physical and mechanical properties of European Hophornbeam (Ostrya carpinifolia Scop.) wood. Bioresource Technology 99, 4780–4785.

Lautenschlager, M., Keuler, K., Wunram, C., Keup-Thiel, E., Schubert, M., Will, A., Rockel, B., Boehm, U., 2009. Climate Simulation with CLM, Scenario A1B run no.1, Data Stream 3: European region MPI-M/MaD. World Data Center for Climate. http://dx.doi.org/10.1594/WDCC/CLM_A1B_1_D3.

Lischke, H., Löffler, T.J., Fischlin, A., 1998. Aggregation of Individual Trees and Patches in Forest Succession Models: Capturing Variability with Height Structured, Random, Spatial Distributions. Theoretical Population Biology 54, 213–226.

Lischke, H., Zimmermann, N.E., Bolliger, J., Rickebusch, S., Löffler, T.J., 2006. TreeMig: A forest-landscape model for simulating spatio-temporal patterns from stand to landscape scale. Ecological Modelling 199, 409–420.

Mitchell, T., Carter, T., Jones, P., , Hulme, M., New, M., 2003. A comprehensive set of climate scenarios for Europe and the globe. Tyndall centre Working paper 55.

Nakicenovic, N. et al., 2000. IPCC Special Report on Emissions Scenarios. Cambridge University Press.

Noack, H., 1979. Das Portrait. Ostrya carpinifolia Scop. (Hopfenbuche). Mitteilungen der Deutschen Dendrologischen Gesellschaft, Nr 71, 257-259.

Rickebusch, S., Lischke, H., Bugmann, H., Guisan, A., Zimmermann, N.E., 2007. Understanding the low-temperature limitations to forest growth through calibration of a forest dynamics model with tree-ring data. For. Ecol. Manage. 246, 251–263.

Svenning, J.C., Skov, F., 2007. Could the tree diversity pattern in Europe be generated by postglacial dispersal limitation? Ecology Letters 10, 453–460.

Swiss National Forest Inventory (NFI), 2004/06. Occurrence of *Ostrya Carpinifolia* in the different biogeographical regions of Switzerland according to the NFI3 grid. Accessed from http://www.lfi.ch/resultate/regionen-en.php, on 28.01.2012.

Thuiller, W., Albert, C., Araújo, M.B., Berry, P.M., Cabeza, M., Guisan, A., Hickler, T., Midgley, G.F., Paterson, J., Schurr, F.M., Sykes, M.T., Zimmermann, N.E., 2008. Predicting global change impacts on plant species' distributions: Future challenges. Perspectives in Plant Ecology, Evolution and Systematics 9, 137–152.

Chapter 3

Interannual climate variability and population density thresholds can have a substantial impact on simulated tree species' migration

Published in Ecological Modelling Volume 257, 2013, Pages 88–100

Julia E. M. S. Nabel[a,b], *Natalie Zurbriggen*[a,c], *Heike Lischke*[a]

[a] *Landscape Dynamics, Swiss Federal Institute for Forest, Snow and Landscape Research WSL, Zürcherstrasse 111, 8903 Birmensdorf, Switzerland*
[b] *Department of Environmental Systems Science, Swiss Federal Institute of Technology ETH, 8092 Zurich, Switzerland*
[c] *Forest Ecology, Institute of Terrestrial Ecosystems, Swiss Federal Institute of Technology ETH, Universitätstr. 22, 8092 Zurich, Switzerland*

Abstract

Assessments of future tree species' distributions should account for time lags in the adaptation of their external range limits to climatic changes. In simulation experiments it is therefore necessary to capture processes that influence such time lags, in particular tree species' migration. We hypothesise that directional processes such as migration are sensitive to the exact sequence of simulated climate influences, and that the uncertainty associated with a given interannual climate variability has to be accounted for when simulating migration explicitly. In this paper we used the intermediate-complexity multi-species model TreeMig to examine whether different realisations of future climate influences with the same temporal mean and the same interannual variability cause fundamental differences in simulated migration. We assume that the impact of interannual climate variability becomes most apparent in situations which critically influence regeneration and survival. Such situations arise, for example, when species' sensitivities to climate, competition and spatial fragmentation interact. We therefore developed an illustrative and realistic simulation setup representing this situation. We simulated the northwards migration of the submediterranean tree species *Ostrya carpinifolia* Scop. (European Hop Hornbeam) through the highly fragmented and climatically heterogeneous landscape of the Swiss Alps.

Situations critically influencing regeneration and survival can lead to low species' abundances. Before investigating effects of interannual climate variability, we therefore tested whether the continuous representation of species' cell populations in TreeMig, which allows for infinitesimal population densities, can have side effects on simulated migration. Specifically, we tested for effects of minimum density thresholds, i.e. thresholds below which a species is treated as absent. We found that small thresholds in the magnitude of one individual per km^2 cell have a considerable impact on simulated migration, and can even impede migration in situations critical for regeneration and survival.

To test for effects of interannual climate variability, we compared simulation results from multiple repetitions driven by different annual climate time series generated stochastically from the same probability distribution. Results from these repetitions were additionally compared to results from simulations driven by cyclically repeated climate and steadily applied mean climate, respectively. These comparisons were conducted for different species parameter sets within the plausible parameter range of *O. carpinifolia* to account for potential interactions between species' sensitivities and the environment. Simulated tree species' migration was highly dependent on the species parameters applied and markedly influenced by interannual climate variability. Notable divergence in species' spread resulted amongst multiple realisations of annual climate time series stochastically sampled from the same probability distribution. We conclude that uncertainty associated with interannual climate variability has to be accounted for. Single realisations can be insufficient and mean value simulations as well as averages of output results can be too simplistic to reflect possible outcomes of tree species' migration.

Glossary

External range limits Outermost geographical limits (latitudinal/longitudinal) to species' occurrences (cf. Gaston, 2003)
Internal range limits Limits to species' occurrences (e.g. altitudinal and habitat limits) within the external range (cf. Gaston, 2003)
Colonisation Establishment, growth to reproductive maturity and production of viable seeds
Migration Colonisation of locations outside of the external range limits (Keel, 2007), and thus (at least temporarily) shifting them
Species' spread Change in the species' internal or external range limits due to local colonisation/extinction dynamics or migration

3.1 Introduction

Future species' distributions are crucially influenced by their capabilities to adapt their external range limits to climatic changes, which therefore also influences future vegetation composition (Fischlin et al., 2007; Midgley et al., 2007; Sato and Ise, 2012). Species with limited dispersal distances and long generation times, such as many tree species, can lag behind rapid climatic changes, particularly in fragmented landscapes (Pitelka et al., 1997; Collingham and Huntley, 2000; Rosenzweig et al., 2007; Hof et al., 2011). Such time lags can lead to remnant trees in areas where changed environmental conditions prevent new establishment and can be accompanied by a lack of propagules in climatically inhabitable areas (Davis, 1989; Svenning and Skov, 2004; Zhu et al., 2011; Matías and Jump, 2012). To adequately project the availability of propagules, and to overcome the simplistic but common assumption that propagules are available everywhere, migration (sensu Keel, 2007 – see glossary) needs to be simulated explicitly (Neilson et al., 2005; Morin and Thuiller, 2009; Huntley et al., 2010). Many modelling studies which project future tree species' distributions do not simulate migration explicitly (Thuiller et al., 2008). One key problem is the requirement to represent the processes involved, i.e. seed dispersal, establishment, growth to reproductive maturity and production of viable seeds (Neilson et al., 2005; Keel, 2007), in a sufficiently accurate spatial and temporal resolution under consideration of competition and environmental influences. Several of these processes can only be represented in dynamic, spatially linked models and computational costs and data constraints currently presuppose intermediate complexity (Lischke et al., 2006; Pearson, 2006; Thuiller et al., 2008; Huntley et al., 2010).

When simulating migration, different uncertainties have to be taken into account (e.g. Higgins et al., 2003 and for a general framework of uncertainties in models Refsgaard et al., 2007). Uncertainties in model drivers, in particular climate influences, are a key difficulty. Shifts of species' external range limits operate on long time spans over centuries or millennia. At the same time, available climate records often only cover the recent past, and climate projections are mostly only calculated for scenarios described up to the end of this century (Hickler et al., 2012). In order to study trends in simulated species' range shifts, the climate is therefore often extrapolated to generate input for longer time spans, with approaches differing amongst simulation studies. The most simplistic approaches to extrapolate climate time series are to steadily apply mean values, or to adapt observed climatic conditions with projected mean climatic changes. However, not only temperature and precipitation means, but also their variances are changing, which has been observed at the continental (Schär et al., 2004)

and at the global scale (Frich et al., 2002; Trenberth et al., 2007). Several simulation studies with different model types have discussed effects of changes in interannual climate variability on simulated forest compositions, tree species' distributions and range limits (Bugmann and Pfister, 2000; Morin and Chuine, 2005; Miller et al., 2008; Giesecke et al., 2010). Generally, climate variability was found to strongly influence natural systems (Brubaker, 1986; Easterling et al., 2000; Camarero and Gutiérrez, 2004). Changes in geographical ranges can, for example, result from favourable periods enabling recruitment pulses or unfavourable periods causing extirpation (Jackson et al., 2009). The need to include interannual variability has already been demonstrated for statistical projections of current species' distributions and range limits (Zimmermann et al., 2009) and for projections of mean global vegetation distributions with a dynamic global vegetation model (Notaro, 2008).

Interannual climate variability can be incorporated in extrapolations by, for example, cyclically repeating a certain base period as done by Hickler et al. (2012) for the model LPJ-Guess and by Sato and Ise (2012) for the SEIB-DGVM. Another possibility is to stochastically sample annual climate influences from a distribution obtained from a base period of a climate change scenario as done in Lischke et al. (2006) and Epstein et al. (2007) for the model TreeMig. The listed simulation studies all applied single realisations of a multitude of possible climate time series with the same temporal mean and variability. The restriction to a single realisation can be motivated by computational costs, where single runs already require extensive computational resources. Applying single realisations may be justifiable when assuming a general availability of propagules (e.g. Hickler et al., 2012), because in this case the timing of stochastic events might be less important. When propagules are available in each cell of the simulation area at each point in time, suitable establishment years automatically co-occur with available seeds. In contrast, when simulating migration explicitly, recruitment happens only where and when environmental conditions are favourable and seeds were previously dispersed to or in the cell. We therefore hypothesise that simulated migration can be affected by the actually realised time series of annual climate influences and that a single simulation driven by one out of multiple possible realisations of climate influences with the same statistical properties can be insufficient to adequately project possible outcomes of tree species' migration.

We used the multi-species, spatially linked and dynamic intermediate-complexity model TreeMig (Lischke et al., 2006) to examine our hypothesis. The impact of interannual climate variability probably becomes most obvious in situations which critically influence regeneration and survival of a species. We assume that such critical situations are where species' limitations, competition and spatial fragmentation interact, and therefore examined an illustrative and realistic anticipated migration situation which includes these critical conditions. We simulated the northwards migration of the submediterranean tree species *Ostrya carpinifolia* Scop. (European Hop Hornbeam) through the highly fragmented and climatically heterogeneous landscape of the Swiss Alps. Spatial fragmentation, species' sensitivities to climate and competition can lead to low species' abundances, particularly at the range boundaries of a species. Because previous simulation studies found that species' abundances at the external range boundaries can be an important factor influencing migration rates (e.g. Iverson et al., 2004), we revisited the representation of species' cell populations in TreeMig. TreeMig's cell populations are represented as continuous densities and hence allow for infinitesimal values. We examined whether simulated migration is affected when such infinitesimal values are prevented by minimum density thresholds, i.e. thresholds below which a species is treated as absent (density set to zero).

Overall we investigated the following research questions in TreeMig, using the example of *O. carpinifolia* and multiple simulations driven by different realisations of the stochastically sampled annual future climate time series:

Q1: Do minimum thresholds for species' presence, which prevent infinitesimal densities, have an impact on simulated migration?

Q2: Does interannual climate variability influence migration outcomes, i.e. do simulations driven by climate time series generated with different extrapolation methods (steady application of mean values, cyclic repetition and stochastic sampling) differ in resulting migration success, speed and species' spread?

Q3: What are the uncertainty ranges in simulated species' spread associated with interannual climate variability?

A pre-study with TreeMig highlighted that species parameter uncertainty can be particularly important when explicitly simulating tree species' migration (Nabel et al., 2012). We therefore conducted our investigations with different species parameter sets covering the plausible parameter range of *O. carpinifolia*. Examining interactions between input uncertainty and species parameter uncertainty is a critical approach, which often has been neglected in sensitivity analysis of computationally intensive models. Sensitivity analyses often either concentrated on species parameter uncertainty (e.g. Harper et al., 2011) or on climate influences (e.g. Bugmann and Pfister, 2000; Morin and Chuine, 2005).

3.2 Methods

3.2.1 Model

TreeMig is a multi-species, spatially linked and dynamic intermediate-complexity model which was developed with the aim to simulate spatio-temporal patterns of tree species' distributions with emphasis on endogenous dynamics, such as competition and migration (Lischke et al., 2006). TreeMig includes many processes required to simulate migration explicitly, for example, seed production, seed dispersal and seed bank dynamics. TreeMig-Netcdf 1.0, the TreeMig version applied in this study, is based on TreeMig 1.0 (Lischke et al., 2006) with amendments described in Rickebusch et al. (2007) and several technical revisions and refactorings. Here, we only summarise the properties most important to our study.

TreeMig simulations are driven by three bioclimate variables per year and per cell (default cell size: 1km^2): the annual sum of daily mean temperatures above $5.5\,^{\circ}\mathrm{C}$ (DDsum$_{>5.5\,^{\circ}\mathrm{C}}$), the minimum winter temperature and an index describing the severity of drought events. These bioclimate variables directly influence various processes such as simulated tree species' growth, establishment and mortality (Lischke et al., 2006). The value for the minimum required DDsum$_{>5.5\,^{\circ}\mathrm{C}}$, for example, directly influences the maximum possible growth (see electronic supplementary material Fig. 3.A.2 for the maximum possible growth functions of *O. carpinifolia*), operates as a threshold on the establishment, and has an indirect effect on the mortality of a species (Lischke et al., 2006). The establishment in a cell is only possible for years with DDsum$_{>5.5\,^{\circ}\mathrm{C}}$ higher than the species specific parameter value, which can strongly affect simulated regeneration in cold regions. In addition to the three yearly bioclimate variables, a static zero-one mask is required, which determines the stockability for each cell of the simulation area, i.e. if trees can grow in the cell (e.g. Fig. 3.1b). A stockability of zero can represent big water bodies, solid rock surfaces and different kinds of human land use. Together with extreme climate influences, non-stockable cells are the main cause of spatial fragmentation in a simulation area.

When developing TreeMig, the trade-off between computational efficiency and accuracy has been approached by employing a distribution-based representation of the local spatial forest heterogeneity per simulated grid cell (Lischke et al., 1998, 2006). The forest in each cell is described by a density of seeds per species in the seed bank and by tree densities per species in a constant number of distinct height classes. These state variables are real-valued and represent mean densities, each determining a Poisson distribution of the density on a given unit area, so called patch area (cf. Bugmann, 1994). The resulting vertical and horizontal structure can be regarded as a deterministic representation of multiple patch repetitions – as used in ForClim (Bugmann, 1994), the forest gap model preceding TreeMig – retaining the small-scale variability originally resulting from stochastic establishment and mortality. This deterministic representation counterbalances the increase in computational complexity (memory and time) accompanying the increased spatial extent – compared to simulating single stands – and the spatial linkage through seed dispersal. However, the model still has a high computational complexity and the approximate computation time for each 1km^2 cell and each year amounts to one millisecond on a 2.8GHz AMD Opteron CPU[1].

[1]A single run with a simulation area entailing Switzerland (350km x 220km) for 1000 years thus would nearly take one day.

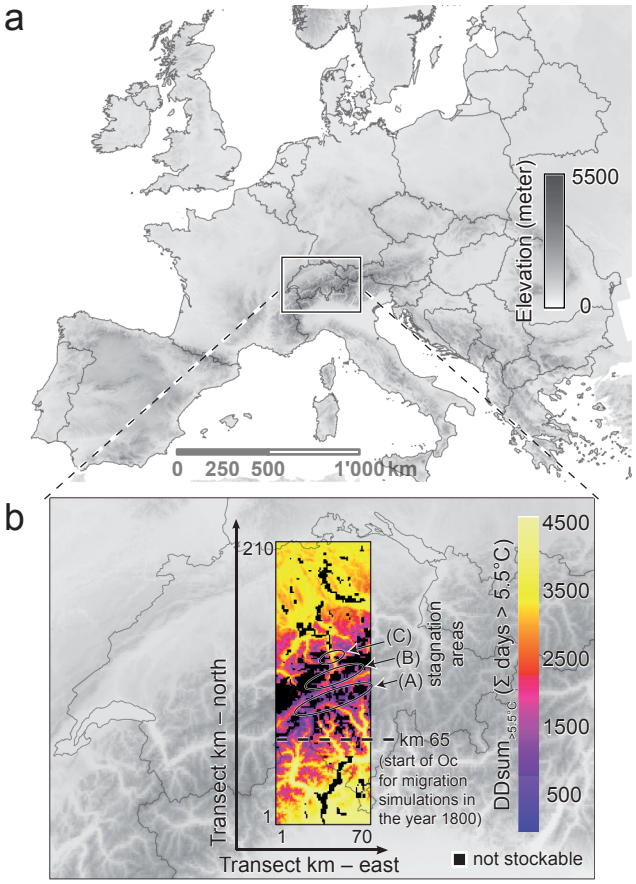

Figure 3.1 : Simulation transect. Panel a: Location in Europe (digital elevation model from Jarvis et al., 2008). Panel b: 210km x 70km simulation transect through the climatically heterogeneous and fragmented landscape of the Swiss Alps. The northern and the southern part of the transect are characterised by higher temperatures than the pass in the middle of the simulation transect. Future mean $\mathrm{DDsum}_{>5.5\,^{\circ}\mathrm{C}}$ (sum of daily mean temperatures above $5.5\,^{\circ}\mathrm{C}$) is depicted by a colour gradient (refer to the online version for a coloured map). Black cells represent big water bodies and solid rock surfaces, defining non-stockable cells, i.e. cells where trees cannot grow. The circled stagnation areas (A), (B) and (C) mark the bottlenecks of the pass. The dashed line marks the approximate northern edge of the current distribution of *Ostrya carpinifolia*, used as starting point for the migration simulations in the simulation year 1800.

Due to the deterministic description of local dynamics and motivated by the computational costs involved, repetitions of simulation runs were not considered in applications of TreeMig so far (e.g. in Lischke et al., 2006; Epstein et al., 2007). However, the model still has to deal with stochasticity. In particular bioclimate influences are often stochastically extrapolated, as described in the introduction and discussed in this paper. As a simplification, further stochastic processes which are optional in TreeMig (stochastic dispersal and non-climatic stochastic disturbances) were not considered in this study.

3.2.2 Implementation of a minimum density threshold

As described above, an area simulated with TreeMig is represented by continuous seed densities per species in the seed bank and tree densities per species in the height classes of each cell. None of the processes of the initial TreeMig version required a minimum density for any of these variables, and no process included a mechanism – beyond computational precision – which could lead to the extinction of a species in a cell. Since there were no minimum threshold requirements, infinitesimally small values in the densities were allowed for all processes, for example, for seed production, seed dispersal, germination, growth and mortality. It was in particular possible to disperse subinteger fractions of seeds, which – if not prevented by the computational precision or the

minimum temperature thresholds – ultimately caused minuscule population densities in their sink cell, since establishment is realised as a deterministic processes in TreeMig (see Lischke et al., 2006). Infinitesimally small densities could also be caused by other local dynamics, for example, by mortality which only had a thinning effect under severe environmental conditions but did not lead to extinction in a cell. Hence, TreeMig's model formulations enabled subinteger fractions of densities to spread through inhospitable terrain, and to rapidly develop in more favourable distant locations. This problem is connected to the problem of continuous tails of dispersal kernels where a discretisation of seeds can prevent seed fractions from spreading unrealistically far from the source (Higgins et al., 2003; Nathan et al., 2011).

Small densities are important to represent sporadically far dispersed seeds and low-density populations localised in small-scale microclimates (Pearson, 2006; Giesecke, 2007). Infinitesimal densities, on the other hand, can probably weaken the barrier effect of large areas of inhospitable environments and the effects of severe climatic conditions. To test for such problems, a minimum threshold for TreeMig's real-valued state variables was introduced in this study. At the end of each simulation step (i.e. each year), densities of height classes falling below the threshold are set to zero. To ensure conservation of individuals, the corresponding amount is added to the next lower height class. In the lowest height class, however, any amount smaller than the threshold is ultimately removed. This mechanism in particular prevents the germination of infinitesimally small seed fractions into the lowest height class, which could also have been realised by only allowing integer valued seed densities, i.e. discrete seeds (as proposed in Higgins et al., 2003). However, since the life stage 'seed' is involved in several processes represented in TreeMig, i.e. seed production, seed dispersal from sink to source cells, storage in the seed bank and finally germination, rounding or truncation would have been required at several different process steps.

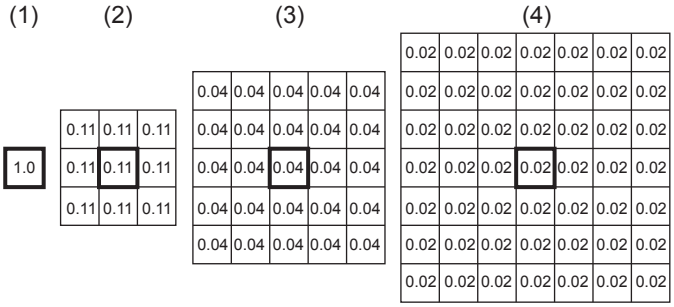

Figure 3.2 : Number of cells and densities theoretically required in the neighbourhood of the focal cell (highlighted cell) to have a total expected value of approximately one occurrence. Depicted are the requirements for a minimum density threshold of (1) 1.0, (2) 0.11, (3) 0.04 and (4) 0.02.

Determining a meaningful threshold depends on the spatial extent considered. To permit solitary individuals with regard to a single km^2 cell, we applied a threshold of one occurrence per km^2. To test the sensitivity of the simulation results to this threshold we additionally conducted simulations with other thresholds. As described in Section 3.2.1 TreeMig's state variables represent expected occurrences per cell. When the seed or population density in a cell is smaller than one, the reciprocal value of the density for a $1km^2$ cell can therefore be interpreted as the number of similar cells in the cell neighbourhood required to obtain a total expected value of one occurrence (see Fig. 3.2 for a visualisation). A threshold on the minimum required density can thus be interpreted as the maximum tolerated area size in which the expected occurrence theoretically has to amount to one – assuming homogeneous conditions. The thresholds applied in addition to one occurrence per km^2 represent an increasing number of this maximum tolerated area (thresholds of 0.11, 0.04 and 0.02, which correspond approximately to a maximum tolerated area of $9km^2$, $25km^2$ and $49km^2$, respectively – Fig. 3.2).

3.2.3 Simulation setup

3.2.3.1 Simulated area and simulated species

To investigate the impact of minimum density thresholds and of interannual climate variability on simulated migration, a realistic migration setup was developed, providing an illustrative example in which species' limitations, spatial fragmentation and competition interact. *Ostrya carpinifolia*, the focal species of this study (see electronic supplementary material Section 3.A.2 for the reasoning), is a submediterranean species currently limited to the southern side of the Swiss Alps (Swiss National Forest Inventory, 2004/06; European Forest Data Center, 2012). In order to simulate its northwards migration, a 210km x 70km simulation transect through the Swiss Alps was defined (Fig. 3.1). Many transect cells in the area of the Swiss Alps are solid rock surfaces, which are classified as not stockable in TreeMig (Fig. 3.1b), i.e. cells where trees cannot grow (see electronic supplementary material Section 3.B.1.3 for the derivation of the stockability map). As a consequence the transect is highly fragmented and a successful northwards migration of *O. carpinifolia* presupposes crossing the only pass contained in the transect, which has several bottlenecks (Fig. 3.1b – stagnation areas A-C). The transect covers different climate conditions and different climate transitions under the climate change scenario applied (see Section 3.2.3.2) and therefore enables the assessment of the model behaviour under different climate situations. To account for competition, further species occurring in the simulated area were included in the simulations (see electronic supplementary material Section 3.A.3).

Previous simulations with TreeMig have indicated a high sensitivity of migration to species parameter uncertainty (Nabel et al., 2012). Therefore some of the experiments conducted here were simulated for different species parameter sets in the plausible range of parameters for *O. carpinifolia*. Table 3.1 shows the parameter sets applied and their abbreviations. Temperature sensitivity, expressed as the minimum required $5.5\,^{\circ}\mathrm{C}$ degree-day sum ($\mathrm{DDsum}_{>5.5\,^{\circ}\mathrm{C}}$), was treated separately when compiling the species parameter sets, because *O. carpinifolia* is known to be temperature limited (e.g. Noack, 1979; Brändli, 1998). Temperature sensitivity was furthermore the parameter which influenced a successful northwards migration of *O. carpinifolia* most in previous simulations (Nabel et al., 2012). For a description of the effects of $\mathrm{DDsum}_{>5.5\,^{\circ}\mathrm{C}}$ see Section 3.2.1.

Table 3.1 : Parameter sets applied for *Ostrya carpinifolia* in the simulations and their abbreviations: all nine combinations of the most optimistic, moderate and most pessimistic parameters for (1) the sensitivity to temperature represented by the minimum required $\mathrm{DDsum}_{>5.5\,^{\circ}\mathrm{C}}$ (sum of daily mean temperatures above $5.5\,^{\circ}\mathrm{C}$) and (2) all other parameters, which describe species' traits influencing fertility, competitiveness and sensitivity to drought. See Nabel et al. (2012) for the parameter values and their uncertainty ranges.

		Temperature sensitivity (T) (Min. required $\mathrm{DDsum}_{>5.5\,^{\circ}\mathrm{C}}$)		
		Pessimistic (1440)	Moderate (1200)	Optimistic (960)
All other parameters (O)	Optimistic	$\mathrm{T_{pess}} \times \mathrm{O_{opt}}$	$\mathrm{T_{mod}} \times \mathrm{O_{opt}}$	$\mathrm{T_{opt}} \times \mathrm{O_{opt}}$
	Moderate	$\mathrm{T_{pess}} \times \mathrm{O_{mod}}$	$\mathrm{T_{mod}} \times \mathrm{O_{mod}}$	$\mathrm{T_{opt}} \times \mathrm{O_{mod}}$
	Pessimistic	$\mathrm{T_{pess}} \times \mathrm{O_{pess}}$	$\mathrm{T_{mod}} \times \mathrm{O_{pess}}$	$\mathrm{T_{opt}} \times \mathrm{O_{pess}}$

3.2.3.2 Extrapolation of bioclimate time series

All simulation experiments conducted in this study were run for 1600 years (1400-3000). The bioclimate variables required in the simulations were derived from monthly data of past climate (1901-2000: CRU data Mitchell et al., 2003) and projections of monthly data up to 2100 based on the SRESA1B scenario (Nakicenovic et al., 2000) (see electronic supplementary material Section 3.B.1 for details). The derived bioclimate was used directly for the corresponding simulation years (i.e. 1901-2100). Past and future time spans exceeding the available climate data (1400-1900 and 2101-3000) were extrapolated from the available data. As mentioned in the introduction,

there are different common extrapolation approaches (for a visualisation on the example of $\mathrm{DDsum}_{>5.5\,^{\circ}\mathrm{C}}$ see Fig. 3.3): (1) steady application of the mean of a selected base period (*mean values extrapolation*), (2) cyclic repetition of a selected base period (*cyclic extrapolation*) and (3) stochastic sampling of annual bioclimate influences from a distribution obtained from a selected base period (*stochastic extrapolation*). Extrapolations with each of these approaches were based on 30 year base periods of derived bioclimate – 1901-1931 for extrapolations of the past and 2071-2100 for extrapolations of the future (see electronic supplementary material Section 3.B.2 for further information).

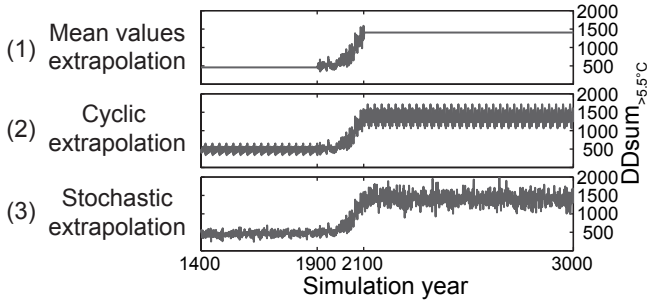

Figure 3.3 : Realised time series for the different extrapolation methods on the example of the $\mathrm{DDsum}_{>5.5\,^{\circ}\mathrm{C}}$ (sum of daily mean temperatures above $5.5\,^{\circ}\mathrm{C}$) and an illustrative example cell (119 transect km north and 42 transect km east), which reflects the average temperature conditions of the Alpine region. The three time series share the data for 1900-2100 (see text). Past (future) data was extrapolated from the base period 1901-1931 (2071-2100) by (1) steady application of the mean of the base period (mean values extrapolation), (2) cyclic repetition of the base period (cyclic extrapolation) and (3) stochastic sampling of the annual $\mathrm{DDsum}_{>5.5\,^{\circ}\mathrm{C}}$ from the distribution obtained from the base period (stochastic extrapolation).

With the cyclic and the mean values extrapolation, deterministic time series for each cell of the simulation area are generated. With the stochastic extrapolation, a bioclimate time series is stochastically generated through sampling each year from a distribution derived separately for each cell and bioclimate variable (see electronic supplementary material Section 3.B.2.3 for further information).

3.2.3.3 Simulation phases and scenarios

TreeMig simulations start with an initialisation phase used as a computationally efficient way to generate an initial forest by assuming that saplings of all species are available in all cells, instead of simulating seed production, dispersal and germination (cf. Lischke et al., 2006; Epstein et al., 2007). The initialisation phase for this study comprised the first 400 simulation years (1400-1800). To investigate the effects of interannual climate variability and of minimum density thresholds on migration, a *migration scenario* was set up by restricting *O. carpinifolia* in the initialisation phase to the lower 65km of the transect (Fig. 3.1b), in congruence with the approximate northern edge of its current distribution (cf. Brändli, 1998). Additionally, a *no-restriction scenario* was simulated, to test for the effects of minimum density thresholds in a setting without prescribed restrictions. In the subsequent main simulation phase, seed production and dispersal were simulated explicitly in both scenarios (migration scenario and no-restriction scenario) and the restriction of *O. carpinifolia* used in the initialisation phase for the migration scenario simulations was removed.

3.2.4 Simulation experiments and output

Each research question was addressed with several simulation experiments (Table 3.2). Simulations with stochastic extrapolation of the driving bioclimate time series were initially repeated ten times only, because of the long computation times. However, additional repetitions were conducted for simulation experiments most sensitive to the actual realisation of annual bioclimate influences (Table 3.2). Repetitions of stochastic extrapolations only varied in the seed of the pseudo-random number (PRN) stream used to sample the bioclimate time series. The PRN streams were generated with the pseudo-random number generator mtprng (Ladd, 2004), a Fortran implementation of the Mersenne Twister (Matsumoto and Nishimura, 1998).

Table 3.2 : Simulation experiments performed to address the research questions (Q1 - Q3). The table lists all simulated combinations of species parameter sets, threshold variants and methods used to extrapolate the driving bioclimate time series. All simulations with stochastically extrapolated bioclimate time series were initially repeated ten times. Additional repetitions were conducted for most sensitive and relevant combinations of species parameters and threshold variants.

Research Question	Scenario	Simulation experiments
Q1	Migration scenario	10 repetitions with stochastic extrapolation of the driving bioclimate time series × all 9 parameter sets for *Ostrya carpinifolia* (Table 3.1) × without, and with each of the 4 minimum density thresholds (1, 1/9, 1/25, 1/50 per km^2)
	No-restriction scenario	10 repetitions with stochastic extrapolation × 2 parameter sets for *O. carpinifolia* ($T_{mod} \times O_{mod}$ and $T_{opt} \times O_{opt}$) × without, and with each of the 4 minimum density thresholds (1, 1/9, 1/25, 1/50 per km^2)
Q2	Migration scenario	10 repetitions with stochastic extrapolation × all 9 parameter sets for *O. carpinifolia* × without, and with 2 minimum density thresholds (1, and 1/9 per km^2)
		20 additional repetitions with stochastic extrapolation × 3 parameter sets for *O. carpinifolia* ($T_{opt} \times \{O_{pess}, O_{mod}, O_{opt}\}$) × without, and with 2 minimum density thresholds (1, and 1/9 per km^2)
		One simulation run with cyclic and one with mean value extrapolation × all 9 parameter sets for *O. carpinifolia* × without, and with 2 minimum density thresholds (1, and 1/9 per km^2)
Q3	Migration scenario	One simulation run with cyclic and one with mean value extrapolation and 230 repetitions with stochastic extrapolation × 1 parameter set for *O. carpinifolia* ($T_{opt} \times O_{mod}$) × 1 minimum density thresholds (1 per km^2)

The biomass of *O. carpinifolia* was tracked yearly for all simulations of the migration scenario and was calculated as a cell sum over the population densities of all height classes, i.e. excluding the seed bank. Two aggregative indicators were derived from the biomass distribution of *O. carpinifolia*: the northernmost occurrence at each time step (in transect km – counted from the southernmost point of the transect) and the number of cells inhabited north of transect km 65, to which *O. carpinifolia* was restricted in the initialisation phase (see Section 3.2.3.3), i.e. the change of its distribution relative to the simulation year 1800. A cell was counted as inhabited if *O. carpinifolia* was present. As a consequence, arbitrarily small fractions of individuals led to inhabited cells in simulations in which no threshold was applied. The northernmost occurrence at each time step is used as an indicator for migration success and speed and the number of inhabited cells is used as an indicator for species' spread. Both indicators were smoothed with a moving window of ten years, to remove short term fluctuations and reveal the general trend.

To test the influence of minimum density thresholds on the model behaviour, additional output variables were derived: total biomass of all species per cell [t/ha] and biomass per species per cell [t/ha]. These variables were calculated for each century starting in the year 2100 and were tracked as snapshots, i.e. annual maps of the values for a variable in all cells of the transect area (see Fig. 3.4 for snapshots of the biomass of *O. carpinifolia*).

Snapshots of different simulation runs were compared with a similarity coefficient (SC – Equation 3.1) ranging from zero (no similarity) to one (complete agreement). This measure has already been used for inter- and intramodel comparisons (Bugmann and Fischlin, 1994; Lischke, 2005), as well as in comparisons of forest stands (Bray and Curtis, 1957).

$$SC_{sh_1,sh_2} = 1 - \frac{\sum_i^{cell} D_{sum_i}}{\sum_i^{cell} S_{sum_i}} \tag{3.1}$$

SC_{sh_1,sh_2} for two snapshots sh_1 and sh_2 is calculated as the relationship of the sum of the biomass differences

Table 3.3 : Effect of the most restrictive minimum density threshold on different output variables (total biomass, biomass per species and biomass of *Ostrya carpinifolia*) for simulations with the two application scenarios (no-restriction scenario and migration scenario) and different species parameter sets for *O. carpinifolia* ($T_{mod} \times O_{mod}$ and $T_{opt} \times O_{opt}$). Each number represents the average similarity coefficient (SC) of ten snapshot-comparisons between simulations with no threshold and with the most restrictive threshold (minimum of one occurrence per km^2). Each comparison was conducted between simulations driven by the same stochastically extrapolated bioclimate time series. Effects on simulations with the moderate ($T_{mod} \times O_{mod}$) and the optimistic species parameter set ($T_{opt} \times O_{opt}$) did not differ for the no-restriction scenario. Standard deviations amongst the ten snapshot-comparisons were very low: differences of SCs $< \pm 0.01$ for total biomass and biomass comparisons per species and $< \pm 0.015$ for comparisons of the biomass of *O. carpinifolia*.

Output	Scenario	2100	2300	2500	2700	2800	2900	3000
Total Biomass	No-restriction scenario ($T_{opt} \times O_{opt}$)	0.999	0.997	0.997	0.998	0.998	0.998	0.998
	Migration scenario ($T_{mod} \times O_{mod}$)	0.999	0.997	0.997	0.998	0.998	0.998	0.998
	Migration scenario ($T_{opt} \times O_{opt}$)	0.999	0.997	0.997	0.996	0.995	0.993	0.991
Biomass per species	No-restriction scenario ($T_{opt} \times O_{opt}$)	0.997	0.984	0.980	0.980	0.981	0.982	0.983
	Migration scenario ($T_{mod} \times O_{mod}$)	0.997	0.985	0.981	0.982	0.982	0.983	0.984
	Migration scenario ($T_{opt} \times O_{opt}$)	0.997	0.984	0.980	0.978	0.975	0.970	0.967
Biomass of *Ostrya carpinifolia*	No-restriction scenario ($T_{opt} \times O_{opt}$)	0.998	0.994	0.995	0.996	0.997	0.997	0.997
	Migration scenario ($T_{mod} \times O_{mod}$)	0.990	0.982	0.967	0.957	0.950	0.939	0.908
	Migration scenario ($T_{opt} \times O_{opt}$)	0.994	0.981	0.982	0.948	0.909	0.873	0.859

D_{sum} between corresponding cells (i) and their sum S_{sum}. In comparisons of the biomass per species, differences are calculated for each species separately and summed before dividing by the total sum.

3.3 Results

3.3.1 Q1 – Effects of minimum density thresholds

To assess whether minimum density thresholds for TreeMig's state variables cause differences in the model results, simulations with no threshold and with different thresholds were compared (see Table 3.2 - Q1 for the simulation experiments performed).

3.3.1.1 Impact on simulated total biomass and biomass per species

Minimum density thresholds had negligible effects on total biomass and biomass per species (Table 3.3). Snapshots of these variables from simulations with the same bioclimate influences, but with the most restrictive threshold and without a threshold, were generally very similar (SCs close to 1), regardless of the application scenario (no-restriction scenario and migration scenario). The lowest – but still very high – SC of 0.967 for biomass per species comparisons was found in the migration scenario for the last simulation year in simulations with the most optimistic parameter set for *Ostrya carpinifolia* ($T_{opt} \times O_{opt}$). The main share of these differences can be attributed to the influence of the threshold on the migration of *O. carpinifolia* (see Section 3.3.1.2 and last row of Table 3.3).

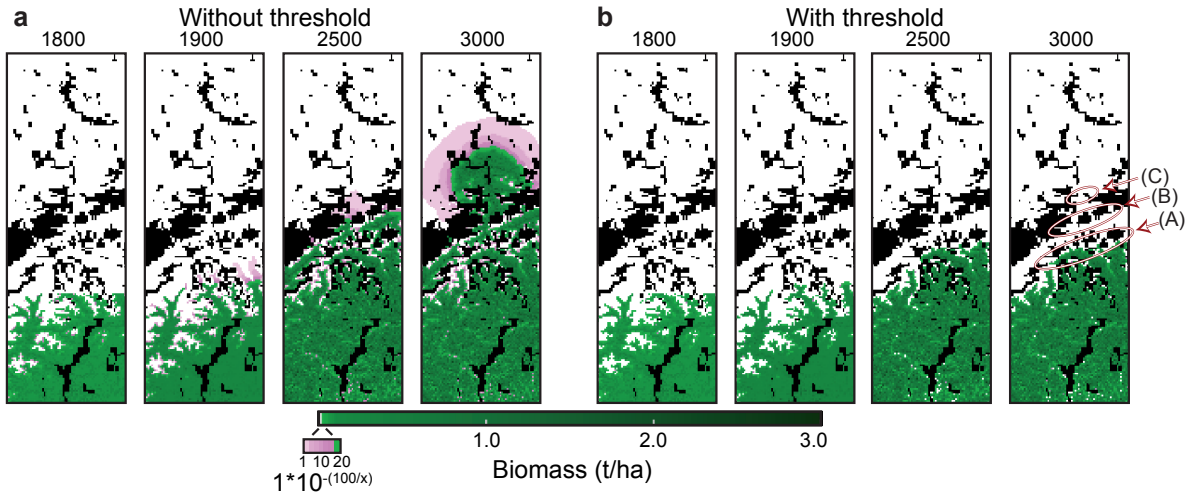

Figure 3.4 : Snapshots of the biomass [t/ha] of *Ostrya carpinifolia* (see Section 3.2.4) in the years 1800, 1900, 2500 and 3000 for migration scenario simulations without (panel a) and with the most restrictive threshold (minimum of one occurrence per km^2 – panel b). Both simulations applied the moderate species parameter set for *O. carpinifolia* ($T_{mod} \times O_{mod}$) and were driven by the same stochastically extrapolated bioclimate time series. The selected colour gradient highlights abundances close to zero (pink cells – refer to the online version for coloured maps), illustrating the spread of infinitesimal population densities in simulations without a threshold (panel a). The scale insert shows the colours used for values smaller than $1 \cdot 10^{-5}$ (= $1 \cdot 10^{-(100/20)}$). The biomass was plotted with ParaView 3.10.0 (Ahrens et al., 2005). The circled stagnation areas (A), (B) and (C) mark the bottlenecks of the pass; white cells are not inhabited and black cells not stockable (Fig. 3.1b).

The SCs in Table 3.3 resulted from comparisons of simulations with no threshold and with the most restrictive threshold (minimum of one occurrence per km^2). Snapshots of simulations with less severe thresholds (e.g. 1/50 = one occurrence per 50km^2) were slightly more similar (difference of SCs < 0.02).

3.3.1.2 Impact on simulated migration

Minimum density thresholds were found to have a considerable impact on simulated migration of *O. carpinifolia*. In simulations without a threshold, *O. carpinifolia* sooner or later passed at least the first two stagnation areas (Fig. 3.4a, Fig. 3.5) and – for most species parameter sets applied – *O. carpinifolia* successfully migrated through the pass within the simulated time span, irrespective of the driving bioclimate time series (see electronic supplementary material Appendix 3.C for illustrations of all migration scenario experiments performed for Q1). Simulations without a threshold mainly differed in migration speed among different species parameter sets (Fig. 3.5 and Appendix 3.C). For parameter sets with the pessimistic temperature sensitivity value (Table 3.1 – T_{pess}) the annual bioclimate influences became important for migration in the area of the pass (Fig. 3.5a and first column of Fig. 3.C.2 and Fig. 3.C.3), which is discussed in more detail in Section 3.3.2.

In simulations with a minimum density threshold, migration of *O. carpinifolia* experienced an initial slowdown compared to simulations with no threshold, irrespective of the species parameter set applied (Fig. 3.5 and Appendix 3.C). In the year 1800, the artificial simulated restriction of *O. carpinifolia* to the lower 65km of the transect (Fig. 3.1b) was removed. *O. carpinifolia* suddenly was able to disperse to the northern parts of the transect, which, as described in Section 3.2.2, led to distant spread of infinitesimal seed fractions in simulations without a minimum density threshold (change from 1800 to 1900 in Fig. 3.4a compared to Fig. 3.4b). Apart from this initial slowdown, simulated migration was mainly affected in the area of the pass (Fig. 3.5, Fig. 3.C.2). Although driven by the same bioclimate time series and simulated with the same species parameter set, *O. carpinifolia* often only migrated successfully through the pass in simulations without a threshold (Fig. 3.4a compared to Fig. 3.4b, Fig. 3.5b and Appendix 3.C). For simulations with most of the species parameter sets threshold size had no relevance for migration success (Fig. 3.5, Fig. 3.C.2, but see Fig. 3.C.2b,f). Migration success resulting from test simulations with a different base year set used to extrapolate the bioclimate time series indicated

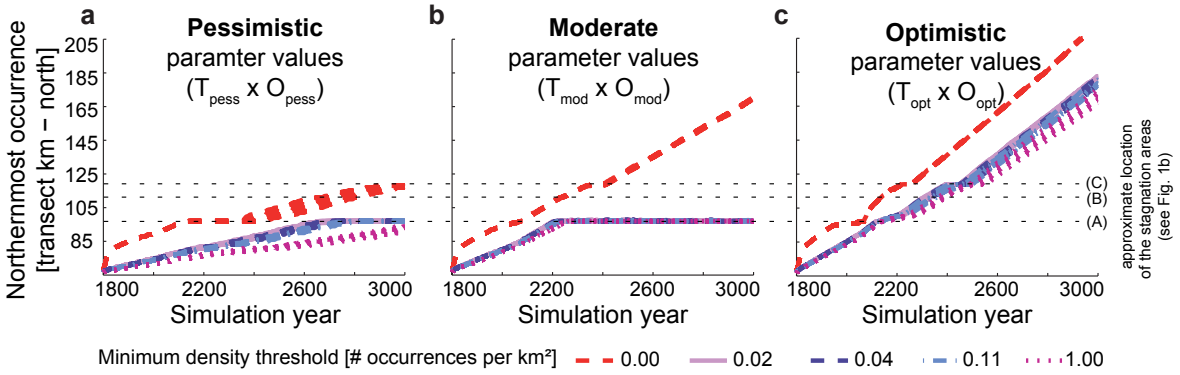

Figure 3.5 : Northernmost occurrence (transect km - north, smoothed over ten years) simulated for *Ostrya carpinifolia* for the years 1800-3000, starting at km 65, to which *O. carpinifolia* was restricted until 1800 in the migration scenario simulations. Simulations were performed without a minimum density threshold and with four different thresholds (different colours discriminate the corresponding thresholds – refer to the online version for a coloured figure). The panels show the results for three of the nine species parameter sets used for *O. carpinifolia* (Table 3.1): all pessimistic ($T_{pess} \times O_{pess}$, panel a), all moderate ($T_{mod} \times O_{mod}$, panel b) and all optimistic ($T_{opt} \times O_{opt}$, panel c). Series of lines with the same colour depict the results of ten repetitions driven by stochastically extrapolated bioclimate time series and simulated with the corresponding threshold and species parameter set. The dashed horizontal lines (A-C) mark the approximate location of the three main stagnation areas (Fig. 3.1b). See electronic supplementary material Appendix 3.C for illustrations of all migration scenario experiments performed for Q1.

that the sensitivity to threshold size depends on the species parameter set applied and on interactions with the driving bioclimate time series (see Appendix 3.C). Outside of the pass, density thresholds had a minor influence on simulated migration and the trajectories for the northernmost occurrence of *O. carpinifolia* were almost parallel (e.g. Fig. 3.5c).

When considering the snapshot comparisons for the migration scenario (Table 3.3), notable differences were only found in comparisons of the biomass of *O. carpinifolia* with the smallest SC being 0.859, indicating that the compared snapshots were predominantly similar. The biomass of *O. carpinifolia* in the lower parts of the transect was indeed hardly influenced by the minimum density threshold (see e.g. Fig. 3.4). For simulations with the optimistic parameter set ($T_{opt} \times O_{opt}$) differences between snapshots were greater (difference of SCs $>$0.05) than for simulations with the moderate parameter set ($T_{mod} \times O_{mod}$), which seemingly is a contradiction to the impact of the thresholds on migration success (Fig. 3.5). However, the SC depends less on migration distance than on the size of the inhabited area, which was much larger for the optimistic parameter set (e.g. in the year 3000: approximately 8000km^2 for $T_{opt} \times O_{opt}$ compared to 4500km^2 for $T_{mod} \times O_{mod}$ for the no threshold case and for the most severe threshold approximately 4000km^2 for $T_{opt} \times O_{opt}$ compared to 1000km^2 for $T_{mod} \times O_{mod}$ – see Fig. 3.C.1 electronic supplementary material).

3.3.2 Q2 – Comparison of the different extrapolation methods

Simulations driven by bioclimate time series extrapolated with all three approaches (Section 3.2.3.2) were conducted with either of two thresholds or no threshold, and for all nine species parameter sets used for *O. carpinifolia* (see Table 3.2 – Q2 for the simulation experiments performed). The influence of annual bioclimate on simulated migration was found to depend on interactions of species parameters used for *O. carpinifolia* (in particular sensitivity to temperature) and the density threshold applied (see Appendix 3.D in the electronic supplementary material for illustrations of all experiments performed for Q2).

Simulations driven by different stochastic realisations of annual bioclimate influences resulted in notably diverging northernmost occurrence trajectories for some threshold and species parameter set combinations (Fig. 3.6b, c, Fig. 3.D.1 and Fig. 3.D.3). Simulations driven by cyclically repeated bioclimate (cyclic extrapolation) mostly led to northernmost occurrences of *O. carpinifolia* at the lower end of the range spanned by stochastic realisations (Fig. 3.6, Fig. 3.D.1 and Fig. 3.D.3). This was especially noticeable for one species parameter set where

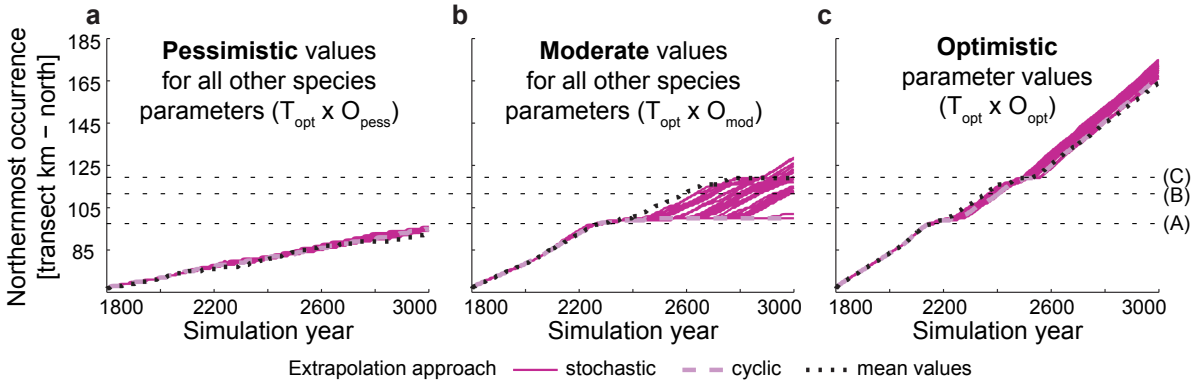

Figure 3.6 : Northernmost occurrence (transect km - north, smoothed over ten years) of *Ostrya carpinifolia* in simulations with a minimum density threshold of one occurrence per km^2 for the years 1800-3000, starting at km 65, to which *O. carpinifolia* was restricted until 1800 in the simulations. The panels show results for the three species parameter sets with optimistic temperature sensitivity (T_{opt} – Table 3.1). Each colour (refer to the online version for a coloured figure) represents one extrapolation approach (see Section 3.2.3.2). Bioclimate time series from cyclic extrapolation and from mean values extrapolation are deterministic and are therefore represented by one line per panel. Series of lines with the same colour depict the results of 30 repetitions driven by stochastically extrapolated bioclimate time series. The dashed horizontal lines (A-C) mark the approximate location of the three main stagnation areas (Fig. 3.1b). See electronic supplementary material Appendix 3.D for illustrations of all experiments performed for Q2.

migration through the pass was successful for most, but not for all stochastic realisations, and also not for the simulation driven by cyclically repeated bioclimate (Fig. 3.6b).

For most species parameter sets and thresholds applied, *O. carpinifolia* tended to migrate slower in simulations driven by steady application of the mean bioclimate values (mean values extrapolation) than in simulations driven by stochastic realisations (Fig. 3.6a, c, Fig. 3.D.1 and Fig. 3.D.3, but see Fig. 3.6b) and led to fewer inhabited cells (Fig. 3.D.2 and Fig. 3.D.4). Furthermore, the trajectory of simulated spread under steady application of mean values differed greatly from simulations with interannual variability (Fig. 3.7, Fig. 3.D.2 and Fig. 3.D.4).

3.3.3 Q3 – Uncertainty associated with interannual climate variability

Uncertainty in the simulated spread of *Ostrya carpinifolia* associated with the interannual climate variability was determined for simulations with the most sensitive combination examined. Simulations were conducted with a minimum density threshold of one occurrence per km^2 and the moderate parameters for *O. carpinifolia*, except for the temperature sensitivity, which was set to the optimistic value ($T_{opt} \times O_{mod}$). 230 repetitions were simulated and the temporal development of the uncertainty ranges was calculated (Fig. 3.7). Trajectories of the spread of *O. carpinifolia* started to diverge when the species entered the area of the pass around simulation year 2400 (Fig. 3.6b, Fig. 3.7). Uncertainty accumulated over time and the number of cells newly inhabited north of transect km 65 was more than 1.5-fold higher for the run with the largest than for the run with the smallest extent in the last simulation year. The total range of possible outcomes of spread covered approximately 600 cells (600km^2) and the likely (>66%) range approximately 350 cells (350km^2).

3.4 Discussion

The aim of the present study was to examine whether different realisations of future climate influences with the same temporal mean and the same interannual variability can lead to fundamental differences in the outcomes of simulated tree species' migration. To discuss the influence of interannual climate variability, we developed an illustrative realistic simulation setup, which was anticipated to be sensitive to the exact sequence of simulated annual climate influences. Because species' abundances at the external range boundaries are particularly

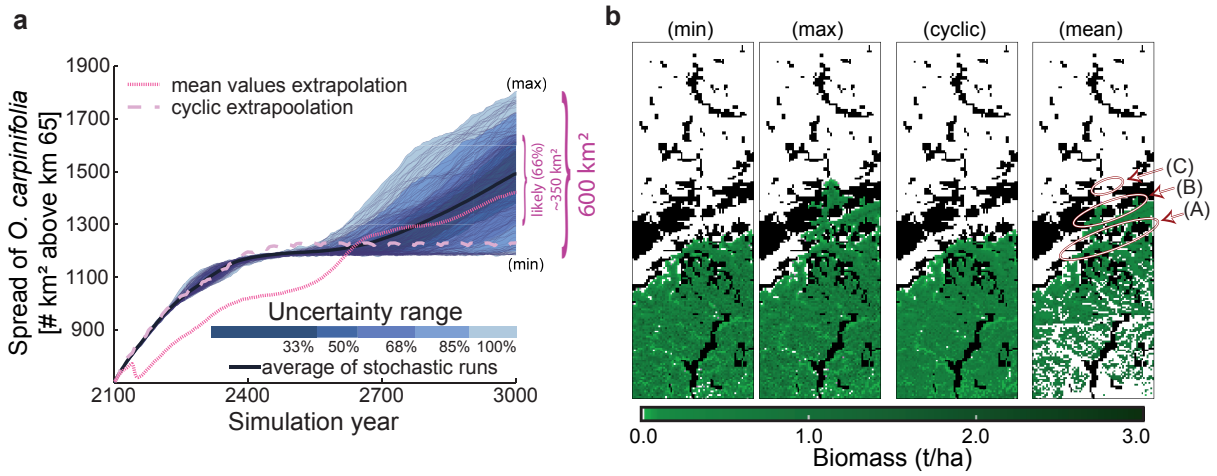

Figure 3.7 : Differences in the spread of *Ostrya carpinifolia* for simulations with a minimum density threshold of one occurrence per km^2 and the species parameter set $T_{opt} \times O_{mod}$ (Table 3.1). Panel a: Number of cells (km^2) newly inhabited north of transect km 65, to where *O. carpinifolia* was restricted up to the simulation year 1800. 230 simulations (single trajectories displayed as half-transparent lines) driven by stochastically extrapolated bioclimate time series were used to calculate the temporal development of uncertainty in the spread of *O. carpinifolia*. Percentages on each uncertainty bar denote the probability that the spread resulting for a simulation lies in the range framed by the corresponding colour (refer to the online version for a coloured figure). The total and the likely range of spread are indicated on the right side of panel a. The average result for the stochastic runs is highlighted as a black line. Additionally, the results for the runs driven by mean values and cyclically extrapolated bioclimate time series are shown. Panel b: Snapshot of the biomass [t/ha] of *O. carpinifolia* in the year 3000 for the runs with the smallest and largest extent, as well as for the runs with mean values and cyclic extrapolation. The biomass was plotted with ParaView 3.10.0 (Ahrens et al., 2005). The circled stagnation areas (A), (B) and (C) mark the bottlenecks of the pass; white cells are not inhabited and black cells not stockable (Fig. 3.1b).

important for migration, we first explored whether simulated migration is affected by minimum density thresholds preventing infinitesimal small densities in the model state variables.

3.4.1 Impact of minimum density thresholds

Introducing a minimum density threshold had a considerable effect on simulated migration in our study. Recognising the discrete nature of seeds (cf. Higgins et al., 2003; Nathan et al., 2011), at least in a probabilistic sense, prevented the initial unrealistic spread of minuscule fractions of seeds (see e.g. Fig. 3.4). Furthermore, for most of the simulated species parameter sets *Ostrya carpinifolia* no longer succeeded in migrating through the area of the pass, where spatial fragmentation, competition and severe climate influences interact, not even for the smallest threshold applied. This complete inhibition of migration through the pass suggests that, in simulations with no threshold, some of the bottlenecks of the pass must have been crossed in form of minuscule populations. And indeed, in simulations without a threshold and, for example, with the moderate parameter set ($T_{mod} \times O_{mod}$), several bottleneck cells of the first stagnation area (Fig. 3.1b – area A) showed population densities with biomass values smaller than $1 \cdot 10^{-5}$ [t/ha] throughout the simulation time (Fig. 3.4a). Hence, without a threshold, the inhospitable conditions prevailing in these bottleneck cells, i.e. the small $DDsum_{>5.5\,°C}$ and the small number of seed producing source cells within reach of the dispersal kernel, only affected species' abundance, but not migration success. This unrealistic behaviour was prevented in simulations with a threshold.

Minimum density thresholds in the magnitude applied (minimum of one occurrence per km^2) had negligible effects on biomass snapshot comparisons among simulations of the no-restriction scenario (see Section 3.2.3.3). This suggests that the introduction of a threshold did not strongly disturb simulated dynamics other than migration. Maximum abundances of *O. carpinifolia* per cell generally depended strongly on the values applied for the set of species parameters other than temperature sensitivity (rows in Table 3.1) and varied

greatly (see Fig. 3.C.1 electronic supplementary material). Only for parameter sets resulting in the lowest abundances – i.e. sets with the pessimistic values (O_{pess}) – thresholds had a visible influence on occurrences below transect km 65, where in both scenarios (migration and no-restriction scenario) only local dynamics operated (Fig. 3.C.1a).

3.4.2 Influence of interannual variability

In some of the simulation experiments, trajectories of the northernmost occurrence and of the spread of *Ostrya carpinifolia* diverged for different bioclimate time series stochastically generated from a base period, the cyclic repetition of the base period and the steady application of mean values. This confirms that interannual climate variability has a critical influence in our illustrative example, which is consistent with previous model studies showing that tree species' distributions and range limits can be influenced by the magnitude of climate variation (Bugmann and Pfister, 2000; Miller et al., 2008; Notaro, 2008; Giesecke et al., 2010) as well as by changes in the generation process of climate time series (Morin and Chuine, 2005; Stratton et al., 2011). Here we demonstrated that even realisations with the same statistical properties can lead to substantially different results.

In simulations driven by steadily applied mean values *O. carpinifolia* tended to be slower and systematically fewer cells were inhabited than in simulations driven by bioclimate time series with the same temporal mean but including interannual variability. And, even more important, simulations driven by different realisations of bioclimate time series with the same temporal mean and the same interannual variability resulted in notable differences for some simulation experiments. The relevance of the actual sequence of annual bioclimate influences on migration is reasonable. Migration is based on several entangled processes, where dispersal is only the first step (Pitelka et al., 1997). Each of the processes involved, such as germination and maturation, faces certain climatic requirements and sequences of favourable years or single extremely unfavourable years can strongly determine establishment and local persistence (Brubaker, 1986; Camarero and Gutiérrez, 2004; Miller et al., 2008; Jackson et al., 2009).

Observed variations in the simulated migration distance emphasised the relevance of the actual sequence of annual climate influences and showed the need to simulate multiple repetitions driven by different realisations of the stochastically extrapolated annual bioclimate time series. Furthermore, the results highlighted the importance of interactions between spatial fragmentation, climate influences and species' sensitivities to climate.

3.4.2.1 Impact of spatial fragmentation at the pass

In our illustrative example study, simulated migration of *O. carpinifolia* was mainly affected in the area of the pass, which highlights the impact of spatial fragmentation on migration. Spatial fragmentation was also found to be an important factor in other simulation studies (e.g. Malanson and Cairns, 1997; Collingham and Huntley, 2000). The importance of spatial fragmentation for simulated migration is reasonable, because spatial fragmentation not only increases distances between uninhabited areas and propagule sources, but also generally reduces the number of propagule sources (Malanson and Cairns, 1997; Pitelka et al., 1997). Effects on migration comparable to the ones observed are conceivable for situations other than the simulated pass, in particular with current landscapes being highly fragmented due to human land use (Pitelka et al., 1997; Hof et al., 2011).

3.4.2.2 Interactions of species' sensitivities and climate influences

By simulating several species parameter sets covering the plausible range for *O. carpinifolia*, we accounted for species parameter uncertainty and laid the foundation for a more general interpretation. At the same time, we enabled assessments of interactions between the temperature sensitivity parameter and climate influences. Our results underline the strong interaction of species' climate sensitivities and climate influences at the range boundaries. Test simulations with an additional bioclimate base year set with different temporal mean and interannual variability generally had comparable trajectories (see electronic supplementary material C and D).

For some thresholds and species parameter sets, however, they showed different sensitivities to the interannual variability in the bioclimate driver, i.e. divergences amongst multiple runs. Comparable changes in the sensitivity are to be expected if drivers are extrapolated based on projections of other climate scenarios or of the same scenario calculated with another climate model.

Interannual climate variability is suggested to influence the migration of many tree species, in particular, because of the combined effect between changes in the climate suitability (Svenning and Skov, 2004; Rosenzweig et al., 2007) and species' sensitivities at the external range boundaries (Camarero and Gutiérrez, 2004; Zimmermann et al., 2009) in the current, highly fragmented landscapes (Pitelka et al., 1997; Hof et al., 2011). In the studied case of the thermophile tree species *O. carpinifolia* and the simulated migration in the Alps, temperature was the main limiting climate factor and comparably warm years promoted the establishment and growth of *O. carpinifolia* in the simulations. However, depending on species' sensitivities and the prevailing abiotic and biotic conditions, interannual variation of other climate influences, such as precipitation, as well as interactions between different climate influences can be important. Single or episodes of years deviating from the mean can, furthermore, have promoting as well as inhibiting effects (Jackson et al., 2009). When, for example, drought is the limiting factor preventing establishment of a species, years with above average precipitation can enable recruitment (Mendoza et al., 2009; Matías and Jump, 2012). Extreme dry years, on the other hand, can cause extensive mortality. Finally, climate variability often also has indirect (positive or negative) effects by facilitating or inhibiting competitors or antagonists (Breshears et al., 2005; Gray et al., 2006; Matías and Jump, 2012).

In our study, results differed more amongst simulations with different species parameter sets than amongst simulations with the same species parameter set but driven by different realisations of the stochastically extrapolated annual bioclimate time series. This, however, does not necessarily imply that the uncertainty associated with the interannual climate variability is less important. Uncertainty in species parameters and uncertainty associated with the applied stochastic extrapolation of future climate influences are different kinds of uncertainty (cf. Refsgaard et al., 2007). The latter is a non-reducible stochastic uncertainty (Refsgaard et al., 2007) and, as long as no better informed approaches to generate climate input for longer time spans are applied, has to be accounted for by simulating multiple repetitions for each simulation setup. Hence, for example, each simulated species parameter set and each set of bioclimate base years requires multiple repetitions. Species parameters uncertainty, in contrast, could theoretically be partially reduced through further investigations of species' traits, particularly given that the assumed plausibility parameter ranges are rough assessments (Nabel et al., 2012) and that the parameter sets applied in this study are the most extreme ones. Specifically, the simulated combinations were not selected based on realistic or plausible combinations, but instead were combinations of the most favourable, the original, and the most unfavourable values for the single parameters, respectively.

Nevertheless, also competing species might have uncertain parameters, which was not considered in our study and could lead to a substantial increase in uncertainty associated with species parameterisation. A further point which is assumed to aggravate the uncertainty associated with the interannual variability is the stochastic approach currently applied in TreeMig. As described in Section 3.2.3.2, the bioclimate is sampled independently for each year from distributions separately derived for each cell and each bioclimate variable. This leads to an unrealistic disruption of the spatial autocorrelation found for each bioclimate variable and of the correlation amongst them. We suspect that accounting for spatial autocorrelation, in particular, could amplify the differences among simulations driven by stochastically generated annual bioclimate time series. Further investigations, however, exceed the scope of this paper.

3.4.2.3 Other stochastic influences

The simplification of not using the other two stochastic influences available in TreeMig – stochastic dispersal and non-climatic stochastic disturbances – was motivated by the reduced number of experiments required to examine the sensitivity to interannual climate variability. Preliminary test experiments with additional stochastic disturbances resulted in a higher output variability (simulations not shown), indicating that even more repetitions could be required.

3.4.3 Further challenges when simulating future tree species' migration

This study has revealed several pitfalls which have to be considered when simulating species' migration, in particular in fragmented terrain under unfavourable environmental conditions. It highlighted that computational complexity and model complexity are major challenges for sensitivity analyses and a constraint to manageable investigations and need to be further addressed in order to enable extensive studies. Generally, processes and influences represented in a model result from trade-offs between accuracy on one side, and computational efficiency as well as parameterisation requirements and simplicity on the other side (Huntley et al., 2010), leading to certain advantages and drawbacks. TreeMig, for example, offers the rare advantage to allow for explicit simulation of tree species' migration and of competition, driven by climate influences. Other multi-species models often assume general seed availability (e.g. Hickler et al., 2012) or only include predefined migration rates estimated from paleoecological studies (e.g. Morin and Thuiller, 2009). Models explicitly simulating migration on the other hand often simplify competition by simulating single species and only representing competition indirectly by, for example, constant (e.g. Collingham and Huntley, 2000; Iverson et al., 2004) or stepwise adapted carrying capacities (e.g. Fitzpatrick et al., 2011) or random effects on establishment (e.g. Malanson and Cairns, 1997).

A drawback common to many models, including TreeMig, is that changes in geographical distribution are the only possible mechanism for species to respond to climatic changes in the simulations. While it is often expected that adaptations of geographical range limits are the predominant response to rapid climatic changes (e.g. Huntley et al., 2010; Zhu et al., 2011), recent studies have discussed the potentially pivotal role that species' plasticity might play in how plants respond to climate changes (Hof et al., 2011) and have argued that models should contain a mechanistic representation of phenology (Chuine, 2010). Mechanistically representing phenology, however, is not possible when simulating with an annual time step, which is often the case in intermediate-complexity models such as TreeMig.

Further problems common to intermediate-complexity models are involved with the representation of environmental influences. Typically, a couple of bioclimate variables, such as $\mathrm{DDsum}_{>5.5\,^{\circ}\mathrm{C}}$, are used as proxies for direct influences, such as temperature and radiation. These relationships are empirically derived under current conditions and are not necessarily valid for future conditions (Williams and Jackson, 2007; Jackson et al., 2009). Another problem involved is whether the important aspects of the environment are covered for the simulated species. For example, bedrock types are assumed to play an important role for the distribution of *Ostrya carpinifolia* (Gobet et al., 2000), but as in many models, bedrock type differences are not represented in TreeMig other than by their water holding capacity. Such restrictions need to be discussed when model results are used for purposes other than methodological studies.

Models with a certain degree of complexity, finally, share the challenge of validation (e.g. Oreskes et al., 1994; Fitzpatrick et al., 2011). Migration rates resulting in the presented simulations for our example species (e.g. 25-85 meter per year in simulations with the most restrictive minimum density threshold) are consistent with recent estimates of tree species' migration rates (Svenning and Skov, 2007). However, a thorough validation of the model is a central challenge outside of the scope of this paper. Moreover the findings of this study further emphasised the prominence of one of the main hurdles: for a thorough validation, long-term time series on climate influences are required and need to contain the actual sequences of annual climate conditions. Our knowledge about past climate, however, is incomplete and, in particular the prevailing interannual climate variability is difficult to reconstruct (Giesecke et al., 2010).

3.5 Conclusions

Testing for side effects of continuous representations of species' cell populations revealed unrealistic migration behaviour, which was corrected by introducing minimum population density thresholds. We suggest that models which explicitly simulate migration applying continuous densities for seeds and other life stages should generally be tested for similar issues.

When studying trends in simulated species' migration, climate time series are commonly extrapolated to generate long-term inputs and this approach will be difficult to replace as long as no long-term climate projections are available. However, important pitfalls involved with this approach have to be accounted for. We demonstrated that interannual climate variability can markedly influence migration success, speed and species' spread. Simulation studies therefore have to explore the effects of different realisations of driving climate time series, i.e. they have to simulate multiple realisations with the same temporal mean and variability. The uncertainty in species' spread found amongst simulations driven by different climate realisations in our study furthermore demonstrated that average results can be misleading. For example, when a successful migration through the Alps results for some realisations, but migration is impeded for other realisations, then the average result cannot appropriately reflect both outcomes.

Our study examined the specific example of the simulated migration of one submediterranean tree species through one pass in the Swiss Alps. The conditions under which the species migrated, however, might be representative for several tree species migrating in the highly fragmented today's landscape under rapid changes of climate conditions.

Acknowledgements

We would like to thank James Kirchner, Felix Kienast and two anonymous reviewers for their valuable comments, Thomas Wüst for the support with the cluster, Dirk Schmatz for assistance with the data preparation, Signe Normand for discussions about the Glossary and Heiko Klein from the IT Department of the Norwegian Meteorological Institute for the help in applying FIMEX. This work was funded by the Swiss National Science Foundation (SNF) Grant 315230-122434. N. Zurbriggen was supported by the research project MOUNTLAND funded by the Competence Center Environment and Sustainability of the ETH Domain (CCES).

References

Ahrens, J., Geveci, B., Law, C., 2005. ParaView: An End-User Tool for Large-Data Visualization, in: Hansen, C.D., Johnson, C.R. (Eds.), Visualization Handbook. Butterworth-Heinemann.

Brändli, U.B., 1998. Die häufigsten Waldbäume der Schweiz. Ergebnisse aus dem Landesforstinventar 1983-85: Verbreitung, Standort und Häufigkeit von 30 Baumarten. Berichte der Eidgenöss. Forschungsanstalt für Wald, Schnee und Landschaft.

Bray, J.R., Curtis, J.T., 1957. An Ordination of the Upland Forest Communities of Southern Wisconsin. Ecological Monographs 27, 326–349.

Breshears, D.D., Cobb, N.S., Rich, P.M., Price, K.P., Allen, C.D., Balice, R.G., Romme, W.H., Kastens, J.H., Floyd, M.L., Belnap, J., Anderson, J.J., Myers, O.B., Meyer, C.W., 2005. Regional vegetation die-off in response to global-change-type drought. Proceedings of the National Academy of Sciences of the United States of America 102, 15144–15148.

Brubaker, L.B., 1986. Responses of Tree Populations to Climatic-change. Vegetatio 67, 119–130.

Bugmann, H., 1994. On the Ecology of Mountainous Forests in a Changing Climate: A Simulation Study. Ph.D. thesis. Swiss Federal Institute of Technology Zurich.

Bugmann, H., Fischlin, A., 1994. Comparing the behaviour of mountainous forest succession models in a changing climate. Mountain environments in changing climates. M. Beniston, Ed., Routledge, London, UK, 204–219.

Bugmann, H., Pfister, C., 2000. Impacts of interannual climate variability on past and future forest composition. Regional Environmental Change 1, 112–125.

Camarero, J.J., Gutiérrez, E., 2004. Pace and Pattern of Recent Treeline Dynamics: Response of Ecotones to Climatic Variability in the Spanish Pyrenees. Climatic Change 63, 181–200.

Chuine, I., 2010. Why does phenology drive species distribution? Philosophical Transactions of the Royal Society B: Biological Sciences 365, 3149–3160.

Collingham, Y.C., Huntley, B., 2000. Impacts of Habitat Fragmentation and Patch Size upon Migration Rates. Ecological Applications 10, 131–144.

Davis, M.B., 1989. Lags in vegetation response to greenhouse warming. Climatic Change 15, 75–82.

Easterling, D.R., Meehl, G.A., Parmesan, C., Changnon, S.A., Karl, T.R., Mearns, L.O., 2000. Climate Extremes: Observations, Modeling, and Impacts. Science 289, 2068–2074.

Epstein, H., Yu, Q., Kaplan, J., Lischke, H., 2007. Simulating Future Changes in Arctic and Subarctic Vegetation. Computing in Science Engineering 9, 12–23.

European Forest Data Center, 2012. Distribution of *Ostrya carpinifolia*. Accessed from http://efdac.jrc.ec.europa.eu/index.php/climate, on 28.01.2012.

Fischlin, A., Midgley, G.F., Price, J.T., Leemans, R., Gopal, B., Turley, C., Rounsevell, M.D.A., Dube, O.P., Tarazona, J., Velichko, A.A., 2007. Ecosystems, their properties, goods, and services. Climate Change 2007: Impacts, Adaptation and Vulnerability. Contribution of Working Group II to the Fourth Assessment Report of the Intergovernmental Panel on Climate Change. M.L. Parry, O.F. Canziani, J.P. Palutikof, P.J. van der Linden and C.E. Hanson, Eds., Cambridge University Press, Cambridge, UK, 211-272.

Fitzpatrick, M.C., Preisser, E.L., Porter, A., Elkinton, J., Ellison, A.M., 2011. Modeling range dynamics in heterogeneous landscapes: invasion of the hemlock woolly adelgid in eastern North America. Ecological Applications 22, 472–486.

Frich, P., Alexander, L.V., Della-Marta, P., Gleason, B., Haylock, M., Tank, A.M.G.K., Peterson, T., 2002. Observed coherent changes in climatic extremes during the second half of the twentieth century. Climate Research 19, 193–212.

Gaston, K.J., 2003. The Structure and Dynamics of Geographic Ranges. Oxford, New York.

Giesecke, T., 2007. Changing Plant Distributions, in: Elias, S.A. (Ed.), Encyclopedia of Quaternary Science. Elsevier, Oxford, pp. 2544–2551.

Giesecke, T., Miller, P.A., Sykes, M.T., Ojala, A.E.K., Seppä, H., Bradshaw, R.H.W., 2010. The effect of past changes in inter-annual temperature variability on tree distribution limits. Journal of Biogeography 37, 1394–1405.

Gobet, E., Tinner, W., Hubschmid, P., Jansen, I., Wehrli, M., Ammann, B., Wick, L., 2000. Influence of human impact and bedrock differences on the vegetational history of the Insubrian Southern Alps. Vegetation History and Archaeobotany 9, 175–187.

Gray, S.T., Betancourt, J.L., Jackson, S.T., Eddy, R.G., 2006. Role of Multidecadal Climate Variability in a Range Extension of Pinyon Pine. Ecology 87, 1124–1130.

Harper, E.B., Stella, J.C., Fremier, A.K., 2011. Global sensitivity analysis for complex ecological models: a case study of riparian cottonwood population dynamics. Ecological Applications 21, 1225–1240.

Hickler, T., Vohland, K., Feehan, J., Miller, P.A., Smith, B., Costa, L., Giesecke, T., Fronzek, S., Carter, T.R., Cramer, W., Kühn, I., Sykes, M.T., 2012. Projecting the future distribution of European potential natural vegetation zones with a generalized, tree species-based dynamic vegetation model. Global Ecology and Biogeography 21, 50–63.

Higgins, S., Clark, J., Nathan, R., Hovestadt, T., Schurr, F., Fragoso, J., Aguiar, M., Ribbens, E., Lavorel, S., 2003. Forecasting plant migration rates: managing uncertainty for risk assessment. Journal of Ecology 91, 341–347.

Hof, C., Levinsky, I., Araújo, M.B., Rahbek, C., 2011. Rethinking species' ability to cope with rapid climate change. Global Change Biology 17, 2987–2990.

Huntley, B., Barnard, P., Altwegg, R., Chambers, L., Coetzee, B.W.T., Gibson, L., Hockey, P.A.R., Hole, D.G., Midgley, G.F., Underhill, L.G., Willis, S.G., 2010. Beyond bioclimatic envelopes: dynamic species' range and abundance modelling in the context of climatic change. Ecography 33, 621–626.

Iverson, L.R., Schwartz, M.W., Prasad, A.M., 2004. How fast and far might tree species migrate in the eastern United States due to climate change? Global Ecology and Biogeography 13, 209–219.

Jackson, S.T., Betancourt, J.L., Booth, R.K., Gray, S.T., 2009. Ecology and the ratchet of events: Climate variability, niche dimensions, and species distributions. Proceedings of the National Academy of Sciences of the United States of America 106, 19685–19692.

Jarvis, A., Reuter, H., Nelson, A., Guevara, E., 2008. Hole-filled SRTM for the globe Version 4. Available from the CGIAR-CSI SRTM 90m Database http://srtm.csi.cgiar.org.

Keel, B., 2007. Assisted Migration as a Conservation Strategy for Rapid Climate Change: Investigating Extended Photoperiod and Mycobiont Distributions for Habenaria repens Nuttall (Orchidaceae) as a Case Study. Ph.D. thesis. Antioch University New England.

Ladd, S., 2004. mtprng – An implementation of the Mersenne Twister algorithm for generating psuedo-random sequences. Accessed from http://www.coyotegulch.com, on 03.05.2010.

Lischke, H., 2005. Modeling tree species migration in the Alps during the Holocene: What creates complexity? Ecological Complexity 2, 159–174.

Lischke, H., Löffler, T.J., Fischlin, A., 1998. Aggregation of Individual Trees and Patches in Forest Succession Models: Capturing Variability with Height Structured, Random, Spatial Distributions. Theoretical Population Biology 54, 213–226.

Lischke, H., Zimmermann, N.E., Bolliger, J., Rickebusch, S., Löffler, T.J., 2006. TreeMig: A forest-landscape model for simulating spatio-temporal patterns from stand to landscape scale. Ecological Modelling 199, 409–420.

Malanson, G.P., Cairns, D.M., 1997. Effects of dispersal, population delays, and forest fragmentation on tree migration rates. Plant Ecology 131, 67–79.

Matías, L., Jump, A.S., 2012. Interactions between growth, demography and biotic interactions in determining species range limits in a warming world: The case of *Pinus sylvestris*. Forest Ecology and Management 282, 10–22.

Matsumoto, M., Nishimura, T., 1998. Mersenne twister: A 623-dimensionally equidistributed uniform pseudo-random number generator. ACM Transactions on Modeling and Computer Simulation 8, 3–30.

Mendoza, I., Zamora, R., Castro, J., 2009. A seeding experiment for testing tree-community recruitment under variable environments: Implications for forest regeneration and conservation in Mediterranean habitats. Biological Conservation 142, 1491–1499.

Midgley, G.F., Thuiller, W., Higgins, S.I., 2007. Plant Species Migration as a Key Uncertainty in Predicting Future Impacts of Climate Change on Ecosystems: Progress and Challenges. Terrestrial Ecosystems in a Changing World. Canadell, Josep G. and Pataki, Diane E. and Pitelka, Louis F., Eds., Springer Berlin Heidelberg, 129–137.

Miller, P.A., Giesecke, T., Hickler, T., Bradshaw, R.H.W., Smith, B., Seppä, H., Valdes, P.J., Sykes, M.T., 2008. Exploring climatic and biotic controls on Holocene vegetation change in Fennoscandia. Journal of Ecology 96, 247–259.

Mitchell, T., Carter, T., Jones, P., Hulme, M., New, M., 2003. A comprehensive set of climate scenarios for Europe and the globe. Tyndall centre Working paper 55.

Morin, X., Chuine, I., 2005. Sensitivity analysis of the tree distribution model Phenofit to climatic input characteristics: implications for climate impact assessment. Global Change Biology 11, 1493–1503.

Morin, X., Thuiller, W., 2009. Comparing niche- and process-based models to reduce prediction uncertainty in species range shifts under climate change. Ecology 90, 1301–1313.

Nabel, J.E.M.S., Zurbriggen, N., Lischke, H., 2012. Impact of species parameter uncertainty in simulations of tree species migration with a spatially linked dynamic model. In: R. Seppelt, A.A. Voinov, S. Lange, D. Bankamp (Eds.) (2012): International Environmental Modelling and Software Society (iEMSs) 2012. International Congress on Environmental Modelling and Software. Managing Resources of a Limited Planet: Pathways and Visions under Uncertainty, Sixth Biennial Meeting, Leipzig, Germany.

Nakicenovic, N., Alcamo, J., Davis, G., de Vries, B., Fenhann, J., Gaffin, S., Gregory, K., Grübler, A., Jung, T.Y., Kram, T., La Rovere, E.L., Michaelis, L., Mori, S., Morita, T., Pepper, W., Pitcher, H., Price, L., Riahi, K., Roehrl, A., Rogner, H.H., Sankovski, A., Schlesinger, M., Shukla, P., Smith, S., Swart, R., van Rooijen, S., Victor, N., Z., D., 2000. IPCC Special Report on Emissions Scenarios. Cambridge University Press, Cambridge, United Kingdom and New York, NY, USA.

Nathan, R., Horvitz, N., He, Y., Kuparinen, A., Schurr, F.M., Katul, G.G., 2011. Spread of North American wind-dispersed trees in future environments. Ecology Letters 14, 211–219.

Neilson, R., Pitelka, L., Solomon, A., Nathan, R., Midgley, G., Fragoso, J., Lischke, H., Thompson, K., 2005. Forecasting Regional to Global Plant Migration in Response to Climate Change. BioScience 55, 749–759.

Noack, H., 1979. Das Portrait. Ostrya carpinifolia Scop. (Hopfenbuche). Mitteilungen der Deutschen Dendrologischen Gesellschaft, Nr 71, 257-259.

Notaro, M., 2008. Response of the mean global vegetation distribution to interannual climate variability. Climate Dynamics 30, 845–854.

Oreskes, N., Shrader-Frechette, K., Belitz, K., 1994. Verification, Validation, and Confirmation of Numerical Models in the Earth Sciences. Science 263, 641–646.

Pearson, R., 2006. Climate change and the migration capacity of species. Trends in Ecology & Evolution 21, 111–113.

Pitelka, L.F., Gardner, R.H., Ash, J., Berry, S., Gitay, H., Noble, I.R., Saunders, A., Bradshaw, R., Brubaker, L., Clark, J.S., Davis, M.B., Sugita, S., Dyer, J.M., Hengeveld, R., Hope, G., Huntley, B., King, G.A., Lavorel, S., Mack, R.N., Malanson, G.P., McGlone, M., Prentice, I.C., Rejmanek, M., 1997. Plant migration and climate change. American Scientist 85, 464–473.

Refsgaard, J.C., van der Sluijs, J.P., Højberg, A.L., Vanrolleghem, P.A., 2007. Uncertainty in the environmental modelling process – A framework and guidance. Environ. Model. Softw. 22, 1543–1556.

Rickebusch, S., Lischke, H., Bugmann, H., Guisan, A., Zimmermann, N.E., 2007. Understanding the low-temperature limitations to forest growth through calibration of a forest dynamics model with tree-ring data. Forest Ecology and Management 246, 251–263.

Rosenzweig, C., Casassa, G., Karoly, D., Imeson, A., Liu, C., Menzel, A., Rawlins, S., Root, T., Seguin, B., Tryjanowski, P., 2007. Assessment of observed changes and responses in natural and managed systems. In: Impacts, Adaptation and Vulnerability. Contribution of Working Group II to the Fourth Assessment Report of the Intergovernmental Panel on Climate Change, M.L. Parry, O.F. Canziani, J.P. Palutikof, P.J. van der Linden and C.E. Hanson, Eds., Cambridge University Press, Cambridge, UK, 79-131.

Sato, H., Ise, T., 2012. Effect of plant dynamic processes on African vegetation responses to climate change: Analysis using the spatially explicit individual-based dynamic global vegetation model (SEIB-DGVM). Journal of Geophysical Research-biogeosciences 117, G03017.

Schär, C., Vidale, P.L., Lüthi, D., Frei, C., Haberli, C., Liniger, M.A., Appenzeller, C., 2004. The role of increasing temperature variability in European summer heatwaves. Nature 427, 332–336.

Stratton, T., Price, D.T., Gajewski, K., 2011. Impacts of daily weather variability on simulations of the Canadian boreal forest. Ecological Modelling 222, 3250–3260.

Svenning, J.C., Skov, F., 2004. Limited filling of the potential range in European tree species. Ecology Letters 7, 565–573.

Svenning, J.C., Skov, F., 2007. Could the tree diversity pattern in Europe be generated by postglacial dispersal limitation? Ecology Letters 10, 453–460.

Swiss National Forest Inventory, 2004/06. Stem numbers of observed tree species (woody species, 56 classes) in the different biogeographical regions of Switzerland according to the NFI3 grid. Accessed from http://www.lfi.ch/resultate/regionen-en.php, on 28.01.2012.

Thuiller, W., Albert, C., Araújo, M.B., Berry, P.M., Cabeza, M., Guisan, A., Hickler, T., Midgley, G.F., Paterson, J., Schurr, F.M., Sykes, M.T., Zimmermann, N.E., 2008. Predicting global change impacts on plant species' distributions: Future challenges. Perspectives in Plant Ecology, Evolution and Systematics 9, 137–152.

Trenberth, K., Jones, P., Ambenje, P., Bojariu, R., Easterling, D., Tank, A.K., Parker, D., Rahimzadeh, F., Renwick, J., Rusticucci, M., Soden, B., Zhai, P., 2007. Observations: Surface and Atmospheric Climate Change. In: Climate Change 2007: The Physical Science Basis. Contribution of Working Group I to the Fourth Assessment Report of the Intergovernmental Panel on Climate Change [Solomon, S., D. Qin, M. Manning, Z. Chen, M. Marquis, K.B. Averyt, M. Tignor and H.L. Miller (eds.)]. Cambridge University Press, Cambridge, United Kingdom and New York, NY, USA.

Williams, J.W., Jackson, S.T., 2007. Novel climates, no-analog communities, and ecological surprises. Frontiers in Ecology and the Environment 5, 475–482.

Zhu, K., Woodall, C.W., Clark, J.S., 2011. Failure to migrate: lack of tree range expansion in response to climate change. Glob Change Biol 18, 1042–1052.

Zimmermann, N.E., Yoccoz, N.G., Edwards, T.C., Meier, E.S., Thuiller, W., Guisan, A., Schmatz, D.R., Pearman, P.B., 2009. Climatic extremes improve predictions of spatial patterns of tree species. Proceedings of the National Academy of Sciences 106, 19723–19728.

Appendix

Appendix 3.A Simulation setup

The assumption underlying the definition of the simulation setup was that the impact of interannual variability on explicitly simulated migration becomes most obvious in critical situations arising from the interaction of species' sensitivities to climate, competition and spatial fragmentation. Therefore, an illustrative and realistic anticipated migration situation including these critical conditions was aimed for.

3.A.1 Simulation area

A transect through the fragmented Swiss Alps was selected to achieve a successful trade-off between computational costs (area size) and required properties (competition with other tree species, spatial fragmentation and climatic limitations – here through cold temperatures). The transect was additionally chosen in a way to cover different climatic conditions and different climate transitions under the selected climate change scenario (see Section 3.B.1.1), which allowed to assess the model behaviour under different climatic situations. The southern part of the transect (Lago Maggiore up to the western parts of the Ticino) currently has a warm climate with moderate drought stress, and high temperatures with extreme drought stress projected for the future. The northern part of the transect (Swiss Plateau) currently has moderate temperatures without drought stress, and warm temperatures with little drought stress projected for the future. The Swiss Alps, in the middle of the transect, are characterised by a very cold climate without drought stress at present, and by still comparably cold temperatures under the climate change scenario.

Simulations were conducted with absorbing boundaries, i.e. seeds falling outside of the transect were lost and no seeds were dispersed into the transect from outside of the boundaries.

3.A.2 Focal species for the migration simulations

Only three of the 55 species listed as species with "statistically significant statements" in the third Swiss National Forest Inventory (NFI) (Brändli, 2010 – Table 065 page 84-85) are restricted to the southern side of the Swiss Alps (Swiss National Forest Inventory, 2004/06), namely *Quercus cerris*, *Ostrya carpinifolia* and *Fraxinus ornus*. Among these three species, *O. carpinifolia* is the most abundant (Swiss National Forest Inventory, 2004/06) and was therefore selected as focal species for the migration simulations. This decision was supported by results from a study with statistical models on tree species' range shifts conducted for the Italian peninsula (Attorre et al., 2011), where *O. carpinifolia* belonged to the few species projected to profit from climate change by means of a broader distribution, in particular towards higher altitudes. The importance of *Q. cerris* was projected to markedly decrease in the study of Attorre et al. (2011), and *F. ornus*, which is often socialised with *O. carpinifolia* (Gobet et al., 2000), was also projected to be negatively influenced by climate change. Additionally, *Quercus cerris* appeared to be least suitable for migration experiments in TreeMig, because of the slow migration found for *Quercus* species in general in a previous study with TreeMig (Meier et al., 2011).

3.A.2.1 Current and projected future distribution of *O. carpinifolia*

Ostrya carpinifolia Scop. (European Hop Hornbeam) is an important pioneer species (Puncer and Zupančič, 1982; Piškur et al., 2011), with the potential to grow under conditions which are too dry for *Fagus sylvatica* (Noack, 1979; Ellenberg, 1996; Brändli, 1998). The habitat suitability maps of the European Commission Joint Research Centre (Fig. 3.A.1), which are based on a large number of predictor variables, agree with the current

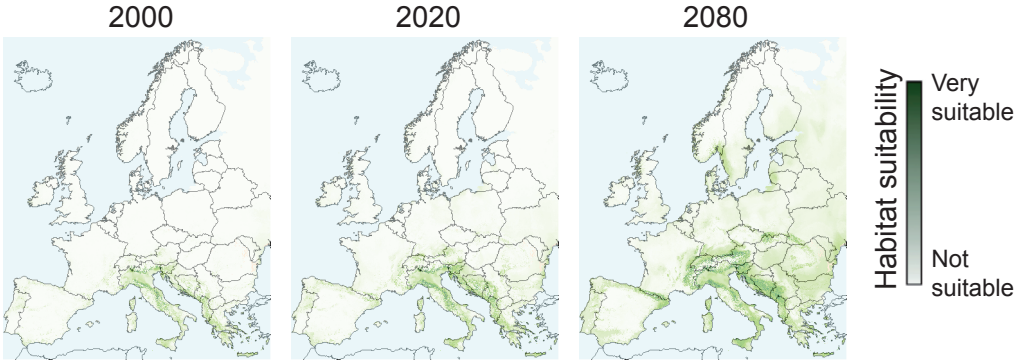

Figure 3.A.1 : Habitat suitability projected for *O. carpinifolia* in an ensemble run of the European Forest Data Center under the scenario SRESA2 (Casalegno et al., 2009) - the individual maps were downloaded from: http://efdac.jrc.ec.europa.eu/index.php/climate (European Forest Data Center, 2012).

distribution of *O. carpinifolia* and project that climate change leads to an expansion of its habitat suitability to the northern side of the Swiss Alps (European Forest Data Center, 2012). Regional simulation studies also predict substantial increase of abundance and growing stocks for *O. carpinifolia* (e.g. in Slovenia: Kobler and Kutnar, 2010 and in Italy: Attorre et al., 2011).

3.A.2.2 Representation of *O. carpinifolia* in TreeMig

The parameters used in TreeMig for *O. carpinifolia* were mostly derived from the Mediterranean mountain forest gap model GREFOS (Fyllas and Troumbis, 2009) and are listed in (Nabel et al., 2012). The functions for the maximum possible growth of *O. carpinifolia* resulting for the three values used for the parameter *minimum required* $5.5\,^{\circ}$C *degree-day sum* in the simulations are depicted in Fig. 3.A.2.

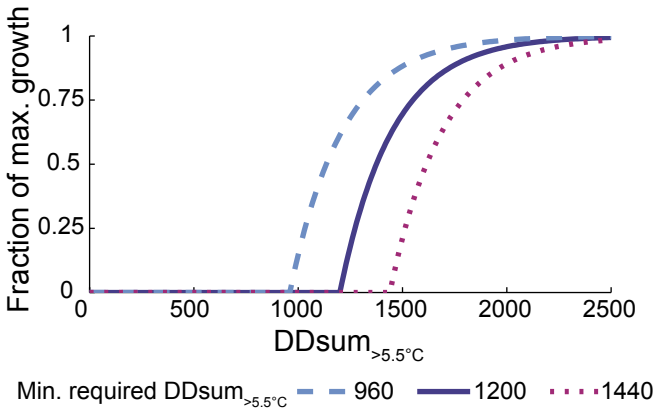

Figure 3.A.2 : Fraction of maximum growth as a function of $\mathrm{DDsum}_{>5.5\,^{\circ}\mathrm{C}}$ (sum of daily mean temperatures above $5.5\,^{\circ}$C) – one of the three bioclimate drivers in TreeMig (see Section 3.B.1). The shape of the function depends on the parameter *minimum required* $DDsum_{>5.5\,^{\circ}\mathrm{C}}$. Coloured lines depict the functions resulting from the three different values applied for *O. carpinifolia*.

The probability kernel (see Lischke et al., 2006 for more details) used for the simulated seed dispersal of *O. carpinifolia* was taken from *Carpinus betulus*, which was already parameterised in TreeMig and – like *O. carpinifolia* – belongs to the *Coryloideae* subfamily. The selected kernel allowed for slightly further dispersal than a kernel estimated from dispersal distances calculated for *O. carpinifolia* with the mechanistic wind dispersal model PAPPUS (Tackenberg, 2003) for the average falling velocity of 1.15 m/s and an average release height of 15 m (Fig. 3.A.3). The applied PAPPUS dispersal kernel, however, was calculated for lowland conditions (Tack-

enberg, personal communication), which generally tend to have shorter dispersal distances (Tackenberg and Stöcklin, 2008).

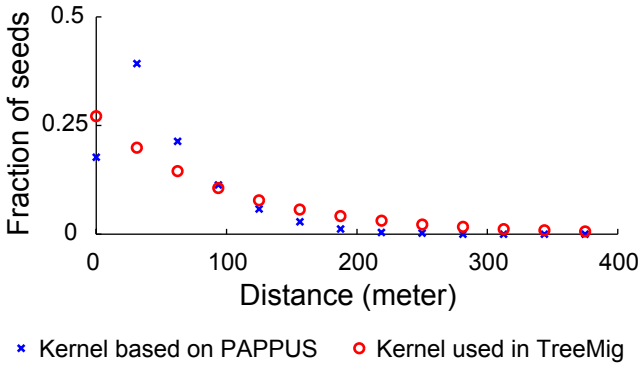

Figure 3.A.3 : Dispersal kernel applied for *O. carpinifolia* in the simulations – depicted as open circles – and a kernel calculated with PAPPUS (Tackenberg, 2003) – depicted as crosses. TreeMig's dispersal kernels are calculated with a centre to centre dispersal on a subgrid of 32m x 32m (for more details see Lischke et al., 2006). The continuous PAPPUS kernel was binned taking bin centres corresponding to this subgrid.

3.A.3 Additional species

The simulations were conducted with 21 additional species already parameterised for previous TreeMig applications (parameters from Lischke et al., 2006 altered according to the findings in Rickebusch et al., 2007), namely *Abies alba*, *Larix decidua*, *Picea abies*, *Pinus cembra*, *P. sylvestris*, *Taxus baccata*, *Acer platanoides*, *A. pseudoplatanus*, *Alnus incana*, *Betula pendula*, *Carpinus betulus*, *Castanea sativa*, *Fagus sylvatica*, *Fraxinus excelsior*, *Populus tremula*, *Quercus petraea*, *Q. pubescens*, *Sorbus aucuparia*, *Tilia cordata*, *T. platyphyllos* and *Ulmus scabra*. These species were selected as a trade-off between computational costs (number of species) and inclusion of a variety of competing species. 20 of these species (and *O. carpinifolia*) are in the list of the 30 species identified as most important for the region of Switzerland in the first Swiss National Forest Inventory (NFI1) (Brändli, 1998). Quercus pubescences was added to the simulated species because of its importance under conditions with increased drought stress. The nine NFI1 species excluded for our simulations (*Pinus mugo*, *Quercus robur*, *Sorbus aria*, *Salix alba*, *Alnus glutinosa*, *Acer campestre*, *Fraxinus ornus*, *Prunus avium* and *Robinia pseudoacacia*) either had a close related species already contained or were only sparsely present in the simulated area.

Appendix 3.B Bioclimate time series

3.B.1 Derivation of bioclimate variables and of the zero-one stockability mask

TreeMig simulations require three bioclimate input variables on an annual time-step for each cell: $\mathrm{DDsum}_{>5.5\,^\circ\mathrm{C}}$ (the sum of daily mean temperatures above $5.5\,^\circ$C), minimum winter temperature (the average temperature of the coldest winter month) and an index describing the severity of drought events. The bioclimate variables and the zero-one stockability map were calculated with a program based on ForClim-E (Bugmann and Cramer, 1998; Lischke et al., 2006), which, in turn, requires monthly average temperatures, monthly precipitation sums, as well as static information on slope and aspect of the terrain and water storage capacity for each cell.

3.B.1.1 Average temperatures and precipitation sums

Monthly average temperatures and precipitation sums for the past climate (1901-2000) were derived from the CRU data (Mitchell et al., 2003), and for the future climate (2001-2100) from SRESA1B (Nakicenovic et al., 2000) projections calculated with the regional climate model CLM (Lautenschlager et al., 2009). Both data sets were

downscaled to 30″ using WorldClim data (Hijmans et al., 2005) and subsequently projected to an Albers equal area projection[2] with 1km^2 resolution using FIMEX-0.28 (Klein, 2012) with a nearest neighbour interpolation.

3.B.1.2 Slope and aspect of the terrain and water storage capacity

To calculate the yearly drought index of a cell, the soil water balance model used in ForClim-E (Bugmann and Cramer, 1998) requires information on slope and aspect of the terrain and on water storage capacity usable for plants, the so-called bucketsize. The maps for slope and aspect were derived with the ESRI®Spatial Analyst tool in ArcMap™9.3.1 from the digital elevation model of the Shuttle Radar Topography Mission (Jarvis et al., 2008).

Information on water storage capacity was available for the transect part located in Switzerland. It has been measured for several soil types in Switzerland (Richard et al., 1978-1987) and, within their study, Löffler and Lischke (2001) used these measured capacities to calculate the bucketsize on a 1km^2 grid for the whole of Switzerland by means of a linear regression on the variables water retention potential and soil wetness found in the Swiss soil suitability map (Frei et al., 1980). Our study required additional, coherent values for the part of the transect area which lies outside of Switzerland (see main text Fig. 3.1, panel B). Therefore, the available water capacities (AWC) for top- and subsoil from the 1km^2 raster library of the European soil database (Panagos et al., 2012) and the bucketsize derived in (Löffler and Lischke, 2001) were compared for the area of Switzerland. AWC-types occurring in Switzerland were assigned by majority rule, AWC-types not occurring in Switzerland were extrapolated from the bucketsize values for the occurring types.

Similar to the climate data, slope and aspect of the terrain, as well as water storage capacity maps were projected to an Albers equal area projection with 1km^2 resolution and a nearest neighbour interpolation using FIMEX-0.28 (Klein, 2012).

3.B.1.3 Zero–one stockability mask

The stockability of the simulation area was derived directly from the bucketsize, which was based on the Swiss soil suitability map (see Section 3.B.1.2). Since this map does not provide values for solid rock surfaces and water bodies, corresponding cells were interpreted as not stockable. Land use was not considered and did not lead to additional non-stockable cells. Non-stockable cells are implemented as absorbing, i.e. seeds falling into non-stockable cells are lost.

3.B.2 Base period, derivation of the base year sets and derivation of distributions for the stochastic extrapolation

3.B.2.1 Base period

The extrapolation approaches applied in this study were all based on the last 30 years for future climate and the first 30 years for past climate, respectively. The number of base years is somewhat arbitrary. Previous studies often used 30 years (e.g. Epstein et al., 2007) or 50 years (e.g. Hickler et al., 2012) as base period. The number of years can influence the variability in a cell. Single extreme situations, for example, can have a higher influence on the variability of shorter time spans. Tests with a 50 year base period, however, did not lead to notable different simulation results in our study.

3.B.2.2 Derivation of the base year sets

As described in Section 3.B.1, the bioclimate was derived from monthly temperature and precipitation data. We tested if the time period used as base years for extrapolations (see main text Section 3.2.3.2) of future climate, i.e. 2071-2100, would contain any long-term trends. Whilst the monthly precipitation time series did not contain a noticeable long-term trend, the temperature time series for most months and cells did (Fig. 3.B.1a).

[2] See http://spatialreference.org/ref/esri/102013/ (last access date: 10.06.12).

Two separate sets of bioclimate base years were therefore derived from differently preprocessed monthly temperature time series. The first set (*bioclimate with trend* – Fig. 3.B.1, first column) was derived from the climate data as is (see Section 3.B.1). For the second set (*detrended bioclimate* – Fig. 3.B.1, second column), the average monthly temperature time series were detrended and – to achieve a continuation of the extrapolated time series – offset with the end of the trend in case of future climate (and the beginning of the trend in case of past climate, respectively). Detrending and offsetting a time series can influence its mean and standard deviation (e.g. increase in the mean $\mathrm{DDsum}_{>5.5\,^{\circ}\mathrm{C}}$ and decrease in the standard deviation in Fig. 3.B.1e compared to Fig. 3.B.1b). Fig. 3.B.1c and f show examples for extrapolations with each of the three approaches: (1) mean values extrapolation, (2) cyclic extrapolation and (3) stochastic extrapolation (see main text Section 3.2.3.2) based on the bioclimate with trend and the detrended bioclimate, respectively.

The simulation experiments described in the main text were conducted with the detrended bioclimate base years. Additionally, we conducted simulations with the bioclimate base years with trend to test if changes in the construction of the base year set leading to changes in its mean and standard deviation would lead to different results (see Appendix 3.C and Appendix 3.D).

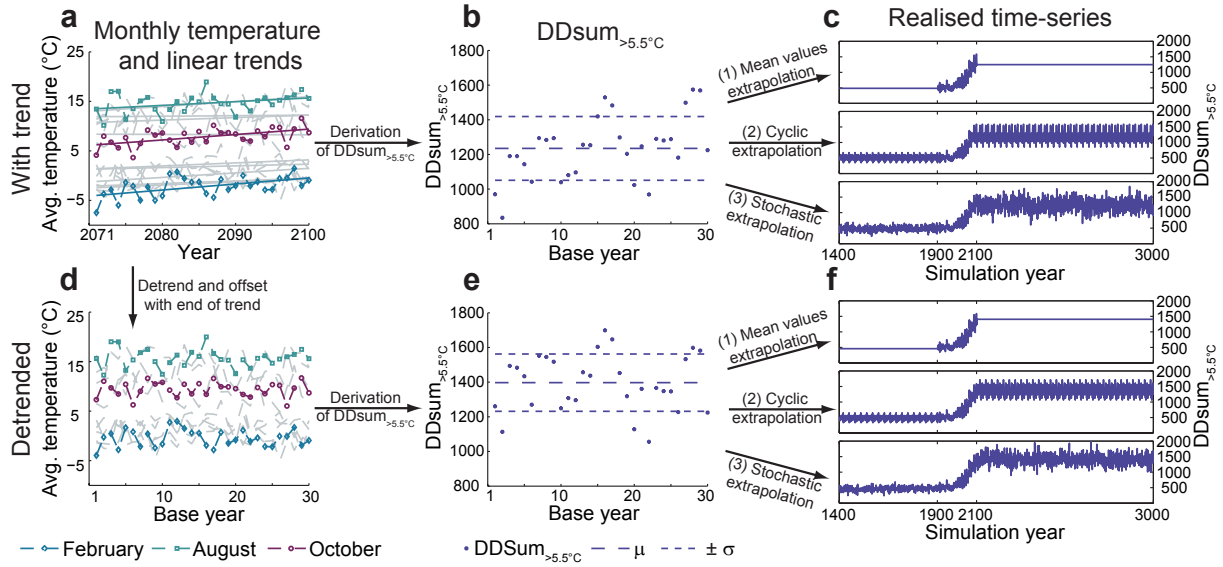

Figure 3.B.1 : Generation and extrapolation of bioclimate time series on the example of the $\mathrm{DDsum}_{>5.5\,^{\circ}\mathrm{C}}$ (sum of daily mean temperatures above $5.5\,^{\circ}\mathrm{C}$). Monthly average temperature values predicted under the climate change scenario SRESA1B for 2071 to 2100 (panel a – for a better readability three months are highlighted) were used to derive the $\mathrm{DDsum}_{>5.5\,^{\circ}\mathrm{C}}$ base years (panel b) required for the extrapolation of future time spans (panel c). Because most of the monthly temperature time series were found to contain a trend, an alternative set of $\mathrm{DDsum}_{>5.5\,^{\circ}\mathrm{C}}$ base years (panel e) was derived from the detrended and offset (= shifted to the end of the trend) temperature time series (panel d). Panel a, b, d and e depict the average conditions in the Alpine region in the centre of the transect (average of 105 to 125 transect km north and 30 to 50 transect km east – see main text Fig. 3.1b). Both sets of $\mathrm{DDsum}_{>5.5\,^{\circ}\mathrm{C}}$ base years (panel b, e) were used for the extrapolation of future bioclimate influences. Panel c and f show entire simulation time series for the different extrapolation approaches for an illustrative example cell (119 transect km north and 42 transect km east), which is representative for the average temperature conditions of the Alpine region. (1) steady application of the mean of the base period (mean values extrapolation), (2) cyclic repetition of the base period (cyclic extrapolation) and (3) stochastic sampling of the annual $\mathrm{DDsum}_{>5.5\,^{\circ}\mathrm{C}}$ from the distribution obtained from the base period (stochastic extrapolation).

3.B.2.3 Derivation of distributions for the stochastic extrapolation

The stochastic extrapolation approach used in the study (see main text Section 3.2.3.2) extrapolates the bioclimate by sampling annual bioclimate influences from probability distributions. These distributions were calculated independently for each cell and each bioclimate variable. The variables $\mathrm{DDsum}_{>5.5\,^{\circ}\mathrm{C}}$ and minimum winter temperature were assumed to be Gaussian distributed, because these variables are linear transformations of average monthly temperatures, which are approximately Gaussian distributed (Schär et al., 2004). The

index describing the severity of drought events, in contrast, is a skewed distribution with frequent zero values (Lischke, 2005). Therefore, drought stress is not only represented by a Gaussian distribution for non-zero values, but in addition by a probability for the occurrence of drought events in each cell (Lischke, 2005).

Appendix 3.C Q1 – Effects of minimum density thresholds

Ten repetitions with stochastic extrapolation (see main text Section 3.2.3.2) of both bioclimate base year sets (detrended and with trend – see Section 3.B.2.2) with no threshold and with different thresholds were conducted for all nine *Ostrya carpinifolia* parameter sets to investigate how species' migration is affected by introducing minimum density thresholds, i.e. thresholds below which a species was regarded to be absent. Fig. 3.C.1 shows snapshots of the biomass [t/ha] of *O. carpinifolia* in the year 3000 driven by one realisation of a stochastically extrapolated bioclimate time series based on the detrended bioclimate base years and simulated for three species parameter sets and without as well as with a minimum density threshold of one occurrence per km^2. Fig. 3.C.2 and Fig. 3.C.3 show the northernmost occurrences resulting for *O. carpinifolia* (Fig. 3.C.2 – detrended bioclimate and Fig. 3.C.3 – bioclimate with trend).

3.C.1 Detrended bioclimate

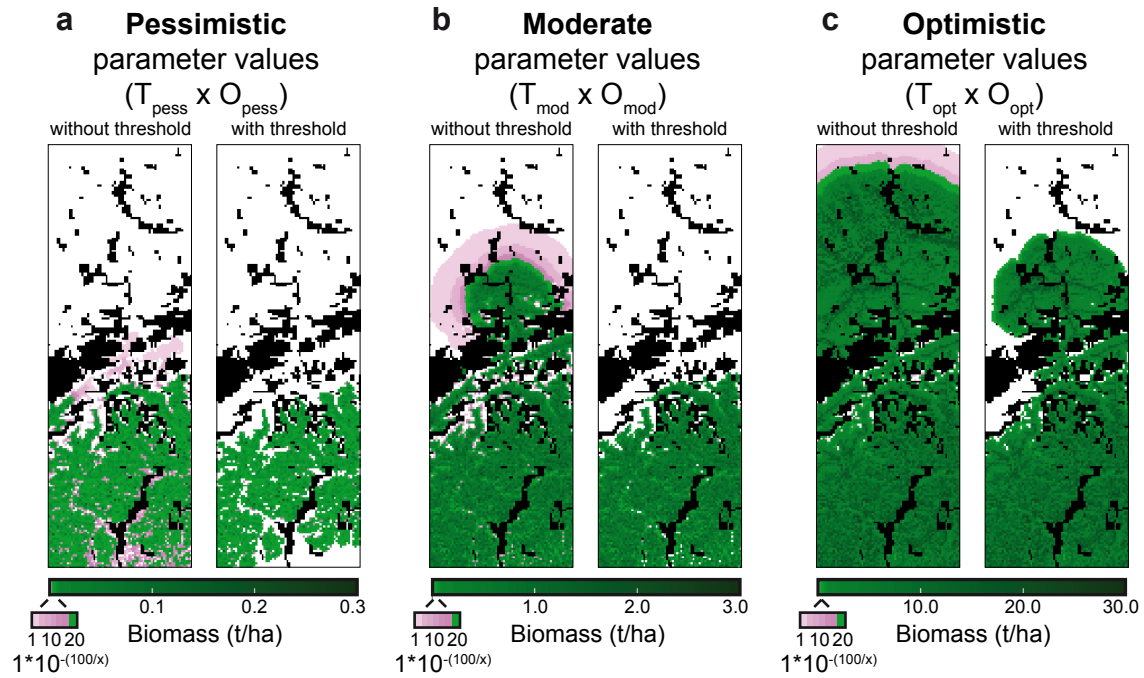

Figure 3.C.1 : Year 3000 snapshots of the biomass [t/ha] of *Ostrya carpinifolia* for simulations with no threshold and with a minimum density threshold of one occurrence per km^2, simulated with three of the nine species parameter sets used for *O. carpinifolia* (see main text Table 3.1): all pessimistic ($T_{pess} \times O_{pess}$, panel a), all moderate ($T_{mod} \times O_{mod}$, panel b) and all optimistic ($T_{opt} \times O_{opt}$, panel c). Simulations were driven by the same bioclimate time series extrapolated stochastically from detrended bioclimate base years (see Section 3.B.2.2). Resulting abundances differed for the different species parameter sets applied. The selected colour gradient highlights abundances close to zero (pink cells), illustrating the spread of infinitesimal seed fractions in simulations without a threshold. The insertion shows the colours used for values smaller than $1 \cdot 10^{-5}$ ($= 1 \cdot 10^{-(100/20)}$). White cells are not inhabited and black cells not stockable (see main text Fig. 3.1b). The biomass was plotted with ParaView 3.10.0 (Ahrens et al., 2005). Note that scales other than the insertion differ among the snapshots of the different parameter sets.

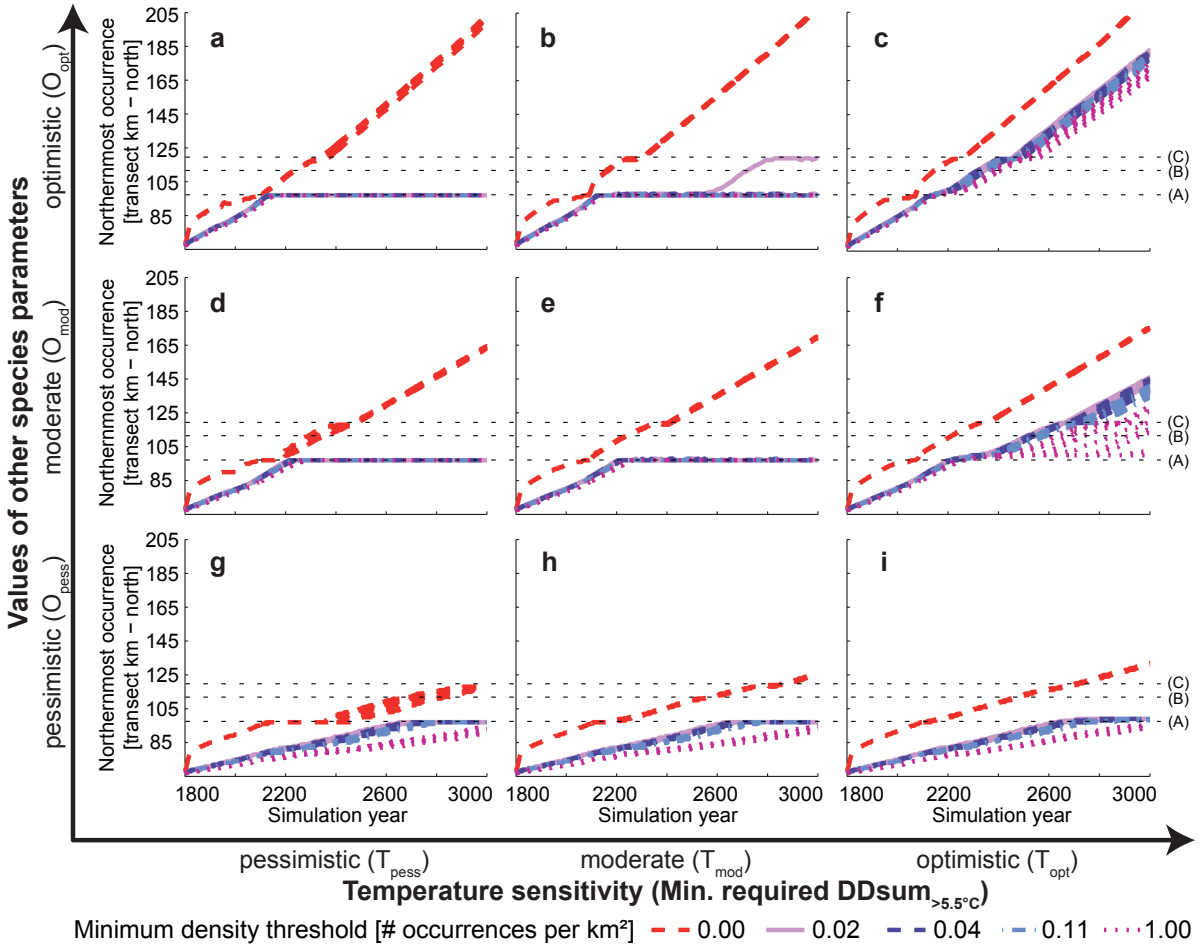

Figure 3.C.2 : Northernmost occurrence (in transect km - north, smoothed over ten years) of *Ostrya carpinifolia* resulting for simulations with bioclimate time series stochastically extrapolated based on the detrended bioclimate base years (see Section 3.B.2.2 – **detrended bioclimate**). Results from simulations for all nine species parameter sets without a density threshold and with four different thresholds are depicted. Lines with the same colour represent results for ten stochastic repetitions with the corresponding density threshold and parameter set. The dashed horizontal lines (A-C) mark the approximate location of the three main stagnation areas (see main text Fig. 3.1b).

3.C.2 Bioclimate with trend

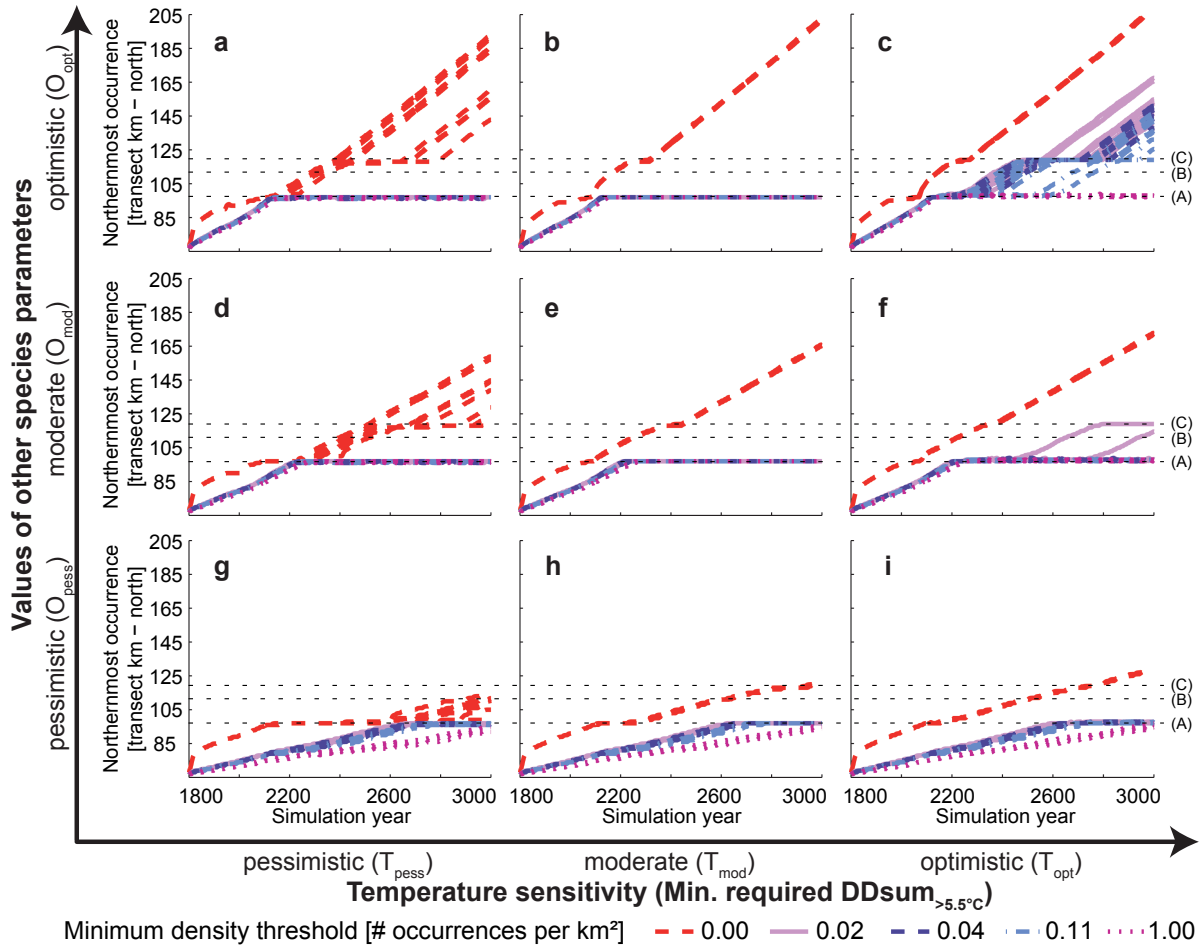

Figure 3.C.3 : Northernmost occurrence (in transect km - north, smoothed over ten years) of *Ostrya carpinifolia* resulting for simulations with bioclimate time series stochastically extrapolated based on the bioclimate base years with trend (see Section 3.B.2.2 – **bioclimate with trend**). Results from simulations for all nine species parameter sets without a density threshold and with four different thresholds are depicted. Lines with the same colour represent results for ten stochastic repetitions with the corresponding density threshold and parameter set. The dashed horizontal lines (A-C) mark the approximate location of the three main stagnation areas (see main text Fig. 3.1b).

Appendix 3.D Q2 – Comparison of different bioclimate time series

To investigate the influence of the interannual climate variability, simulations were conducted driven by differently generated (bioclimate with trend and detrended bioclimate – see Section 3.B.2.2) and extrapolated bioclimate time series (stochastic extrapolation, mean values extrapolation and cyclic extrapolation – see main text Section 3.2.3.2); without a threshold and with two different thresholds (1, and 1/9 individuals per km^2) and for all nine parameter sets applied for *Ostrya carpinifolia* (see main text Table 3.1). Illustrations for the simulated northernmost occurrences (Fig. 3.D.1 – detrended bioclimate and Fig. 3.D.3 – bioclimate with trend), as well as for the spread of *O. carpinifolia* (Fig. 3.D.2 – detrended bioclimate and Fig. 3.D.4 – bioclimate with trend) are displayed in this appendix.

3.D.1 Detrended bioclimate

3.D.1.1 Northernmost occurrence

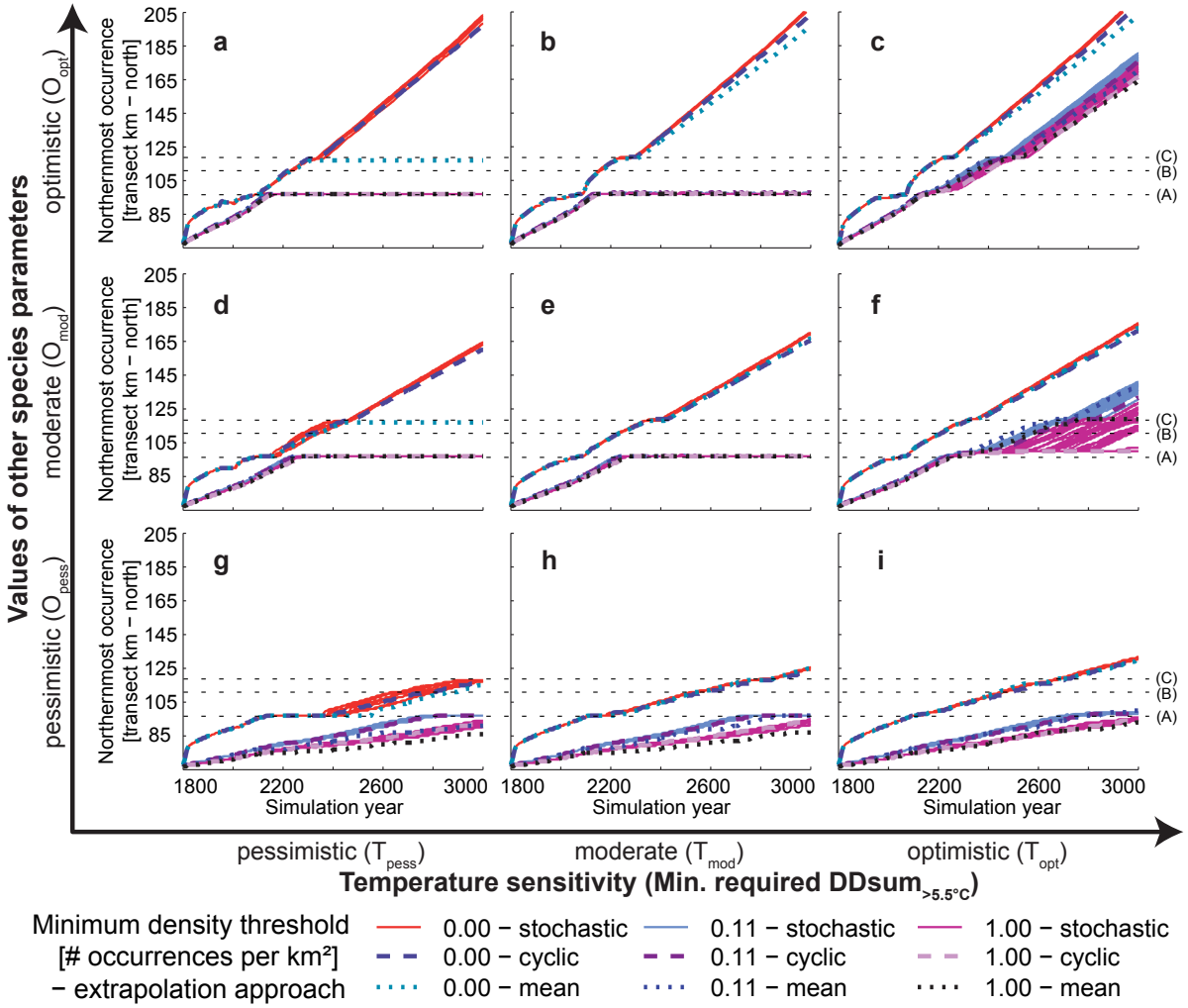

Figure 3.D.1 : Northernmost occurrence (in transect km - north, smoothed over ten years) of *Ostrya carpinifolia* resulting for simulations driven by bioclimate time series extrapolated from the detrended bioclimate base years (see Section 3.B.2.2 – **detrended bioclimate**). Results from simulations for all nine species parameter sets without a density threshold and with two different thresholds are depicted for each of the three approaches to extrapolate bioclimate time series (see main text Section 3.2.3.2). Each colour represents one combination of a density threshold and an extrapolation approach. Bioclimate time series generated with cyclic and mean values extrapolation are deterministic and are therefore represented by one line in each panel. The stochastic extrapolation was repeated 30 times for simulations with species parameter sets with the optimistic parameter value for temperature sensitivity (T_{opt} – see main text Table 3.1), else ten times. Repetitions are depicted by lines with the same colour. The dashed horizontal lines (A-C) mark the approximate location of the three main stagnation areas (see main text Fig. 3.1, panel b).

3.D.1.2 Spread – newly inhabited cells north of transect km 65

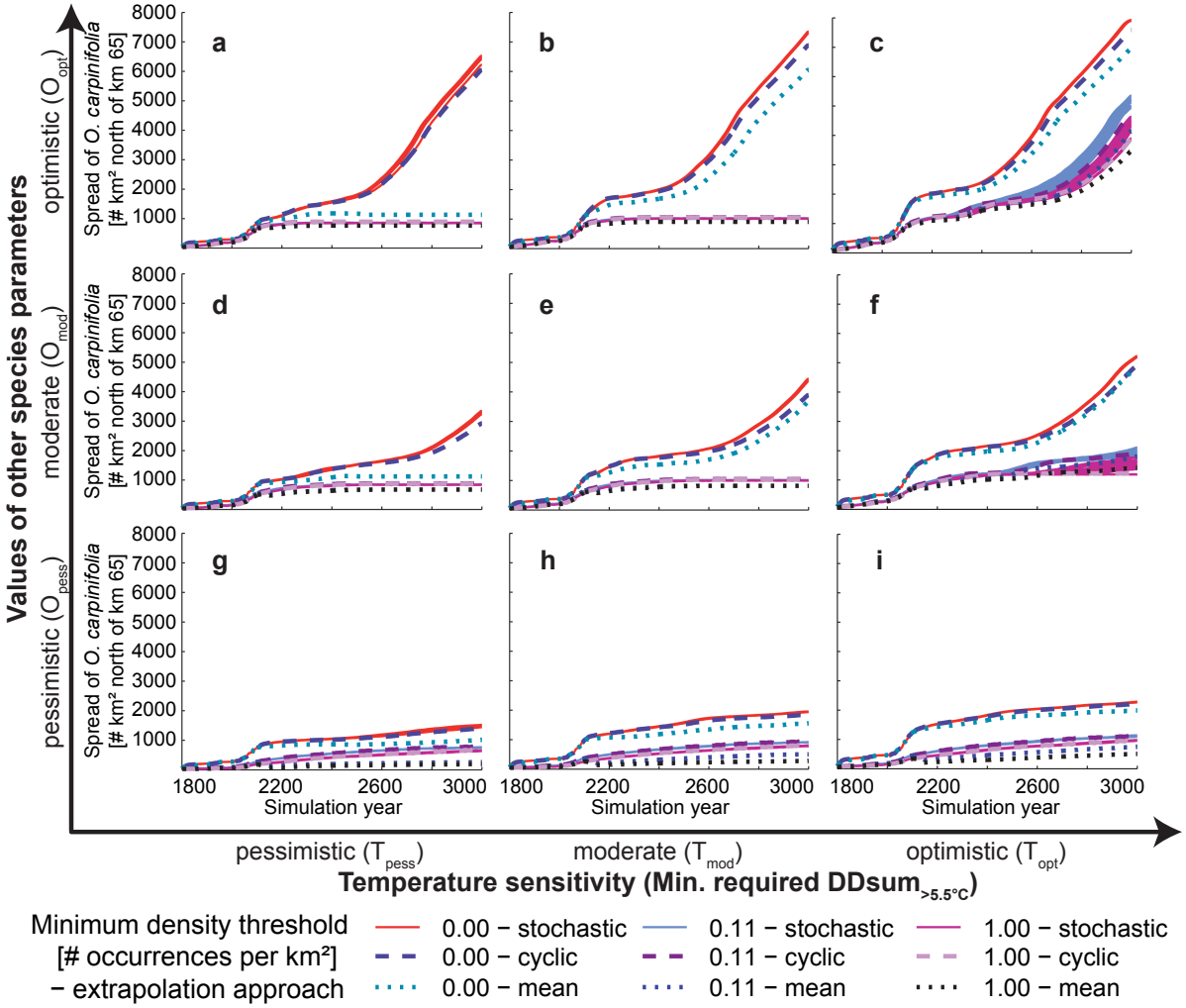

Figure 3.D.2 : Spread of *Ostrya carpinifolia* (smoothed over ten years) represented as the number of cells (km^2) newly inhabited north of transect km 65 – to where *O. carpinifolia* was restricted up to the simulation year 1800 in the migration scenario (see main text Fig. 3.1, panel b). Simulations were driven by bioclimate time series extrapolated from the detrended bioclimate base years (see Section 3.B.2.2 – **detrended bioclimate**). Results from simulations for all nine species parameter sets without a density threshold and with two different thresholds are depicted for each of the three approaches to extrapolate bioclimate time series (see main text Section 3.2.3.2). Each colour represents one combination of a density threshold and an extrapolation approach. Bioclimate time series generated with cyclic and mean values extrapolation are deterministic and are therefore represented by one line in each panel. The stochastic extrapolation was repeated 30 times for simulations with species parameter sets with the optimistic parameter value for temperature sensitivity (T_{opt} – see main text Table 3.1), else ten times. Repetitions are depicted by lines with the same colour.

3.D.2 Bioclimate with trend

3.D.2.1 Northernmost occurrence

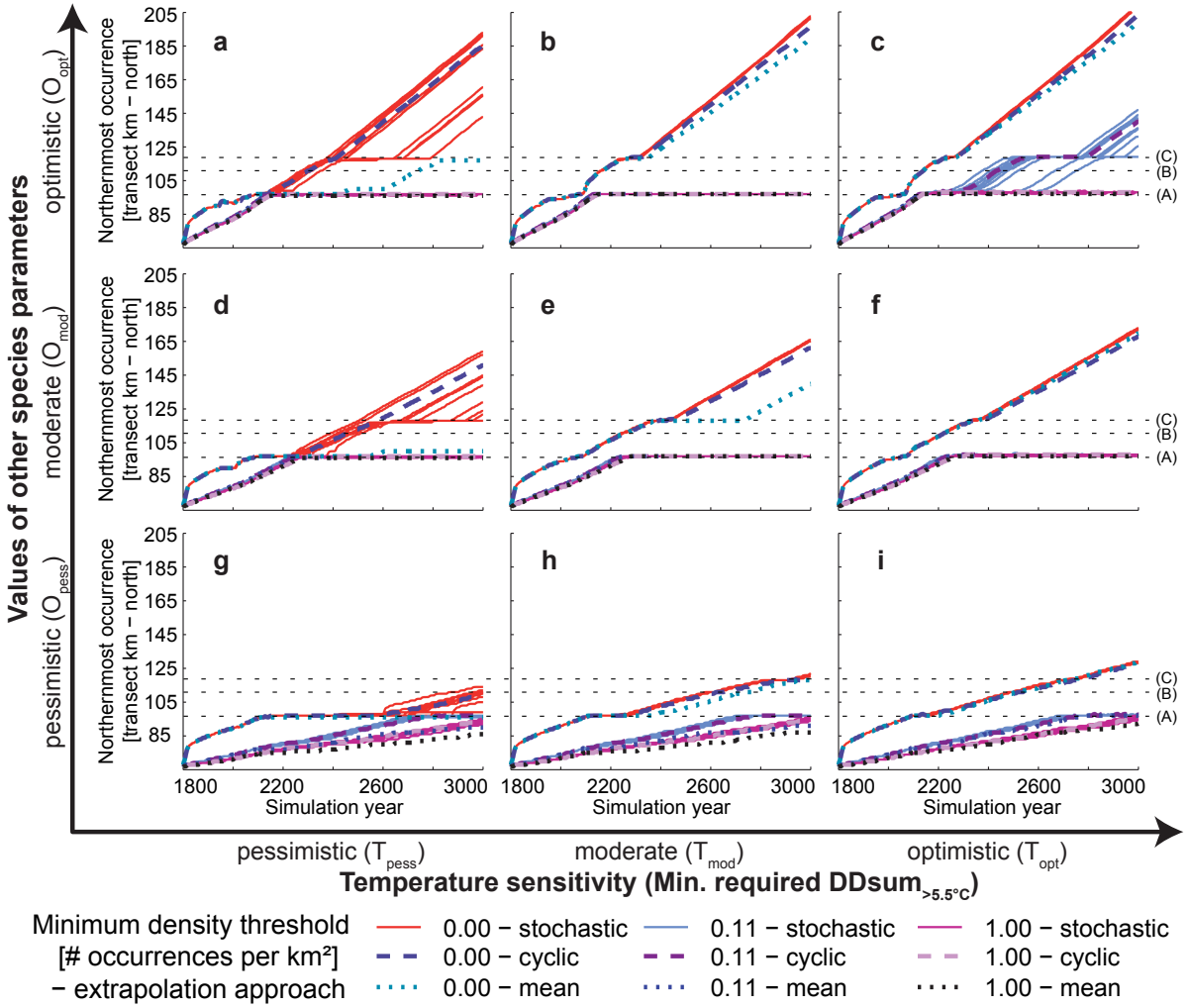

Figure 3.D.3 : Northernmost occurrence (in transect km - north, smoothed over ten years) of *Ostrya carpinifolia* resulting for simulations driven by bioclimate time series extrapolated from the bioclimate base years with trend (see Section 3.B.2.2 – **bioclimate with trend**). Results from simulations for all nine species parameter sets without a density threshold and with two different thresholds are depicted for each of the three approaches to extrapolate bioclimate time series (see main text Section 3.2.3.2). Each colour represents one combination of a density threshold and an extrapolation approach. Bioclimate time series generated with cyclic and mean values extrapolation are deterministic and are therefore represented by one line in each panel. The stochastic extrapolation was repeated ten times for each combination and these repetitions are depicted by lines with the same colour. The dashed horizontal lines (A-C) mark the approximate location of the three main stagnation areas (see main text Fig. 3.1, panel b).

3.D.2.2 Spread – newly inhabited cells north of transect km 65

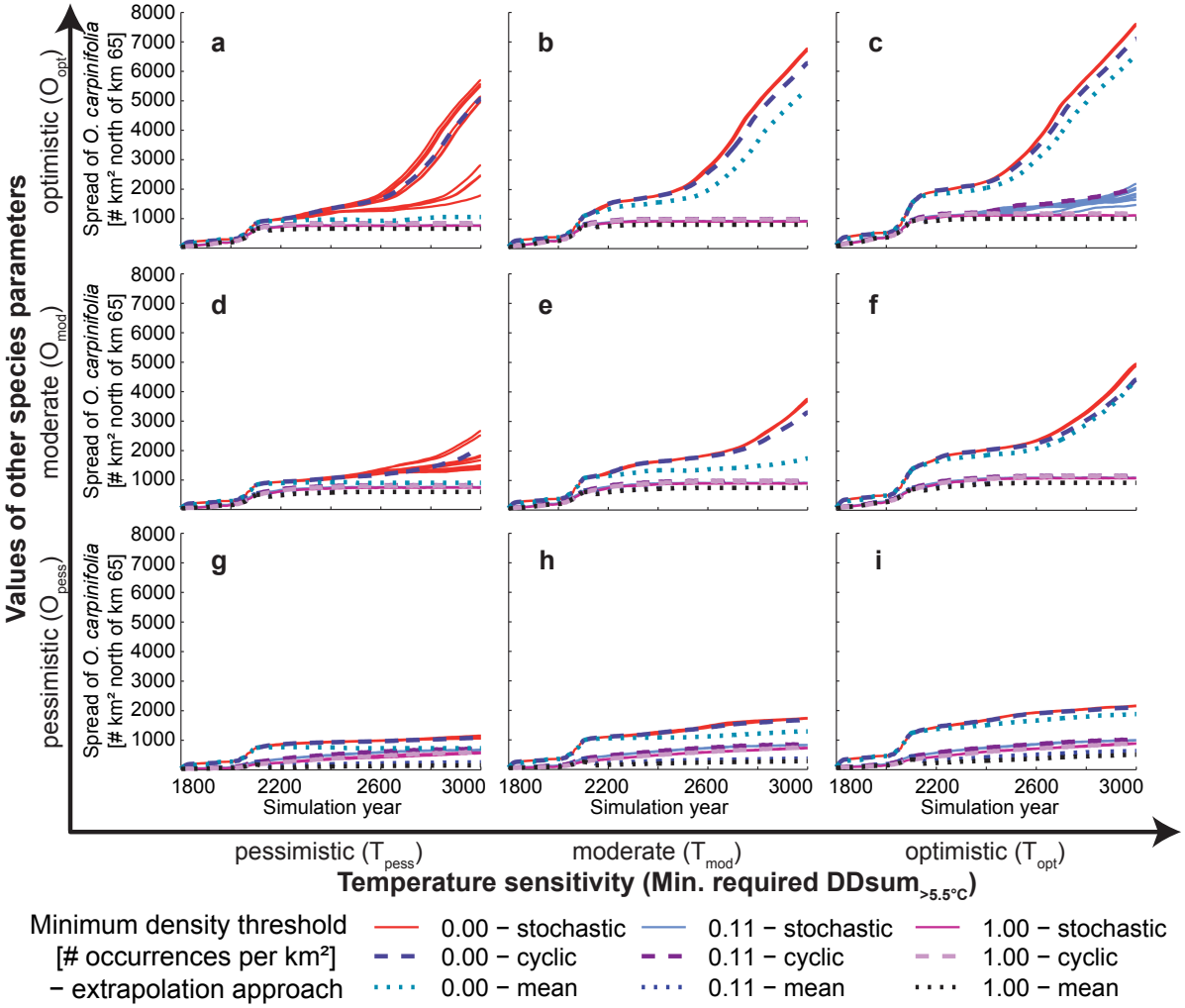

Figure 3.D.4 : Spread of *Ostrya carpinifolia* (smoothed over ten years) represented as the number of cells (km^2) newly inhabited north of transect km 65 – to where *O. carpinifolia* was restricted up to the simulation year 1800 in the migration scenario (see main text Fig. 3.1, panel b). Simulations were driven by bioclimate time series extrapolated from the bioclimate base years with trend (see Section 3.B.2.2 – **bioclimate with trend**). Results from simulations for all nine species parameter sets without a density threshold and with two different thresholds are depicted for each of the three approaches to extrapolate bioclimate time series (see main text Section 3.2.3.2). Each colour represents one combination of a density threshold and an extrapolation approach. Bioclimate time series generated with cyclic and mean values extrapolation are deterministic and are therefore represented by one line in each panel. The stochastic extrapolation was repeated ten times for each combination and these repetitions are depicted by lines with the same colour.

References

Ahrens, J., Geveci, B., Law, C., 2005. ParaView: An End-User Tool for Large-Data Visualization, in: Hansen, C.D., Johnson, C.R. (Eds.), Visualization Handbook. Butterworth-Heinemann.

Attorre, F., Alfò, M., De Sanctis, M., Francesconi, F., Valenti, R., Vitale, M., Bruno, F., 2011. Evaluating the effects of climate change on tree species abundance and distribution in the Italian peninsula. Applied Vegetation Science 14, 242–255.

Brändli, U.B., 1998. Die häufigsten Waldbäume der Schweiz. Ergebnisse aus dem Landesforstinventar 1983-85: Verbreitung, Standort und Häufigkeit von 30 Baumarten. Berichte der Eidgenöss. Forschungsanstalt für Wald, Schnee und Landschaft.

Brändli, U.B., 2010. (Red.): Schweizerisches Landesforstinventar. Ergebnisse der dritten Erhebung 2004–2006. Birmensdorf, Eidgenössische Forschungsanstalt für Wald, Schnee und Landschaft WSL. Bern, Bundesamt für Umwelt, BAFU. 312 S.

Bugmann, H., Cramer, W., 1998. Improving the behaviour of forest gap models along drought gradients. Forest Ecology and Management 103, 247–263.

Casalegno, S., Amatulli, G., Camia, A., Nelson, A., Pekkarinen, A., 2009. Vulnerability of Pinus cembra L. in the Alps and the Carpathian mountains under present and future climates. Forest Ecology and Management 259, 750–761.

Ellenberg, H., 1996. Vegetation Mitteleuropas mit den Alpen. Hohenheim, Germany.

Epstein, H., Yu, Q., Kaplan, J., Lischke, H., 2007. Simulating Future Changes in Arctic and Subarctic Vegetation. Computing in Science Engineering 9, 12–23.

European Forest Data Center, 2012. Habitat suitability for *Ostrya Carpinifolia* in an ensemble run under the scenario SRESA2. Accessed from http://efdac.jrc.ec.europa.eu/index.php/climate, on 28.01.2012.

Frei, E., Vökt, U., R., F., Brunner, H., Schai, F., 1980. Bodeneignungskarte der Schweiz auf Grund der Bodeneigenschaften ausgewählter physiographischer Landschaftselemente. Bundesämter für Raumplanung, Landwirtschaft und Forstwesen. Bern.

Fyllas, N.M., Troumbis, A.Y., 2009. Simulating vegetation shifts in north-eastern Mediterranean mountain forests under climatic change scenarios. Global Ecology and Biogeography 18, 64–77.

Gobet, E., Tinner, W., Hubschmid, P., Jansen, I., Wehrli, M., Ammann, B., Wick, L., 2000. Influence of human impact and bedrock differences on the vegetational history of the Insubrian Southern Alps. Vegetation History and Archaeobotany 9, 175–187.

Hickler, T., Vohland, K., Feehan, J., Miller, P.A., Smith, B., Costa, L., Giesecke, T., Fronzek, S., Carter, T.R., Cramer, W., Kühn, I., Sykes, M.T., 2012. Projecting the future distribution of European potential natural vegetation zones with a generalized, tree species-based dynamic vegetation model. Global Ecology and Biogeography 21, 50–63.

Hijmans, R.J., Cameron, S.E., Parra, J.L., Jones, P.G., Jarvis, A., 2005. Very high resolution interpolated climate surfaces for global land areas. International Journal of Climatology 25, 1965–1978.

Jarvis, A., Reuter, H., Nelson, A., Guevara, E., 2008. Hole-filled SRTM for the globe Version 4. Available from the CGIAR-CSI SRTM 90m Database http://srtm.csi.cgiar.org.

Klein, H., 2012. FIMEX-0.28. https://wiki.met.no/fimex/start. Last access date: 09.01.12.

Kobler, A., Kutnar, L., 2010. Potential forest change in Slovenia due to climate warming. Small Scale Forestry in a Changing World: Opportunities and Challenges and the Role of Extension and Technology Transfer, IUFRO Conference: 3.08 Small Scale Forestry, 6.06.02 Extension, 6.06.01 Technology Transfer.

Lautenschlager, M., Keuler, K., Wunram, C., Keup-Thiel, E., Schubert, M., Will, A., Rockel, B., Boehm, U., 2009. Climate Simulation with CLM, Scenario A1B run no.1, Data Stream 3: European region MPI-M/MaD. World Data Center for Climate. http://dx.doi.org/10.1594/WDCC/CLM_A1B_1_D3.

Lischke, H., 2005. Modeling tree species migration in the Alps during the Holocene: What creates complexity? Ecological Complexity 2, 159–174.

Lischke, H., Zimmermann, N.E., Bolliger, J., Rickebusch, S., Löffler, T.J., 2006. TreeMig: A forest-landscape model for simulating spatio-temporal patterns from stand to landscape scale. Ecological Modelling 199, 409–420.

Löffler, T.J., Lischke, H., 2001. Incorporation and influence of variability in an aggregated forest model. Natural Resource Modeling 14, 103–137.

Meier, E.S., Lischke, H., Schmatz, D.R., Zimmermann, N.E., 2011. Climate, competition and connectivity affect future migration and ranges of European trees. Global Ecology and Biogeography 21, 164–178.

Mitchell, T., Carter, T., Jones, P., Hulme, M., New, M., 2003. A comprehensive set of climate scenarios for Europe and the globe. Tyndall centre Working paper 55.

Nabel, J.E.M.S., Zurbriggen, N., Lischke, H., 2012. Impact of species parameter uncertainty in simulations of tree species migration with a spatially linked dynamic model. In: R. Seppelt, A.A. Voinov, S. Lange, D. Bankamp (Eds.) (2012): International Environmental Modelling and Software Society (iEMSs) 2012. International Congress on Environmental Modelling and Software. Managing Resources of a Limited Planet: Pathways and Visions under Uncertainty, Sixth Biennial Meeting, Leipzig, Germany.

Nakicenovic, N., Alcamo, J., Davis, G., de Vries, B., Fenhann, J., Gaffin, S., Gregory, K., Grübler, A., Jung, T.Y., Kram, T., La Rovere, E.L., Michaelis, L., Mori, S., Morita, T., Pepper, W., Pitcher, H., Price, L., Riahi, K., Roehrl, A., Rogner, H.H., Sankovski, A., Schlesinger, M., Shukla, P., Smith, S., Swart, R., van Rooijen, S., Victor, N., Z., D., 2000. IPCC Special Report on Emissions Scenarios. Cambridge University Press, Cambridge, United Kingdom and New York, NY, USA.

Noack, H., 1979. Das Portrait. Ostrya carpinifolia Scop. (Hopfenbuche). Mitteilungen der Deutschen Dendrologischen Gesellschaft, Nr 71, 257-259.

Panagos, P., Van Liedekerke, M., Jones, A., Montanarella, L., 2012. European Soil Data Centre: Response to European policy support and public data requirements. Land Use Policy 29, 329–338.

Piškur, B., Pavlic, D., Slippers, B., Ogris, N., Maresi, G., Wingfield, M., Jurc, D., 2011. Diversity and pathogenicity of Botryosphaeriaceae on declining Ostrya carpinifolia in Slovenia and Italy following extreme weather conditions. European Journal of Forest Research 130, 235–249.

Puncer, I., Zupančič, M., 1982. Die ökologische und wirtschaftliche Bedeutung der Ostrya carpinifolia Scop. in Slowenien. Studia Geobotanica. Vol. 2, OSTRYA - SYMPOSIUM, p.25-32.

Richard, F., Lüscher, P., Strobel, T., 1978-1987. Physikalische Eigenschaften von Böden der Schweiz. Vol. 1- 1978, 2-1981, 3-1983, 4-1987. Eidgenössische Anstalt für das forstliche Versuchswesen, Birmensdorf, Switzerland.

Rickebusch, S., Lischke, H., Bugmann, H., Guisan, A., Zimmermann, N.E., 2007. Understanding the low-temperature limitations to forest growth through calibration of a forest dynamics model with tree-ring data. Forest Ecology and Management 246, 251–263.

Schär, C., Vidale, P.L., Lüthi, D., Frei, C., Haberli, C., Liniger, M.A., Appenzeller, C., 2004. The role of increasing temperature variability in European summer heatwaves. Nature 427, 332–336.

Swiss National Forest Inventory, 2004/06. Stem numbers of observed tree species (woody species, 56 classes) in the different biogeographical regions of Switzerland according to the NFI3 grid. Accessed from http://www.lfi.ch/resultate/regionen-en.php, on 28.01.2012.

Tackenberg, O., 2003. Modeling Long-Distance Dispersal of Plant Diaspores by Wind. Ecological Monographs 73, 173–189.

Tackenberg, O., Stöcklin, J., 2008. Wind dispersal of alpine plant species: A comparison with lowland species. Journal of Vegetation Science 19, 109–118.

Chapter 4

Extrapolation methods for climate time series revisited – spatial correlations in climatic fluctuations influence simulated tree species abundance and migration

In Revision at Ecological Complexity

Julia E. M. S. Nabel[a,b,c], *James W. Kirchner*[b], *Natalie Zurbriggen*[a], *Felix Kienast*[a], *Heike Lischke*[a]

[a]*Landscape Dynamics, Swiss Federal Institute for Forest, Snow and Landscape Research WSL, Zürcherstrasse 111, 8903 Birmensdorf, Switzerland*
[b]*Department of Environmental Systems Science, Swiss Federal Institute of Technology ETH, 8092 Zurich, Switzerland*
[c]*now at: Max Planck Institute for Meteorology, Bundesstrasse 53, 20146 Hamburg, Germany*

Abstract

Simulations of tree population dynamics under past and future climatic changes with time- and space-discrete models often suffer from a lack of detailed long-term climate time series that are required to drive these models. Inter- and extrapolation methods which are applied to generate long-term series differ in terms of whether they do or do not account for spatial correlation of climatic fluctuations. In this study we compared tree species abundance and migration outcomes from simulations using extrapolation methods generating spatially correlated (SC) and spatially independent (SI) climatic fluctuations. We used the spatially explicit and linked forest-landscape model TreeMig and a simple cellular automaton to demonstrate that spatial correlation of climatic fluctuations affects simulation outcomes. We conclude that methods to generate long-term climate time series should account for the spatial correlation of climatic fluctuations found in available climate records when simulating tree species abundance and migration.

4.1 Introduction

Climate is regarded as the main determinant of species ranges on broad geographical scales (Pearson and Dawson, 2003; Rosenzweig et al., 2007; Normand et al., 2011). Many processes in the life cycle of plants, such as growth, survival and reproduction, are affected by climatic conditions, whereby long-term trends as well as climatic fluctuations are influential (Brubaker, 1986; Laakso et al., 2001; Jackson et al., 2009). Climatic changes induce changes of ecosystems, including shifts of species ranges and changes in species compositions (Lyford et al., 2003; Rosenzweig et al., 2007; Midgley et al., 2007). These changes, however, seldom occur abruptly but rather slowly, and especially long-lived ecosystems such as forests show lag effects in their reactions to climatic

changes because of the slow nature of tree population dynamics (Pitelka et al., 1997; Fischlin et al., 2007; Sato and Ise, 2012). Therefore, simulations of such ecosystems need to be conducted for long time spans.

Tree population dynamics under past and future climatic changes are often studied with time- and space-discrete models. Studies range from simulations of single sites (e.g. Bugmann, 2001; Giesecke et al., 2010) to spatially explicit simulations with and without spatial linkage of the simulated grid cells (e.g. Lischke et al., 2012; Hickler et al., 2012). One of the main problems of simulation studies for long time spans is the availability of climate data. For simulations of the past often only proxy data for sparse points in time is available, for example from lake sediments or tree rings. From such proxy data climate anomalies can be derived, ranging from 1000-year time periods (e.g. Miller et al., 2008; Giesecke et al., 2010) or approximately 250-year time periods (e.g. Lischke, 2005) to, at the best, around 10 to 20-year time periods (e.g. Lischke et al., 2012). Thus, they miss crucial short-term fluctuations. For simulations of the future, detailed climate projections often only reach until 2100, which is not sufficient to study slow tree population dynamics (Bugmann, 2001; Hickler et al., 2012), especially not trends in tree species migration (Nabel et al., 2013; see Chapter 3).

Generally, to obtain long-term climate drivers with daily, monthly or yearly resolution, past and future climate time series often need to be interpolated or extrapolated. Due to the influence of climate variability on tree population dynamics, the most simplistic approaches, such as linear interpolation, or extrapolation by steadily applying mean values, are not appropriate (Giesecke et al., 2010 and Nabel et al., 2013; see Chapter 3). More sophisticated inter- and extrapolation methods use selected base periods of available climate time series to generate climatic fluctuations. Such methods can directly use the 'empirical distribution' given by the climatic fluctuations that are actually observed in the base years or can sample from probability distributions derived from the statistical properties of the base years. Concordantly, Bugmann (2001) listed three methods applied in forest gap models to extrapolate climatic conditions, namely (1) cyclically repeating available records, (2) randomly selecting from available records and (3) generating random series based on probability distributions derived from available records. Bugmann (2001) recommended the third approach for the application with forest gap models. This approach also has been used in various simulations with the spatially explicit and linked forest-landscape model TreeMig (see e.g. Lischke, 2005; Epstein et al., 2007; Lischke et al., 2012 and Nabel et al., 2013; see Chapter 3). In these TreeMig simulations climatic fluctuations were sampled independently for each single cell of the simulated area.

Whilst sampling from probability distributions might be recommended for forest gap models, which simulate single stands, we question whether it is suitable for models, such as TreeMig, that simulate a landscape of spatially explicit and linked cells. When sampling climatic fluctuations independently for each cell of a landscape, the spatial correlation in the climatic fluctuations among cells is lost and we hypothesise that this eventually could influence spatial correlations of simulated population dynamics. However, biological processes do not necessarily respond linearly to climate drivers (Laakso et al., 2001) and spatial correlation in climatic fluctuations therefore does not automatically have to translate into spatially correlated biotic responses, particularly not in spatially heterogeneous environments (Grenfell et al., 2000; Greenman and Benton, 2001; Currie, 2007). Nevertheless, many studies found that synchronous climatic fluctuations can lead to synchronisations in population dynamics of various (animal and plant) taxa (Koenig, 2002; Liebhold et al., 2004). Examples for observed synchronised events in tree population dynamics attributed to spatial correlations in fluctuations of climatic drivers are synchronised masting behaviour (Koenig and Knops, 2013), pulses of range expansion in favourable years (Lyford et al., 2003; Jackson et al., 2009) and synchronised mortality events in unfavourable years (Breshears et al., 2005). Sampling random fluctuations independently for each cell of a simulation area in order to inter- or extrapolate a climate driver removes such potential synchronisations and we hypothesise that this will affect simulated tree species abundance and migration. Studies on invasive species already demonstrated the importance of climatic fluctuations and of static spatial heterogeneity for migrating species (e.g. With, 2002; Hui et al., 2011). However, the combination, i.e. spatiotemporal heterogeneity (sensu Melbourne et al., 2007), has so far not been well studied (With, 2002; Melbourne et al., 2007; Hui et al., 2011). Furthermore, results of previous studies on the influence of static spatial heterogeneity are not simply transferable to the case studied here, because neglecting the spatial correlation in the fluctuations of a climate driver does not disturb the underlying spatial heterogeneity given

by the mean of the climate driver.

In summary, the overall research questions are whether neglecting spatial correlation in climatic fluctuations (1) leads to a loss in the synchronisation of species abundances and (2) affects simulated tree species migration.

In this study, we used the intermediate-complexity forest-landscape model TreeMig to test for effects of spatial correlation in climatic fluctuations on tree species abundance and migration outcomes. These tests were conducted with an illustrative example setup, simulating the northwards migration of a sub-Mediterranean tree species on a transect through the Swiss Alps (Fig. 4.1). This example was selected because it proved to be sensitive to different realisations of TreeMigs bioclimate drivers in previous studies (Nabel et al., 2012, 2013; see Chapters 2 and 3). The large number of interacting processes and species parameters in TreeMig (see Lischke et al., 2006) hampers a detailed analysis of the influence of spatial correlation in bioclimatic fluctuations on tree species migration. Therefore, we additionally developed a simple individual-based cellular automaton focussing on the first steps required for tree species migration, namely availability of seeds (linked to the presence of adults), germination and survival to maturity. Germination and survival to maturity are critical steps, since juveniles are often more susceptible to climatic influences than adults (Lyford et al., 2003; Jackson et al., 2009). Furthermore, these first steps were the primary bottleneck for migration in previous TreeMig simulations of the illustrative example setup (Nabel et al., 2013; see Chapter 3).

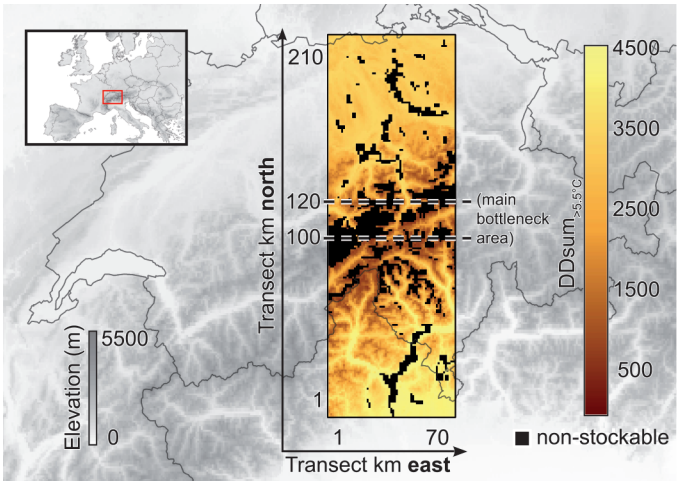

Figure 4.1 : Transect through the climatically heterogeneous and fragmented landscape of the Swiss Alps (210km x 70km; grid-cell size 1km^2). Background: digital elevation model from Jarvis et al. (2008). Colour-gradient: mean value of one of TreeMigs bioclimate variables – the $DDsum_{>5.5\,°C}$ (sum of daily mean temperatures above $5.5\,°C$) for the simulation years 2071-2100 (see Section 4.2.1.3). In this study, the shown transect was used as simulation area in applications of the model TreeMig. Black cells represent cells where trees cannot grow (non-stockable in TreeMig), here: solid rock surfaces and large water bodies. The area between the dashed lines (100^{th} to 120^{th} transect km north) approximately corresponds to the main bottleneck area of the transect.

4.2 Methods

4.2.1 TreeMig

TreeMig is a multi-species, spatially linked and dynamic intermediate-complexity model simulating forest landscapes (Lischke et al., 2006). TreeMig's state variables are height-structured population densities per species. Local stand dynamics are represented by seed-bank dynamics, germination, growth, death and seed production (Lischke et al., 2006; Lischke and Löffler, 2006). The spatial linkage among cells is realised via seed dispersal applying a deterministic dispersal kernel composed of two negative exponentials that are parameterised ac-

cording to dispersal properties of the simulated species (Lischke and Löffler, 2006). TreeMig accounts for inter- and intra-specific competition for light by modulating the local stand dynamics according to light availability (Lischke et al., 2006). Due to the represented processes, TreeMig has the rare advantage of simultaneously allowing for explicit simulation of tree species migration and of inter-specific competition (Lischke et al., 2006 and Nabel et al., 2013; see Chapter 3).

Table 4.1 : Influence of the three bioclimate variables used in TreeMig on TreeMig's processes. All listed processes are additionally influenced by inter-specific competition. For a detailed documentation of TreeMig's processes see (Lischke et al., 2006).

	$DDsum_{>5.5\,^\circ C}$[a]	*Min. WiTemp*[b]	*Drought severity*
Germination	threshold, absolute	threshold, absolute	–
Mortality	threshold, multiplicative thinning effect	–	threshold, multiplicative thinning effect
Growth	asymptotic	–	linear decay with threshold

[a] Sum of daily mean temperatures above $5.5\,^\circ$C. [b] Minimum winter-temperature.

4.2.1.1 Influence of bioclimate variables in TreeMig

TreeMig simulations are driven by three annual bioclimate variables: the sum of daily mean temperatures above $5.5\,^\circ$C ($DDsum_{>5.5\,^\circ C}$), the minimum winter temperature (*Min. WiTemp*) and an index representing the severity of drought events (*Drought severity*). These bioclimate variables were derived from observed (1901-2000) and projected (2001-2100) monthly climate data. $DDsum_{>5.5\,^\circ C}$ and *Min. WiTemp* were derived from monthly average temperatures and *Drought severity* from monthly average temperatures, monthly precipitation sums, water storage capacity as well as slope and aspect of each simulation cell. A detailed description and data sources are given in the electronic supplementary material (ESM). The three bioclimate variables influence different TreeMig processes (see Table 4.1). For successful germination *Min. WiTemp* and $DDsum_{>5.5\,^\circ C}$ need to exceed a species-specific threshold. The maximum possible annual growth of a species is asymptotically influenced by $DDsum_{>5.5\,^\circ C}$ (Rickebusch et al., 2007) and decays as a function of *Drought severity* (Lischke et al., 2006). Mortality is directly influenced when $DDsum_{>5.5\,^\circ C}$ or *Drought severity* exceed a species-specific threshold and indirectly influenced when growth is depleted (Lischke et al., 2006).

4.2.1.2 Methods to extrapolate TreeMig's bioclimate drivers

In previous TreeMig versions, bioclimate time series were inter- or extrapolated by sampling the bioclimate for each year and each cell independently from probability distributions (Lischke et al., 2006). These probability distributions were derived from a selected base period (see e.g. Lischke, 2005; Epstein et al., 2007; Lischke et al., 2012). Thereby the $DDsum_{>5.5\,^\circ C}$, for example, was approximated with an independent normal distribution for each cell of the simulation area (Lischke et al., 2006; Nabel et al., 2013; see Chapter 3). For this study TreeMig (**TreeMig-Netcdf 2.0**) was equipped with two additional methods, which both sample uniformly from the empirical distribution found in the base period, i.e. from the bioclimatic values that actually occur in the base years.

Spatially independent drawing (SI) With this method, the bioclimate of a year is sampled independently from the empirical distribution found in the base years for each cell, i.e. for each cell one base year is drawn (Fig. 4.2a). This base year is used for all bioclimate variables in the cell.

Spatially correlated drawing (SC) When selecting this method, a complete bioclimate map is drawn each year from the base-year set and its values are used for all cells of the simulation area (Fig. 4.2d) and all bioclimate variables.

SI drawing is a simplification of drawing from probability distributions because sampling from probability distributions also allows values outside of the range of the empirical distribution, i.e. outside of the range of the values that actually occur in the base years (Bugmann, 2001). We introduced this simplification to exclude effects solely caused by extreme values, which were not contained in the empirical distribution but were possible when drawing from derived probability distributions. Such effects could else have interfered with effects of spatial correlation in the bioclimate variables when comparing the simulation results for different extrapolation methods.

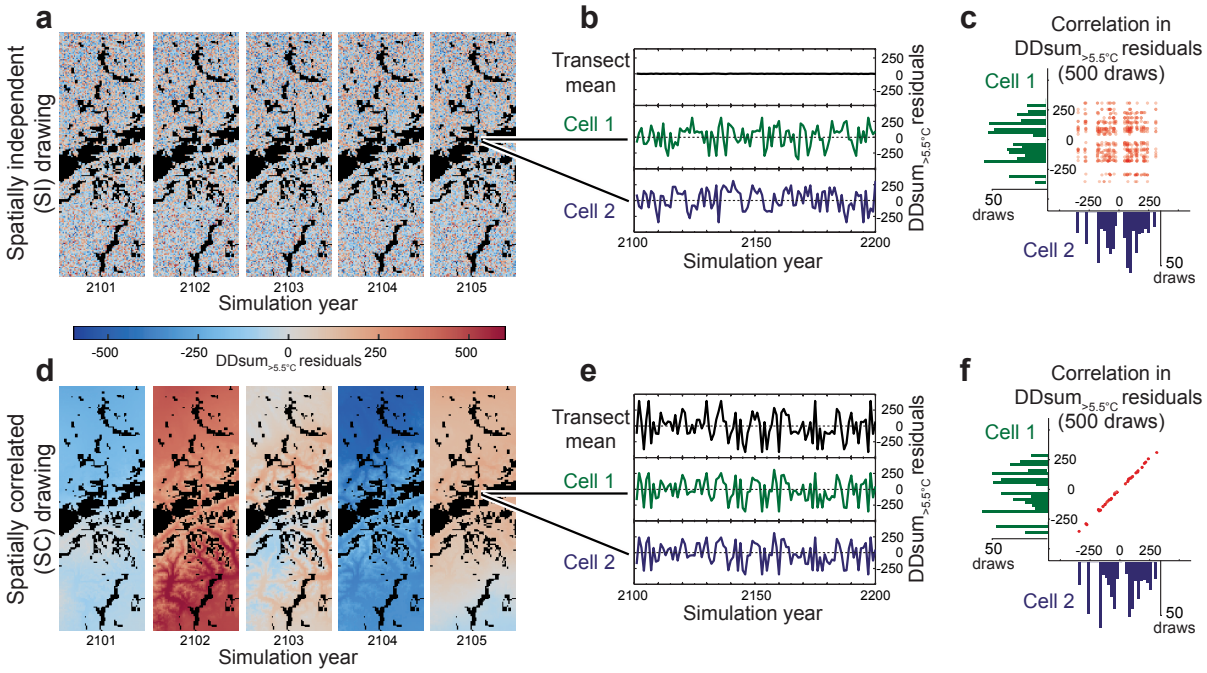

Figure 4.2 : Comparison of the applied extrapolation methods on the example of the bioclimate variable $DDsum_{>5.5\,°C}$. With the first method – spatially independent (SI) drawing – the bioclimate in a year is sampled independently for each cell of the simulation area. With the second method – spatially correlated (SC) drawing – a complete bioclimate map is drawn each year from the base years, i.e. the spatial arrangements and therefore the spatial correlation of the bioclimate found in the drawn base year is directly carried over. The two methods result in dramatic differences in the spatial arrangements of the deviation from the mean of the base years, as illustrated with the five generated $DDsum_{>5.5\,°C}$ maps (panel a: SI, panel d: SC) for the transect through the Swiss Alps (see Fig. 4.1). $DDsum_{>5.5\,°C}$ time series for single cells have comparable distributions, however, their correlation is disrupted for SI drawing (see time series in panel b compared to e and scatter plot with half-transparent markers and histograms in panel c compared to f). The average residuals over all transect cells resulting from simulations with SI drawing are always close to zero (panel b) because the random fluctuations drawn for the single cells tend to cancel each other out. For SC drawing, on the other hand, the average residuals over all transect cells reflect the interannual variability found in the base years.

4.2.1.3 TreeMig simulation setup

The effects of spatially correlated fluctuations in TreeMig's bioclimate drivers on simulated species abundance and migration were studied with an illustrative example. We simulated the northwards migration of the sub-Mediterranean tree species *Ostrya carpinifolia* Scop. (European Hop Hornbeam) in a warming climate on a 210km x 70km simulation transect (grid-cell size of 1km^2) through the Swiss Alps (Fig. 4.1). This example was chosen because it proved to be sensitive to different realisations of the bioclimate time series in previous simulation studies (Nabel et al., 2012, 2013; see Chapters 2 and 3).

For this study, outcomes of simulations applying the two bioclimate extrapolation methods SC and SI were compared. Simulations with SI and SC extrapolation started in the simulation year 2100 from the same model state, i.e. with the same values in the state variables, and used the same set of bioclimate base years (2071-2100). The generation of the bioclimate base-year set and the model state in 2100 follow the simulation setup

as described by Nabel et al. (2013) (see Chapter 3 and summarised in ESM Appendix 4.A). The climate time series used to derive the bioclimate driver showed no consistent signal of autocorrelation (see ESM Section 4.A.1.3). Therefore, temporal autocorrelation was not examined in this study, although its influence on population dynamics has been widely discussed (e.g. Schreiber and Ryan, 2011; van de Pol et al., 2011).

Simulations were run up to the year 3000 and 100 repetitions were conducted for each of the two extrapolation methods and for two different species parameter sets for the focal species. These two species parameter sets represent the moderate to optimistic range of plausible species parameters for *O. carpinifolia* (see ESM Section 4.A.2) and were selected because they resulted in a successful migration through the simulation transect in a previous study (Nabel et al., 2013; see Chapter 3).

In each simulation we tracked the biomass of *O. carpinifolia* and the sum of the biomass of all simulated species (see ESM Section 4.A.2). For each cell of the simulation area these output variables were recorded per century, and their annual development was only tracked for selected single cells and as a sum over the entire transect. As an indicator for the spread of *O. carpinifolia* we recorded the annual development of its northernmost occurrence (NO in transect km – counted from the southernmost point of the transect), i.e. its momentary spread distance. In this paper, figures with maps of the transect were created with Paraview (Ahrens et al., 2005) and graphs with Matlab 11.

4.2.2 Cellular automaton

4.2.2.1 Structure of the cellular automaton

For this study we developed a single-species cellular automaton (CA). Each cell of the CA can be regarded as an abstract representation of one individual or one small stand of same-aged individuals of the focal species. A cell can be in one of three states: **empty**, **juvenile** or **mature** (Fig. 4.3).

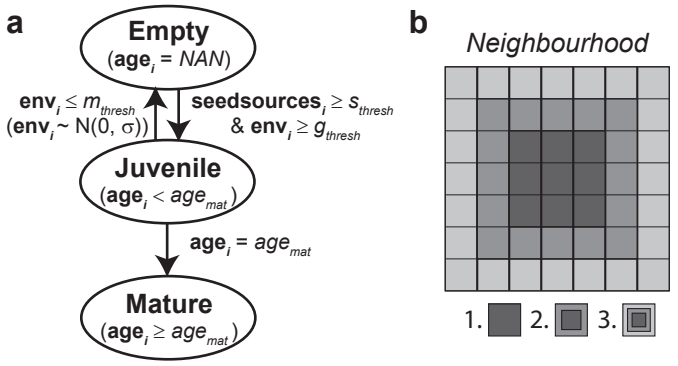

Figure 4.3 : Schematic of the cellular automaton (CA). Each cell of the CA can be in one of three different states: empty, juvenile and mature (panel a). A transition from empty to juvenile has two prerequisites: (1) the number of seed providing sources **seedsources**$_i$, i.e. the number of mature cells in the selected $neighbourhood$ (panel b), needs to exceed the threshold s_{thresh} and (2) the environmental conditions **env**$_i$, which are drawn from a normal distribution with mean 0 and standard deviation σ, need to exceed the germination threshold g_{thresh}. If the environmental conditions **env**$_i$ fall below the mortality threshold m_{thresh} while a cell is in the state juvenile its state changes back to empty. A transition from juvenile to mature happens when the age **age**$_i$ of the cell exceeds age_{mat}. A mature cell stays mature for the rest of the simulation time. Simulations were conducted with three different neighbourhoods (panel b).

In TreeMig, germination presupposes that bioclimate influences exceed certain species-specific thresholds (Table 4.1). Therefore, in the CA, a cell i changes from empty to juvenile only when the environmental conditions (**env**$_i$ drawn from a normal distribution with mean 0 and standard deviation σ) exceed a specified germination threshold (g_{thresh}). Additionally, the number of seed providing sources for cell i (**seedsources**$_i$), i.e. the number of mature cells in the simulated neighbourhood ($neighbourhood$ – Fig. 4.3b), needs to exceed a threshold (s_{thresh}). Thus, the parameter s_{thresh} controls the incidence and the strength of positive density dependency. Moreover, because cells in the CA do not differ in terms of size, age or fitness, they also do not

differ in the number of seeds they produce. Thus, the number of seed providing sources alone is used as a proxy for propagule pressure.

Table 4.2 : Parameters used for simulations with the cellular automaton and their function. The first five parameters are the species parameters of the focal species. The sixth parameter – σ – determines the variability of the environmental fluctuations.

	Parameter values	Function
age_{mat}	{1, 3, 5, 10}	Iterations after which a cell in the state juvenile changes to the state mature
g_{thresh}	{0, 1, 2, 3, 4}	Germination threshold ($\geq$: positive influence of environmental variability; small values (close to 0) imply frequent germination, large values infrequent germination)
m_{thresh}	{-4, -3, -2, -1, 0}	Mortality threshold ($\leq$: negative influence of environmental variability; small values (close to -4) imply infrequent deaths, large values frequent deaths)
s_{thresh}	{1, 3, 5, 10}	Determines the number of required seed sources to achieve a successful germination and therefore the incidence and the strength of positive density dependency
$neighbourhood$	{1, 2, 3}	Determines the neighbourhood that a mature cell provides seeds for (see Fig. 4.3b)
σ	{1, 2}	Standard deviation of the normal distribution used to represent environmental fluctuations (see Fig. 4.B.5 in the ESM for example histograms)

```
PROGRAM CA
SET age (age_i) for each cell to NAN
FOR each time step
    IF spatially correlated (SC) drawing
        CALL draw environment (env_i) for all cells
    END IF
    FOR each cell
        IF spatially independent (SI) drawing
            CALL draw environment (env_i) for this cell
        END IF
        IF age_i < age_mat AND env_i ≤ m_thresh
            SET age_i to NAN
        ELSEIF age_i == NAN AND env_i ≥ g_thresh
            SET seedsources_i to zero
            FOR each other cell j in neighbourhood
                IF age_j ≥ age_mat
                    INCREMENT seedsources_i
                END IF
            END FOR
            IF seedsources_i ≥ s_thresh
                SET age_i to zero
            END IF
        ELSEIF age_i ≠ NAN
            INCREMENT age_i
        END IF
    END FOR
END FOR
```

Figure 4.4 : Pseudocode of the cellular automaton. State variables are printed in bold, parameters in italic type.

Transition from juvenile to mature happens when the age (**age**$_i$) of the cell exceeds age_{mat}, i.e. when the individual survived in the state juvenile for this number of iterations. If the environmental conditions (**env**$_i$) fall below the mortality threshold (m_{thresh}) while the cell is in the state juvenile its state changes back to empty. After reaching the mature state, a cell stays in this state for the rest of the simulation time and can provide seeds to cells in the simulated $neighbourhood$ (Fig. 4.3b). Mortality was implemented not to affect mature individuals, because mortality for adults would have required an independent environmental threshold, since juveniles and adults often have different sensitivities to climatic influences (Lyford et al., 2003; Jackson et al.,

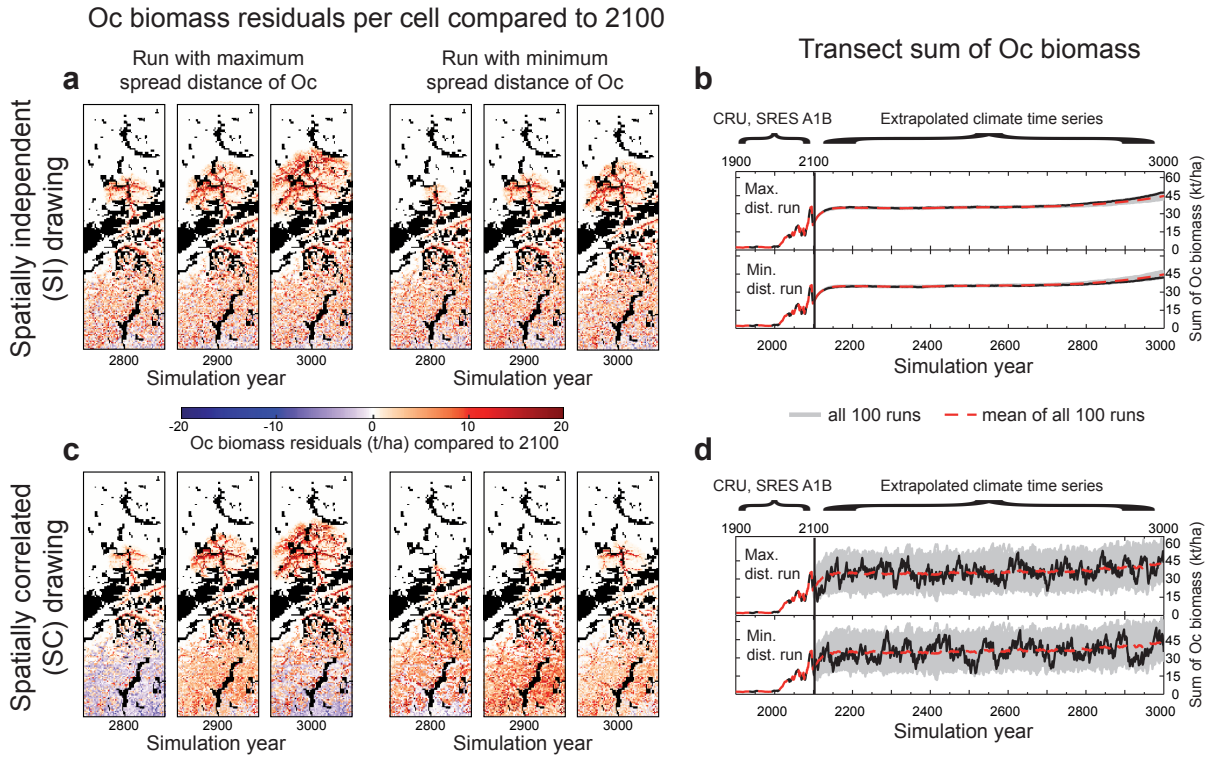

Figure 4.5 : Abundance of *Ostrya carpinifolia* (Oc) resulting from TreeMig simulations for different runs with the two extrapolation methods: spatially independent (SI) and spatially correlated (SC) drawing and the optimistic parameter set for *O. carpinifolia*. Depicted are maps for the simulation years 2800, 2900 and 3000 of simulated biomass residuals (t/ha) after subtracting the biomass resulting for the year 2100, from when on the bioclimate time series were extrapolated. For both, SI (panel a) and SC drawing (panel c), maps show the run with the maximum and the run with the minimum spread distance of *O. carpinifolia* in the simulation year 3000, i.e. the runs in which *O. carpinifolia* expanded most and least, respectively. The maps from simulations with SC drawing show a synchronisation of species abundances (accumulation of negative (blue) or positive (red) residuals), as opposed to maps from simulations with SI drawing in which no synchronisation is visible. Discrepancy of SC-runs and SI-runs get particularly clear when comparing the transect sums of the simulated biomass for *O. carpinifolia* for 1900-3000. The transect sum resulting from SI-runs (panel b) is nearly invariant over time and among realisations. For SC-runs (panel d), by contrast, the transect sum shows much larger and more realistic variability over time and among realisations. Black lines show the run with the maximum and minimum spread distance, respectively. Grey lines in the background are results from all 100 runs and the dashed red line represents the running mean over these 100 runs.

2009). Furthermore, for migration, the development on the range limits is anyway more important than population fluctuations (i.e. mortality of adults) in parts of the simulation area far from the front (Melbourne et al., 2007).

In summary, the CA incorporates stochasticity for transitions between empty and juvenile (germination and mortality). The fluctuating environmental influence is implemented as a normal distribution with mean 0 and standard deviation σ. The two different approaches to draw environmental influences were implemented such that in case of spatially correlated (SC) drawing only one pseudo-random number is drawn for the entire area, whilst in case of spatially independent (SI) drawing an independent pseudo-random number is drawn for each cell. A pseudocode of the CA is given in Fig. 4.4. A vectorised version of the CA was implemented in Matlab 11 (see ESM Appendix 4.C).

4.2.2.2 CA simulation setup

In accordance with the TreeMig simulations, a northwards migration was simulated with the CA. Simulations were conducted on a grid with 50 cells in west-east and 200 cells in north-south direction with cyclic and absorbing boundary conditions, respectively. The lowest two rows; i.e. the first 100 cells, were initialised with

the state juvenile: $\mathbf{age}_i$ = 1 (i = 1,...,100). The mean environmental influence of all cells of the simulation area was assumed to be zero. In case of SC drawing the simulation area was thus spatially homogeneous and only fluctuated among iterations.

Simulations were conducted for different combinations of parameter values (Table 4.2). For both methods to draw environmental influences each combination was simulated with 100 repetitions (in total 480000 runs). In each of 100 iteration steps the northernmost occurrence was tracked (in number of rows from the southernmost row including the lowest two rows).

4.3 Results

4.3.1 TreeMig simulations of tree species abundance

Despite the strong synchronisation of bioclimatic fluctuations (Fig. 4.2d-f), simulations with SC extrapolation only showed partial synchronisation of the simulated biomass, i.e. residuals of the same colour in Fig. 4.5c. However, where fluctuations of the biomass of *O. carpinifolia* were synchronised in simulations with SC extrapolation this synchronisation was disrupted in simulations with SI extrapolation (Fig. 4.5a). In addition to the maps shown in Fig. 4.5 we provide further analyses of biomass correlations over time for selected single cells in the ESM (Figs. 4.B.1 and 4.B.2).

The biomass sum of *O. carpinifolia* (Fig. 4.5b,d) over the whole transect showed similar effects to the transect mean of the bioclimate driver (Fig. 4.2b,e): For simulations with SI extrapolation the sums were nearly invariant over time and among realisations (Fig. 4.5b) – apart from the biomass increase of *O. carpinifolia* due to its northwards migration. For simulations with SC extrapolation, on the other hand, the biomass of *O. carpinifolia* varied greatly (20-55 kt – Fig. 4.5d). The same effects were observed for the sum of the biomass of all simulated species (see ESM Fig. 4.B.3).

4.3.2 Simulations of tree species migration

4.3.2.1 Simulations with TreeMig

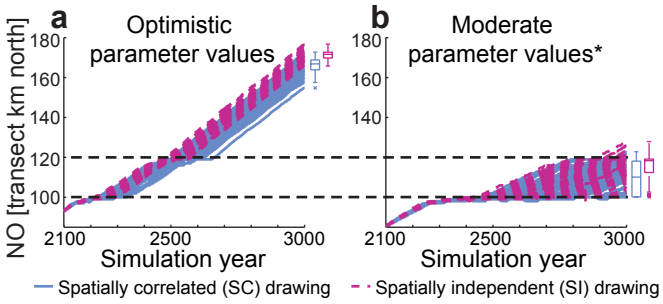

Figure 4.6 : Comparison of spread distances resulting from TreeMig simulations with spatially correlated (SC) and spatially independent (SI) drawing of bioclimate influences. Depicted are northernmost occurrences (NO in transect km north, smoothed over ten years) in the simulation years 2100-3000 resulting from 100 repetitions with the two drawing methods and for two different species parameter sets for *Ostrya carpinifolia*. (Panel a) Optimistic parameter values. (Panel b) Moderate parameter values (* with the optimistic parameter for the required $DDsum_{>5.5\,°C}$, see ESM Section 4.A.2). The box plots on the right side of each panel depict the NO-distribution in the simulation year 3000 resulting from the 100 repetitions for each drawing method. For both parameter sets the NO in the simulation year 3000 show faster migration for and less variability among runs with SI drawing than with SC drawing. Box edges represent the interquartile range, whiskers extreme data points and crosses outliers. The black dashed lines mark the main bottleneck area of the transect (see Fig. 4.1).

Northernmost occurrences among simulations with SI and SC extrapolation and among their repetitions (Fig. 4.6) diverged when *O. carpinifolia* entered the main bottleneck area (approximately at the 100^{th} transect km north, Fig. 4.1). For both extrapolation methods, simulations with the moderate, less favourable parameter

set for *O. carpinifolia* (Fig. 4.6b) resulted in slower migration rates and a higher variability in the northernmost occurrences among the 100 repetitions than simulations with the optimistic parameter set (Fig. 4.6a). In simulations with the optimistic parameter set, trajectories of the northernmost occurrence were almost parallel for all runs, i.e. they have the same migration speed, aside from two bottleneck situations (Fig. 4.6a).

The distributions of the northernmost occurrence in the simulation year 3000 resulting from repetitions with SC extrapolation and SI extrapolation are significantly different: for both species parameter sets, the year-3000 distribution mean for SI repetitions does not fall into the interquartile range of the distribution of SC repetitions (Fig. 4.6). SC repetitions showed a variability approximately 1.2-fold and 1.5-fold the variability of SI repetitions for the moderate parameter set and the optimistic parameter set, respectively.

Differences in the time points when *O. carpinifolia* passed the bottleneck situation of the simulation area led to large differences in the spatial spread of *O. carpinifolia*. Differences between the runs with the maximum and the minimum spread distances in the simulation year 3000, for example, are much smaller in simulations with SI than with SC drawing (e.g. compare differences between SI maps in panel a and SC maps in panel c in Fig. 4.5).

4.3.2.2 Simulations with the CA

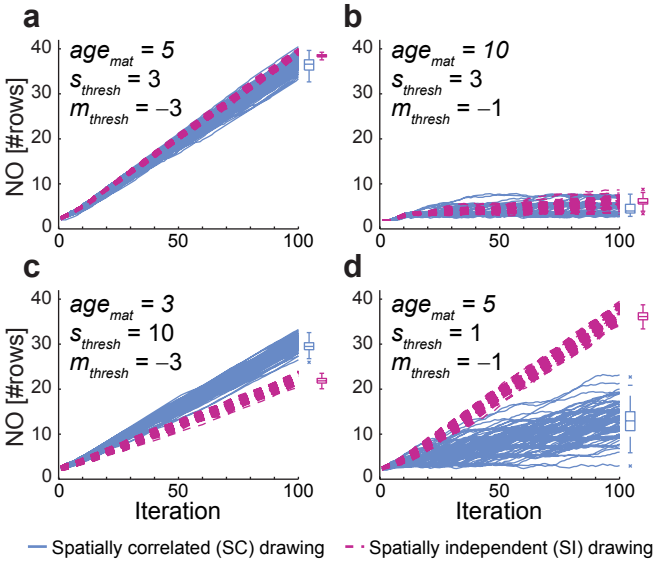

Figure 4.7 : Comparison of spread distances resulting from simulations with the cellular automaton (CA), with spatially correlated (SC) and spatially independent (SI) drawing of environmental influences. Depicted are northernmost occurrences (NO in number of rows, smoothed over ten iterations) resulting from 100 repetitions for each of the two drawing methods and four different parameter sets. The four parameter sets differ in the applied values for the age of maturity (age_{mat}), the required number of seed sources (s_{thresh}) and the mortality threshold (m_{thresh}). All parameter sets were simulated with germination threshold g_{thresh} = 0, $neighbourhood$ 2 (Fig. 4.3) and standard deviation σ = 1. The first two parameter sets (panel a, b) were selected because their migration outcomes visually resemble the TreeMig outcomes for simulations of the migration of *O. carpinifolia* (Fig. 4.6). The two other parameter sets (panel c, d) show examples for the range of possible results within the simulated parameters (Table 4.2). The box plots on the right side of each panel depict the distributions of northernmost occurrences resulting from the 100 repetitions in the 100^{th} iteration for each of the two extrapolation methods. Box edges represent the interquartile range, whiskers extreme data points and crosses outliers.

Whether the migration speed was higher in runs with SC or SI drawn environmental influences in the CA simulations depended on the species parameter values (see e.g. Fig. 4.7). For most of the simulated parameter sets the simulated migration was on average faster in runs with SI than in runs with SC drawn environmental influences (for summary statistics of all simulated parameter combinations see Table 4.B.1 in the ESM). Only for some of the parameter sets with a positive density dependence ($s_{thresh} > 1$) and small to intermediate neighbourhood ($neighbourhood$ 1 or 2) migration was on average slower for SI-runs (see e.g. Fig. 4.7c). In

situations with minor environmental constraints (m_{thresh} close to -4 and g_{thresh} close to 0) migration speed for good dispersers ($neighbourhood$ 2 or 3) was on average equal in SC- and SI-runs (see e.g. Fig. 4.8). Overall, variations in the environmental thresholds led to comparable effects among simulations with SI and SC drawing (Fig. 4.8 and ESM Section 4.B.2.3).

Whilst the number of required seed sources (s_{thresh}) had a strong effect on simulations with SI drawn environmental influences, this parameter had weaker effects on SC-runs (e.g. compare Fig. 4.7a with Fig. 4.7c). This is intuitive, because in SC-runs the environment in each iteration is the same for all cells and, therefore, same-aged cells are perfectly synchronised. Thus, if a row contains one mature cell, then all cells in this row are mature (see the ESM for a visualisation example).

For many parameter sets the variability in spread distances among SI-runs was very low and, in particular, for most simulated parameter sets lower than among SC-runs (see Fig. 4.7, Fig. 4.8 and ESM Section 4.B.2.3).

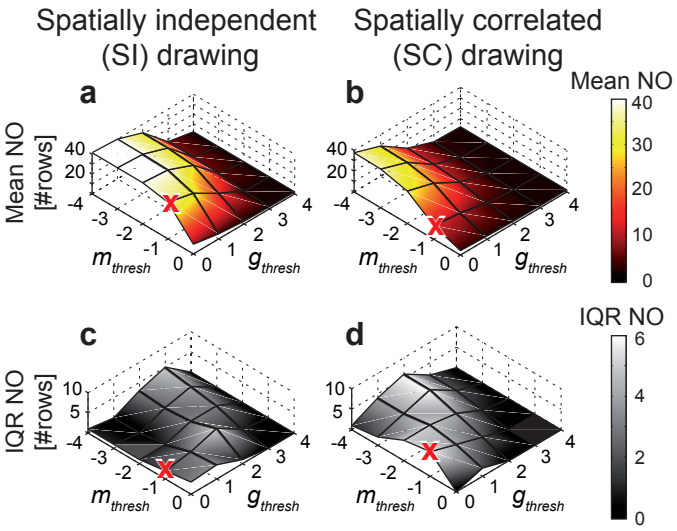

Figure 4.8 : Mean and interquartile range (IQR) of the northernmost occurrences (NO in number of rows) in applications of the cellular automaton as a function of all values simulated for the mortality threshold (m_{thresh}) and the germination threshold (g_{thresh}). Depicted are the mean (panel a and b) and the IQR (panel c and d) of the NO in the 100^{th} iteration, calculated from 100 repetitions with $neighbourhood$ 2 (Fig. 4.3), maturity age age_{mat} = 5, required number of seed sources s_{thresh} = 1 and standard deviation σ = 1 for the spatially independent (SI, panel a and c) and the spatially correlated (SC, panel b and d) drawing. The red crosses in the surface plots depict the parameter combination shown in Fig. 4.7d.

4.4 Discussion

The results of the presented TreeMig simulations confirmed that tree species abundance and migration outcomes are influenced by the spatial correlation of climatic fluctuations. Simulations with the simple cellular automaton, furthermore, affirmed that the different methods to generate fluctuations in the model driver can lead to large differences in migration speed and variability among runs with the same set of species parameters.

4.4.1 Simulated tree species abundance

The ubiquitous synchronism of the fluctuations in the bioclimate driver in TreeMig simulations with SC extrapolation (Fig. 4.2) did not lead to an equally ubiquitous synchronism in simulated tree species abundances (Fig. 4.5). This was expected, because the synchronised fluctuations are only superimposed on the spatially heterogeneous mean bioclimate influences (Fig. 4.1). As already stated in the introduction, this underlying spatial heterogeneity is very important, because population dynamics – in models like TreeMig and in natural systems – can be non-linear (Laakso et al., 2001). Thus, the synchronised fluctuations in the driver do not have to result

in synchronised biotic responses (Greenman and Benton, 2001; Currie, 2007). In fact, species abundance at a certain point in time depends on many factors: the actual climatic influence (mean and superimposed fluctuations), species sensitivities to climatic influences and previous abundance of the species itself and of other species.

Besides synchronised temporal fluctuations of model drivers, dispersal has been discussed as another important factor synchronising species abundances (e.g. Ripa, 2000; Liebhold et al., 2004; Bahn et al., 2008). The low degree of correlations in simulated species biomass among neighbouring single cells in simulations with SI extrapolation (Fig. 4.5a) and the strong similarities of biomass distributions among simulations with SC and SI drawn fluctuations in single cells over time (see ESM Fig. 4.B.2) indicate that dispersal did not lead to a strong synchronising effect in the presented TreeMig simulations. On one hand, this might be due to the weak spatial linkage in TreeMig caused by a strong seed density regulation (see Lischke and Löffler, 2006) which diminishes the possible impact of large amounts of dispersed seeds. On the other hand, dispersal might be less important in synchronising plant abundances than in synchronising abundances of highly mobile taxa with low numbers of offspring, such as large animals (Bahn et al., 2008). Tree species, in particular, usually disperse by seeds, which subsequently are entirely subject to the local dynamics in the new environment.

Even though simulations with SC extrapolation did not show ubiquitous synchronism in species abundances, they showed partially synchronised species abundances. Comparisons between simulations with SC and SI extrapolation revealed greater synchronism in species abundances in simulations with SC extrapolation than in simulations with SI extrapolation (Fig. 4.5). In simulations with SI extrapolation nearly all climatically possible situations are experienced in one year, due to the large number (210 x 70) of transect cells with independently drawn bioclimatic fluctuations. Thus, applying the SI extrapolation method induced a blurring effect, i.e. biomass maps simulated for all years and all repetitions with SI extrapolation look almost identical in the coarse view (Fig. 4.5). This blurring effect was particularly visible when summing the biomass over the entire transect. Simulations with SI extrapolation resulted in biomass sums that were nearly invariant over time and among repetitions for *O. carpinifolia* (Fig. 4.5). Large-scale fluctuations in the biomass that were observed in simulations with SC extrapolation – and are common in natural systems – were missing. This effect was also observed for the sum of the biomass of all simulated species (see ESM Section 4.B.1.2). The observed lack of variability can be explained via the central limit theorem (CLT), which states that sums of independent random variables will converge as long as they are not dominated by a small number of values (Spanos, 1999). The applicability of the CLT is supported by the fact that the moments of the biomass distribution over time are bounded and that the biomass in each cell is only a small fraction of the total. However, even in the SI simulations, biomass values in individual cells are not strictly independent variables, because of the underlying mean bioclimate (Fig. 4.1) and filter effects (Table 4.1), and because of the spatial linkage due to seed dispersal. Furthermore, the simulated biomass in each cell will be temporally correlated. Nevertheless, this lack of strict independence did not prevent convergence in the distributions of the transect sums in the SI simulations.

Overall, the results demonstrated that the SI method, which neglects spatial correlations in the bioclimatic fluctuations, led to a loss in the synchronisation of simulated tree species abundances.

4.4.2 Simulated tree species migration

Because of the large number of species parameters and interacting processes in TreeMig, no experiments were conducted in addition to the example setup. In order to enable a more detailed analysis, instead, a simple cellular automaton (CA) was developed. This CA abstracts from several processes and drivers represented in TreeMig. Each cell of the CA represents one individual (or cohort) which can be in one of three states. Thus, in contrast to TreeMig the CA has a discrete state space and the individuals do not have any attributes, such as fitness or height. Accordingly, there is no feedback between the environmental influences experienced by an individual and its contribution to future colonisations in the CA, which in TreeMig is realised via seed numbers proportional to tree heights (see Lischke et al., 2006). Due to this lack of the feedback in the CA, the number of required seed sources (s_{thresh}) is used as a proxy for propagule pressure, covering effects of species-specific differences in seed production.

Another important difference between the CA and TreeMig is that TreeMig simulations are driven by three bioclimate variables. These variables have different influences on the simulated processes and thus represent different filters (sensu Laakso et al., 2001) that can interfere with each other. The CA, in contrast, was only equipped with one environmental driver. The discrete nature of the CA, moreover, only allows for thresholds and not for other filter types. Whilst germination is implemented as a threshold in TreeMig, mortality only has a threshold effect if the population falls below a minimum density (see ESM Appendix 4.A.3) and otherwise has a multiplicative thinning effect. The influence of the parameter m_{thresh} in CA simulations therefore might be too strong compared to mortality in TreeMig simulations. Finally, the simulation area used for TreeMig simulations has a high background heterogeneity in the bioclimate variables. As discussed in Section 4.4.1 this background heterogeneity can strongly influence species abundance, which in turn influences migration. In the CA simulations such background heterogeneity effects were neglected. In particular, we assumed that all cells in the CA were potentially inhabitable, and thus neglected potentially important effects caused by fragmentation (see e.g. Hof et al., 2011; Nabel et al., 2013; see Chapter 3).

Nevertheless, comparisons between simulations with the CA and with TreeMig demonstrate that observed trends in the northernmost occurrences simulated with TreeMig can be approximated by simulations with the CA (Fig. 4.6a,b compared to Fig. 4.7a,b). TreeMig simulations of the optimistic parameter set for *O. carpinifolia* showed nearly parallel trajectories outside of critical conditions. In CA simulations such behaviour would correspond to situations in which neither the threshold for required seed sources nor one of the environmental thresholds would be limiting (i.e. small values for the germination and the mortality threshold). In such cases, no big differences between SC and SI drawn environmental influences were observed (see e.g. the farthest left corner in the surface plots Fig. 4.8). To represent the migration outcomes of the moderate, less favourable parameter set for *O. carpinifolia*, more severe environmental thresholds were required in the CA simulations. This reflects the limitation by means of the bioclimate in the main bottleneck area in TreeMig simulations and the importance of interannual variability in the bioclimate in this area (see Nabel et al., 2013; see Chapter 3). The CA surface plots (e.g. Fig. 4.8) demonstrated this intuitive response to the applied environmental thresholds, which is consistent for the two extrapolation methods and throughout all applied parameter sets (for further surface plots see ESM Section 4.B.2).

Due to the small number of processes and in particular the small number of species parameters, the CA enabled a more detailed analysis of the influence of spatial correlation in the environmental fluctuations on migration. Simulations with the CA showed a broad range of possible migration outcomes for the different parameter sets (Fig. 4.7). Results of the CA demonstrate that simulations with the same parameter set can show different behaviour for SC and for SI drawn environmental influences. The tendency that SI-runs lead to faster migrations than SC-runs – as long as there is no strong positive density dependence – is intuitive. The environment in SC-runs only fluctuates among iterations but not among cells, i.e. the simulation area has a homogeneous environment in each iteration. Therefore, if the drawn environment falls below the mortality threshold in a SC-run, all cells in the juvenile state switch to the empty state, whilst mortality in SI-runs only affects single cells. Additionally, SC-runs only enable colonisation events in favourable iterations (exceeding the germination threshold). SI-runs, in contrast, potentially provide a colonisation option in each iteration as long as the number of seed sources is sufficiently high (exceeding the threshold for required seed sources), i.e. if propagule availability coincides with good conditions (cf. findings reviewed by Melbourne et al. (2007)). Whenever there is a strong positive density dependence, colonisation of a cell is dependent on the number of mature cells in the specified neighbourhood. In such cases, correlation in the environment is favourable, i.e. migration is faster in SC-runs, which is in agreement with the simulation results by McInerny et al. (2007). Overall, simulation results of the CA demonstrated that spatial correlations in the environmental driver can have promoting as well as inhibiting influences on the migration speed, depending on the simulated species traits. The two extrapolation methods can thus not simply be used interchangeably when simulating migration.

4.4.3 Methods to inter- and extrapolate bioclimate time series

In TreeMig simulations, spatially correlated (SC) fluctuations in the bioclimate driver were generated sampling uniformly from a base-year set and used for all cells of the simulation area. This method resembles the often applied method to cyclically repeat a set of base years (e.g. Hickler et al., 2012; Sato and Ise, 2012), however, without the deterministically fixed temporal pattern. A fixed temporal pattern can lead to an incomplete or biased representation (Nabel et al., 2013; see Chapter 3), particularly in cases without a consistent signal of temporal autocorrelation, as in the current study (see ESM Section 4.A.1.3).

The SC method was compared to a method generating spatially independent (SI) bioclimatic fluctuations, drawing each year and each cell uniformly from the empirical distributions found for single cells. Drawing directly from the empirical distributions is a simplification of drawing from derived probability distributions, which is the method originally suggested to be revisited in this study. This simplification was made in order to prevent effects of extreme values interfering with the effects of spatial correlation in the bioclimate driver. However, observed effects on the spatial arrangements of simulated species abundances will equally occur when drawing from derived probability distributions. In the CA simulations the environmental influence was again simplified and fluctuations were solely drawn from prescribed normal distributions with zero being the expected value. Using a normal distribution was motivated by the fact that (detrended) annual temperatures and derived bioclimate influences are often represented by normal distributions (Schär et al., 2004; Lischke et al., 2006). To obtain a spatial correlation in the driver of the CA simulations, only one pseudo-random number was drawn for the whole simulation area.

The results of this study demonstrated that drawing climatic fluctuations independently for single cells, and thus neglecting the spatial correlation of the fluctuations, led to severe differences in the spatial configuration of simulated tree species abundances. Furthermore, it also had an influence on tree species migration. It is thus not recommended to neglect the spatial correlation in the driver. However, the applied method to draw spatially correlated fluctuations also has drawbacks compared to the originally applied sampling from probability distributions. The main disadvantage is that only climatic patterns which are represented in the base-year set can actually occur in the generated time series (Bugmann, 2001). Thus, the length of the selected base period and the single selected base years could be influential. On one hand, when a series is too short or selected such that years with extreme values are not contained in the base period, no extreme events will occur in the generated time series. On the other hand, when years with extreme conditions are contained, then these will frequently be drawn (with a probability of 1/base period length). For the inter- and extrapolation of climate time series for simulations with spatially explicit and in particular spatially linked models it would thus be desirable to use more sophisticated methods. Ideally, a method should not neglect spatial correlation and the influence of the base period length and the selected base years should be small. One possibility could be to use statistically derived relationships of climatic fluctuations and static spatial properties to generate spatially correlated noise. One could, for example, use lapse-rates with elevation (as e.g. done by Schumacher et al. (2004) for temperature and precipitation). This approach is suitable for small areas, however, these relationships are not invariant on larger extents but vary, for example, with latitude and longitude (Jackson et al., 2009) and with distance to large water bodies (Hutchinson, 1995). Therefore, such a method can be rather data hungry and difficult to parametrise. For a detailed description of such methods see, for example, Hutchinson (1995).

4.5 Conclusions

Overall, the results demonstrated that neglecting the spatial correlations in climatic fluctuations for simulations with spatially explicit models can be a considerable interference because it can have a strong influence on the spatial arrangement of simulated species abundances and on migration outcomes.

The simulations with the illustrative example in TreeMig showed that neglecting the spatial correlation in climatic fluctuations might only be justifiable when one is solely interested in the mean abundance over an area and when abundance fluctuations do not matter. The observed invariance of the biomass sum over the

transect area when neglecting the spatial correlation in bioclimatic fluctuations will also hold for other strongly climatically driven models because it is a consequence of the central limit theorem. For most applications drawing climatic fluctuations independently for single cells is therefore not recommended.

Simulations with the simple CA enabled a more detailed analysis of effects on simulated species migration and showed that the influence of spatial correlation in fluctuations of the environmental driver depends on species traits. Mostly, simulations with spatial correlation in environmental fluctuations resulted in slower migration rates than simulations without spatial correlation, however, it was opposite for species with strong positive density dependence. Simulations driven by environmental time series generated with a method which neglects spatial correlations should thus not even be used to estimate upper or lower limits of migration outcomes. They also should not be used to make comparisons among different species, at least not with models containing species parameters representing positive density dependence.

Acknowledgements

We like to thank David Gutzmann and an anonymous reviewer for their helpful comments, Thomas Wüst for the support with the cluster and Dirk Schmatz for assistance with the data preparation. Julia Nabel was partially funded by the Swiss National Science Foundation (SNF) Grant 315230-122434.

References

Ahrens, J., Geveci, B., Law, C., 2005. ParaView: An End-User Tool for Large-Data Visualization, in: Hansen, C.D., Johnson, C.R. (Eds.), Visualization Handbook. Butterworth-Heinemann.

Bahn, V., Krohn, W.B., O'Connor, R.J., 2008. Dispersal leads to spatial autocorrelation in species distributions: a simulation model. Ecological Modelling 213, 285–292.

Breshears, D.D., Cobb, N.S., Rich, P.M., Price, K.P., Allen, C.D., Balice, R.G., Romme, W.H., Kastens, J.H., Floyd, M.L., Belnap, J., Anderson, J.J., Myers, O.B., Meyer, C.W., 2005. Regional vegetation die-off in response to global-change-type drought. Proceedings of the National Academy of Sciences of the United States of America 102, 15144–15148.

Brubaker, L.B., 1986. Responses of Tree Populations to Climatic-change. Vegetatio 67, 119–130.

Bugmann, H., 2001. A Review of Forest Gap Models. Climatic Change 51, 259–305.

Currie, D.J., 2007. Disentangling the roles of environment and space in ecology. Journal of Biogeography 34, 2009–2011.

Epstein, H., Yu, Q., Kaplan, J., Lischke, H., 2007. Simulating Future Changes in Arctic and Subarctic Vegetation. Computing in Science Engineering 9, 12–23.

Fischlin, A., Midgley, G.F., Price, J.T., Leemans, R., Gopal, B., Turley, C., Rounsevell, M.D.A., Dube, O.P., Tarazona, J., Velichko, A.A., 2007. Ecosystems, their properties, goods, and services. Climate Change 2007: Impacts, Adaptation and Vulnerability. Contribution of Working Group II to the Fourth Assessment Report of the Intergovernmental Panel on Climate Change. M.L. Parry, O.F. Canziani, J.P. Palutikof, P.J. van der Linden and C.E. Hanson (Eds.), Cambridge University Press, Cambridge, UK, 211-272.

Giesecke, T., Miller, P.A., Sykes, M.T., Ojala, A.E.K., Seppä, H., Bradshaw, R.H.W., 2010. The effect of past changes in inter-annual temperature variability on tree distribution limits. Journal of Biogeography 37, 1394–1405.

Greenman, J.V., Benton, T.G., 2001. The impact of stochasticity on the behaviour of nonlinear population models: synchrony and the Moran effect. Oikos 93, 343–351.

Grenfell, B.T., Finkenstadt, B.F., Wilson, K., Coulson, T.N., Crawley, M., 2000. reply: Nonlinearity and the Moran effect. Nature 406, 847–847.

Hickler, T., Vohland, K., Feehan, J., Miller, P.A., Smith, B., Costa, L., Giesecke, T., Fronzek, S., Carter, T.R., Cramer, W., Kühn, I., Sykes, M.T., 2012. Projecting the future distribution of European potential natural vegetation zones with a generalized, tree species-based dynamic vegetation model. Global Ecology and Biogeography 21, 50–63.

Hof, C., Levinsky, I., Araújo, M.B., Rahbek, C., 2011. Rethinking species' ability to cope with rapid climate change. Global Change Biology 17, 2987–2990.

Hui, C., Krug, R.M., Richardson, D.M., 2011. Modelling spread in invasion ecology: a syntesis. In: Fifty years of invasion ecology. D. M. Richardson (Eds.), Wiley-Blackwell, UK, 329–343.

Hutchinson, M., 1995. Stochastic space–time weather models from ground-based data. Agricultural and Forest Metorology 73, 237–264.

Jackson, S.T., Betancourt, J.L., Booth, R.K., Gray, S.T., 2009. Ecology and the ratchet of events: Climate variability, niche dimensions, and species distributions. Proceedings of the National Academy of Sciences of the United States of America 106, 19685–19692.

Jarvis, A., Reuter, H., Nelson, A., Guevara, E., 2008. Hole-filled SRTM for the globe Version 4. Available from the CGIAR-CSI SRTM 90m Database. http://srtm.csi.cgiar.org.

Koenig, W., 2002. Global patterns of environmental synchrony and the Moran effect. Ecography 25, 283–288.

Koenig, W.D., Knops, J.M.H., 2013. Large-scale spatial synchrony and cross-synchrony in acorn production by two California oaks. Ecology 94, 83–93.

Laakso, J., Kaitala, V., Ranta, E., 2001. How does environmental variation translate into biological processes? Oikos 92, 119–122.

Liebhold, A., Koenig, W.D., Bjornstad, O.N., 2004. Spatial synchrony in population dynamics. Annual Review of Ecology Evolution and Systematics 35, 467–490.

Lischke, H., 2005. Modeling tree species migration in the Alps during the Holocene: What creates complexity? Ecological Complexity 2, 159–174.

Lischke, H., von Grafenstein, U., Ammann, B., 2012. Forest dynamics during the transition from the Oldest Dryas to the Bølling-Allerød at Gerzensee – a simulation study. Palaeogeography, Palaeoclimatology, Palaeoecology in press, –.

Lischke, H., Löffler, T.J., 2006. Intra-specific density dependence is required to maintain species diversity in spatio-temporal forest simulations with reproduction. Ecological Modelling 198, 341–361.

Lischke, H., Zimmermann, N.E., Bolliger, J., Rickebusch, S., Löffler, T.J., 2006. TreeMig: A forest-landscape model for simulating spatio-temporal patterns from stand to landscape scale. Ecological Modelling 199, 409–420.

Lyford, M., Jackson, S., Betancourt, J., Gray, S., 2003. Influence of landscape structure and climate variability on a late Holocene plant migration. Ecological Monographs 73, 567–583.

McInerny, G., Travis, J.M.J., Dytham, C., 2007. Range shifting on a fragmented landscape. Ecological Informatics 2, 1–8.

Melbourne, B.A., Cornell, H.V., Davies, K.F., Dugaw, C.J., Elmendorf, S., Freestone, A.L., Hall, R.J., Harrison, S., Hastings, A., Holland, M., Holyoak, M., Lambrinos, J., Moore, K., Yokomizo, H., 2007. Invasion in a heterogeneous world: resistance, coexistence or hostile takeover? Ecology Letters 10, 77–94.

Midgley, G.F., Thuiller, W., Higgins, S.I., 2007. Plant Species Migration as a Key Uncertainty in Predicting Future Impacts of Climate Change on Ecosystems: Progress and Challenges. In: Terrestrial Ecosystems in a Changing World. Canadell, Josep G. and Pataki, Diane E. and Pitelka, Louis F. (Eds.), Springer Berlin Heidelberg, 129–137.

Miller, P.A., Giesecke, T., Hickler, T., Bradshaw, R.H.W., Smith, B., Seppä, H., Valdes, P.J., Sykes, M.T., 2008. Exploring climatic and biotic controls on Holocene vegetation change in Fennoscandia. Journal of Ecology 96, 247–259.

Nabel, J.E.M.S., Zurbriggen, N., Lischke, H., 2012. Impact of species parameter uncertainty in simulations of tree species migration with a spatially linked dynamic model. International Environmental Modelling and Software Society (iEMSs) 2012, Sixth Biennial Meeting, Leipzig, Germany, 909–916, url: http://www.iemss.org/society/index.php/iemss-2012-proceedings.

Nabel, J.E.M.S., Zurbriggen, N., Lischke, H., 2013. Interannual climate variability and population density thresholds can have a substantial impact on simulated tree species' migration. Ecological Modelling 257, 88–100.

Normand, S., Ricklefs, R.E., Skov, F., Bladt, J., Tackenberg, O., Svenning, J.C., 2011. Postglacial migration supplements climate in determining plant species ranges in Europe. Proceedings of the Royal Society B: Biological Sciences 278, 3644–3653.

Pearson, R.G., Dawson, T.P., 2003. Predicting the impacts of climate change on the distribution of species: are bioclimate envelope models useful? Global Ecology and Biogeography 12, 361–371.

Pitelka, L.F., Gardner, R.H., Ash, J., Berry, S., Gitay, H., Noble, I.R., Saunders, A., Bradshaw, R.H.W., Brubaker, L., Clark, J.S., Davis, M.B., Sugita, S., Dyer, J.M., Hengeveld, R., Hope, G., Huntley, B., King, G.A., Lavorel, S., Mack, R.N., Malanson, G.P., McGlone, M., Prentice, I.C., Rejmanek, M., 1997. Plant migration and climate change. American Scientist 85, 464–473.

Rickebusch, S., Lischke, H., Bugmann, H., Guisan, A., Zimmermann, N.E., 2007. Understanding the low-temperature limitations to forest growth through calibration of a forest dynamics model with tree-ring data. Forest Ecology and Management 246, 251–263.

Ripa, J., 2000. Analysing the Moran Effect and Dispersal: Their Significance and Interaction in Synchronous Population Dynamics. Oikos 89, 175–187.

Rosenzweig, C., Casassa, G., Karoly, D., Imeson, A., Liu, C., Menzel, A., Rawlins, S., Root, T., Seguin, B., Tryjanowski, P., 2007. Assessment of observed changes and responses in natural and managed systems. In: Impacts, Adaptation and Vulnerability. Contribution of Working Group II to the Fourth Assessment Report of the Intergovernmental Panel on Climate Change, M.L. Parry, O.F. Canziani, J.P. Palutikof, P.J. van der Linden and C.E. Hanson (Eds.), Cambridge University Press, Cambridge, UK, 79-131.

Sato, H., Ise, T., 2012. Effect of plant dynamic processes on African vegetation responses to climate change: Analysis using the spatially explicit individual-based dynamic global vegetation model (SEIB-DGVM). Journal of Geophysical Research-biogeosciences 117, G03017.

Schär, C., Vidale, P.L., Lüthi, D., Frei, C., Haberli, C., Liniger, M.A., Appenzeller, C., 2004. The role of increasing temperature variability in European summer heatwaves. Nature 427, 332–336.

Schreiber, S.J., Ryan, M.E., 2011. Invasion speeds for structured populations in fluctuating environments. Theoretical Ecology 4, 423–434.

Schumacher, S., Bugmann, H., Mladenoff, D.J., 2004. Improving the formulation of tree growth and succession in a spatially explicit landscape model. Ecological Modelling 180, 175–194.

Spanos, A., 1999. Probability theory and statistical inference: econometric modeling with observational data. Cambridge University Press.

van de Pol, M., Vindenes, Y., Sæther, B., Engen, S., Ens, B., Oosterbeek, K., Tinbergen, J., 2011. Poor environmental tracking can make extinction risk insensitive to the colour of environmental noise. Proceedings of the Royal Society B: Biological Sciences 278, 3713–3722.

With, K.A., 2002. The Landscape Ecology of Invasive Spread. Conservation Biology 16, 1192–1203.

Appendix

Appendix 4.A Summary of the setup used for the TreeMig simulations

For this study, simulations with the intermediate-complexity forest-landscape model TreeMig (Lischke et al., 2006) were compared for two different methods to extrapolate the fluctuations in its bioclimate drivers from empirical distributions. Compared simulations used the same set of bioclimate base years (Section 4.A.1.2) and started in the simulation year 2100 from the same model state (Section 4.A.2), i.e. with the same set of values in TreeMig's state variables. The simulation setup of this study was based on the setup used in the study of Nabel et al. (2013)(see Chapter 3) and is summarised below.

4.A.1 Bioclimate time series

4.A.1.1 Derivation of bioclimate variables

TreeMig simulations are driven by annual time series of three bioclimate variables: the sum of daily mean temperatures above $5.5\,^{\circ}\mathrm{C}$ ($DDsum_{>5.5\,^{\circ}\mathrm{C}}$), the minimum winter-temperature (*Min. WiTemp*) and an index representing drought severity (*Drought severity*). These bioclimate variables were calculated with a program based on ForClim-E (Bugmann and Cramer, 1998; Lischke et al., 2006). $DDsum_{>5.5\,^{\circ}\mathrm{C}}$ and *Min. WiTemp* were derived from time series of monthly averaged temperatures; *Drought severity* from monthly averaged temperatures, monthly precipitation sums and static information on water storage capacity, slope and aspect of each cell of the simulation area.

Slope and aspect were derived from the digital elevation model of the Shuttle Radar Topography Mission (Jarvis et al., 2008). Water storage capacity was taken from a study by Löffler and Lischke (2001) based on the Swiss soil suitability map (Frei et al., 1980) for the Swiss part of the transect and supplemented with data of the European soil database (Panagos et al., 2012) for transect parts outside of Switzerland (for details see supplementary material to Nabel et al., 2013; see Appendix 3.A). For solid rock surfaces and big water bodies no information on water storage capacity was available and transect cells belonging to these types were considered non-stockable, i.e. as cells in which trees are not able to grow.

Bioclimate time series were derived from monthly climate data for the years 1901-2100. Historical data (1901-2000) was taken from CRU (Mitchell et al., 2003) and for future data (2001-2100) a CLM (Lautenschlager et al., 2009) calculation of the SRESA1B scenario (Nakicenovic et al., 2000) was used. Monthly temperature averages and precipitation sums were downscaled to 30″ with WorldClim data (Hijmans et al., 2005) and projected to 1km^2 with FIMEX-0.28 (Klein, 2012) with a nearest neighbour interpolation (see supplementary material to Nabel et al., 2013; see Appendix 3.B).

4.A.1.2 The bioclimate base-year set

Both extrapolation methods applied in this study (see main text Section 4.2.1.2) used the same set of base years, which were derived from the last 30 years (2071-2100) of the downscaled and interpolated version of the CLM SRESA1B scenario calculations (Section 4.A.1.1). Because monthly temperature averages of this time series contained a long-term trend, monthly temperature time series were detrended and subsequently offset with the end of the trend before deriving the bioclimate variables (for details see supplementary material to Nabel et al., 2013; see Appendix 3.B).

The length of the base period was selected to be 30 because previous studies often used a base period of approximately 30 years to inter- or extrapolate bioclimate time series (e.g. Lischke, 2005; Epstein et al., 2007;

Hickler et al., 2012; Lischke et al., 2012). Other studies, however, used different base period lengths (e.g. Sato and Ise (2012) used 10 years and Miller et al. (2008) used 50 years) and the length of the base period could potentially influence migration outcomes (see discussion in the main text Section 4.4.3).

4.A.1.3 Temporal autocorrelation

Time series of single cells and of the transect sum of monthly temperature averages (detrended) and precipitation sums used to calculate the set of base years (see Section 4.A.1.2) were tested for temporal autocorrelation with Pearson correlation tests for lags of 1 to 15 years. For these time series no significant correlations were observed for any of the lags. Subsequently, the same tests were conducted for time series with all 100 years of monthly temperature averages (detrended) and precipitation sums of the downscaled and interpolated version of the CLM SRESA1B scenario calculations and still no significant correlations were observed for the tested time lags. Only for the full available time series of 200 years – CRU data followed by the CLM SRESA1B scenario calculations (see Section 4.A.1.1) – an autoregressive signal was observed for both, the monthly average temperatures and the precipitation sums.

4.A.2 Generation of the model state in the simulation year 2100

Comparisons between the two extrapolation methods were conducted for simulations with two different species parameter sets for the focal species *Ostrya carpinifolia* Scop. (European Hop Hornbeam). The applied parameters sets represent the moderate to optimistic range of plausible species parameters for *O. carpinifolia* (Nabel et al., 2012; see Chapter 2), whereby in the moderate parameter set, the required $DDsum_{>5.5\,^{\circ}\mathrm{C}}$ parameter was replaced with the optimistic parameter value. These two parameter sets were selected because they resulted in a successful migration through the simulation transect in a previous study (Nabel et al., 2013; see Chapter 3).

In this study, all simulations with the same species parameter set started in the simulation year 2100 from the same model state, i.e. with the same set of values in TreeMig's state variables. Thus, for each of the two species parameter sets an own initial model state was generated.

Simulations to generate the model state in the simulation year 2100 started in 1400. In addition to *O. carpinifolia* (with its two different parametrisations, respectively) 21 other species occurring in the simulation area were included in the simulations (see supplementary material to Nabel et al., 2013; see Appendix 3.A). In the initialisation phase (1400-1800) of the TreeMig simulations saplings of all species, except of *O. carpinifolia*, were available throughout the whole simulation area. *O. carpinifolia* was restricted to the southern part of the transect up to the 65^{th} transect km north, which corresponds approximately to its current northern range limit (cf. Brändli, 1998). In the simulation year 1800 this restriction was removed and *O. carpinifolia* started to migrate northwards.

For the initialisation phase (1400-1800) and for 100 subsequent years the bioclimate was extrapolated following the original TreeMig method drawing from distributions derived from a base period – here the first 30 years (1901-1930) of the downscaled and interpolated CRU data (Section 4.A.1.1). For 1901-2100 the available deterministic annual time series of interpolated and downscaled climate data from CRU and the CLM calculated SRESA1B scenario was used. In 2100 all state variables were recorded (including hidden state variables such as the current x-axis position of the mast seeding sine-curve – see formula in the supplementary material to Lischke et al., 2006). The recorded values were then loaded as state variables for each simulation with the according species parameter set for *O. carpinifolia*.

4.A.3 Further specification of the simulation setup

For this application no disturbances (other than climatically caused) were applied and seed dispersal was simulated deterministically. Borders of the simulation area were absorbing, i.e. no seeds came from outside the simulation area and all seeds dispersed over the borders were lost. To avoid the spread of infinitesimal population densities a minimum population density threshold of one individual per km^2 was applied (see Nabel et al.,

2013; see Chapter 3). This minimum population density threshold thus also provides a threshold for mortality in such cases in which mortality leads to less then one individual per km^2.

Appendix 4.B Additional simulation results

4.B.1 Additional results from simulations with TreeMig

4.B.1.1 Abundance of *Ostrya carpinifolia*

In order to compare effects of the two applied extrapolation methods – spatially correlated (SC) and spatially independent (SI) drawing – on the abundance of *O. carpinifolia*, the temporal development of the biomass of *O. carpinifolia* was tracked for selected single cells. Selected were two neighbouring cells from the main bottleneck area (see Fig. 4.1, main text) on the 42^{th} transect km south and 119^{th} km north (cell 1) as well as 118^{th} km north (cell 2), which were already used to show bioclimate influences resulting from the two different drawing methods (see Fig. 4.2, main text). Additionally, three neighbouring cells on the southern side of the transect were selected on the 21^{th} transect km south: 42^{th} transect km north (cell 3), 43^{th} km north (cell 4) and 44^{th} km north (cell 5). The temporal development of the biomass of *O. carpinifolia* in these cells is shown in Fig. 4.B.1 for the run with the maximum and the run with the minimum spread distance of *O. carpinifolia* in the simulation year 3000, i.e. the runs in which *O. carpinifolia* expanded most and least, respectively. For these runs, additionally, the correlation in the simulated biomass over time among cell 3, cell 4 and cell 5 is depicted in Fig. 4.B.2 to stress the reduction in biomass correlations among cells in SI-runs compared to SC-runs.

4.B.1.2 Sum of the biomass of all simulated species (Total biomass)

Additional to the biomass of *O. carpinifolia*, the sum of the biomass of all simulated species (see Section 4.A.2) in each cell of the simulation area was tracked for each century and as a sum over the simulation area on an annual basis (Fig. 4.B.3). Similar to the sum of the biomass of *O. carpinifolia* (Fig. 4.5b,d in the main text), the sum of the biomass of all species over the transect was invariant over time and repetitions for simulations with SI extrapolation, while it varied (between 1 and 2Mt/ha) for simulations with SC extrapolation (Fig. 4.B.3b,d). In panel a and c in Fig. 4.B.3, and in the same panels in Fig. 4.5 in the main text, the biomass residuals after subtracting the biomass resulting for the year 2100 are shown. The results for the biomass of all species resemble the results for the biomass of *O. carpinifolia*: different years and different runs simulated with SI extrapolation are not visually discernible, whilst different years and different runs simulated with SC extrapolation perceivably differ.

Among all runs and all years, several cells in the area of the Alps showed a loss in simulated species biomass compared to the simulation year 2100 (blue coloured cells in Fig. 4.B.3a,c). This biomass loss compared to the simulation year 2100 can be attributed to an overshooting in the biomass in TreeMig simulations after early succession from bare ground (Lischke et al., 1998; Zurbriggen, 2013). Before the pronounced warming under the SRESA1B scenario, the cells in the area of the Alps were too cold for any tree species to establish. A warmer climate driver allowed several tree species to germinate and quickly grow in these cells due to little light-competition – and a lack of other important processes restricting Alpine forests in the applied TreeMig version (Zurbriggen, 2013). The sum of the simulated biomass of all species peaked around 2100 in the area of the Alps followed by a subsequent decrease and stabilisation around 2300.

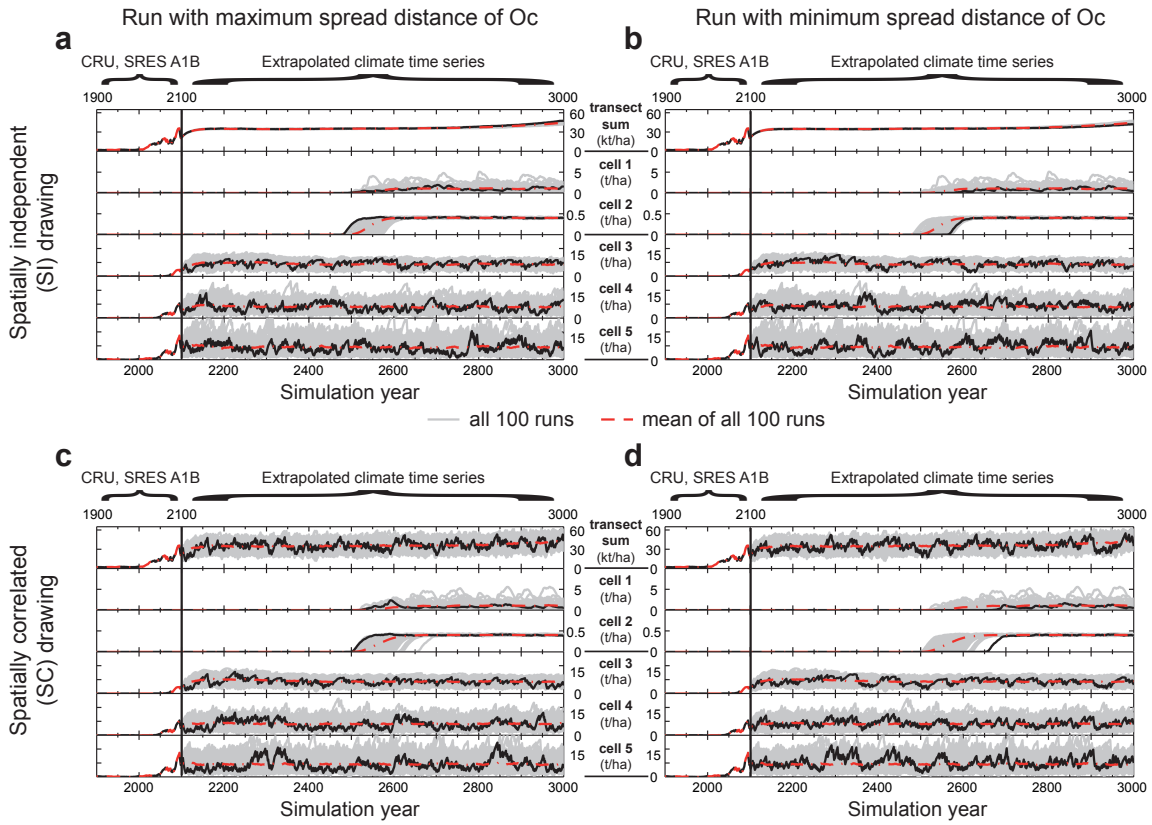

Figure 4.B.1 : Comparison of the development of the abundance of *Ostrya carpinifolia* (Oc) over time for simulations with spatially independent (SI – panel a and b) and spatially correlated (SC) drawing (panel c and d). Shown are time series for the runs with the maximum and the minimum spread distance of *O. carpinifolia* in the simulation year 3000, i.e. the runs in which *O. carpinifolia* expanded most and least, respectively. All simulations were conducted with the optimistic parameter set for *O. carpinifolia*. Depicted is the biomass of *O. carpinifolia* for the years 1900-3000 in five different cells (in t/ha) and as transect sum (kt/ha). Selected were two cells from the main bottleneck area (see Fig. 1, main text) on the 42^{th} transect km south and 119^{th} km north (cell 1) as well as 118^{th} km north (cell 2), which were already used to show bioclimate influences resulting from the two different drawing methods (see Fig. 4.1, main text). Additionally, three neighbouring cells on the southern side of the transect were selected on the 21^{th} transect km south: 42^{th} transect km north (cell 3), 43^{th} km north (cell 4) and 44^{th} km north (cell 5). Whilst resulting biomasses appear to be generally unsynchronised between cell 1 and 2 for all depicted runs, cell 3, 4 and 5 show correlations of the resulting biomass over time for SC simulations (see also Fig. 4.B.2). Grey lines in the background are results from all 100 runs and the dashed red line represents the running mean over these 100 runs. It should be noted that the y-axis of the different cells and the transect sum are varied.

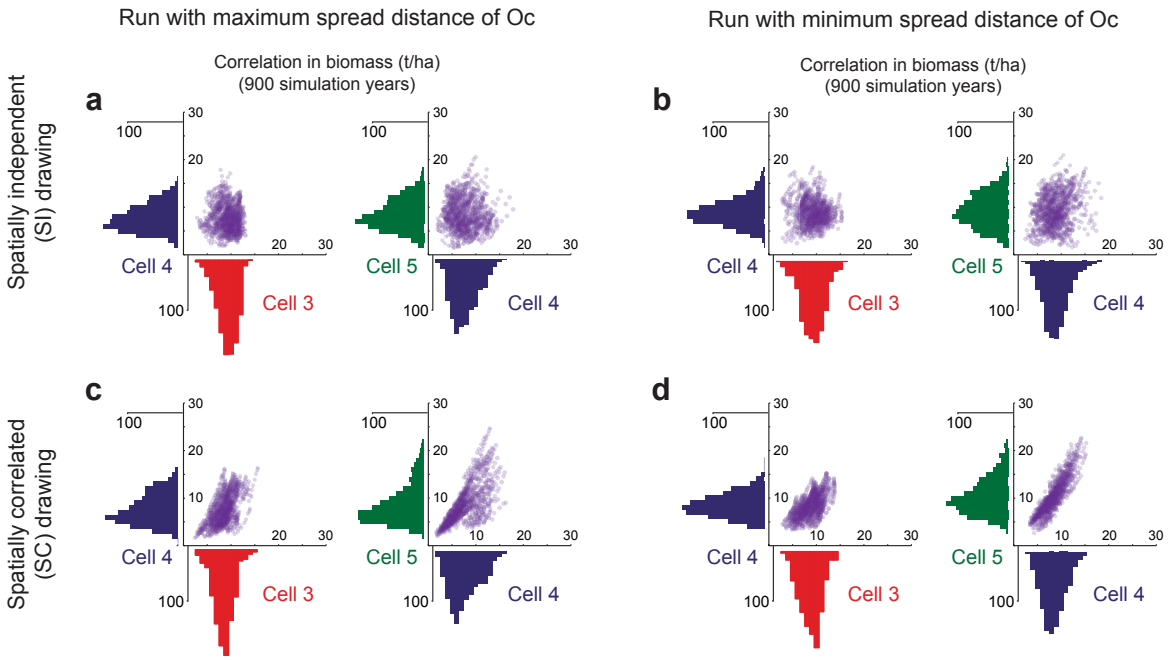

Figure 4.B.2 : Comparison of the histograms and correlations of the biomass of *Ostrya carpinifolia* (Oc) among single cells for simulations with spatially independent (SI – panel a and b) and spatially correlated (SC) drawing (panel c and d). Shown are results from runs with the maximum and the minimum spread distance of *O. carpinifolia* in the simulation year 3000, i.e. the runs in which *O. carpinifolia* expanded most and least, respectively. All simulations were conducted with the optimistic parameter set for *O. carpinifolia*. The histograms and correlations were calculated for the biomass of *O. carpinifolia* (t/ha) for the years 2100-3000 and three neighbouring cells on the 21^{th} transect km south: 42^{th} transect km north (cell 3), 43^{th} km north (cell 4) and 44^{th} km north (cell 5). Scatter plots showing biomass values for cells resulting from simulations conducted with SC extrapolated bioclimate indicate correlations. These correlations are not visible in the plots resulting from simulations with SI extrapolated bioclimate. Markers in the scatter plot are printed half-transparent.

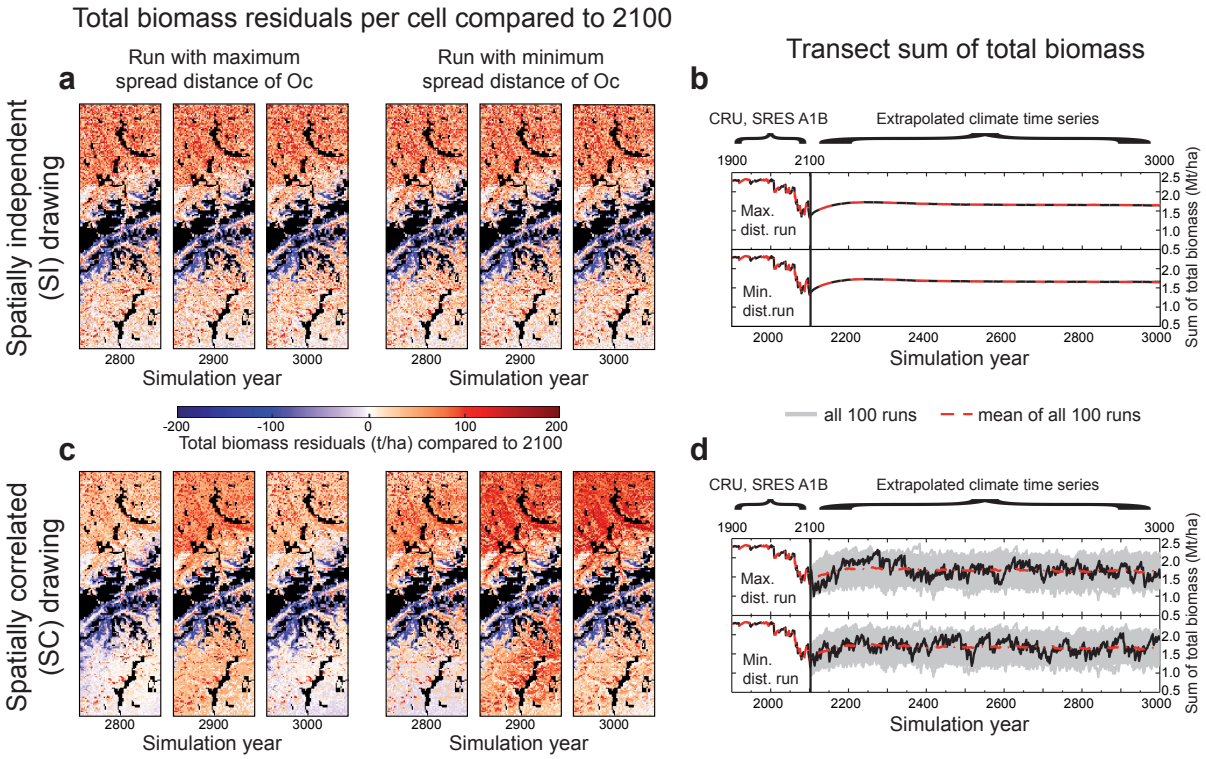

Figure 4.B.3 : Sum of the biomass of all simulated species (total biomass) for different runs with the two extrapolation methods: spatially independent (SI) and spatially correlated (SC) drawing. Depicted are maps for 2800, 2900 and 3000 of simulated total biomass residuals (t/ha) after subtracting the total biomass resulting for the simulation year 2100, from when on the bioclimate time series were extrapolated (panel a: SI drawing and panel c: SC drawing). In compliance with Fig. 4.5 in the main text, the run with the maximum and the minimum spread distance of *Ostrya carpinifolia* (Oc) in the simulation year 3000 are shown, i.e. the runs in which *O. carpinifolia* expanded most and least, respectively. In all runs the optimistic parameter set for *O. carpinifolia* was used. Maps from simulations with SC drawing differ visibly over time and between the depicted runs, whilst in maps from simulations with SI drawing hardly any differences are discernible. Discrepancy of SC and SI runs get particularly clear when comparing the transect sums of the simulated biomass for 1900-3000. The transect sum resulting from runs with SI drawing is nearly invariant over time and among realisations (panel b). For the SC drawn simulations, by contrast, the transect sum shows much larger and more realistic variability over time and among realisations (panel d). Grey lines in the background are results from all 100 runs and the dashed red line represents the running mean over these 100 runs. Several cells in the area of the Alps show a loss in simulated species biomass compared to the year 2100 for all runs, which is due to a known overshooting problem in TreeMig (see text).

4.B.2 Additional results from simulations with the cellular automaton

4.B.2.1 Summary statistics of conducted simulations

In total 2400 parameter combinations (see Table 4.2, main text) were simulated with the cellular automaton (CA). Of these 2400 parameter combinations 1482 were successful, whereby we called a combination successful if the northernmost occurrence in the furthest run for the parameter set exceeded the 5^{th} row in the last iteration. Of the 918 unsuccessful combinations 802 were unsuccessful for simulations with both methods to generate environmental influences, 83 were only unsuccessful for simulations with spatially independent (SI) and 33 for simulations with spatially correlated (SC) drawing. For all successful runs Table 4.B.1 shows whether simulations with SC or SI drawing lead to on average faster migration, i.e. further northernmost occurrences.

Table 4.B.1 : Summary statistics of simulations conducted with the cellular automaton. 2400 different combinations of parameter values were simulated with 100 repetitions each (see Table 4.2, main text). 1482 of these combinations were successful (here, a combination is called successful if the northernmost occurrence in the repetition with the furthest spread distance exceeds the 5^{th} row in the last iteration). For all successful combinations this table summarises whether the mean (μ) and the standard deviation (σ) of the distribution over the northernmost occurrence found in the 100 repetitions for the 100^{th} iteration are larger for the runs with spatially correlated (SC) or spatially independent (SI) drawing. For cases were the mean northernmost occurrences differed, it was additionally tested (1) if the larger mean was greater than the 75th percentile of the distribution with the smaller mean and (2) if the lowest (min) northernmost occurrence for the distribution with the larger mean was greater than the furthest (max) occurrence of the distribution with the smaller mean. The mean, standard deviation and 75th percentile, as well as min and max occurrences were rounded to integers (i.e. to row numbers).

μ of 100 repetitions							σ of 100 repetitions		
SI > SC			SC > SI			SC = SI	SI > SC	SC > SI	SC = SI
total	$\mu_{SI} > \text{Q75}_{SC}$*	$\text{min}_{SI} > \text{max}_{SC}$	total	$\mu_{SC} > \text{Q75}_{SI}$*	$\text{min}_{SC} > \text{max}_{SI}$	total	total	total	total
1113	865[a], [b]	357[d]	285	267	42[c]	84	103[b]	1173[a], [c], [d]	206
(75%)	(58%)	(24%)	(19%)	(18%)	(3%)	(6%)	(7%)	(79%)	(14%)

[a] Fig. 4.7a [b] Fig. 4.7b [c] Fig. 4.7c [d] Fig. 4.7d, main text
* Q75: 75th percentile

4.B.2.2 Spatial representation of the state of the cellular automaton

In simulations with the CA and SC drawn environmental influences the driver in each iteration is the same for all cells, therefore, all same-aged cells are perfectly synchronised Fig. 4.B.4c,d.

4.B.2.3 Sensitivity to the environmental thresholds

As expected, mean spread distances of the 100 repetitions were higher for small thresholds for germination (g_{thresh}) and mortality (m_{thresh}) for both drawing methods, independently of the other parameter values (see Fig. 4.8 in the main text and Figs. 4.B.6 and 4.B.7). Variability among repetitions tended to be higher for intermediate thresholds than for large or small thresholds (Figs. 4.8, 4.B.6 and 4.B.7). This is also expected, because for mortality, large thresholds nearly always and small thresholds seldom lead to transitions from juvenile to empty, and for germination, small thresholds nearly always allow and large thresholds nearly always prevent transition from empty to juvenile.

Two different normal distributions were used to generate the environmental driver for simulations with the CA (Fig. 4.B.5). Both distributions had the expectation value zero, one with standard deviation one (σ = 1), the other with standard deviation two (σ = 2). In simulations with σ = 1 mean northernmost occurrences differed stronger among different values for g_{thresh} and m_{thresh} than in simulations with σ = 2 (Fig. 4.B.6). This is logical because the normal distribution with the higher standard deviation is flatter and accordingly the probability for more extreme environmental influences is higher (Fig. 4.B.5).

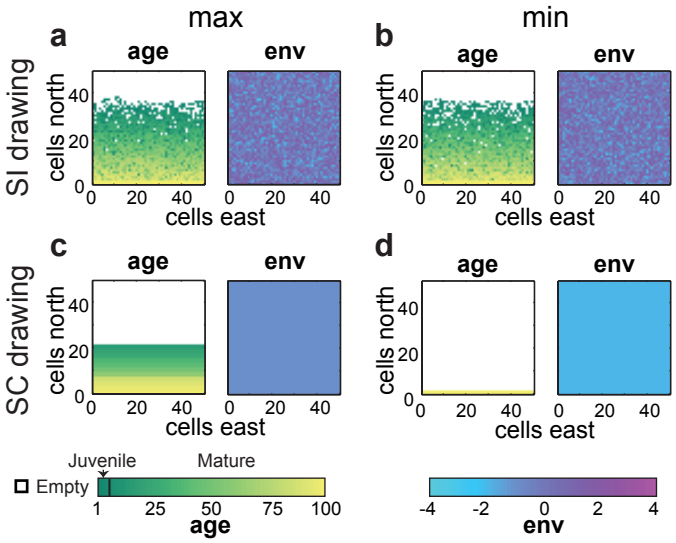

Figure 4.B.4 : Spatial representation of the driver and the state of the cellular automaton for different runs with the two methods to draw environmental influences: spatially independent (SI) and spatially correlated (SC) drawing. Depicted are the driver and the age in the last iteration (iteration = 100) for the run with the maximum (max) and the minimum (min) spread distance, i.e. the run with the furthest and the lowest northernmost occurrence, for the parameters: age_{mat} = 5, s_{thresh} = 1, m_{thresh} = -1, $neighbourhood$ = 2 and σ = 1 (see Fig. 4.7d main text for the northernmost occurrences of all 100 repetitions for SI and SC drawn environment and this parameter set).

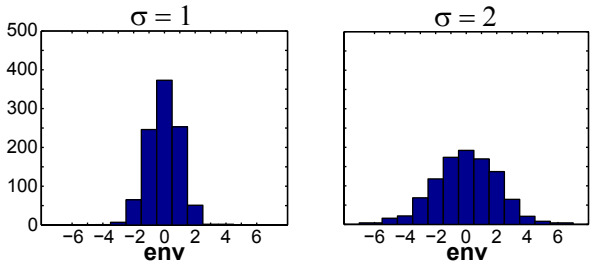

Figure 4.B.5 : Histograms for 1000 draws with each of the two normal distributions used to generate the environmental driver in the simulations with the cellular automaton. Panel a: N(0, 1), panel b: N(0, 2).

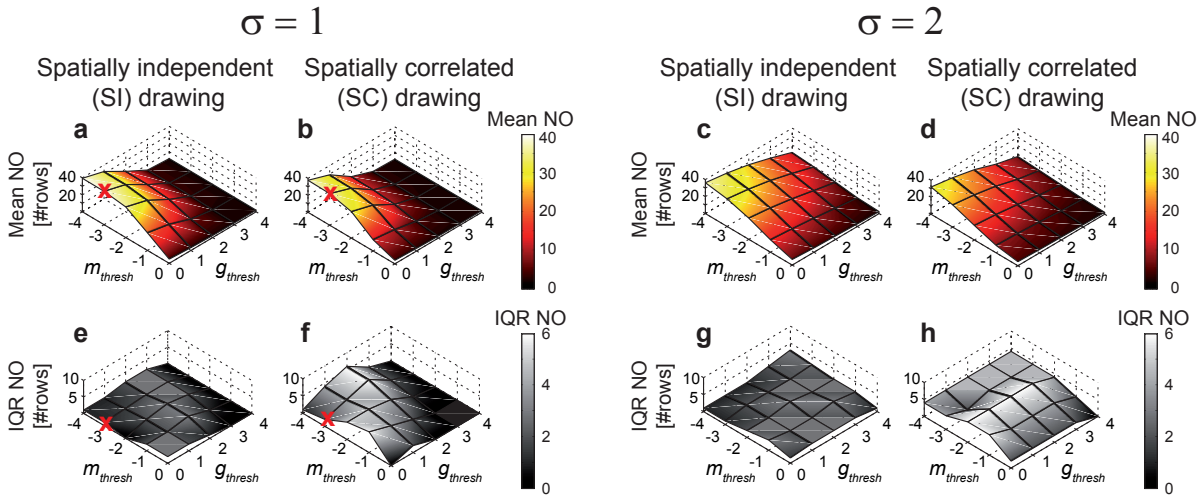

Figure 4.B.6 : Mean and interquartile range (IQR) of the northernmost occurrences (NO in number of rows) in applications of the cellular automaton as a function of all values simulated for the mortality threshold (m_{thresh}) and the germination threshold (g_{thresh}), for the two different normal distributions used to generate the environmental driver. Depicted are the mean (panel a-d) and the IQR (panel e-h) of the northernmost occurrences in the 100^{th} iteration, calculated from 100 repetitions with $neighbourhood$ 2 (see Fig. 4.3, main text), maturity age age_{mat} = 5 and number of required seed sources s_{thresh} = 3, for spatially independent (SI) and spatially correlated (SC) drawing and the two different values for σ, respectively. The red crosses in the surface plots for σ = 1 (panel a,b,e and f) depict the parameter combination shown in Fig. 4.7a, main text.

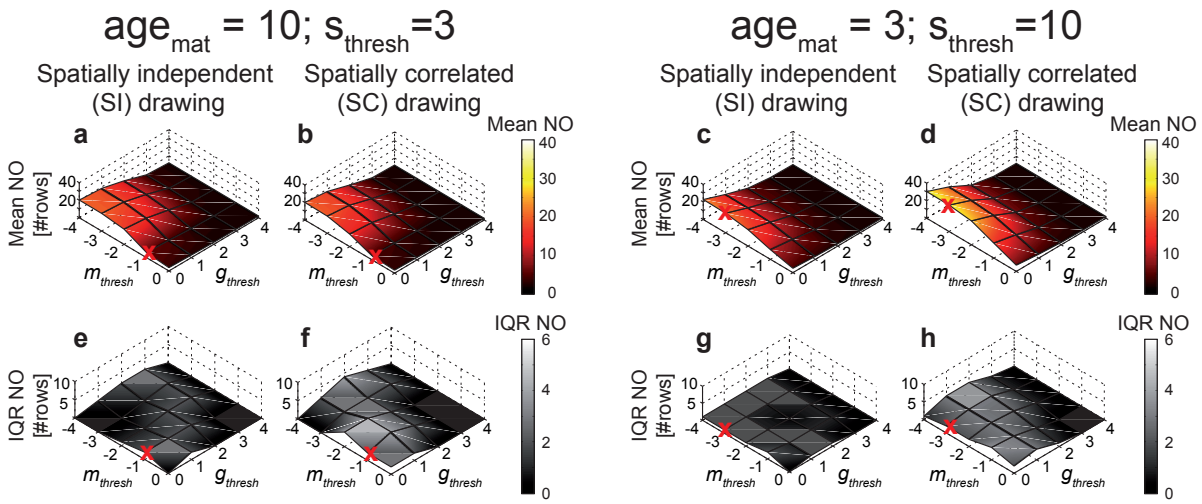

Figure 4.B.7 : Mean and interquartile range (IQR) of the northernmost occurrences (NO in number of rows) in applications of the cellular automaton as a function of all values simulated for the mortality threshold (m_{thresh}) and the germination threshold (g_{thresh}). Depicted are the mean (panel a-d) and the IQR (panel e-h) of the northernmost occurrences in the 100^{th} iteration, calculated from 100 repetitions for spatially independent (SI) and spatially correlated (SC) drawing and two different parameter sets, respectively. Panel a,b,e and f depict results from simulations with $neighbourhood$ 2 (see Fig. 4.3 main text), maturity age age_{mat} = 10 and number of required seed sources s_{thresh} = 3. Panel c,d,g and h depict results from simulations with $neighbourhood$ 2, maturity age age_{mat} = 3 and number of required seed sources s_{thresh} = 10. The red crosses in the surface plots depict the parameter combination shown in Fig. 4.7b (panel a,b,e and f) and Fig. 4.7c (panel c,d,g and h) in the main text, respectively.

Appendix 4.C Cellular Automaton

```
%%%%%%%%%%%%%%%%%%%%%%%%%%%%%%%%%%%%%%%%%%%%%%%%%%%%%%%%%%%%%%%%%%%%%%%%%%%%%%%
%%%%%%%%%%%%%%%%%%%%%%%%%%%%%%%%%%%%%%%%%%%%%%%%%%%%%%%%%%%%%%%%%%%%%%%%%%%%%%%
% Electronic supplementary material C for
%
%  "Extrapolation methods for climate time series revisited --
%    spatial correlations in climatic fluctuations influence
%        simulated tree species abundance and migration"
%
% by Julia E.M.S. Nabel (jemsnabel@gmail.com) [a,b,c]
% a: Landscape Dynamics, Swiss Federal Institute for Forest, Snow and Land-
%     scape Research WSL, Zürcherstrasse 111, 8903 Birmensdorf, Switzerland
% b: Department of Environmental Systems Science, Swiss Federal Institute
%     of Technology ETH, Universitätstrasse 16, 8092 Zürich, Switzerland
% c: now at: Max Planck Institute for Meteorology, Bundesstrasse 53,
%     20146 Hamburg, Germany
%%%%%%%%%%%%%%%%%%%%%%%%%%%%%%%%%%%%%%%%%%%%%%%%%%%%%%%%%%%%%%%%%%%%%%%%%%%%%%%
%%%%%%%%%%%%%%%%%%%%%%%%%%%%%%%%%%%%%%%%%%%%%%%%%%%%%%%%%%%%%%%%%%%%%%%%%%%%%%%
function furthestRowPerIteration = cellular_automaton(useSCDrawing, ...
    prngSeed, numberOfIterations, numberOfCellsNorthSouth, ...
    numberOfCellsWestEast, meanOfEnvDistribution, sigma, ...
    age_mat, neighbourhood, g_thresh, m_thresh, s_thresh)

% CELLULAR_AUTOMATON
% this matlab function comprises a vectorised version of the single-species
% cellular automaton (CA) developed and used for the simulations of the
% northwards migration of a focal species as described in the main text.
%
%-------------------------------------------------------------------------
% The CA consists of a two dimensional grid. Each cell of the grid can be
% regarded as an abstract representation of one individual or small stand
% of same-aged individuals of a simulated focal species. Each cell can be
% in one of three states: empty, juvenile or mature, whereby this state is
% uniquely defined by the cell-value of the matrix 'age' (state-variable)
% and the species parameter 'age_mat' which is given as input to the CA.
%
% The northwards migration simulated for a function call is determined by
% the drawing method (useSCDrawing), the seed (prngSeed) of the
% pseudo-random number (prn) generator [mt19937ar - Matlab implementation
% of the Mersenne twister], the number of iterations (numberOfIterations),
% the extent of the simulation area (numberOfCellsNorthSouth,
% numberOfCellsWestEast), the mean and standard deviation of the normal
% distribution used to generate environmental influences
% (meanOfEnvDistribution, sigma) and a set of species parameters (age_mat,
% neighbourhood, g_thresh, m_thresh, s_thresh).
% The function retuns a vector with the number of the northernmost occupied
% row for each iteration (furthestRowPerIteration), i.e. the northernmost
% row with at least one cell which is not in the state empty.
%
%--------------------
% state-variables:
% * age             m x n matrix (numberOfCellsNorthSouth+2*neighbourhood x
%                                 numberOfCellsWestEast) -
%                   stores the number of iterations since when a cell is
%                   occupied, i.e. not empty.
% * seedSources     m x n matrix - stores the number of available seed
%                   sources, i.e. mature neighbouring cells
%                   (determined by the species parameter 'neighbourhood')
% * envStream       state of the pseudo-random number generator
%
%--------------------
```

```
% rules:
% 1. A cell changes its state from juvenile to empty when the environmental
%    influence (prn 'thisClim' drawn from N(meanOfEnvDistribution, sigma)
%    falls below the mortality threshold (thisClim <= m_thresh)
%    -> in this case the age of the cell is set to NAN
% 2. A cell changes its state from empty to juvenile when the environmental
%    influence exceeds the germination threshold (thisClim >= g_thresh) and
%    enough seed sources are available (seedSources >= s_thresh), i.e.
%    enough neighbouring cells (determined by neighbourhood) are mature
%    -> in this case the age of the cell is set to one
% 3. At the end of each iteration the age of all occupied cells is
%    increased by one
%
%-------------------
% boundary conditions:
% * west-east: cyclic
% * north-south: absorbing (realised with a 2*neighbourhood sized buffer
%                           which is emptied after each iteration)
%
%------------------------------------------------------------------------
% REQUIRES: RandStream, imfilter, fspecial
%
% INPUT:
% useSCDrawing: (logical) - a Boolean which indicates if spatially
%               correlated (SC) drawing or spatially independent (SI)
%               drawing should be applied.
%               True = SC drawing: in this case only one prn is drawn per
%               iteration for the whole simulation area.
%               False = SI drawing: in this case each cell of the
%               simulation area is assigned an independent prn.
% prngSeed: (integer) - a non-negative scalar integer with which the
%               pseudo-random number generator is initialised
% numberOfIterations: (integer) - a non-negative scalar integer determining
%               the number of simulated iterations
% numberOfCellsNorthSouth: (integer) - a non-negative scalar integer
%               defining the number of rows in the simulation area
% numberOfCellsWestEast: (integer) - a non-negative scalar integer
%               defining the number of columns in the simulation area
% meanOfEnvDistribution: (integer) - a non-negative scalar integer
%               determining the mean of the (discrete) normal distribution
%               used to sample the environmental influences
% sigma: (integer) - a non-negative scalar integer determining the standard
%               deviation of the normal distribution
% age_mat: (integer) - non-negative scalar integer representing a species
%               parameter determining after how many iterations an occupied
%               cell is in the state mature
% neighbourhood: (integer) - scalar integer which can take a restricted
%               number of values ({1,2,3}) representing a species parameter
%               determining the number of neighbours considered when
%               testing the transition from empty to juvenile (rule 2)
% g_thresh: (integer) - scalar integer representing a species parameter
%               specifying a lower threshold on the environmental
%               influences for transition from empty to juvenile (rule 2)
% m_thresh: (integer) - scalar integer representing a species parameter
%               specifying an upper threshold on the environmental
%               influences for transition from juvenile to empty (rule 1)
% s_thresh: (integer) - non-negative scalar integer representing a species
%               parameter specifying a lower threshold on the number of
%               available seed sources (seedSources) for transition from
%               empty to juvenile (rule 2)
```

```
% OUTPUT:
% furthestRowPerIteration: (integer) - non-negative vector of integers with
%               the number of the northernmost occupied row for each
%               iteration, i.e. the northernmost row with at least one cell
%               which is not in the state empty.
%
%-------------------------------------------------------------------------
%-------------------------------------------------------------------------
% (c) Written by Julia Nabel, WSL, 2012/2013.
% This file is shared under a "Attribution-NonCommercial-ShareAlike 3.0"
% licence, which means that you must give credit to the author, are not
% allowed to use it for commercial purposes and you may share your
% derivatives of this work only under a similar licence. Other than that,
% you are free to copy, display, use, modify the code. The details of this
% licence are given at: http://creativecommons.org/licenses/by-nc-sa/3.0/
%
% version: 130319
% author: Julia Nabel (jemsnabel@gmail.com)
%-------------------------------------------------------------------------
%-------------------------------------------------------------------------

%%%%%%%%%%%%%%%%%%%%%%%%%%%%%%%%%%%%%%%%%%%%%%%%%%%%%%%%%%%%%%%%%%%%%%%%%%%
%%%%%%%%%%%%%%%%%%%%%%%%%%%%%%% TEST INPUT %%%%%%%%%%%%%%%%%%%%%%%%%%%%%%%%
error(nargchk(12,12,nargin));

if ~islogical(useSCDrawing) ...
        || ~(isnumeric(prngSeed) && isscalar(prngSeed)) ...
        || ~(isnumeric(numberOfIterations) ...
            && isscalar(numberOfIterations)) ...
        || ~(isnumeric(numberOfCellsNorthSouth) ...
            && isscalar(numberOfCellsNorthSouth)) ...
        || ~(isnumeric(numberOfCellsWestEast) ...
            && isscalar(numberOfCellsWestEast)) ...
        || ~(isnumeric(age_mat) && isscalar(age_mat)) ...
        || ~(isnumeric(meanOfEnvDistribution) ...
            && isscalar(meanOfEnvDistribution)) ...
        || ~(isnumeric(sigma) && isscalar(sigma)) ...
        || ~(isnumeric(neighbourhood) && isscalar(neighbourhood)) ...
        || ~(isnumeric(g_thresh) && isscalar(g_thresh)) ...
        || ~(isnumeric(m_thresh) && isscalar(m_thresh)) ...
        || ~(isnumeric(s_thresh) && isscalar(s_thresh))
    error('Error in one of the input types, please check.')
end

%The number of iterations needs to be positive
if(numberOfIterations < 1 || numberOfIterations > 1000)
    error(['Number of iterations needs to be larger than 1 and ' ...
        'should be smaller than 1000, please check.'])
end
%The number of cells in each direction needs to be positive
if(numberOfCellsNorthSouth < 1 || numberOfCellsNorthSouth > 1000 ...
        || numberOfCellsWestEast < 1 || numberOfCellsWestEast > 1000 )
    error(['Number of cell needs to be larger than 1 and should be ' ...
        'smaller than 1000, please check.'])
end
%The maturity age needs to be positive
if(age_mat < 1 || age_mat > 100)
    error(['Age of maturity needs to be larger than 1 and should ' ...
        'be smaller than 100, please check.'])
end
```

```
181 %The number of required seed sources needs to be positive
182 if(s_thresh < 1 || s_thresh > 100)
183     error(['Number of required seed sources needs to be larger than 1 ' ...
184         'and should be smaller than 100, please check.'])
185 end
186 
187 %%%%%%%%%%%%%%%%%%%%%%%%%%%%%%%%%%%%%%%%%%%%%%%%%%%%%%%%%%%%%%%%%%%%%%%%%%%%
188 %%%%%%%%%%%%%%%%%%%%%%%%%%%%%%%% INIT %%%%%%%%%%%%%%%%%%%%%%%%%%%%%%%%%%%%%
189 switch neighbourhood
190     case 1
191         cellRadius = 3;
192         numberOfNeighbouringCells = 9;
193     case 2
194         cellRadius = 5;
195         numberOfNeighbouringCells = 25;
196     case 3
197         cellRadius = 7;
198         numberOfNeighbouringCells = 49;
199     otherwise
200         error(['This function is only implemented for certain types ' ...
201             'of neighbourhood - please use one out of {1, 2, 3}.']);
202 end
203 
204 %Initialisation of a buffer zone (+ 2*neighbourhood) to ensure absorbing
205 %  north-south boundaries. This is required in order to apply a filter
206 %  for this vectorised version of the cellular automaton
207 bufferedNumberOfCells = numberOfCellsNorthSouth+2*neighbourhood;
208 %Initialisation of the filter used to determine mature cells in the
209 %  neighbourhood for this vectorised version of the cellular automaton
210 myFilter = fspecial('average', [cellRadius, cellRadius]);
211 
212 %Initialisation of the state-variables
213 age = nan(bufferedNumberOfCells, numberOfCellsWestEast);
214 seedSources = zeros(bufferedNumberOfCells, numberOfCellsWestEast);
215 envStream = RandStream('mt19937ar','Seed', prngSeed); %set seed for prng
216 
217 %If not SC but SI drawing is used, an array for the to be independently
218 %  drawn prns needs to be initalised
219 if(~useSCDrawing)
220     prnPerCell = zeros(bufferedNumberOfCells, numberOfCellsWestEast);
221 end
222 
223 %Initialisation of the output vector
224 furthestRowPerIteration = zeros(numberOfIterations, 1);
225 
226 %Initial distribution: lowest two cells of the "real" simulation area, i.e.
227 %  outside of the buffer zone
228 age(neighbourhood+1:neighbourhood+2, :) = 1;
229 
230 %Auxiliary matrix (logicals) used to identify the "real" simulation area
231 %   above the lowest two 'real' cells, i.e. the area outside of the buffer
232 %   zone and outside of the area of the initial distribution.
233 %   This matrix is used to test for transitions from juvenile to empty
234 %   ensuring that the cells of the initial distribution are not subject to
235 %   transitions from juvenile to empty, i.e. that this area of initial
236 %   distribution can serve as a source over the whole simulation time
237 aboveAreaOfInitialDistribution = ...
238     zeros(bufferedNumberOfCells, numberOfCellsWestEast);
239 aboveAreaOfInitialDistribution(neighbourhood+3:end, :) = 1;
240 
```

```
241 %%%%%%%%%%%%%%%%%%%%%%%%%%%%%%%%%%%%%%%%%%%%%%%%%%%%%%%%%%%%%%%%%%%%%%%%%%%%
242 %%%%%%%%%%%%%%%%%%%%%%%%%%%%%%%% ITERATE %%%%%%%%%%%%%%%%%%%%%%%%%%%%%%%%
243 for iteration = 1:numberOfIterations
244
245     %Derive boolean matrix indicating if a cell is empty or occupied
246     isEmpty = isnan(age);
247
248     %Derive boolean matrix indicating if a cell is in the state juvenile
249     isJuvenile = (age < age_mat) & ~isEmpty;
250
251     %Derive boolean matrix indicating if the number of available seed
252     %  sources is sufficient
253     hasEnoughSeedSources = seedSources >= s_thresh;
254
255     %Reset number of potentially supplied neighbouring cells (i.e.
256     %  according to 'neighbourhood') - this auxiliary matrix is required
257     %  for the filter to derive the number of accessible mature neighbours
258     %  later
259     suppliedNeighbours = repmat(numberOfNeighbouringCells, ...
260         bufferedNumberOfCells, numberOfCellsWestEast);
261
262     %--- Transitions: empty <-> juvenile
263     %Test which drawing kind is used
264     if(useSCDrawing)
265         %In case of SC drawing all cells are subject to the same
266         %  environmental influence, i.e. environmental threshold
267         %  comparisons are conducted with the same prn for all cells
268         thisClim = meanOfEnvDistribution + round(sigma * randn(envStream));
269
270         %-- Rule 1 (SC): transition for all cells in the state juvenile to
271         %  the state empty if the environmental influence falls below the
272         %  mortality threshold
273         if(thisClim <= m_thresh)
274             %Mortality only happens above the area of initial distribution
275             age(isJuvenile & aboveAreaOfInitialDistribution) = NaN;
276
277             %Update boolean matrix identifying cells in the state empty
278             isEmpty = isnan(age);
279         end
280
281         %-- Rule 2 (SC - first part): transition for all cells in the state
282         %  empty to the state juvenile if the environmental influence
283         %  exceeds the germination threshold
284         if(thisClim >= g_thresh)
285             %Rule 2 (SC - second part): transition happens only for cells
286             %  for which enough seed sources are available
287             age(isEmpty & hasEnoughSeedSources) = 0;
288         end
289     else
290         %In case of SI drawing each cell receives an independent prn
291         prnPerCell(:, :) = meanOfEnvDistribution ...
292             + round(sigma .* randn(envStream, ...
293                 bufferedNumberOfCells, numberOfCellsWestEast));
294
295         %Derive boolean matrix indicating if the environmental influence
296         %  falls below the mortality threshold
297         mortalEnvironment = prnPerCell <= m_thresh;
298
299         %-- Rule 1 (SI): transition from juvenile to empty for all cells
300         %  for which the environmental influence falls below the mortality
```

```
301         %  threshold (no mortality in the area of initial distribution)
302         age(isJuvenile & mortalEnvironment ...
303             & aboveAreaOfInitialDistribution) = NaN;
304 
305         %Update boolean matrix identifying cells in the state empty
306         isEmpty = isnan(age);
307 
308         %Derive boolean matrix indicating if the environmental influence
309         %  exceeds the germination threshold
310         suitableForGermination = prnPerCell >= g_thresh;
311 
312         %-- Rule 2 (SI): transition from empty to juvenile for all cells
313         %  for which the environmental influence exceeds the germination
314         %  threshold (transition happens only for cells for which enough
315         %  seed sources are available)
316         age(isEmpty & suitableForGermination & hasEnoughSeedSources) = 0;
317     end % if useSCDrawing
318 
319     %--- Increment age
320     %Update Boolean array indicating which cells are in the state empty
321     isEmpty = isnan(age);
322     %then increment not empty cells
323     age(~isEmpty) = age(~isEmpty) + 1;
324 
325     %--- Prepare available seed sources array for next iteration
326     %Find mature cells
327     isage_mature = age >= age_mat;
328     %Supplied neighbours in all cells not in the state mature is zero
329     suppliedNeighbours(~isage_mature) = 0;
330     %Imfilter applies the averaging filter 'myFilter' on the array of
331     %  supplied neighbours (which only contains values for mature cells),
332     %  thus, each cell is assigned the number of neighbouring mature cells
333     seedSources = imfilter(suppliedNeighbours, myFilter, 'circular');
334 
335     %--- Empty the buffer zone to ensure absorbing north-south boundaries
336     age(1:neighbourhood, :) = nan;
337     age(end-neighbourhood+1:end, :) = nan;
338     seedSources(1:neighbourhood, :) = 0;
339     seedSources(end-neighbourhood+1:end:end, :) = 0;
340 
341     %--- Calculate output (last row with occurrences) for this iteration
342     existing = ~isnan(age);
343     if(any(existing))
344         [furthestRowPerIteration(iteration), ~, ~] ...
345             = find(existing, 1, 'last');
346 
347         %-- Care for the buffer-zone
348         if furthestRowPerIteration(iteration) > numberOfCellsNorthSouth
349             %If the number of rows is above the maximum number of 'real'
350             %  rows it is set to the maximum possible number of rows
351             furthestRowPerIteration(iteration) = numberOfCellsNorthSouth;
352         else
353             %Else halve the buffer size is subtracted
354             furthestRowPerIteration(iteration) ...
355                 = furthestRowPerIteration(iteration) - neighbourhood;
356         end
357     end
358 end %for iteration = 1:numberOfIterations
359 end %function
```

References

Brändli, U.B., 1998. Die häufigsten Waldbäume der Schweiz. Ergebnisse aus dem Landesforstinventar 1983-85: Verbreitung, Standort und Häufigkeit von 30 Baumarten. Berichte der Eidgenöss. Forschungsanstalt für Wald, Schnee und Landschaft.

Bugmann, H., Cramer, W., 1998. Improving the behaviour of forest gap models along drought gradients. Forest Ecology and Management 103, 247–263.

Epstein, H., Yu, Q., Kaplan, J., Lischke, H., 2007. Simulating Future Changes in Arctic and Subarctic Vegetation. Computing in Science Engineering 9, 12–23.

Frei, E., Vökt, U., Flückiger, R., Brunner, H., Schai, F., 1980. Bodeneignungskarte der Schweiz auf Grund der Bodeneigenschaften ausgewählter physiographischer Landschaftselemente. Bundesämter für Raumplanung, Landwirtschaft und Forstwesen. Bern.

Hickler, T., Vohland, K., Feehan, J., Miller, P.A., Smith, B., Costa, L., Giesecke, T., Fronzek, S., Carter, T.R., Cramer, W., Kühn, I., Sykes, M.T., 2012. Projecting the future distribution of European potential natural vegetation zones with a generalized, tree species-based dynamic vegetation model. Global Ecology and Biogeography 21, 50–63.

Hijmans, R.J., Cameron, S.E., Parra, J.L., Jones, P.G., Jarvis, A., 2005. Very high resolution interpolated climate surfaces for global land areas. International Journal of Climatology 25, 1965–1978.

Jarvis, A., Reuter, H., Nelson, A., Guevara, E., 2008. Hole-filled SRTM for the globe Version 4. Available from the CGIAR-CSI SRTM 90m Database. http://srtm.csi.cgiar.org.

Klein, H., 2012. FIMEX-0.28. https://wiki.met.no/fimex/start. Last access date: 09.01.12.

Lautenschlager, M., Keuler, K., Wunram, C., Keup-Thiel, E., Schubert, M., Will, A., Rockel, B., Boehm, U., 2009. Climate Simulation with CLM, Scenario A1B run no.1, Data Stream 3: European region MPI-M/MaD. World Data Center for Climate. http://dx.doi.org/10.1594/WDCC/CLM_A1B_1_D3.

Lischke, H., 2005. Modeling tree species migration in the Alps during the Holocene: What creates complexity? Ecological Complexity 2, 159–174.

Lischke, H., von Grafenstein, U., Ammann, B., 2012. Forest dynamics during the transition from the Oldest Dryas to the Bølling-Allerød at Gerzensee – a simulation study. Palaeogeography, Palaeoclimatology, Palaeoecology in press, –.

Lischke, H., Löffler, T.J., Fischlin, A., 1998. Aggregation of Individual Trees and Patches in Forest Succession Models: Capturing Variability with Height Structured, Random, Spatial Distributions. Theoretical Population Biology 54, 213–226.

Lischke, H., Zimmermann, N.E., Bolliger, J., Rickebusch, S., Löffler, T.J., 2006. TreeMig: A forest-landscape model for simulating spatio-temporal patterns from stand to landscape scale. Ecological Modelling 199, 409–420.

Löffler, T.J., Lischke, H., 2001. Incorporation and influence of variability in an aggregated forest model. Natural Resource Modeling 14, 103–137.

Miller, P.A., Giesecke, T., Hickler, T., Bradshaw, R.H.W., Smith, B., Seppä, H., Valdes, P.J., Sykes, M.T., 2008. Exploring climatic and biotic controls on Holocene vegetation change in Fennoscandia. Journal of Ecology 96, 247–259.

Mitchell, T., Carter, T., Jones, P., Hulme, M., New, M., 2003. A comprehensive set of climate scenarios for Europe and the globe. Tyndall centre Working paper 55.

Nabel, J.E.M.S., Zurbriggen, N., Lischke, H., 2012. Impact of species parameter uncertainty in simulations of tree species migration with a spatially linked dynamic model. International Environmental Modelling and Software Society (iEMSs) 2012, Sixth Biennial Meeting, Leipzig, Germany, 909–916, url: http://www.iemss.org/society/index.php/iemss-2012-proceedings.

Nabel, J.E.M.S., Zurbriggen, N., Lischke, H., 2013. Interannual climate variability and population density thresholds can have a substantial impact on simulated tree species' migration. Ecological Modelling 257, 88–100.

Nakicenovic, N., Alcamo, J., Davis, G., de Vries, B., Fenhann, J., Gaffin, S., Gregory, K., Grübler, A., Jung, T.Y., Kram, T., La Rovere, E.L., Michaelis, L., Mori, S., Morita, T., Pepper, W., Pitcher, H., Price, L., Riahi, K., Roehrl, A., Rogner, H.H., Sankovski, A., Schlesinger, M., Shukla, P., Smith, S., Swart, R., van Rooijen, S., Victor, N., Dadi, Z., 2000. IPCC Special Report on Emissions Scenarios. Cambridge University Press.

Panagos, P., Van Liedekerke, M., Jones, A., Montanarella, L., 2012. European Soil Data Centre: Response to European policy support and public data requirements. Land Use Policy 29, 329–338.

Sato, H., Ise, T., 2012. Effect of plant dynamic processes on African vegetation responses to climate change: Analysis using the spatially explicit individual-based dynamic global vegetation model (SEIB-DGVM). Journal of Geophysical Research-biogeosciences 117, G03017.

Zurbriggen, N., 2013. Avalanche disturbance and regeneration in mountain forests under climate change: experimental and modeling approaches. Ph.D. thesis. Swiss Federal Institute of Technology Zurich.

Chapter 5

Upscaling of spatially explicit and linked time- and space-discrete models simulating vegetation dynamics under climate change

Published in Proceedings of the 27th International Conference on Environmental Informatics for Environmental Protection, Sustainable Development and Risk Management, EnviroInfo 2013, Hamburg, Germany, 2013

Julia E. M. S. Nabel[a,b], *Heike Lischke*[a]

[a]*Landscape Dynamics, Swiss Federal Institute for Forest, Snow and Landscape Research WSL, Zürcherstrasse 111, 8903 Birmensdorf, Switzerland*
[b]*Department of Environmental Systems Science, Swiss Federal Institute of Technology ETH, 8092 Zurich, Switzerland*

Abstract

Models applied to simulate the impact of climate change on vegetation dynamics generally face the trade-off between computational expenses (computation time and memory) and modelled detail. Models used for simulations of large areas (e.g. continental) often abstract processes entailing spatial linkages, e.g. species migration, and have too coarse resolutions to depict microsite heterogeneity. Regional to local models, on the other hand, are more detailed, but their computational expenses prevent applications on larger scales. For manageable and accurate simulations of vegetation dynamics on large scales, small-scale dynamics need to be integrated with large-scale applications in a balanced way. Several methods have been proposed and applied to expedite the integration of scales. However, each method has different advantages and drawbacks and the applicability of a method also strongly depends on the initial model and on the research question.

Here we present a conceptual framework for a further step integrating the scales in simulations with spatially explicit, time- and space-discrete models simulating vegetation dynamics under climate change. In such models, grid cells with similar environmental drivers and species compositions often entail repetitive calculations. Our method strives to reduce this redundancy and aims to disentangle repetitive calculations from processes specific to single cells. The proposed method is based on a dynamic two-layer classification (D2C) concept, in which the majority of processes is simulated in representative cells constituting the coarse layer, and only processes which might lead to changes specific to a single cell are simulated on the original grid, i.e. the fine layer. This new concept is a further step to enable the simulation of more detailed small-scale dynamics on a larger scale. We provide an example applying the D2C concept with the forest-landscape model TreeMig and shortly discuss its advantages and limitations.

5.1 Introduction

Spatiotemporal vegetation dynamics play a central role in earth system processes, and large-scale changes in vegetation structure and distribution can influence the entire system (Fischlin et al., 2007). Changes in the vegetation structure, in turn, are driven by processes on various scales, ranging from photosynthesis on very small

scales and competition for light and disturbances on intermediate scales up to large-scale disturbances and species' migration (Neilson et al., 2005; Fischlin et al., 2007). Models applied to study vegetation dynamics suffer from limitations when trying to simulate interacting small and large-scale forest dynamics on a large extent. Generally, processes and influences represented in a model result from trade-offs between accuracy on one side, and computational feasibility and efficiency as well as parametrisation requirements on the other side (Huntley et al., 2010). Available dynamic vegetation models can broadly be classified into large and small-scale models. Large-scale models – essentially dynamic global vegetation models (DGVMs) – avoid spatially linking processes and use coarse spatial (e.g. 50-200 km^2) or taxonomic resolutions (plant functional types instead of single species). Furthermore, they disregard or strongly simplify processes requiring small-scale information, such as local competition for light (Fisher et al., 2010). Small-scale models, on the other hand, often incorporate important small-scale processes and drivers, but are computationally too expensive (time and required memory) to be used for large area simulations. Particularly, the naïve approach to enable simulations of larger areas by coarsening the grid cell resolution has been shown to introduce large discretisation errors (e.g. Bocedi et al., 2012). Furthermore, high computational expenses often not only result from the fine resolution, but from the simulation of processes which are usually neglected in large-scale models, for example, spatial linkages between grid cells (Nabel et al., 2013; see Chapter 3). Typical cell side lengths of small-scale models are 25m to 1km and simulated extents seldom exceed the size of a small country or federal state.

Several methods have been proposed and applied to reach a stronger integration of the scales, either in a top-down manner refining large-scale models (Fisher et al., 2010) or as bottom-up approaches to upscale small-scale models (Urban et al., 1999; Lischke et al., 2007; Auger et al., 2012). The majority of upscaling methods assume that fine-scale components of a modelled system can be represented on a coarse scale through skilful selections and aggregations (Lischke et al., 2007). Such aggregations can be temporal, spatial or functional, i.e. regarding processes or state variables. There is a manifold of methods, ranging from analytical aggregations (Auger et al., 2012) to adaptive grid methods, in which discretisations in time and space are dynamically refined or coarsened according to local gradients (Zumbusch, 2003). Other methods use parts of the original model to obtain information for coarser scales. This is for example the case with so-called equation free approaches, which calculate and evaluate selected small-scale experiments to attain the state on the coarse scale at a certain point in time (Kevrekidis and Samaey, 2009). A common way to completely change the computation scale is the so-called meta-modelling, involving the development of a new coarse-scale model, parameterised with results of representative small-scale model simulations (Urban et al., 1999).

Most of the listed methods are constrained by certain assumptions, some are not suitable for more complex models and others replace the complex fine-scale model by a simpler coarse-scale model, which then is only valid under specific conditions. In the end, the applicability of a method strongly depends on the initial model and on the investigated research question. Models simulating vegetation dynamics are often implemented as discrete grid-based systems with or without spatial linkage of the single cells. For this kind of models we developed a method which aims to provide a further step in the integration of detailed small-scale dynamics with larger-scale applications. In the following we describe the concept of the method and present a first implementation and test.

5.2 The dynamic two-layer classification concept

The proposed dynamic two-layer classification (D2C) concept relies on the fact that in many grid-based models simulating sessile organisms, grid cells with similar abiotic drivers are covered by comparable species compositions. Provided the abiotic drivers influencing the cells follow the same temporal pathways, cells with similar species compositions will continue to follow the same successional paths until cell-specific influences, such as immigration or disturbances, cause deviations of the species compositions among single cells. Cells with comparable abiotic drivers can hence lead to repetitive calculations. The D2C concept aims to reduce this redundancy by disentangling repetitive calculations from processes specific to single cells in a dynamic and adaptive way.

When upscaling a model with the D2C concept, processes which might lead to changes specific to a single cell, such as dispersal, recruitment and disturbances, are simulated on the original fine grid constituting the first layer. All other processes (e.g. light competition, growth and seed production) are simulated on the second layer solely consisting of representatives to which the cells of the first layer are assigned. Each element of the second layer represents all first-layer cells with similar environmental influences and similar species compositions, i.e. one type of first-layer cells. In order to classify the first-layer cells into types, thresholds have to be specified determining similarity of environmental drivers and of the model state variables describing species quantities and properties (e.g. size or age) in a cell. The number of these representatives, i.e. the number of types, can be dynamic, since processes simulated on the first layer can cause splits, and therefore new types. A split would, for example, be necessary when formerly absent species establish in only some of the cells assigned to one type. On the other hand, representatives which are similar enough according to the specified thresholds can be merged. This can, for example, happen when two representatives both reach a similar state, after being simulated separately because a species immigrated at different points in time (e.g. Fig. 3.1).

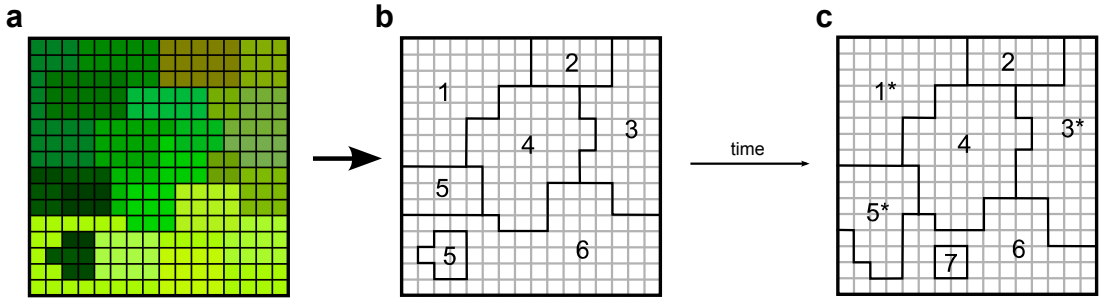

Figure 5.1 : Simple example for the dynamic two-layer classification concept. (Panel a) Cells with similar species compositions are depicted in the same shade of green. (Panel b) Similarity thresholds the species compositions and on model drivers determine the classification of first-layer cells (grey underlying grid) in different types (numbers) each constituting a second layer representative. The assignment of first-layer cells to their representatives (frames formed by the black lines) can change over time: processes simulated on the first layer can cause splits, for example seed dispersal, leading to new representatives (e.g. 7 – panel c). Second-layer processes change properties of the representatives (panel c – asterisks). Dynamics simulated on both layers can lead to changed associations due to merges and splits (e.g. changed frames panel b, c).

5.2.1 How to apply the D2C concept

In order to apply the D2C concept for a certain model, the following steps have to be conducted:

1. Modelled processes have to be assigned to the two different layers, i.e. the layer representing the fine scale, where processes are calculated for each cell, and the coarse-scale layer, where only representatives are evaluated. Processes which might lead to changes specific to a single cell, such as dispersal, recruitment and cell-specific disturbances need to be simulated on the first layer. All other processes (e.g. light competition, growth and seed production) can be simulated on the second layer.

2. Similarity thresholds have to be specified for the environmental drivers and for model state variables describing species quantities and properties in a cell. These thresholds determine the number of resulting representatives and therefore control large parts of the trade-off between computational expenses (computation time and memory) and accuracy[1]. There are multiple ways to specify the similarity thresholds. The simplest way would be to predefine a maximum number and to equidistantly stratify the range of environmental influences and expected species abundances. Alternatively, heuristics could be developed to determine the thresholds and to control similarity comparisons. One example are heuristics linked to

[1]Here accuracy is defined as the similarity of simulation results with two layers compared to results when simulating all processes on the original fine layer.

ingrowth: small changes in the ingrowth of established species might not lead to changes in the species composition, as opposed to changes for non- or underrepresented species. Thresholds in this example hence depend on the momentary situation of a considered site.

3. Whilst splits are required as soon as any of the thresholds would be violated, merges on the second layer do not necessarily have to be conducted in each iteration. Testing for similarity among all different representatives in each iteration would involve high computational expenses. An efficient application of the D2C concept therefore should also implement heuristics to reduce the overhead involved with these membership decisions. Merging could, for example, only be considered after certain time intervals or for representatives with a specific age. Another applicable heuristic would be to restrict comparisons among representative cells to groups with similar environmental conditions.

The assignment of the first-layer cells to representatives on the second layer at the beginning of a simulation depends on how the state variables of a model run are initialised. Many models simulating vegetation dynamics are initialised by a so-called spin-up from bare ground, i.e. without pre-assigned species' distributions. In this case, a simulation will start with a small number of representatives classified according to the similarity thresholds for the environmental drivers and will increase with simulation time. If the simulation area, on the other hand, is initialised based on species occurrence or abundance data, this data also needs to be classified, which is done according to the similarity thresholds for species compositions.

5.2.2 When to apply the D2C concept

We expect the D2C concept to be suitable for spatially explicit and linked, time- and space-discrete models in which repetitive calculations for cells with similar environmental drivers and species compositions constitute a big share of the computational expenses. In such cases, the separation into two different layers reduces the memory usage, since not all state variables have to be stored for the fine layer anymore and reduces the computation time for processes now executed on the coarse layer. Hence, the concept is expected to be suitable when the main share of the local processes are realised as deterministic processes (as done in the forest-landscape model TreeMig – see below and Lischke et al., 2006) or if stochastic processes are only realised as patch replications within each cell (as in the second generation DGVM LPJ-Guess – Hickler et al., 2012). The D2C concept will not be suitable when processes linking first-layer cells predominate the computational expenses or in case of a high variability in species compositions among first-layer cells with similar environmental influences. A high variability in species compositions can especially be expected when the species composition in a cell strongly depends on stochastic processes which are not realised as within cell patch replications (as in the forest-landscape model Landclim – Schumacher et al., 2004).

5.3 Applying the D2C concept to the forest-landscape model TreeMig

The forest-landscape model TreeMig is a dynamic time- and space-discrete intermediate-complexity model simulating the dynamics and spatial interactions of multiple competing tree species (Lischke et al., 2006). Depending on the simulation setup, the TreeMig Fortran implementation used in the following (TreeMig-Netcdf 2.0 – Nabel et al., submitted) has a computation time of approximately 0.2-0.7 millisecond for each cell and year on a 2.8GHz AMD Opteron CPU and a memory usage of approximately 5kB per cell (see Table 5.1 for some examples). The computational expenses hence constrain large-scale applications.

TreeMig simulations are driven by annual time series of three bioclimate variables per simulation cell (listed in Fig. 5.2b). These bioclimate variables are derived from monthly average temperatures and precipitation sums in combination with static information on slope and aspect of the terrain and water storage capacity for each cell (Lischke et al., 2006). Hence, the number of fluctuating environmental drivers is small and they are, moreover, correlated among each other and in space (Nabel et al., submitted; see Chapter 4). These properties imply

that TreeMig potentially requires a smaller number of representatives than a model with more or uncorrelated fluctuating environmental drivers.

TreeMig itself is already the result of a previous upscaling. The state variables are real-valued densities of seeds per tree species in the seed bank and of population densities of tree species in a constant number of distinct height classes per grid cell. These state variables represent mean densities determining Poisson distributions of the population density on a given unit area (the 'patch' area) and can be regarded as a deterministic representation of the local spatial forest heterogeneity (Lischke et al., 1998, 2006). This deterministic representation of the species composition on a constant number of height classes makes TreeMig particularly suitable for the application of the D2C concept because it implies less variability among different cells with similar environmental drivers. The discretisation to a constant number of height classes, furthermore, reduces the number of similarity thresholds required to test if representatives can be merged.

The first step to apply the D2C concept to a model requires the assignment of simulated processes to the two layers. In simulations with TreeMig the main share of the local processes are realised as deterministic processes which can be assigned to the coarse layer. Stochastic influences on the local processes can stem from purely random cell-specific disturbances (Lischke et al., 2006) or from random but spatially autocorrelated bioclimatic influences (Nabel et al., submitted; see Chapter 4). Therefore, single-cell disturbances and bioclimatic influences have to be simulated on the fine layer. Additionally, TreeMig simulations can be conducted with or without spatial linkage via seed dispersal. In simulations without spatial linkage all seeds stay in the producing cell which is what is typically done in models applied on larger scales. In simulations with spatial linkage seeds produced in a cell are distributed to its neighbourhood following deterministic or stochastic species-specific dispersal kernels. Since seeds are distributed to the neighbours of a cell, dispersal has to be simulated on the fine layer, together with associated seedbank dynamics (see Lischke et al., 2006).

5.3.1 Preclustering the bioclimate influences to assign representatives

In a first attempt to apply the D2C concept to TreeMig and to assess possible gains of its implementation, we established static assignments to representatives following a clustering of the bioclimate space. This approach was selected because TreeMig simulations are strongly influenced by its three bioclimate drivers (listed in Fig. 5.2b), whose interannual fluctuations are highly spatially correlated (Nabel et al., submitted; see Chapter 4). For these first tests we selected a nested set of three simulation areas: a small transect embedded in a larger transect, which itself is embedded in Switzerland (Fig. 5.2a). All of these simulation areas are gridded with a cell side length of 200m. We clustered the bioclimate influences with three sets of bioclimate classes (E1, E2, E3 – Fig. 5.2b) equidistantly distributed over the bioclimate space derived for Switzerland from an SRES A1B scenario simulation with RCA3 (Kjellström et al., 2005) downscaled to 200m cell side length based on an interpolated grid of MeteoSwiss weather stations.

To derive the representatives for each of the three simulation areas and to assign the single cells to these representatives we clustered the bioclimate time series of the SRES A1B scenario (1961-2100) following four steps: (1) We defined the average of the first and the last 30 years, as well as the average over the whole time span as sampling points. (2) For all cells we calculated the sampling points for each bioclimate variable and assigned them to the closest bioclimate class of the applied sets (Fig. 5.2b). (3) Cells with the same class for all three bioclimate variables and all sampling points were assigned to the same representative. (4) Finally, we derived bioclimate time series for the representatives by averaging the values of the associated cells for each year and variable.

Results from TreeMig simulations with two layers based on the assignment to the obtained representatives were compared to results from simulations on the single layer[2]. Comparisons of the overall resulting biomass and the biomass resulting for single species were conducted with a similarity coefficient (Equation 5.1) previ-

[2]All simulations were conducted for 1100 years starting in 1400 with a spin-up from bare ground. Bioclimate for years exceeding the scenario (i.e. 1400-1960 and 2101-2500) was extrapolated by sampling single years for the entire simulation area from a base set derived from the first (1961-1990) and the last 30 years (2071-2100), respectively (see Nabel et al., submitted; Chapter 4).

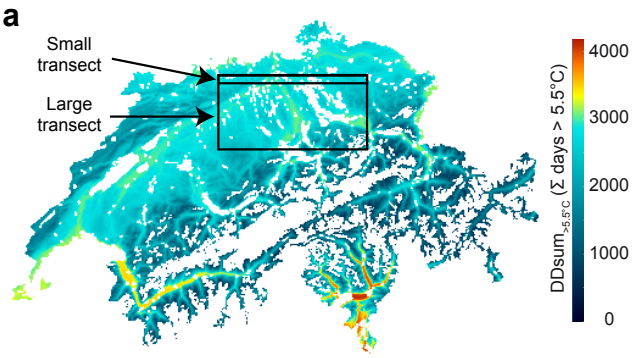

b

Bioclimate variable	Range min	Range max	# Classes E1	# Classes E2	# Classes E3
DDeg$_{>5.5°C}$ [a]	0	4200	85	43	22
Min. wtmp. [b]	-14	10	49	25	13
DrStr. [c]	0	0.7	29	15	6

[a] DDeg$_{>5.5°C}$: Sum of daily mean temperatures above 5.5°C
[b] Min. wtmp.: Minimum winter temperature
[c] DrStr.: An index describing drought severity

Figure 5.2 : (Panel a) Nested simulation areas used for simulations with a D2C TreeMig implementation. The map shows the values of the bioclimate variables $DD_{sum} > 5.5°C$ (sum of daily mean temperatures above 5.5°C) derived from the applied climate scenario for the year 2100. (Panel b) Applied sets of bioclimate classes.

ously used in various inter- and intramodel comparisons (e.g. Lischke et al., 1998; Nabel et al., 2013; see Chapter 3).

$$SC_y = 1 - \frac{\sum_{i=1}^{\#cells} |D_{sum_{i,y}}|}{\sum_{i=1}^{\#cells} S_{sum_{i,y}}} \tag{5.1}$$

The similarity coefficient (SC) for a year (y) of a run with two layers compared to the run on the single layer is calculated as the ratio of the sum of the absolute biomass differences ($|D_{sum}|$) of cells with the same coordinates (i) in this year and their sum (S_{sum}). When comparing the biomass per species, differences for each species are calculated separately. The SC can range from zero to one, with one resulting for a perfect match and zero for no similarity.

5.3.1.1 Simulating without spatial linkage

We calculated the similarity coefficient (SC) to compare simulations with two layers and the single layer over time, for simulations without spatial linkage, i.e. without seed dispersal to neighbouring cells and with an additional steady supply of seeds of all species in all cells (Fig. 5.3). The SCs resulting from the comparisons indicate that the simulation results are fairly similar. The nearly identical results in the spin-up diverge in the transient phase of climate warming after 2000 and subsequently stabilise on different levels depending on the resolution of the applied set of representatives (E1-E3). Since these simulations were conducted without spatial linkage and with no other stochastic influences than the bioclimate extrapolation, these comparisons show the error due to the clustering of the bioclimate and could further be reduced using a finer classification or additional sampling points. Simulations with different sets of representatives involve large differences in computational expenses compared to the simulation on one layer (see Table 5.1).

5.3.1.2 Simulating with spatial linkage

Simulations with the same setup as described above but with spatial linkage via seed dispersal and without additionally supplied seeds were conducted. These simulations, in which ingrowth to a representative was simply averaged from the associated fine layer cells, led to a reduction in the similarities (Fig. 5.4). The memory usage was about the same as for the simulations without spatial linkage, however, computation times increased strongly for both, simulations on one and simulations on two layers (Table 5.1). This increase in computation time was expected and is due to the higher common expenses due to the simulation of dispersal between fine layer cells. One consequence of this increase in 'base load' is that the gain in computation time between simulations on one and on two layers is also decreased.

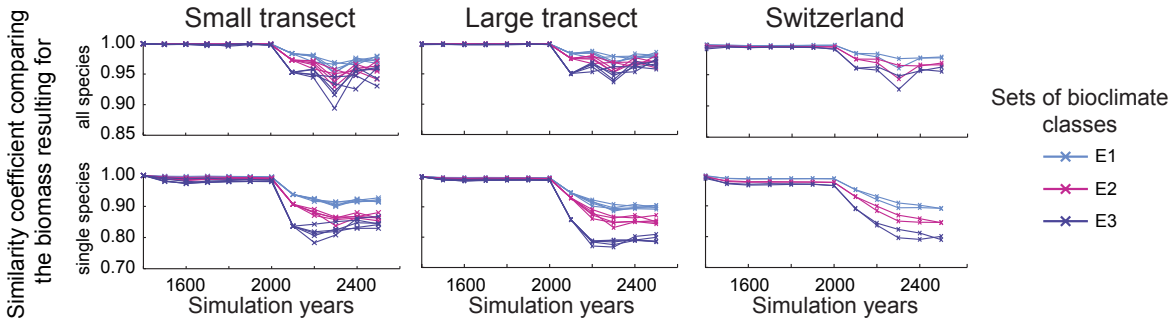

Figure 5.3 : Similarity coefficients (SCs) comparing results from simulations without spatial linkage conducted with one or two layers. The graphs show SCs for the biomass resulting for all and for the single species over time. Each colour represents SCs comparing results of the simulations with one layer to simulations with one of the applied sets of bioclimate classes (E1-E3 – Fig. 5.2b); lines of the same colour are repetitions with different pseudo-random number streams (PRNS) used to extrapolate bioclimate influences (five for the two transects, two for Switzerland). Comparisons were conducted between runs with the same PRNS.

Table 5.1 : Statistics for simulations with the three applied clustering schemes (E1-E3 – Fig. 5.2b) compared to simulation on one layer. Simulations were conducted without (F) and with spatial linkage (T) via seed dispersal.

			Small transect				Large transect					Switzerland			
			ORG	E1	E2	E3	ORG	E1	E2	E3		ORG	E1	E2	E3
	Reps.[a]	#100	125	12	3	1	1250	35	8	2	#1000	1920	56	11	2
		(%)		(9.6)	(2.4)	(0.8)		(2.8)	(0.6)	(0.2)			(2.9)	(0.6)	(0.1)
F	CPU time[b]	min.	63.2	6.3	1.8	0.5	618.1	23.2	5.6	1.7	hours	68.1	32.4	8.1	1.5
		(%)		(10.0)	(2.8)	(0.8)		(3.8)	(0.9)	(0.3)	(%)		(47.6)	(11.9)	(2.2)
T	CPU time[b]	min.	79.2	30.5	26.4	24.7	859.3	336.5	323.8	322.0	hours	95.6	40.6	37.1	36.7
		(%)		(38.5)	(33.3)	(31.2)		(39.2)	(37.7)	(37.5)	(%)		(42.5)	(38.8)	(38.4)
	Heap mem.[c]	MB	83.7	29.1	25.0	23.8	679.0	92.4	79.4	76.5	GB	10.2	1.2	1.0	0.9
		(%)		(34.8)	(30.0)	(28.4)		(13.6)	(11.7)	(11.3)	(%)		(11.4)	(9.8)	(8.8)

[a] Reps.: Rounded number of representatives (E1-E3) or cells (ORG) divided by 100 (small and large transect) and 1000 (Switzerland).

[b] CPU-time: computation time on a 2.8GHz AMD Opteron CPU measured with the intrinsic Fortran procedure CPU_TIME and averaged over five (small and large transect) or two (Switzerland) repetitions for each simulation setup.

[c] Peak heap memory: measured with the heap profiler Massif, a tool included in the Valgrind framework (Nethercote and Seward, 2003).

5.3.2 Discussion and Outlook

The example application of the D2C concept with TreeMig showed a reasonable gain in computational expenses which, for example, could be used to increase the simulated extent or to refine the resolution of the simulation area. At the same time, the application demonstrated limitations of the concept, in particular the loss of accuracy in simulations with spatial linkage caused by the averaging of the ingrowth from the fine layer. The introduced error will in particular cause problems in simulations where many species migrate in the simulation area, or where the migration of single species should be tracked. The next step to address such situations needs to be the implementation of dynamic partitioning and merging of representatives. However, the overhead introduced with these dynamic decisions will inevitably further reduce the gain in computational expenses, in addition to the reduction already involved with the spatial linkage. For simulations with spatial linkage, the D2C concept will hence only lead to reductions in computational expenses if efficient heuristics for the partitioning and the merging can be identified (see Section 5.2.1 for examples). Despite these pitfalls, the D2C concept has several advantages compared to other methods. It particularly allows retaining the fine

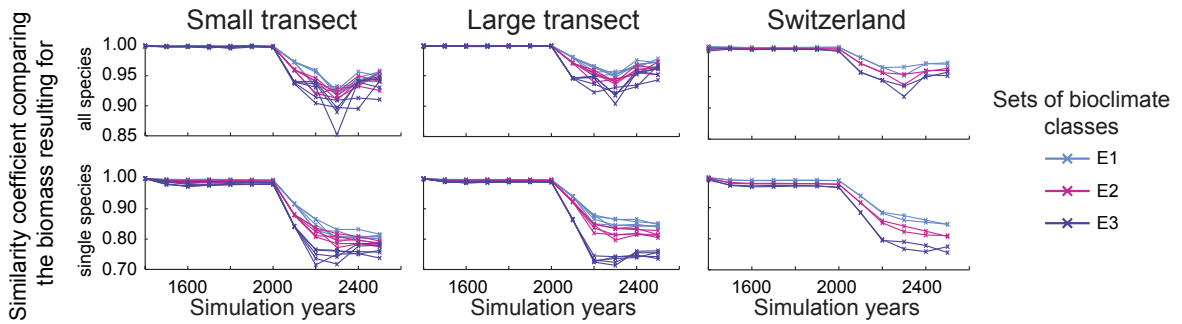

Figure 5.4 : Similarity coefficients (SCs) resulting for simulations with spatial linkage (Please see caption of Fig. 5.3).

resolution for important small-scale processes and for the simulation results, as opposed to other methods, such as equation free approaches or meta-modelling, which work with model results on a coarser scale. A further important advantage is that the representatives are not constrained to predefined spatial arrangements in contrast to, for example, adaptive meshing methods, which can only aggregate cells to compact regular shapes.

Acknowledgements

We like to thank Felix Kienast, James Kirchner, Natalie Zurbriggen and David Gutzmann for valuable discussions and comments and Dirk Schmatz for providing the downscaled data. Julia Nabel was partly funded by the Swiss National Science Foundation (SNF) Grant 315230-122434.

References

Auger, P., Poggiale, J., Sánchez, E., 2012. A review on spatial aggregation methods involving several time scales. Ecological Complexity 10, 12–25.

Bocedi, G., Pe'er, G., Heikkinen, R.K., Matsinos, Y., Travis, J.M., 2012. Projecting species' range expansion dynamics: sources of systematic biases when scaling up patterns and processes. Methods in Ecology and Evolution 3, 1008–1018.

Fischlin, A., Midgley, G.F., Price, J.T., Leemans, R., Gopal, B., Turley, C., Rounsevell, M.D.A., Dube, O.P., Tarazona, J., Velichko, A.A., 2007. Ecosystems, their properties, goods, and services. Climate Change 2007: Impacts, Adaptation and Vulnerability. Contribution of Working Group II to the Fourth Assessment Report of the Intergovernmental Panel on Climate Change. M.L. Parry, O.F. Canziani, J.P. Palutikof, P.J. van der Linden and C.E. Hanson, Eds., Cambridge University Press, Cambridge, UK, 211-272.

Fisher, R., McDowell, N., Purves, D., Moorcroft, P., Sitch, S., Cox, P., Huntingford, C., Meir, P., Woodward, F.I., 2010. Assessing uncertainties in a second-generation dynamic vegetation model caused by ecological scale limitations. New Phytologist 187, 666–681.

Hickler, T., Vohland, K., Feehan, J., Miller, P.A., Smith, B., Costa, L., Giesecke, T., Fronzek, S., Carter, T.R., Cramer, W., Kühn, I., Sykes, M.T., 2012. Projecting the future distribution of European potential natural vegetation zones with a generalized, tree species-based dynamic vegetation model. Global Ecology and Biogeography 21, 50–63.

Huntley, B., Barnard, P., Altwegg, R., Chambers, L., Coetzee, B.W.T., Gibson, L., Hockey, P.A.R., Hole, D.G., Midgley, G.F., Underhill, L.G., Willis, S.G., 2010. Beyond bioclimatic envelopes: dynamic species' range and abundance modelling in the context of climatic change. Ecography 33, 621–626.

Kevrekidis, I.G., Samaey, G., 2009. Equation-Free Multiscale Computation: Algorithms and Applications. Annual Review of Physical Chemistry 60, 321–344.

Kjellström, E., Bärring, L., Gollvik, S., Hansson, U., Jones, C., Samuelsson, P., Rummukainen, M., Ullerstig, A., U., W., Wyser, K., 2005. A 140-year simulation of European climate with the new version of the Rossby Centre regional atmospheric climate model (RCA3). SMHI Reports Meteorology and Climatology No. 108, SMHI, SE-60176, Norrköping, Sweden, 54 pp.

Lischke, H., Löffler, T.J., Fischlin, A., 1998. Aggregation of Individual Trees and Patches in Forest Succession Models: Capturing Variability with Height Structured, Random, Spatial Distributions. Theoretical Population Biology 54, 213–226.

Lischke, H., Löffler, T.J., Thornton, P.E., Zimmermann, N.E., 2007. Model Up-scaling in Landscape Research. A Changing World. Challenges for Landscape Research. Springer. chapter 16. pp. 259–282.

Lischke, H., Zimmermann, N.E., Bolliger, J., Rickebusch, S., Löffler, T.J., 2006. TreeMig: A forest-landscape model for simulating spatio-temporal patterns from stand to landscape scale. Ecological Modelling 199, 409–420.

Nabel, J.E.M.S., Kirchner, J.W., Zurbriggen, N., Kienast, F., Lischke, H., submitted. Extrapolation methods for climate time series revisited – spatial correlations in climatic fluctuations influence simulated tree species' abundance and migration.

Nabel, J.E.M.S., Zurbriggen, N., Lischke, H., 2013. Interannual climate variability and population density thresholds can have a substantial impact on simulated tree species' migration. Ecological Modelling 257, 88–100.

Neilson, R., Pitelka, L., Solomon, A., Nathan, R., Midgley, G., Fragoso, J., Lischke, H., Thompson, K., 2005. Forecasting Regional to Global Plant Migration in Response to Climate Change. BioScience 55, 749–759.

Nethercote, N., Seward, J., 2003. Valgrind: A Program Supervision Framework. In Proceedings of the Third Workshop on Runtime Verifcation (RV'03), Boulder, Colorado, USA, July 2003. Available at http://valgrind.org/docs/valgrind2003.ps.

Schumacher, S., Bugmann, H., Mladenoff, D.J., 2004. Improving the formulation of tree growth and succession in a spatially explicit landscape model. Ecological Modelling 180, 175–194.

Urban, D., Acevedo, M., Garman, S., 1999. Scaling fine-scale processes to large-scale patterns using models derived from models: meta-models. Advances in spatial modeling of forest landscape change: approaches and applications. Cambridge University Press, Cambridge, UK. chapter 4. pp. 70–98.

Zumbusch, G., 2003. Parallel Multilevel Methods. Adaptive Mesh Refinement and Loadbalancing. Teubner.

Chapter 6

The dynamic two-layer classification concept: a dynamic upscaling method to reduce computational expenses in spatial simulations of vegetation dynamics

Manuscript

Julia E. M. S. Nabel[a,b]

[a]*Department of Environmental Systems Science,*
Swiss Federal Institute of Technology ETH, 8092 Zurich, Switzerland
[b]*Landscape Dynamics, Swiss Federal Institute for Forest,*
Snow and Landscape Research WSL, Zürcherstrasse 111, 8903 Birmensdorf, Switzerland

Abstract

1. Models used to conduct spatio-temporal impact studies of climatic changes on vegetation dynamics need to balance required accuracy with computational feasibility. To enhance the computational efficiency of these models, upscaling methods are required that maintain important fine-scale processes influencing vegetation dynamics.
2. In this paper, an adjustable method – the dynamic two-layer classification (D2C) concept – for the upscaling of time- and space-discrete models is presented which aims to disentangle potentially repetitive calculations from processes specific to single cells. The idea of the method is to extract processes that do not require information on the spatial position of a cell in the simulation area to a reduced-size non-spatial layer, which is introduced in addition to the original two-dimensional layer. Cells on the two-dimensional layer are dynamically associated with elements on the non-spatial layer, on which the extracted processes are simulated.
3. I present how the method can be implemented in an intermediate-complexity forest-landscape model and provide different application examples. Based on these examples, the trade-off between computational expenses and accuracy, as well as the applicability of the D2C concept to upscale time- and space-discrete models, are discussed.
4. The application examples demonstrate that the D2C concept has the potential to strongly reduce computational expenses required for processes calculated on the non-spatial layer, and that the D2C concept is a valuable upscaling method for models and applications in which spatial processes constitute the minor share of the overall computational expenses.

6.1 Introduction

Spatio-temporal impact studies of climatic changes on vegetation dynamics are often conducted with so-called dynamic vegetation models (DVMs, sensu Snell et al., accepted; see Appendix A). DVMs are usually imple-

mented as time- and space-discrete models, simulating important ecological processes, such as establishment, growth and mortality, under consideration of biotic and abiotic influences. As all models do, DVMs need to balance accuracy with computational feasibility and parametrisation requirements (Huntley et al., 2010; He et al., 2011). Modelled processes and their level of detail vary among DVMs, with a close link to the apparent trade-off between spatial resolution and spatial extent of the simulation area: DVMs which simulate small-scale processes with a fine spatial resolution ($< 1\text{km}^2$) often have high computational expenses and can only operate on much smaller spatial extents than those with coarser resolution neglecting small-scale heterogeneity (see examples listed in Snell et al., accepted; see Appendix A). There is a steady increase in the spatial extents that small-scale models can be applied on, due to increasing computational capacities and the availability of cost reductions via pure computational methods (mainly code optimisations and different parallelisation techniques). Nevertheless, there is still a gap in what can be studied with small- and large-scale models. One of the main reasons for this gap is the fact that the spatial resolution on which a process is simulated can markedly influence simulation results, such that decreasing the spatial resolution to increase the spatial extent risks introducing strong biases, such as replacing rare with dominant forest types (He et al., 2011), or overestimating dispersal distances and population sizes (Bocedi et al., 2012). Thus, there is a need to develop upscaling methods that maintain required fine resolution for important small-scale processes (Bocedi et al., 2012).

Many upscaling methods have been proposed and applied in the context of ecological modelling (see e.g. Urban et al., 1999; Lischke et al., 2007; Auger et al., 2012). Most of these methods seek to aggregate small-scale information to a coarser scale; these aggregations can be temporal, spatial or thematical, i.e. regarding simulated processes or state variables. When the fine spatio-temporal resolution should be maintained (as recommended by Bocedi et al., 2012) remaining possibilities for cost reductions are thus thematical. One example finding broad application in DVMs is the aggregation of individuals with similar properties into cohorts, such that solely one representative calculation, instead of multiple replicate calculations, needs to be conducted (for this and further examples see Snell et al., accepted; see Appendix A). In this paper I present an adjustable upscaling method which also is based on such a similarity approach: the dynamic two-layer classification (D2C) concept.

The motivation for the D2C concept is the observation that simulations with time- and space-discrete DVMs entail redundant replicate calculations when different simulation cells share similar state variables and drivers for long periods of time. The D2C concept aims to avoid such redundant calculations by dynamically combining cells to groups with similar properties, for which subsequently only one representative calculation is conducted. The property of time- and space-discrete DVMs to lead to redundant replicate calculations has already been used to decrease computational expenses in finite state individual based models with a simple age based succession (Yang et al., 2011) and for spatially-explicit models without spatial linkage (Nabel and Lischke, 2013; see Chapter 5). These two cases can be regarded as restricted application cases and will be picked up in the discussion.

In the following I will outline the basic principles of the D2C concept. Subsequently I will present an implementation of the D2C concept using the example of an intermediate-complexity DVM, the forest-landscape model TreeMig (Lischke et al., 2006), and I will examine its applicability with two different applications scenarios.

6.2 The dynamic two-layer classification (D2C) concept

The D2C concept aims to increase the computational efficiency of time- and space-discrete DVMs through identification and elimination of redundant calculations. Such redundancies can occur in simulations with a DVM because cells with comparable species' composition and abundances, i.e. comparable values in the cells' state variables, tend to follow the same successional paths provided that their abiotic drivers follow the same temporal pathways and provided that none of the cells is subject to any cell-specific deviations, such as entailed by disturbances or immigration. The target models for the D2C concept considered here are complex, two-dimensional (i.e. spatially linked) DVMs, as opposed to spatially one-dimensional DVMs (sensu Fisher et al.,

2010) or such with a decreased complexity (e.g. only considering species' presence and absence). Such DVMs can be considered restricted application cases and are picked up in the discussion.

The idea behind the D2C concept is to only simulate such processes on the original two-dimensional layer, i.e. for all simulated cells, which use information on the spatial position of a cell relative to other cells in the simulation area. One example for such processes is seed dispersal using source and sink positions. Processes using information on the spatial position of a cell can entail cell-specific deviations, for example inflow of seeds of a new species not contained in otherwise similar cells. All other processes, such as light competition, growth or seed production are simulated on a new associated non-spatial layer (Fig. 6.1). Each element of the non-spatial layer represents a certain type of cells on the two-dimensional layer, characterised by prevailing abiotic conditions and momentary species' composition and abundances. Each cell of the two-dimensional layer, in turn, is associated with one element of the non-spatial layer (visualised in Fig. 6.1 with numbers). However, neither this association, nor the number of elements on the non-spatial layer need to be static. Processes simulated on the two-dimensional layer can require addition of new elements to the non-spatial layer, for example, when a species newly establishes after being dispersed to some but not all cells represented by one element. It is on the other hand possible that elements on the non-spatial layer can be merged when they are similar enough in all state variables and in their abiotic drivers.

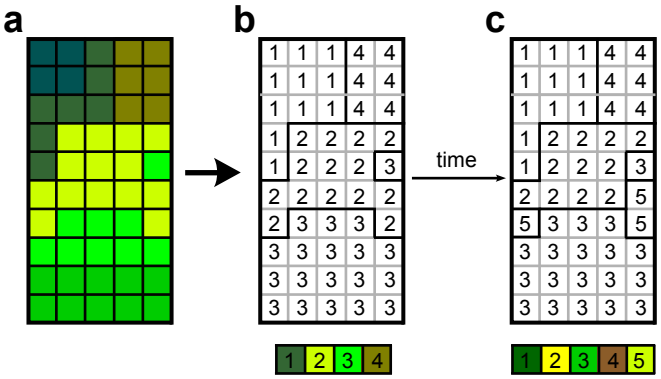

Figure 6.1 : Visualisation of the dynamic two-layer classification concept. (Panel a) Pre-defined similarity criteria (e.g. on climate and species' compositions) are used to classify similar cells to distinct types. Cells of the same type are coloured with the same shade of green. (Panel b) For each type of cells one element is required on the non-spatial layer (coloured row, bottom). Cells on the two-dimensional layer (2D-grid, top) are associated to these elements (numbers represent associations). Species' compositions can change over time due to processes simulated on both layers (changes from panel b to c in the coloured row, bottom). Furthermore, associations between the layers can change (changes of numbers from panel b to c), for example, when processes simulated on the spatial-layer (e.g. seed dispersal) lead to differences among cells associated with the same element of the non-spatial layer violating any specified similarity criteria.

To apply the D2C concept, the processes of a model and its state variables need to be disentangled and assigned to the two layers, the two-dimensional layer and the non-spatial layer. Additionally, one must define the exchange of status information between cells on the two-dimensional layer and their associated elements on the non-spatial layer. The assignment of processes and the definition of the interface between the two layers are critical steps because the information directed from the cell to the elements on the non-spatial layer is used to test if associations are still valid, or if an element needs to be split up. To control splits, but also to test if two elements on the non-spatial layer are similar enough to be merged, similarity criteria need to be defined for the abiotic driver and for the model state variables. The potential for reductions of computational expenses with the D2C concept will be influenced by (1) the base load due to processes simulated on the two-dimensional layer, i.e. processes requiring information on the spatial position of a cell; (2) the number of elements on the non-spatial layer, which in turn is controlled by the specified similarity criteria; and (3) the overhead introduced for managing elements on the non-spatial layer, associations between the two layers and the exchange of status information between the layers.

6.3 Methods

6.3.1 Implementation of TreeMig-2L

I demonstrate the implementation of the D2C concept using the example of the forest-landscape model TreeMig (Lischke et al., 2006). TreeMig is an intermediate-complexity DVM simulating multiple competing tree species and allowing for explicit simulation of tree species' migration, with the rare advantage of including seed dispersal and subsequent regeneration processes (Thuiller et al., 2008). Descriptions in the following refer to the TreeMig two-layer implementation **TreeMig-2L**, implemented in Fortran and based on TreeMig-Netcdf 2.0 (Nabel et al., submitted; see Chapter 4) . Additional details on the implementation are given in Appendix 6.A.

6.3.1.1 TreeMig's drivers and state variables

TreeMig simulations require time series of three different annual bioclimatic drivers: the minimum winter temperature, the sum of daily mean temperatures above $5.5\,^{\circ}\mathrm{C}$, and an index denoting the severity of droughts (Lischke et al., 2006; Nabel et al., submitted; for the latter see Chapter 4). TreeMig's state variables are population densities of tree species in a constant number of height classes per grid cell (Lischke et al., 2006). In addition to these population densities describing established individuals, TreeMig also stores densities of seeds per tree species, representing the seed bank of a cell.

6.3.1.2 Assigning processes to the different layers

Most of the processes simulated with TreeMig do not require information on the position of the cell relative to other cells in the grid: competition for light, growth, mortality and production of seeds in a cell only use information that is independent of other cells. Therefore, these processes can be simulated on the new non-spatial layer (Fig. 6.2). In TreeMig-Netcdf 2.0, the only process which requires information on the position of a cell is seed dispersal, which thus has to be simulated on the two-dimensional layer. For TreeMig-2L simulations to be efficient, associations between cells on the two-dimensional layer and elements on the non-spatial layer need to be as long-lived as possible, i.e. re-merging of elements with a very recent split needs to be prevented, and splits should only be conducted if they entail actual changes in species' compositions. The availability of seeds of a species, however, does not necessarily have to lead to changes in the species' composition, because a species might not be able to regenerate in a cell. Therefore, the entire regeneration process was assigned to the two-dimensional layer (Fig. 6.2), although seed dispersal is the only process in the current version actually requiring information on the position relative to other cells. Further processes requiring such information could, for example, be spatially connected disturbances (e.g. Zurbriggen, 2013), these are however not included in TreeMig-2L.

6.3.1.3 Architecture of TreeMig-2L

When designing TreeMig-2L the two main requirements were a fast exchange of status information between the two layers and an efficient organisation of the elements on the non-spatial layer. The architecture of TreeMig-2L had to accomondate the circumstance that the number of elements on the non-spatial layer is not known in advance but is an emergent property of the temporal development during a simulation. The array data structure used in previous TreeMig implementations was therefore only kept for the two-dimensional layer. The elements on the non-spatial layer in contrast are stored in linked lists. A linked list is a dynamic data structure that can grow and shrink dynamically in size, and that allows for a fast traversal (for more information see Section 6.A.1). Elements stored in the same list share similarities to reduce the organisational overhead during runtime for comparison of elements. Instead of comparing all elements to all other elements, which would be very inefficient, only elements in the same list are compared. To pre-define which element is stored in which list , the fact is used that for cells to be similar not only species' compositions need to satisfy the given similarity criteria but also bioclimatic influences need to be comparable. As opposed to species' compositions,

which develop during runtime, bioclimatic drivers are an input to TreeMig-2L. Information about the bioclimate drivers can thus be used in advance to pre-structure a simulation area. In this pre-structuring, cells with a comparable bioclimate driver are assigned to what I refer to as bioclimate types in the following. For each of these bioclimate types an own list is used to store elements on the non-spatial layer (Figs. 6.2 and 6.A.1). Each bioclimate type has a pointer – a data type allowing direct access – to the first element in its list. In addition, each cell of the two-dimensional layer has a pointer to the element with which it is currently associated, to allow for a direct and therefore fast exchange of the status information.

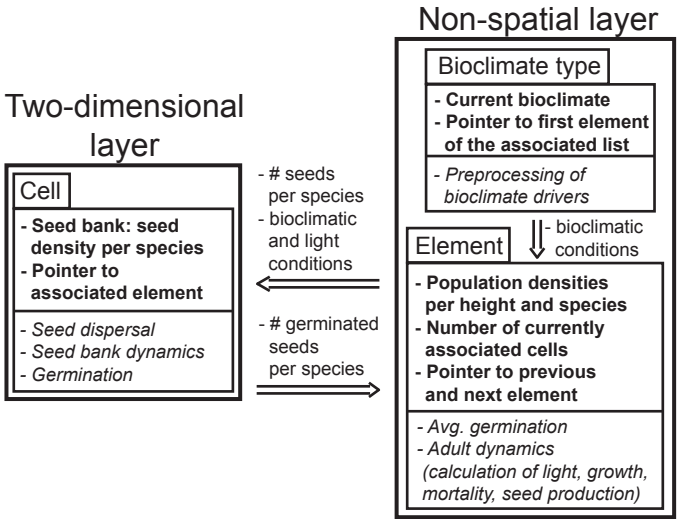

Figure 6.2 : Outline of the architecture of TreeMig-2L. The two-dimensional layer consists of single cells whose state variables are seed densities per species in the seed bank. Additionally, each cell has a pointer – a data type allowing direct access – to the element of the non-spatial layer with which the cell is currently associated. The non-spatial layer consists of bioclimate types and linked lists of associated elements (for more information see Section 6.A.1). State variables are printed in bold, processes in italic type. Items listed on the arrows represent information exchanged between the layers and between bioclimate types and elements of their associated list.

Pre-structuring of a simulation area The organisation of the non-spatial layer in TreeMig-2L is based on a pre-structuring of the bioclimate drivers (for an example see Fig. 6.A.2). For this pre-structuring a set of bins for each of the three bioclimate influences needs to be defined (see e.g. Table 6.2) and a set of periods ('supporting periods') has to be selected over which the bioclimate influences are averaged. These averages are compared among all cells of a simulated area. Cells whose averages fall into the same bioclimate bins for all supporting periods are clustered into the same bioclimate type. These bioclimate types constitute the static basic structure of the non-spatial layer. The bioclimate influence for a bioclimate type is then calculated as the average of all associated cells for each point in time. In two-layer simulations with TreeMig-2L the bioclimate information is thus not processed on the cell level, but on the non-spatial layer in the bioclimate types. Although it is common to (stochastically) extrapolate required bioclimate drivers from available data (Nabel et al., 2013; see Chapter 3), spatial autocorrelations in bioclimate influences should always be maintained (Nabel et al., submitted; see Chapter 4). Thus, as long as the extrapolation method does not violate the spatial autocorrelation of the bioclimatic influences, a pre-structuring based on the available data will also be valid for possible extrapolations.

Information exchange between the two layers Because the number of elements and their associations with cells on the two-dimensional layer change over time, only cells have pointers to the element with which they are currently associated (Fig. 6.2) and elements only have information about how many but not which cells are associated with them. The communication between the layers is thus asymmetric, and each cell accesses the densities of produced seeds per species from the associated element. In addition, current bioclimatic and

light conditions are accessed and used to calculate the densities of newly germinated seeds per species. Newly germinated seeds are used to determine if splits are necessary (see Section 6.3.1.4). After dynamic changes in associations between the layers, cells push their number of germinated seeds to the currently associated element and each element of the non-spatial layer calculates the average of the germinated seeds. In the special case that germination is close to zero for a species, i.e. if the density of germinated seeds falls below the threshold which defines presence, germinated seeds of this species are not averaged but set to zero for this element.

6.3.1.4 Dynamic associations

In order to account for spatial processes resulting from seed dispersal, associations between the two-dimensional and the non-spatial layer need to be dynamic. In a TreeMig-2L simulation, elements on the non-spatial layer can be split up or merged (see Section 6.A.3 for details on the execution sequence of a TreeMig-2L simulation).

Splitting elements Splitting, and thus introduction of new elements on the non-spatial layer is required as soon as the density of germinated seeds among any two cells associated with the same element is considered not similar enough. In TreeMig-2L, similarity in the density of germinated seeds is defined by a set of thresholds. The simplest possible set consists of a single threshold which defines presence, i.e. species with a density below this threshold are assumed to be absent. However, other thresholds are also possible, for example dividing sparse occurrences from more frequent ones. If the density of germinated seeds of any two cells associated with the same element fall on different sides of any of these thresholds for a single species, a split is required. One determinant for the efficiency of a TreeMig-2L simulation is assumed to be the number of considered splits. When $k-1$ thresholds are specified and n species are simulated, k^n different combinations could possibly entail splits. In TreeMig-2L this trade-off between accuracy and possible splits is approached by only considering splitting for species previously specified as species to be tracked. Deviations in the germinated seed densities of species which are not tracked are thus not controlled in a simulation.

Merging elements The state variables stored in the elements on the non-spatial layer are population densities per species for a fixed set of height classes (Section 6.3.1.1). In TreeMig-2L, two elements belonging to the same bioclimatic type (Section 6.3.1.3) are merged when deviations between each pair of their population densities do not exceed a similarity threshold pre-specified for each of the height classes. To avoid immediately re-merging of elements that were recently split up, newly germinated seed densities also need to satisfy a similarity test. As opposed to splitting, merging of elements on the non-spatial layer potentially decreases accuracy and there is a trade-off between costs involved with merging and the reduction of repetitive calculations caused by similar elements. In TreeMig-2L merging is therefore only performed after a pre-defined number of iterations.

6.3.2 Simulations with TreeMig-2L

6.3.2.1 Influences on the expected benefit

Previous TreeMig simulations were conducted with different spatial resolution (cell side lengths of 25m to 1km) and extents (up to 77000 km^2) for different numbers of interacting tree species (up to 31) and for simulation areas with different spatio-temporal complexity (see e.g. Epstein et al., 2007; Nabel et al., 2013; Nabel and Lischke, 2013; Zurbriggen, 2013; see Chapters 3 and 5 and Section 1.2.4.4). Differences in such simulation settings are expected to strongly influence the potential benefit of the D2C implementation, because they control two of the properties assumed to be most important (see Section 6.2): (1) the base load due to computation time spent with processes simulated on the two-dimensional layer, and (2) the ratio between the number of cells on the two-dimensional layer and the number of bioclimate types. A simulation area with a high spatio-temporal

complexity, i.e. with a high heterogeneity in its bioclimate drivers, for example, is expected to end up with a large number of bioclimate types. Increasing the spatial extent of a simulation area will, up to a certain point, also potentially increase the number of bioclimate types, however, there might be a certain threshold beyond which the number of already contained types exceeds the number of newly added types. A similar effect is expected for increases in spatial resolution: bioclimate influences in a cell are always averages and with increased resolution fewer bioclimate extremes might be smoothed out, increasing the number of required bioclimate types. However, especially in areas with a homogeneous bioclimate, an increase in resolution might lead to a larger number of similar cells, increasing the potential benefit of a D2C application. An increase in spatial resolution, on the other hand, will lead to a larger amount of sink cells considered for each source cell for seed dispersal. In TreeMig, seed dispersal is simulated from the perspective of the source cell, providing seeds to sink cells according to a pre-calculated truncated probabilistic density function (see supplementary material of Lischke et al., 2006). As a direct consequence, the number of sink cells depends on the resolution of the original grid. A finer resolution implies a larger number of sink cells for each source cell, which necessarily will increase the computational costs involved with the seed dispersal calculations, i.e. the base load due to processes simulated on the two-dimensional layer, and therefore will decrease the benefit of the D2C implementation. Finally, the benefit is expected to be influenced by the number of tracked species, the splitting and merging thresholds, and the number of iterations after which merging is considered.

Table 6.1 : Main characteristics of the two application scenarios. For an in-depth description see Appendix 6.B. Scenario A1 was previously used for a preliminary study with a pre-version of TreeMig-2L without dynamic associations between the layers (Nabel and Lischke, 2013; see Chapter 5). Scenario A2 was used to investigate the influence of interannual bioclimate variability on the simulated northwards migration of *Ostrya carpinifolia* (Nabel et al., 2012, 2013; see Chapters 2 and 3).

	Spatial complexity	Spatial resolution[a]	Spatial extent	Number of cells (stockable cells[b])	Competing species	Time span simulated	Tracked species	Number of repetitions
A1	Rather homogeneous	200m	5000 km^2	125000 (110789)	31	1400-2500	Most drought resistant	5
A2	Very heterogeneous	1km	14700 km^2	14700 (12230)	22	1400-3000	*Ostrya carpinifolia*	100

[a] Cell side length

[b] Stockable cells denote cells in which trees can grow in a TreeMig simulation (trees cannot grow in cells with large water bodies or solid rock surfaces).

6.3.2.2 Application scenarios

TreeMig-2L simulations were conducted for two different application scenarios (A1 and A2). These application scenarios were selected because they strongly differ in the simulation settings mentioned above. Fig. 6.3 shows the location of the simulation areas in Switzerland. A1 stems from a preliminary study with a pre-version of TreeMig-2L without dynamic associations between the layers (Nabel and Lischke, 2013; see Chapter 5), and A2 was used to investigate the influence of interannual bioclimate variability in a scenario of the northwards migration of *Ostrya carpinifolia* Scop. (European Hop Hornbeam) (Nabel et al., 2012, 2013; see Chapters 2 and 3). Table 6.1 lists the main characteristics of the application scenarios; an in-depth description can be found in Appendix 6.B.

Application scenario A1 has a spatially rather homogeneous simulation area and a finer spatial resolution, such that a better ratio between the number of cells on the two-dimensional layer and the number of bioclimate types is expected for scenario A1 than for scenario A2. On the other hand, due to the finer spatial resolution higher base load costs are expected for scenario A1. Whilst the tracked species in the scenario of a northwards migration in A2 is naturally the migrating species (*Ostrya carpinifolia*), four species with high drought tolerance indices in TreeMig (*Quercus pubescens*, *O. carpinifolia*, *Larix decidua*, *Pinus silvestris*) were selected as tracked species for scenario A1, because with increasing drought severity (and increasing temperatures), these species are expected to extend their spatial distributions. For both scenarios, merging was considered every 100 simulation years and the same splitting and merging thresholds were used (for these settings and some sensitivity tests see Appendix 6.C).

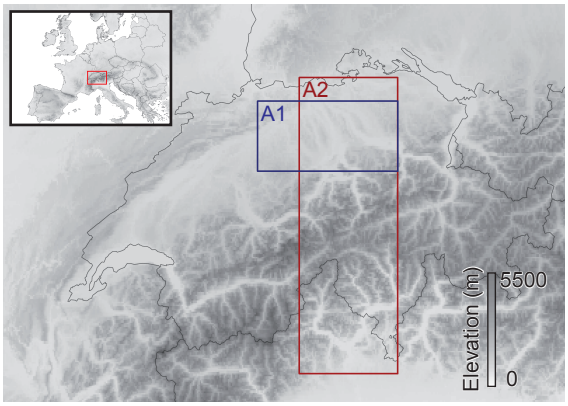

Figure 6.3 : Location of the two simulation areas in Switzerland, superimposed on the digital elevation model by Jarvis et al. (2008), illustrating the differences in elevational heterogeneity between the simulation areas of application scenario A1 and application scenario A2.

Both application scenarios were driven by bioclimate time series derived from SRESA1B (Nakicenovic et al., 2000) scenario projections, although from different models and downscaled with different observational data (see Appendix 6.B). To cover the entire simulation time spans of the examples, a stochastic extrapolation method accounting for the spatial correlation of the fluctuations found in the available bioclimate time series was used (see Appendix 6.B and Nabel et al., submitted; see Chapter 4).

6.3.2.3 Pre-structuring of the simulation areas

Bioclimate types for both application scenarios were derived with the same set of bioclimate bins (Table 6.2). For both scenarios three sampling periods were averaged: the first 30 (Scenario A1: 1961-1991; A2: 1901-1931) and the last 30 years (both: 2071-2100), as well as the whole time span (A1: 1961-2100; A2: 1901-2100).

Table 6.2 : Sets of bioclimate bins applied for the pre-structuring of the simulation areas. Minimum and maximum ranges of the bioclimate variables cover the bioclimate ranges of both application scenarios. For each of the three sets, the three bioclimate variables are discretised with different resolution (E1: fine, E2: moderate, E3: coarse).

	Range		Resolution (#bins)		
Bioclimate variable	min	max	E1	E2	E3
$DDsum_{>5.5\,°C}$ [a]	0	4200	50 (85)	100 (43)	200 (22)
Min. witemp.[b]	-14	10	0.5 (49)	1.0 (25)	2.0 (13)
Drought index	0.0	0.7	0.025 (29)	0.05 (15)	0.1 (8)

[a] $DDsum_{>5.5\,°C}$: Sum of daily mean temperatures above $5.5\,°C$
[b] Min. witemp.: Minimum winter temperature [°C]

6.3.2.4 Conducted simulations

Simulations were conducted with bioclimate types from pre-structurings of the simulation areas with each of the three sets of bioclimate bins (E1, E2 and E3 – Table 6.2) and with multiple repetitions to account for the stochasticity involved with the extrapolation of the bioclimate drivers. For application scenario A1 five repetitions were calculated. For scenario A2, which requires one-tenth of the computation time of scenario A1, 100 repetitions were calculated[1]. To disentangle the effects of the pre-structuring and of dynamic associations, three different kinds of simulations were conducted with E1-E3 derived bioclimate types: (1) simulations with two layers and with dynamic associations (2L); (2) simulations with two layers but without dynamic associations

[1]The average CPU-time with the original one-layer approach (1L-ORG) was 50353s (average of five runs with σ = 784s) for A1 runs and 5195s (average from 100 runs with σ = 38).

(2L-NDA), i.e. with only one element for each bioclimate type; and (3) simulations with the pre-structured bioclimate driver but with all processes simulated on one layer (1L-PB). Finally, in order to obtain reference values, a further kind of simulations were conducted, namely simulations with the original bioclimate driver and the original one-layer approach (1L-ORG).

6.3.2.5 Applied performance measures

The ratio of computation costs spent on different processes was profiled with callgrind (Weidendorfer, 2008). As described above, simulation costs spent with processes simulated on the two-dimensional layer are expected to determine the main share of the base load not reducible with the D2C concept. To assess the performance of the D2C concept two measures were calculated: an accuracy measure and the required CPU time[2]. As a measure of accuracy, different output variables were compared with a similarity coefficient (Equation 6.1) already used in previous studies for intra-model comparisons (e.g. Lischke et al., 1998; Nabel et al., 2013; for the latter see Chapter 3), ranging from zero (no similarity) to one (identical output).

$$SC_y = 1 - \frac{\sum_i^{cell} |D_{sum_i}|}{\sum_i^{cell} S_{sum_i}} \tag{6.1}$$

The similarity coefficient SC_y for a year y is calculated as the ratio of the sum of an output variable of two runs S_{sum_i} and their differences $|D_{sum_i}|$ summed over all cells of the simulation area. The SC was used to compare 1L-ORG simulations to simulations with E1-E3 derived bioclimate types (see Section 6.3.2.4), whereas each comparison was conducted with runs with the same pseudo-random number stream used to extrapolate the driving bioclimate time series. For both application scenarios, the SC for the sum of the biomass of all species (SC_{sum}) and the SC of the biomass per species (SC_{spec}) were calculated, for A1 every century and for A2 every 50 years. For A2 simulations, furthermore, the SC of the biomass of *O. carpinifolia* (SC_{OC}) was calculated for each year. In addition to SC comparisons, the northernmost occurrences over time, as well as the spatial spread of *O. carpinifolia* in the last simulation year, were compared for E1-E3 and 1L-ORG simulations of the application scenario A2.

6.4 Results and discussion

6.4.1 Pre-structuring of the simulation areas

The pre-structuring resulted in a considerably smaller number of bioclimate types compared to cells of the simulation area for both application scenarios but was very different for the two scenarios in absolute as well as relative terms (Table 6.3). The simulation area of application scenario A1 always contained fewer bioclimate types than A2 (E1: ∼factor 2; E2 and E3: ∼factor 4) and especially the resulting ratio of bioclimate types to the number of cells of the simulation area was much smaller (E1: ∼factor 20; E2 and E3: ∼factor 40). As suggested in Section 6.3.2.1, this is due to the increased spatial homogeneity, the coarser resolution and the smaller bioclimatic range covered in the simulation area of scenario A1 compared to the simulation area of A2. A2's simulation area is divided in a larger number of bioclimate types, with two-thirds as many bioclimate types as cells for the finest set of bioclimate bins (E1). For this set, thus, more than half of the cells end up with their own bioclimate type (Fig. 6.C.1 shows the distribution of numbers of cells to bioclimate types).

The averaging of the bioclimate driver of single cells to obtain the driver for the bioclimate types led to small but visible deviations in the bioclimate (e.g. Figs. 6.4, 6.C.5 and 6.C.6). These deviations in the bioclimate driver entail deviations in the simulation results from the simulations on one layer, i.e. simulations with the original cell-based bioclimate (see column 1L-PB in Table 6.4 and Section 6.4.2). The larger the deviations in the bioclimate, i.e. the coarser the division into bioclimate bins, the larger are the entailed deviations in the simulation results (Table 6.4). In the current implementation of TreeMig-2L these deviations can only be reduced using a

[2]Measured with the intrinsic Fortran procedure CPU_TIME; computations were conducted on 2.8GHz AMD Opteron CPUs.

Table 6.3 : Number of bioclimate types resulting from the three different sets of bioclimate bins (E1-E3 – Table 6.2). For both application scenarios (A1 and A2), absolute numbers of bioclimate types and percentages relative to the number of stockable cells of the simulation area (see Table 6.1) are listed.

	Application scenario A1		Application scenario A2	
	#Bioclimate types	[% #Cells]	#Bioclimate types	[% #Cells]
E1	3460	3.1%	7941	64.9%
E2	798	0.7%	3424	28.0%
E3	213	0.2%	884	7.2%

finer division into bioclimate bins or more supporting periods. The dynamic association of cells to elements on the non-spatial layer does not reduce this error, because the bioclimate driver is not processed on the single elements but on the bioclimate types. The pre-structuring of the simulation area is fundamental for the efficiency of TreeMig-2L, because the thereby obtained static structure is used for the organisation and maintenance of the elements on the non-spatial layer. However, averaging of the bioclimate in the pre-structuring step could potentially be replaced by a dynamic approach. In a dynamic approach, preprocessing of the bioclimate drivers could be re-transferred to the two-dimensional layer, and the bioclimate influences of each element could be calculated by averaging the bioclimate of its currently associated cells in each time step of the simulation. Whilst this could reduce deviations in the simulation results compared to original one-layer simulations, it would also require more computations and thus lead to less CPU time reductions (see Section 6.4.2.2).

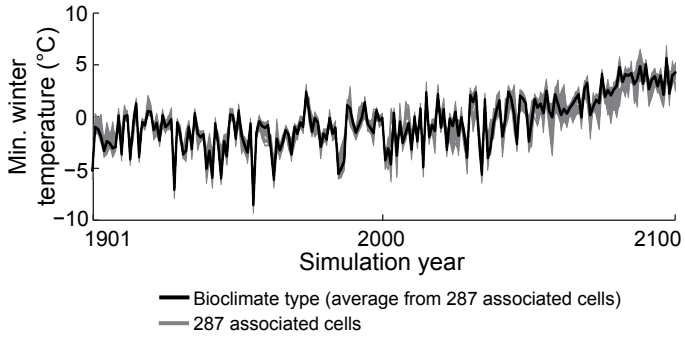

Figure 6.4 : Minimum winter temperature of an example bioclimate type (black line) resulting from a pre-structuring of the simulation area of application scenario A2 with E3, the coarsest applied set of bioclimate bins (Table 6.2). Depicted is the bioclimate type with the largest deviations in minimum winter temperature from one of its associated cells. The minimum winter temperatures of all associated cells are displayed in grey. Further examples are provided in Appendix 6.C (Figs. 6.C.2 and 6.C.3)

Applying bioclimate types in their current static form is reminiscent of the stratified sampling methods used in explicit spatial upscalings of single site models (Bugmann et al., 2000), and is comparable to the ecoregions used in the forest-landscape model LANDIS (see e.g. Mladenoff and He, 1999; Scheller and Mladenoff, 2004). Similarly to cells associated with the same bioclimate type in TreeMig-2L, cells associated with the same ecoregion in LANDIS share important process rates influencing establishment and biomass development (e.g. Scheller and Mladenoff, 2004). Ecoregions in LANDIS, similar to bioclimate types in TreeMig-2L, do not need to be contiguous but can be distributed in space (He et al., 1999). This is an important advantage over other upscaling methods, which are often based on local spatial aggregations, such as naive upscalings that decrease the spatial resolution of a simulation area (as described in Bocedi et al., 2012). The possibility for bioclimate types, which are defined over similarity and not over spatial proximity, to be arbitrarily distributed in space, potentially reduces the number of required bioclimate types and, even more important, prevents errors involved with inappropriate averaging of neighbouring cells. Thus, bioclimate types have the advantage that they conserve the spatio-temporal heterogeneity to a large degree (Fig. 6.C.4 in the supplementary material gives an example for the conservation of the spatial variability; Figs. 6.4, 6.C.5 and 6.C.6 for the conservation of the temporal variability).

6.4.2 Performance of TreeMig-2L simulations

To evaluate the performance of TreeMig-2L, different performance measures (Section 6.3.2.5) were used to compare two-layer (2L) simulations, with bioclimate types derived with each of the three different sets of bioclimate bins (E1-E3 – Table 6.2), to one-layer simulations (1L-ORG – all processes simulated on the two-dimensional layer), with the original bioclimate. To assess to what extent different approximations involved with the D2C concept led to performance decreases, additionally two different pre-stages of the 2L implementation were simulated and compared to 1L-ORG simulations: (1) one-layer simulations with averaged bioclimate according to the bioclimate types (1L-PB) and (2) two-layer simulations with static assignments, i.e. without dynamic associations (2L-NDA). Furthermore, sensitivity tests on splitting and merging thresholds, merging intervals and tracked species were conducted (see Appendix 6.C).

6.4.2.1 Accuracy

The accuracy of TreeMig-2L simulations was evaluated by comparing biomass distributions in space resulting from the different simulations settings. For both application scenarios, biomass distributions in space were compared with a similarity coefficient (SC) ranging from zero (no similarity) to one (identical biomass distributions). SCs resulting from comparisons of 2L and 1L-ORG simulations were generally in the upper range for all compared output variables (ranging from about 0.8 to about 1.0 – Table 6.4) for both application scenarios. The level of the SC was largely determined by the selected set of bioclimate bins, with coarser sets leading to decreases in the SC for all compared variables (differences in the SCs of up to 0.14 – Table 6.4). To be able to assess the relevance of deviations from one in the SCs, results from 1L-ORG runs with different pseudo-random number streams used to extrapolate the bioclimate driver were compared with each other, i.e. the deviation from one in the SC due to interannual variability in the bioclimate driver was calculated (see Section 6.C.2). The only SCs which were markedly larger than the SCs resulting from these 1L-ORG intra-comparisons were SCs from comparisons of 1L-ORG runs and runs with bioclimate types derived with E3 (Tables 6.4 and 6.C.2).

In all cases, SCs from comparisons between 1L-ORG and 2L simulations were very close to the SCs from comparisons of 1L-ORG simulations and simulations on one layer with bioclimate drivers averaged according to the bioclimate types (1L-PB; differences in the SCs $\leq$ 0.01). This indicates that the deviations in TreeMig-2L simulations are mainly due to the averaging of the bioclimate drivers. SCs from 2L simulations were, in particular, larger than SCs from simulations without dynamic associations (differences between 2L and 2L-NDA up to 0.04 in SC_{spec} and up to 0.21 in SC_{OC}). The four tracked species in the application scenario A1 (see Section 6.3.2.2) and *Ostrya carpinifolia* in the application scenario A2 thus seem to be good indicators to test for required splits. Sensitivity tests showed that fewer tracked species increased the error (up to 0.03 smaller SC_{spec} values – Fig. 6.C.11, supplementary material) and more species only slightly decreased it (only $\sim$ 0.01 larger SC_{spec} values – Fig. 6.C.11). The sensitivity tests further showed that the choice of merging and splitting thresholds had only limited impact on the SCs in the application scenarios (Figs. 6.C.11 to 6.C.13). Strong differences in the SC were only observed for simulations that tested elements for merging after a decade instead of after a century (Figs. 6.C.11 to 6.C.13).

The development of the SC_{spec} over time was comparable among simulations with E1-E3 derived bioclimate types in all simulation settings (2L, 1L-PB and 2L-NDA) and for both application scenarios: SC_{spec} decreased in the transient phase of climate change (from around 2000 on) and stabilised after a few centuries (Fig. 6.5 and Figs. 6.C.6 and 6.C.7). The stabilisation on a lower level is mainly due to a stronger impact of differences in the drought index between bioclimate types and single cells due to overall larger drought indices in the second half of the 20^{th} century (see Figs. 6.C.2 and 6.C.3). A comparable effect resulted for inter-comparisons of 1L-ORG runs (see Section 6.C.2). While the temporal development in the SC_{spec} was comparable among all simulations (2L, 1L-PB and 2L-NDA), trajectories resulting from 2L-NDA simulations differed from trajectories form 2L and 1L-PB simulations for the SC_{OC}. Having no dynamic associations, the SC_{OC} for the 2L-NDA simulations mainly reflects changes in the bioclimate over time (see Section 6.C.2 for details).

Being a single index for the whole simulation area, the SC is a rough indicator for the similarity between two

Table 6.4 : Performance measures from simulations with both application scenarios (A1 and A2) for simulations with bioclimate types derived with all three sets of bioclimate bins (E1-E3 – Table 6.2). For both scenarios, the table lists the mean similarity coefficients (SC) from comparisons of last simulation year results from 1L-PB, 2L and 2L-NDA simulations to 1L-ORG simulations for different target variables (biomass sum over all species, biomass per species and, for scenario A2, also biomass of *Ostrya carpinifolia*). The temporal development of the SCs is depicted in Fig. 6.5, Figs. 6.6 and 6.C.9 to 6.C.11. In addition to the SCs, average peak element-cell ratios and mean CPU time reductions relative to the mean CPU time for 1L-ORG simulations are listed. All means for A1 runs stem from five repetitions, for A2 runs from 100 repetitions. SCs from 2L simulations were always very close to SCs from 1L-PB simulations, indicating that the dynamics in the 2L simulations follow the dynamics in the 1L-ORG simulations and that most of the deviations are due to the averaging of the bioclimate drivers for the bioclimate types. SCs from 2L-NDA are smaller, in particular for SC_{OC}, underlining the importance to track changes in species' compositions.

		Application scenario A1 (5 repetitions)				Application scenario A2 (100 repetitions)				
		Avg. SCs[a]		Avg. peak element-cell ratio[b] (σ)	Avg. CPU time[c] reduction [%[d]]	Avg. SCs[a]			Avg. peak element-cell ratio[b] (σ)	Avg. CPU time[c] reduction [%[d]]
		SC_{sum}	SC_{spec}			SC_{sum}	SC_{spec}	SC_{OC}[e]		
E1	1L-PB	0.98	0.90	–	∅	0.99	0.95	0.97	–	∅
	2L	**0.98**	**0.89**	**56.5% (±3.5%)**	**52.4%**	**0.99**	**0.95**	**0.96**	**71.2% (±0.8%)**	**32.6%**
	2L-NDA	0.97	0.85	3.1%	59.6%	0.98	0.92	0.71	64.9%	33.7%
E2	1L-PB	0.97	0.86	–	∅	0.96	0.88	0.89	–	∅
	2L	**0.97**	**0.85**	**39.9% (±2.9%)**	**56.0%**	**0.96**	**0.87**	**0.88**	**38.3% (±1.4%)**	**65.6%**
	2L-NDA	0.96	0.82	0.7%	61.0%	0.96	0.85	0.67	28.0%	68.3%
E3	1L-PB	0.96	0.78	–	∅	0.94	0.82	0.83	–	∅
	2L	**0.96**	**0.78**	**29.4% (±1.4%)**	**57.8%**	**0.94**	**0.81**	**0.82**	**18.1% (±1.3%)**	**84.7%**
	2L-NDA	0.96	0.75	0.2%	61.4%	0.94	0.80	0.63	7.2%	87.0%

[a] SC comparisons were conducted for the last year of the simulations, i.e. for the simulation year 2500 in case of A1 simulations and in the simulation year 3000 in case of A2 simulations. Runs of the listed simulations (1L-PB, 2L, 2L-NDA – see Section 6.3.2.4) were compared with 1L-ORG simulations with the same pseudo-random number streams used to extrapolate the driving bioclimate time series. Examples of the development of the SC over time are given in Fig. 6.5, Fig. 6.6 and in the Appendix 6.C. Standard deviations for 2L and 1L-PB simulations, as well as the 2L-NDA simulations for A1 were always smaller than 0.02. For 2L-NDA simulations for A2 standard deviations were much larger and reached up to 0.04.

[b] Ratio between the number of elements in the non-spatial layer and the number of stockable cells in the simulation area of the application scenario (see Table 6.1).

[c] Standard deviations of CPU times were always smaller than 1.5%, therefore only average CPU times are shown.

[d] Reduction relative to the average CPU time required for 1L-ORG runs (for the average CPU time for 1L-ORG runs please refer to footnote 1).

[e] OC: *Ostrya carpinifolia*, the tree species whose northwards migration is simulated in application scenario A2.

runs and could in particular conceal biases in the distribution of the biomass in space. Furthermore, depending on the research question, other aspects than comparisons of the absolute biomass values per cell could be important, for example when studying the migration of a species. Therefore, 2L and 1L-ORG simulations of application scenario A2 were additionally compared focussing on the migration of the tracked species. Comparisons of the northernmost occurrences of *O. carpinifolia* – an indicator for the migration distance – and of its spread in space showed a good approximation of the 1L-ORG simulations by 2L simulations with bioclimate types derived with all three sets of bioclimate bins (Fig. 6.7). A sensitivity test with another species parameter confirmed the good results for E1 and E2 derived bioclimate types, however, E3 derived types led to an overestimation of the northernmost occurrences (see Fig. 6.C.12).

In summary, SCs comparing 2L and 1L-ORG runs were within the magnitude of deviations due to interannual variability and in particular larger than reported for previous upscalings (e.g. Lischke et al., 1998), and comparisons of the spatial distributions of the biomass of *O. carpinifolia* between 1L-ORG and 2L simulations did not indicate spatial biases.

6.4.2.2 Computational costs

Simulations with two layers led to considerable reductions in CPU time for both application scenarios (Table 6.4). When considering the ratio between the number of bioclimate types and the cells of the simulation

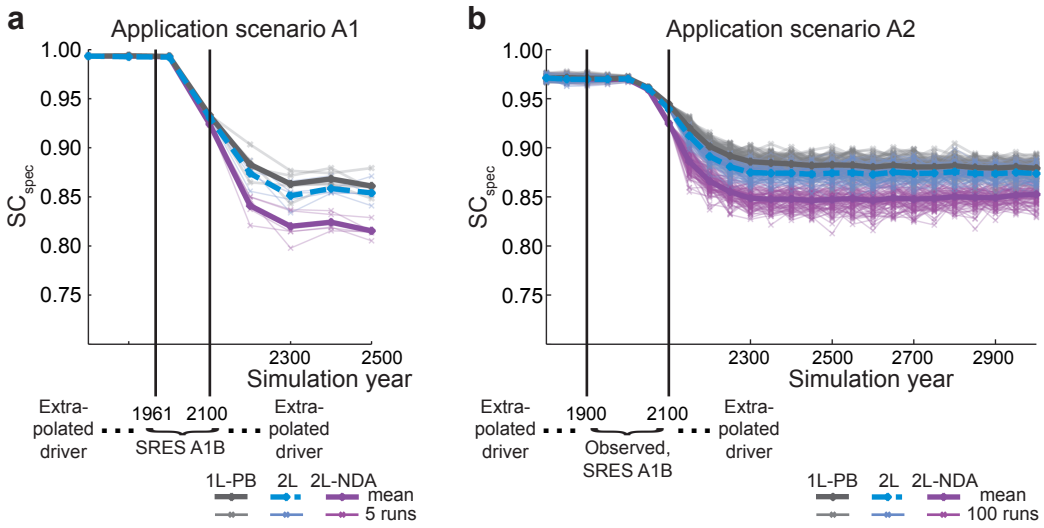

Figure 6.5 : Temporal development of the SC_{spec} for both application scenarios (A1: panel a, A2: panel b) from comparisons of 1L-ORG runs to runs with bioclimate types derived with the moderate set of bioclimate bins (E2 – Table 6.2; for simulations with other bins see Figs. 6.C.6 and 6.C.7 in the supplementary material). SC_{spec} values for A1 were calculated every 100 years, values for A2 every 50 years. Depicted are SC_{spec} values for two-layer runs with and without dynamic associations (2L and 2L-NDA, respectively) and runs on one layer but with the bioclimate of the associated bioclimate types (1L-PB). For each setting several repetitions were compared, which were simulated with different pseudo-random number streams used to extrapolate the bioclimate driver before 1961 (A1) and 1901 (A2) and after 2100. Five runs were simulated for A1, 100 runs for A2. Single runs and their means are printed half-transparent and bold, respectively. All depicted SC_{spec} time series decline in the transient phase of climate change and continue to decline for about 200 years after which the SC_{spec} stabilises. Over the whole simulated time span SC_{spec} values of 2L simulations are much closer to SC_{spec} values from 1L-PB simulations than to SC_{spec} values from 2L-NDA simulations, indicating that the deviations are mainly due to the averaging of the bioclimate drivers.

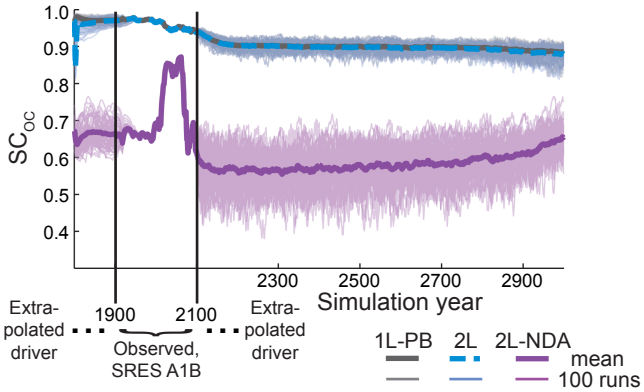

Figure 6.6 : Temporal development of the SC_{OC} comparing simulations of application scenario A2. Depicted SC_{OC} values stem from comparisons of 1L-ORG runs to runs with bioclimate types derived with the moderate set of bioclimate bins (E2 – Table 6.2; for simulations with other bins see Fig. 6.C.8 in the supplementary material). Simulations were conducted with two layers with and without dynamic associations (2L and 2L-NDA, respectively) and with one layer but with the bioclimate of the associated bioclimate types (1L-PB). For each setting 100 repetitions were compared, which were simulated with different pseudo-random number streams used to extrapolate the bioclimate driver before 1901 and after 2100. Single runs and their means are printed half-transparent and bold, respectively. Comparable to SC_{spec} values (Fig. 6.5), SC_{OC} values of comparisons between 1L-ORG and 2L simulations are very close to SC_{OC} values from comparisons with 1L-PB simulations over the whole simulated time span. While these SC_{OC} time series slowly decline, SC_{OC} values from comparisons of 1L-ORG simulations with 2L-NDA simulations mainly reflect the reaction of *Ostrya carpinifolia* to climatic changes on the whole simulation area (see Section 6.C.2), since 2L-NDA simulations were conducted without dynamic associations.

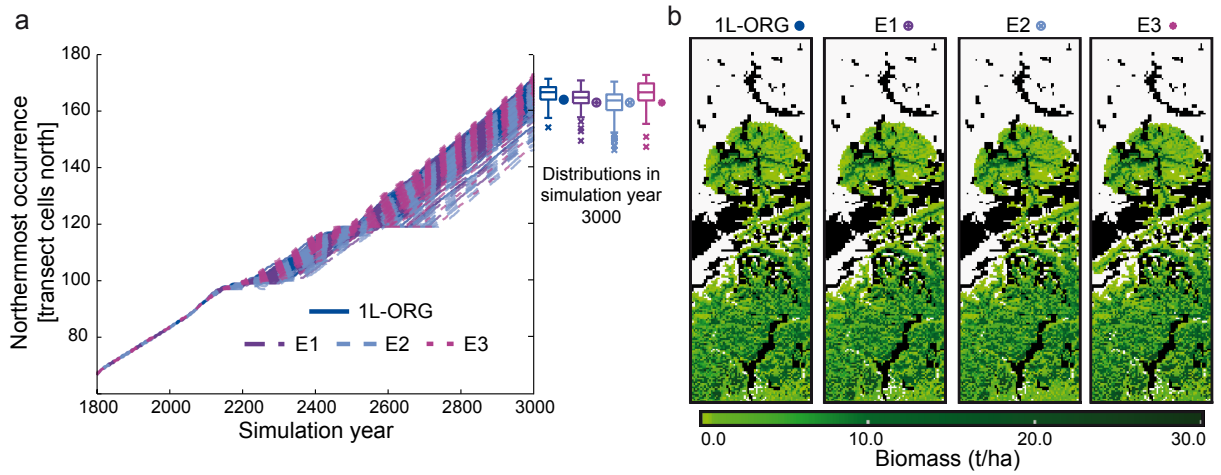

Figure 6.7 : Accuracy of the simulation of migration with TreeMig-2L. (Panel a) The temporal development of the simulated northwards migration of *Ostrya carpinifolia* (depicted as the northernmost occurrence over time; smoothed over ten-year intervals) resulting from 2L simulations with bioclimate types derived with the three sets of bioclimate bins E1-E3 (Table 6.2) strongly resemble the results from the 1L-ORG simulations (lines are superposed). Distributions of the northernmost occurrences in the last simulation year (box-plots on the right side of panel a), calculated from 100 repetitions with different pseudo-random number streams (PRNSs) used to extrapolate the bioclimate driver, are quite similar in mean and standard deviations. (Panel b) Depicted maps of the spatial spread of *O. carpinifolia* in the last simulation year are hardly visually discernible. The only notable difference between the depicted maps is one valley in the west of the transect, which is inhabited by *O. carpinifolia* in the E3 simulation run, but not in the other depicted runs. The absence of notable spatial biases in the biomass distribution indicates that a large share of the differences in the biomass of *O. carpinifolia* between 2L simulations and 1L-ORG simulations (i.e. SC_{OC} values) stem from local biomass variations. All depicted maps stem from runs with the same PRNS and led to SC_{OC} values close to the means: 0.97, 0.88, 0.82 for E1, E2 and E3, respectively. The northernmost occurrences in the last simulation year of the four runs depicted in panel b are marked with differently coloured symbols on the right side of panel a. Maps of the biomass of *O. carpinifolia* were created with Paraview (Ahrens et al., 2005).

areas (Table 6.3), much larger reductions in computational costs could have been expected for application scenario A1 simulations than for application scenario A2 simulations. Yet, the actual reductions are not systematically larger for A1 simulations (E1: 52.9%, E2: 56.0%, E3: 57.8%) than for A2 simulations (E1: 32.6%, E2: 65.6%, E3: 84.7%). To a small part this is due to increased dynamics in the number of elements on the non-spatial layer in A1 simulations than in A2 simulations (Fig. 6.8), leading to a comparable magnitude in the peak element-cell ratio for both application scenarios (Table 6.4).

Table 6.5 : Percentage of instructions executed for selected computation tasks. Shown are results from a callgrind (Weidendorfer, 2008) profiling of simulations with one layer (1L-ORG) and of 2L simulations with bioclimate types derived with the three sets of bioclimate bins E1-E3 (Table 6.2). The measured percentage of instructions executed for selected computation tasks is a performance measure comparable to the relative amount of CPU time spent with the tasks. Measures stem from simulations with the same pseudo-random number stream used to extrapolate the driving bioclimate time series.

	Application scenario A1				Application scenario A2			
	Seed dispersal	Bioclimate prep.[a]	Adult dynamics	2L org. [b]	Seed dispersal	Bioclimate prep.[a]	Adult dynamics	2L org. [b]
1L-ORG	44.31%	3.75%	49.61%	–	6.03%	4.80%	85.97%	–
2L: E1	83.71%	0.21%	14.66%	0.11%	9.02%	4.62%	83.04%	0.15%
2L: E2	88.40%	0.05%	10.19%	0.10%	17.69%	3.84%	74.16%	0.24%
2L: E3	91.80%	0.01%	6.84%	0.10%	39.52%	2.20%	51.42%	0.47%

[a] Bioclimate prep.: Preprocessing of the bioclimate driver, which involves reading of the current values from a NetCDF file and derivation of species-specific coefficients for later calculations with bioclimate dependencies, such as growth, mortality and establishment.

[b] 2L org.: Organisation of the dynamic association between the two-dimensional and the non-spatial layer.

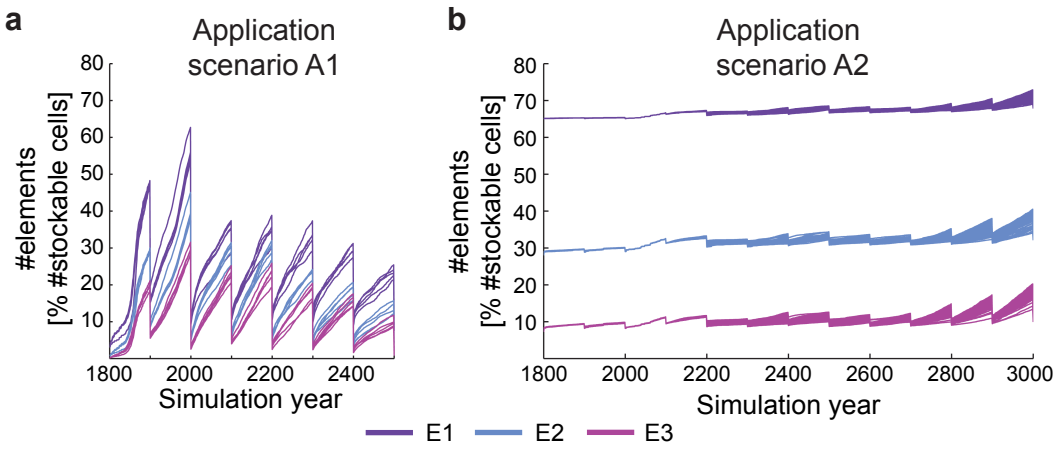

Figure 6.8 : Ratio of the number of elements on the non-spatial layer to cells in the simulation area over time from simulations with bioclimate types derived with the three sets of bioclimate bins (E1-E3 – Table 6.2) and for both application scenarios. For A1 five repetitions with different pseudo-random number streams used to extrapolate the bioclimate driver are depicted; for A2 100 repetitions are shown. The number of elements in A1 simulations increased strongly in between the merging intervals with smaller increases in the course of the simulation. For A2 simulations, in contrast, the number of elements increased faster towards the end of the simulation time, which was due to the growing perimeter of the migration front of the tracked species *Ostrya carpinifolia* (see Fig. 6.C.9).

Sensitivity tests for the application scenario A1, however, showed that changes in the number of tracked species and in the merging interval leading to large changes in the peak element-cell ratio did not lead to large changes in the CPU time reductions: Simulations with a shorter merging interval of a decade and a smaller number of tracked species reduced the peak element-cell ratio from 60% to less than 10% (Fig. 6.C.10), but reductions in the CPU time did not increase much above 60% (Fig. 6.C.11). An increased number of tracked species only decreased reductions in the CPU time to around 49%, although the peak element-cell ratio increased to 70%. Whilst reductions in CPU time thus ranged between 49% and 60% for A1 simulations (Fig. 6.C.11), they ranged between 33% to 84% for A2 simulations (Figs. 6.C.13 and 6.C.14). In A2 simulations, differences in CPU times were nearly entirely driven by the applied set of bioclimate bins used to derive the bioclimate types (Figs. 6.C.13 and 6.C.14). The small difference in the CPU time reductions among A1 simulations with E1, E2 and E3 derived bioclimate types in combination with notable differences in the peak element-cell ratio (Table 6.4) and notable differences in SC_{spec} values indicate that the peak element-cell ratio is not the main cause for the limits in the achieved reduction in CPU time for A1 simulations. The actual main cause for this limitation is revealed when looking at the percentage of executed instructions for the different processes (Table 6.5): the percentage of executed instructions spent on seed dispersal was simply much larger for A1 simulations than for A2 simulations. 1L-ORG simulations for application scenario A1 spent about 45% of executed instructions on seed dispersal and only about 50% on adult dynamics, i.e. on processes simulated on the non-spatial layer. A2 simulations, in contrast, only spent about 6% of the executed instructions on seed dispersal and about 86% on adult dynamics (Table 6.5). Differences in the execution ratios were already expected (see Section 6.3.2.1) because of the increased number of sink cells considered in seed dispersal calculations for the grid with 200m cell side length in A1 simulations compared to the grid with 1km cell side length in A2 simulations. As a consequence, the base load that cannot be reduced with the D2C concept was more than seven times larger in the A1 simulations than in the A2 simulations.

6.4.3 Applicability of the D2C concept

In Section 6.2 three different aspects were hypothesised to influence the benefit of the implementation of the D2C concept: (1) the non-reducible base load, (2) the number of elements on the non-spatial layer, and (3) the organisational overhead for maintaining the non-spatial layer. The implementation and the applications

of TreeMig-2L confirmed the importance of these aspects. Differences in the benefit comparing application scenarios A1 and A2 demonstrated the key role of the non-reducible base load due to time spent with spatially linked processes. This key role is also underlined when comparing the applications including spatial linkages in this study to the application of a predecessor of TreeMig-2L without spatial linkages by Nabel and Lischke (2013): for applications without spatial linkages relative reductions in CPU times were much larger. In TreeMig-2L applications, the second aspect – the number of elements on the non-spatial layer – was on one hand controlled by the number of bioclimate types derived in the pre-structuring (particularly for application scenario A2) and, on the other hand, by the number of tracked species (particularly for A1). The number of bioclimate types, as well as the number of tracked species influenced the reductions in the CPU time via the number of elements on the non-spatial layer. The third aspect – the organisational overhead – was kept very low in the TreeMig-2L applications (see Table 6.5), which was mainly possible due to the developed architecture: the pre-structuring to bioclimate types and the asymmetric relationship between cells and associated elements enabled an efficient maintenance of the dynamic non-spatial layer and the pointers kept in each cell enabled the direct access of the element a cell is associated with.

The three aspects listed above can be used to assess the applicability of the D2C concept for other dynamic vegetation models (DVMs). For example, the number and complexity of processes requiring information on the spatial position of a grid cell relative to other grid cells, i.e. spatially linked processes, will influence the non-reducible base load. Moreover, the number and complexity of spatially linked processes might also influence the number of required elements due to induced splits and will thereby also influence the organisational overhead for the maintenance of the non-spatial layer, not only due to the required splits but also due to the required information exchange between the layers. Thus, the D2C concept might be less suitable for models with many complex and interacting spatially linked processes, such as LANDIS-II (Scheller et al., 2007), if used with several spatially linked extensions (e.g. Sturtevant et al., 2012). It should, however, be applicable for most models with few and simple spatially linked processes, such as TreeMig (provided a relatively coarse spatial resolution is used) and for spatially independent one-dimensional DVMs (sensu Fisher et al., 2010), such as ED (Fisher et al., 2010) and most implementations of LPJ-Guess (e.g. Smith et al., 2001; Hickler et al., 2012). An upscaling with the D2C concept of a one-dimensional DVM could perhaps free computational resources for the inclusion of a simple seed dispersal algorithm, which is an important step towards the explicit simulation of migration. Simulating migration explicitly would be highly desirable (Neilson et al., 2005; Thuiller et al., 2008), which is also underlined by the results of this study comparing 1L-ORG and 2L-NDA simulations (Fig. 6.C.9).

Besides the number and complexity of the spatially linked processes, also properties of the local processes will influence the applicability of the D2C concept: The D2C concept will be suitable for a model in which local processes are rather deterministic, as in TreeMig, or in which the stochasticity in local processes is realised as patch replicates calculated for each iteration within a cell, as for example done in LPJ-Guess (Smith et al., 2001). For models with such properties, grid cells with similar values in the climatic drivers will tend to also have comparable species' compositions, and these grid cells can thus be represented by the same element. The D2C concept will be less suitable for a model in which stochasticity in the local processes is realised on the cell level, such as LANDCLIM (Schumacher et al., 2004), because local stochasticity entails diverging species' composition which would necessitate frequent splits of elements.

The implementation of the D2C concept with a specific model will ultimately depend on the modelled processes, the model drivers and its state variables. Besides the assignment of the processes to the two layers and the specification of the exchanged information, various similarity criteria need to be specified controlling the composition and the dynamics of the non-spatial layer. For merging, for example, criteria need to be specified to determine when the state variables that are stored for an element are similar enough. Because TreeMig's state variables are real-valued population densities on a constant number of height classes, a set of similarity thresholds for the density in each height class was required for merging. A model with, for example, continuous height values for each individual (or cohort) and a discrete but arbitrary number of individuals would require the specification of similarity thresholds on both the continuous heights and the discrete individuals. For the special case of a model with bounded discrete state variables Yang et al. (2011) showed a very efficient technical solution with hash maps – data structures with unique key-value pairs enabling a fast lookup

of associations – having a similar approach as the D2C concept. Because the state variables are discrete and bounded, this method can aggregate cells with identical states (identical keys) and thus, no similarity criteria need to be specified. This method, however, will not be applicable whenever any state variable is continuous or unbounded because then possible states can not be uniquely represented with a finite set of elements on the non-spatial layer. An infinite number of possible states necessitates the specification of similarity criteria and an active management of the associations between the two layers as provided by the D2C concept.

6.5 Conclusions

The implementation of TreeMig-2L and the example simulations demonstrated that the D2C concept can be applied to strongly reduce computational expenses for processes which do not require information on the spatial position of a cell relative to other cells. The D2C concept is adaptable regarding the criteria used to define similarity for the drivers of a model and for its state variables. The implementation and application with TreeMig-2L indicated that these similarity criteria can be used to adjust the resulting discretisation errors. In the application examples, no strong spatial biases were detected, and differences in simulation results between the original and the two-layer implementation were in the magnitude of differences among 1L-ORG runs with different pseudo-random number streams used to extrapolate the bioclimate driver, i.e. differences due to interannual climate variability. Finally, the D2C concept maintained the spatio-temporal resolution of the driver and the simulated processes (as recommended by Bocedi et al., 2012).

As discussed, the D2C concept is applicable for a broad range of DVMs and probably also for time- and space-discrete models simulating other predominantly sessile organisms. The expected benefit when using the D2C concept to upscale a model depends on different model properties, such as for example the ratio of spatially linked to spatially unlinked processes, the scale on which the model applies stochasticity, and the numerical properties of the state variables. However, if this approach would be implemented together with an efficient seed dispersal algorithm, it is expected to improve the extent-resolution trade-off for currently applied DVMs, enabling new applications or greater numbers of stochastic repetitions to better capture important uncertainties.

Acknowledgements

I would like to thank Natalie Zurbriggen, Heike Lischke, James Kirchner, Felix Kienast and David Gutzmann for their valuable comments. Dirk Schmatz for help with the Data preparation and Thomas Wüst for the support with the cluster. Julia Nabel was partially funded by the Swiss National Science Foundation (SNF) Grant 315230-122434.

References

Ahrens, J., Geveci, B., Law, C., 2005. ParaView: An End-User Tool for Large-Data Visualization, in: Visualization Handbook. Butterworth-Heinemann.

Auger, P., Poggiale, J., Sánchez, E., 2012. A review on spatial aggregation methods involving several time scales. Ecological Complexity 10, 12–25.

Bocedi, G., Pe'er, G., Heikkinen, R.K., Matsinos, Y., Travis, J.M., 2012. Projecting species' range expansion dynamics: sources of systematic biases when scaling up patterns and processes. Methods in Ecology and Evolution 3, 1008–1018.

Bugmann, H., Lindner, M., Lasch, P., Flechsig, M., Ebert, B., Cramer, W., 2000. Scaling Issues in Forest Succession Modelling. Climatic Change 44, 265–289.

Epstein, H., Yu, Q., Kaplan, J., Lischke, H., 2007. Simulating Future Changes in Arctic and Subarctic Vegetation. Computing in Science Engineering 9, 12–23.

Fisher, R., McDowell, N., Purves, D., Moorcroft, P., Sitch, S., Cox, P., Huntingford, C., Meir, P., Woodward, F.I., 2010. Assessing uncertainties in a second-generation dynamic vegetation model caused by ecological scale limitations. New Phytologist 187, 666–681.

He, H.S., Mladenoff, D.J., Crow, T.R., 1999. Linking an ecosystem model and a landscape model to study forest species response to climate warming. Ecological Modelling 114, 213 – 233.

He, H.S., Yang, J., Shifley, S.R., Thompson, F.R., 2011. Challenges of forest landscape modeling – Simulating large landscapes and validating results. Landscape and Urban Planning 100, 400–402.

Hickler, T., Vohland, K., Feehan, J., Miller, P.A., Smith, B., Costa, L., Giesecke, T., Fronzek, S., Carter, T.R., Cramer, W., Kühn, I., Sykes, M.T., 2012. Projecting the future distribution of European potential natural vegetation zones with a generalized, tree species-based dynamic vegetation model. Global Ecology and Biogeography 21, 50–63.

Huntley, B., Barnard, P., Altwegg, R., Chambers, L., Coetzee, B.W.T., Gibson, L., Hockey, P.A.R., Hole, D.G., Midgley, G.F., Underhill, L.G., Willis, S.G., 2010. Beyond bioclimatic envelopes: dynamic species' range and abundance modelling in the context of climatic change. Ecography 33, 621–626.

Jarvis, A., Reuter, H., Nelson, A., Guevara, E., 2008. Hole-filled SRTM for the globe Version 4. Available from the CGIAR-CSI SRTM 90m Database. http://srtm.csi.cgiar.org.

Lischke, H., Löffler, T.J., Fischlin, A., 1998. Aggregation of Individual Trees and Patches in Forest Succession Models: Capturing Variability with Height Structured, Random, Spatial Distributions. Theoretical Population Biology 54, 213–226.

Lischke, H., Löffler, T.J., Thornton, P.E., Zimmermann, N.E., 2007. Model Up-scaling in Landscape Research. A Changing World. Challenges for Landscape Research. Springer. chapter 16. pp. 259–282.

Lischke, H., Zimmermann, N.E., Bolliger, J., Rickebusch, S., Löffler, T.J., 2006. TreeMig: A forest-landscape model for simulating spatio-temporal patterns from stand to landscape scale. Ecological Modelling 199, 409–420.

Mladenoff, D.J., He, H.S., 1999. Spatial modeling of forest landscape change: approaches and applications. Cambridge University Press. Cambridge University Press. chapter Design, behavior and application of LANDIS, an object-oriented model of forest landscape disturbance and succession. pp. 125–162.

Nabel, J.E.M.S., Kirchner, J.W., Zurbriggen, N., Kienast, F., Lischke, H., submitted. Extrapolation methods for climate time series revisited – spatial correlations in climatic fluctuations influence simulated tree species abundance and migration.

Nabel, J.E.M.S., Lischke, H., 2013. Upscaling of spatially explicit and linked time and space discrete models studying vegetation dynamics under climate change. In: Environmental Informatics and Industrial Environmental Protection: Concepts, Methods and Tools.

Nabel, J.E.M.S., Zurbriggen, N., Lischke, H., 2012. Impact of species parameter uncertainty in simulations of tree species migration with a spatially linked dynamic model. In: R. Seppelt, A.A. Voinov, S. Lange, D. Bankamp (Eds.) (2012): International Environmental Modelling and Software Society (iEMSs) 2012. International Congress on Environmental Modelling and Software. Managing Resources of a Limited Planet: Pathways and Visions under Uncertainty, Sixth Biennial Meeting, Leipzig, Germany, 909–916.

Nabel, J.E.M.S., Zurbriggen, N., Lischke, H., 2013. Interannual climate variability and population density thresholds can have a substantial impact on simulated tree species' migration. Ecological Modelling 257, 88–100.

Nakicenovic, N., Alcamo, J., Davis, G., de Vries, B., Fenhann, J., Gaffin, S., Gregory, K., Grübler, A., Jung, T.Y., Kram, T., La Rovere, E.L., Michaelis, L., Mori, S., Morita, T., Pepper, W., Pitcher, H., Price, L., Riahi, K., Roehrl, A., Rogner, H.H., Sankovski, A., Schlesinger, M., Shukla, P., Smith, S., Swart, R., van Rooijen, S., Victor, N., Dadi, Z., 2000. IPCC Special Report on Emissions Scenarios. Cambridge University Press.

Neilson, R., Pitelka, L., Solomon, A., Nathan, R., Midgley, G., Fragoso, J., Lischke, H., Thompson, K., 2005. Forecasting Regional to Global Plant Migration in Response to Climate Change. BioScience 55, 749–759.

Scheller, R.M., Domingo, J.B., Sturtevant, B.R., Williams, J.S., Rudy, A., Gustafson, E.J., Mladenoff, D.J., 2007. Design, development, and application of LANDIS-II, a spatial landscape simulation model with flexible temporal and spatial resolution. Ecological Modelling 201, 409–419.

Scheller, R.M., Mladenoff, D.J., 2004. A forest growth and biomass module for a landscape simulation model, LANDIS: design, validation, and application. Ecological Modelling 180, 211–229.

Schumacher, S., Bugmann, H., Mladenoff, D.J., 2004. Improving the formulation of tree growth and succession in a spatially explicit landscape model. Ecological Modelling 180, 175–194.

Smith, B., Prentice, I.C., Sykes, M.T., 2001. Representation of vegetation dynamics in the modelling of terrestrial ecosystems: comparing two contrasting approaches within European climate space. Global Ecology and Biogeography 10, 621–637.

Snell, R.S., Huth, A., Nabel, J.E.M.S., Bocedi, G., Travis, J.M.J., Gravel, D., Bugmann, H., Gutiérrez, A.G., Hickler, T., Higgins, S.I., Scherstjanoi, M., Reineking, B., Zurbriggen, N., Lischke, H., accepted. Using individual based forest models to simulate species range shifts. Ecography .

Sturtevant, B.R., Miranda, B.R., Shinneman, D.J., Gustafson, E.J., Wolter, P.T., 2012. Comparing modern and presettlement forest dynamics of a subboreal wilderness: Does spruce budworm enhance fire risk? Ecological Applications 22, 1278–1296.

Thuiller, W., Albert, C., Araújo, M.B., Berry, P.M., Cabeza, M., Guisan, A., Hickler, T., Midgley, G.F., Paterson, J., Schurr, F.M., Sykes, M.T., Zimmermann, N.E., 2008. Predicting global change impacts on plant species' distributions: Future challenges. Perspectives in Plant Ecology, Evolution and Systematics 9, 137–152.

Urban, D., Acevedo, M., Garman, S., 1999. Scaling fine-scale processes to large-scale patterns using models derived from models: meta-models. Advances in spatial modeling of forest landscape change: approaches and applications. Cambridge University Press, Cambridge, UK. chapter 4. pp. 70–98.

Weidendorfer, J., 2008. Sequential performance analysis with callgrind and kcachegrind, in: Tools for High Performance Computing. Springer, pp. 93–113.

Yang, J., He, H.S., Shifley, S.R., Thompson, F.R., Zhang, Y., 2011. An innovative computer design for modeling forest landscape change in very large spatial extents with fine resolutions. Ecological Modelling 222, 2623–2630.

Zurbriggen, N., 2013. Avalanche disturbance and regeneration in mountain forests under climate change: experimental and modeling approaches. Ph.D. thesis. Swiss Federal Institute of Technology Zurich. Http://dx.doi.org/10.3929/ethz-a-009933944.

Appendix

Appendix 6.A Additional details on the implementation of TreeMig-2L

6.A.1 Data structures

The architecture of TreeMig-2L comprises different data structures (Fig. 6.A.1 and Fig. 6.2, main text). Processes on the two-dimensional layer require information on the spatial location of a cell relative to other cells and state variables required for these processes are therefore stored in an array data structure. Processes on the non-spatial layer do not require information on the spatial location of a cell relative to other cells. Furthermore, the number of elements on the non-spatial layer, as opposed to the number of cells, is not predetermined by the considered simulation area but emerges during the simulation. Therefore, the elements on the non-spatial layer need to be stored in a dynamic data structure. The dynamic data structure used for TreeMig-2L is a doubly linked list. A doubly linked list is a data structure in which each element is connected to two other elements of the list, its predecessor and its successor[3]. Therefore, such a list can dynamically grow or shrink only changing local information instead of global information and allows for efficient traversal. The dynamic character of the non-spatial layer, i.e. splitting and merging of its elements induces an overhead required for the maintenance of its elements. To pre-constrain this overhead, multiple small lists are used instead of one large list. This enables efficient splitting and merging operations which only apply to a single list, but not to the whole non-spatial layer. In particular the comparison of elements would induce a larger overhead if all elements would be compared to all other elements, instead of restricting comparison to the other elements of a list. To pre-define which element is stored in which list, the fact is used that for cells to be similar not only species' compositions need to satisfy the given similarity criteria but also bioclimatic influences need to be comparable. As opposed to species' compositions which develop during runtime, bioclimatic drivers are an input to TreeMig-2L. Information about the bioclimate drivers can therefore be used in advance to pre-structure a simulation area. In this pre-structuring bioclimate types are derived from the bioclimate drivers according to a given set of bioclimate bins (see Section 6.A.2 and Section 6.3.1.3, main text). Each of the derived bioclimate types is associated with one list (Fig. 6.A.1). Because the number of the bioclimate types is known in advance, information about the bioclimate types can be stored in a one dimensional array structure.

Connections between the different data structures, i.e. the array for the two-dimensional layer, the one-dimensional array for bioclimate types and the linked lists for elements on the non-spatial layer, are asymmetric (Fig. 6.A.1). Each bioclimate type has a pointer – a data type allowing direct access – to the first element in its list. In addition, each cell of the two-dimensional layer has a pointer to the element with which it is currently associated, to allow for a direct and thus fast exchange of the status information.

[3] In a doubly linked list with one element the predecessor and the successor of the element are the element itself.

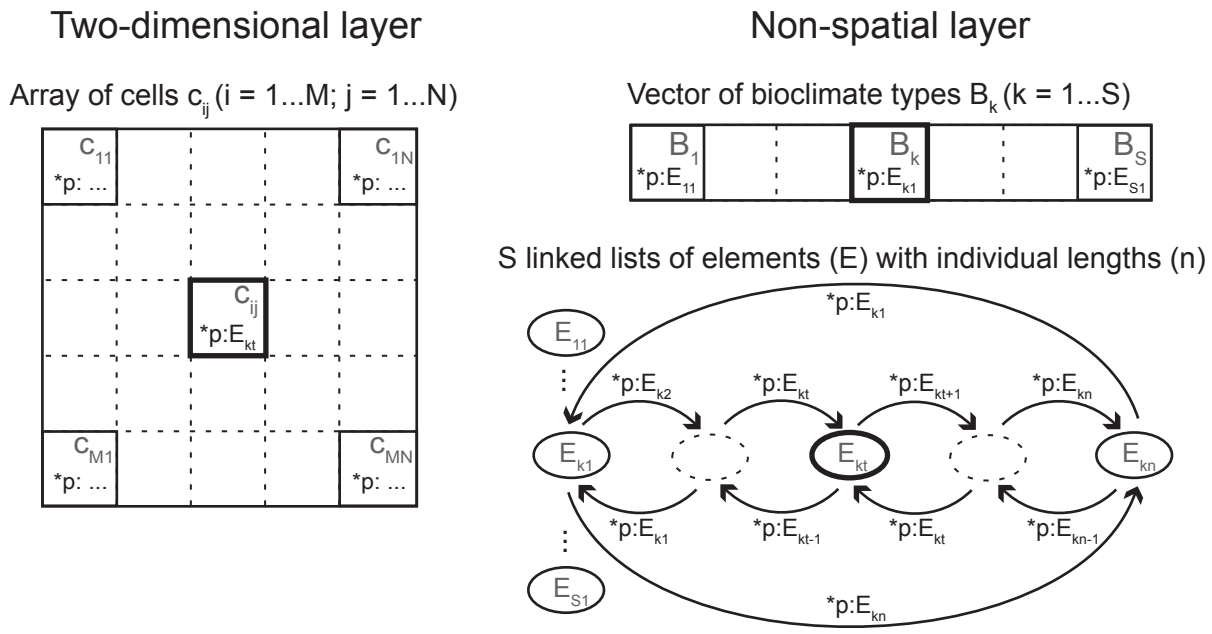

Figure 6.A.1 : Data structures used in TreeMig-2L and their connections. State variables required for processes simulated on the two-dimensional layer (see Fig. 6.2, main text) are kept in cells stored in an M x N array structure (size according to the simulation area). The non-spatial layer comprises different data structures: a vector of bioclimate types (length S) and associated linked lists for each of these types containing the actual elements on the non-spatial layer. The bioclimate types are derived in a pre-processing (see Section 6.A.2 and Section 6.3.1.3, main text). Connections between the different data structures are asymmetric and defined with pointers. A pointer is a data structures holding the memory location of another data structure and therefore allowing direct access. Each cell (c_{ij}) on the two-dimensional layer holds a pointer (*p:E_{kt}) to the element of the non-spatial layer it is currently associated with (E_{kt}). Each bioclimate type (B_k) holds a pointer (*p:E_{k1}) to the first element of its associated list (E_{k1}). Elements stored in the linked lists do not contain pointers to their associated cells because the number of cells changes during simulation time. For explanatory reasons, list k is depicted containing several elements and c_{ij} points to element E_{kt}. However, a list can also consist of only one element which then points to itself.

6.A.2 Pre-structuring of a simulation area

A considered simulation area is pre-structured to bioclimate types according to the bioclimate drivers. The underlying idea of the pre-structuring is that the spatial correlation in the bioclimate among cells of the simulation area is rather persistent (see Nabel et al., submitted; see Chapter 4). Due to this correlation, two cells with similar bioclimate drivers for a certain time span have a good chance to have similar bioclimate drivers beyond this time span (also see the examples in Figs. 6.C.5 and 6.C.6). With this in mind, similarity of cells is only tested for a number of pre-defined supporting periods instead of for the entire time span covered by the bioclimate driver (see Fig. 6.A.2 for an example). For each of the supporting periods and for each of the bioclimate drivers one average per cell is calculated (Fig. 6.A.2a). For each bioclimate driver, the according averages are then clustered into predefined bioclimate bins (Fig. 6.A.2b). Each actually occurring set of classes defines one bioclimate type (Fig. 6.A.2c). The number of possible bioclimate types will therefore be influenced by the number of supporting periods and the number of bioclimate bins (see for example Fig. 6.C.4). A small number of supporting periods and of bioclimate bins will lead to a coarser discretisation to bioclimate types, whilst more periods and more bins will lead to a finer discretisation. After associating each cell with one bioclimate type, the bioclimate influence for this type is calculated as the average of all associated cells for each point in time and each bioclimate variable (e.g. Fig. 6.A.2c).

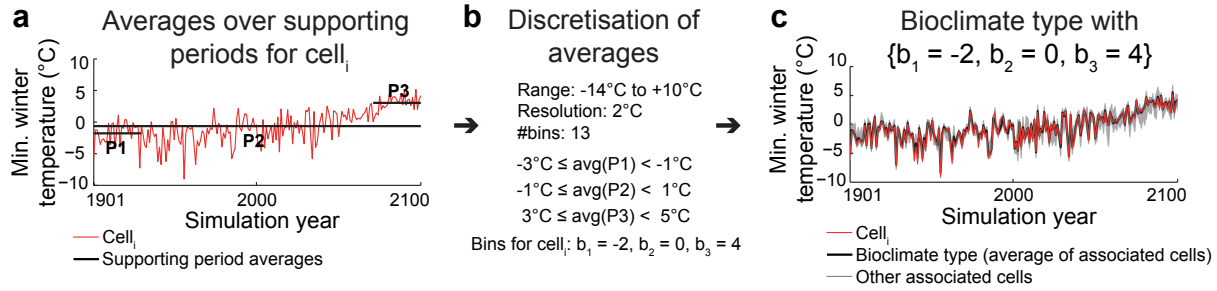

Figure 6.A.2 : Visualisation of the pre-structuring to bioclimate types with the example of the minimum winter temperature (Min. winter temperature), one of TreeMig's three bioclimate drivers. For each of the supporting periods (here P1-P3) the minimum winter temperature driving cell$_i$ is averaged (panel a). In the example the minimum winter temperature is assumed to theoretically range from $-14\,^{\circ}$C to $+10\,^{\circ}$C discretised with a resolution of $2\,^{\circ}$C into 13 bins (as e.g. done for the set E3 of bioclimate bins in Table 6.2, main text). The averages of the supporting periods P1-P3 for cell$_i$ are clustered according to these bins (panel b). All cells with supporting periods clustered into the same bins are associated with the same bioclimate type and the bioclimate influence for a bioclimate type is calculated as the average of all associated cells (panel c) for each point in time.

The bioclimate types receive a unique ID and are stored in a NetCDF file (Unidata - http://www.unidata.ucar.edu/software/netcdf/) used in two-layer simulations to read the bioclimate driver. Depending on the ratio of the number of bioclimate types to the number of cells in the simulation area, this NetCDF file is much smaller than the original NetCDF file which stores bioclimate input data for each single cell (e.g. the NetCDF file for the E1 version of the application scenario A1 having a 1:33 ratio of bioclimate types to cells has a size of 9MB instead of the 400MB required for the original file).

Most TreeMig simulations start with an initialisation phase from bare ground with a reduced number of simulated processes (cf. Lischke et al., 2006; Nabel et al., 2013; for the latter see Chapter 3). One consequence of the pre-structuring of the simulation area in TreeMig-2L is that the linked list of each bioclimate type (see Fig. 6.A.1) will contain exactly one element in this initialisation phase. Simulations not starting from bare-ground but with given species' abundances will require an additional pre-processing step, introducing appropriate numbers of elements according to the different species' abundances occurring for the different bioclimate types.

6.A.3 Execution sequence in TreeMig-2L

The implementation of TreeMig-2L is based on TreeMig-Netcdf 2.0 (Nabel et al., submitted; see Chapter 4) and the gross of the program structure was adopted from there. However, besides the changes in data structures used (see Section 6.A.1) also changes in the execution sequence were required (see Fig. 6.A.3).

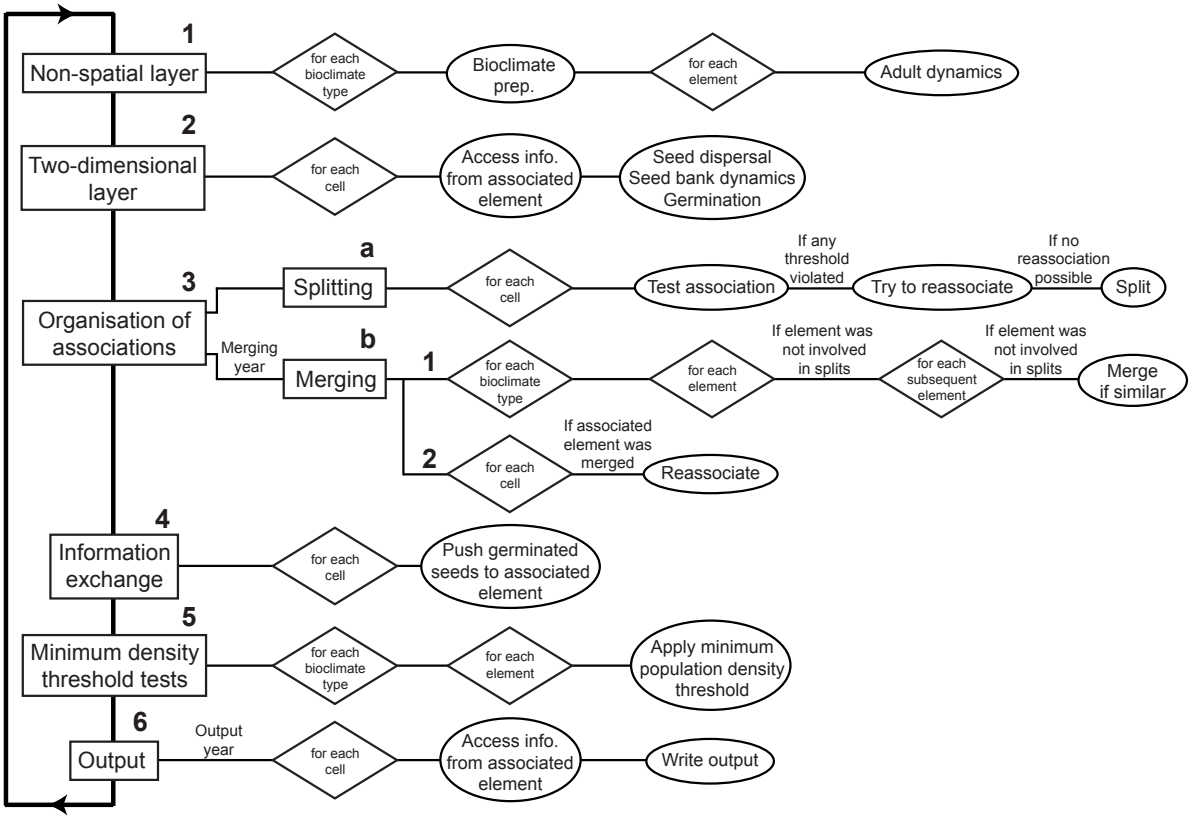

Figure 6.A.3 : Execution sequence per time step in TreeMig-2L. (1) Each time step begins with the execution of the processes simulated on the non-spatial layer. For each bioclimate type the current bioclimate driver is read (or drawn in case of extrapolations) and species-specific influences are derived and are subsequently used for simulations of adult dynamics (described in detail in Lischke et al., 2006) in each element of the linked list of the bioclimate type. (2) Subsequently, processes simulated on the two-dimensional layer are conducted. Since each cell has a pointer to the element it is currently associated with (Fig. 6.A.1 and Fig. 6.2, main text), it can access required information for seed dispersal and germination. (3a) Seeds germinated in the current time step can necessitate splitting of elements. Therefore, current associations are tested for each cell and if any threshold on the density of germinated seeds for any tracked species is violated the association is no longer valid. In case that the current associated element already had splits in the current time step, the cell can be reassociated to an element from a previous split if the thresholds on the germinated seed densities are met. If not, the current element is split up and the cell is associated with the new element. (3b) Merging is only done after a pre-defined number of time steps. In a merging year, (3b.1) all elements in the list of a bioclimate type are compared and similar elements are merged, two elements are thereby only merged if none of them was involved in any splits in this time step. (3b.2) After merging was conducted, cells whose associated elements were merged need to be reassociated. (4) After the associations are reorganised, cells can push the number of seeds germinated in this time step to their associated elements. (5) To prevent infinitesimal values, the population densities per height class kept in each element of the non-spatial layer are tested for adherence of a pre-specified minimum density threshold (see Nabel et al., 2013; see Chapter 3). Values falling below the threshold are added to lower height classes or removed, in case of the lowest height class. (6) The output of TreeMig-2L is written at the end of each time step for each cell, provided the current time step is an output year.

Appendix 6.B Application scenarios

For this study, TreeMig-2L simulations were conducted for two application scenarios with different simulation settings which are briefly characterised in Table 6.1 in the main text. The location of the simulation areas in

Switzerland are depicted in Fig. 6.3 in the main text. In this supplementary material, additional information for the two application scenarios is provided.

As described in Section 6.3.1.1 in the main text, TreeMig simulations require time series of three annual bioclimate drivers. The bioclimate influences used for the two application scenarios were derived from monthly averaged temperatures and monthly precipitation sums from different SRESA1B (Nakicenovic et al., 2000) scenario projections with a program based on ForClim-E (Bugmann and Cramer, 1998; Lischke et al., 2006) – for more details on the actual climate time series see below (B.1 and B.2). Bioclimate types for both application scenarios were derived with the same set of bioclimate bins (see Table 6.2, main text) using three sampling periods: (1) the first 30 years (A1: 1961-1991; A2: 1901-1931), (2) the whole time span (A1: 1961-2100; A2: 1901-2100) and (3) the last 30 years (both: 2071-2100). Because the simulated time spans of both application scenarios exceeded the available bioclimate data, a stochastic method was used to extrapolate the bioclimate driver (see B.3 for further information). Simulations with both scenarios started in 1400 with an initialisation phase lasting 400 years. In this initialisation phase only a restricted set of processes was simulated assuming that saplings of all species are available in all elements (with one restriction in application scenario A2, see B.2 below) instead of simulating seed production, dispersal and germination (cf. Lischke et al., 2006; Nabel et al., 2013; for the latter see Chapter 3).

The two-layer simulations discussed in the main text all applied the same set of splitting and merging thresholds. These thresholds were defined on a unit area, the so-called patch area (cf. Bugmann, 1994), because TreeMig's state variables represent means of Poisson distributions of tree densities per species and height class on this unit area (Lischke et al., 1998, 2006). For the splitting of elements two thresholds were used, namely 0.005 and 0.5 germinated seeds per patch area. These two thresholds were used to divide the number of germinated seeds in three bins: absence of germinated seeds, scattered germinates seeds and more than one seed on every second patch. Elements on the non-spatial area were split if the germinated seeds of any of the species tracked in the application scenario fell on different sides of these thresholds for at least two associated cells. Merging was considered every 100 simulation years and elements were merged if the difference in the densities for all occurring species and height classes did not exceed a height-specific similarity threshold (50.0, 25.0, 20.0, 15.0, 10.0, 7.5, 5.0, 2.5 individuals per patch for the lowest eight height classes, respectively and 1.0 for all other height classes).

In addition to the simulations discussed in the main text, some sensitivity tests were conducted with different splitting and merging thresholds and a different merging interval. Results for these sensitivity tests are shown and discussed in supplementary material C. For A1 and A2 tests were conducted only considering presence and absence of germinated seeds for splitting, i.e. with only one splitting threshold (0.05). For A2, additional tests with a larger set of splitting thresholds were conducted (0.0005, 0.005, 0.05, 0.5, 5.0 and 50.0 germinated seeds per patch area). For both application scenarios, a merging interval of 10 simulation years and merging conditional on smaller differences for the densities in the height classes were tested (5.0 individuals per patch area for the first seven height classes and 1.0 individuals for all other height classes).

All simulations were conducted without disturbances (other than climatically caused) and the boundaries of the simulation areas were assumed to be absorbing, i.e. seeds dispersed beyond the boundaries were lost. In both application scenarios a minimum population density threshold (see Nabel et al., 2013; see Chapter 3) of one individual per grid-cell was applied.

6.B.1 Application scenario A1

Application scenario A1 has already been used in a preliminary study to test the performance of a pre-version of TreeMig-2L in simulations without dynamic associations between the layers (Nabel and Lischke, 2013; see Chapter 5). The bioclimate influences used for A1 simulations were derived from an SRESA1B scenario simulation calculated with RCA3 (1961-2100 – Kjellström et al., 2005) and downscaled to 200m cell side length based on a grid of MeteoSwiss weather stations interpolated with daymet (Thornton et al., 1997). In addition to the monthly climate data, static data for the simulation area on slope, aspect and water holding capacity was used to calculate the bioclimate drivers. Slope and aspect were averaged from the 25m digital elevation model of

the Swiss Federal Office of Topography (DHM25 (c)1994 Bundesamt für Landestopographie). The water holding capacity was derived from data on water retention potential and soil wetness found in the Swiss soil suitability map (Frei et al., 1980) by means of a linear regression based on soil profiles at test sites according to (Löffler and Lischke, 2001).

A1 simulations were conducted for 1100 years (1400-2500) and simulated for 31 species occurring in Switzerland. These species were parameterised for previous TreeMig applications. Parameters for 30 species were taken from Lischke et al. (2006) altered according to the findings in Rickebusch et al. (2007), namely *Abies alba*, *Larix decidua*, *Picea abies*, *Pinus cembra*, *P. montana*, *P. sylvestris*, *Taxus baccata*, *Acer campestre*, *A. platanoides*, *A. pseudoplatanus*, *Alnus glutinosa*, *A. incana*, *A. viridis*, *Betula pendula*, *Carpinus betulus*, *Castanea sativa*, *Corylus avellana*, *Fagus sylvatica*, *Fraxinus excelsior*, *Populus nigra*, *P. tremula*, *Quercus petraea*, *Q. pubescens*, *Q. robur*, *Salix alba*, *Sorbus aucuparia*, *Tilia cordata*, *T. platyphyllos* and *Ulmus scabra*. Parameters for the 31^{th} species *Ostrya carpinifolia* were taken from Nabel et al. (2012) (see Chapter 2).

For the A1 simulations with two layers discussed in the main text, four species were used to decide if an element of the non-spatial layer needs to be split: *Q. pubescens*, *O. carpinifolia*, *L. decidua* and *P. silvestris*. These four species were selected as tracked species because of their high drought tolerance indices in TreeMig. With increasing drought severity (and temperature), these species are expected to increase their distributions. In addition to simulations with these four tracked species, simulations with two tracked species (*P. silvestris* and *Q. pubescens*) and simulations with six tracked species (the four species already listed and the two species most abundant in the simulation area *P. abies* and *F. sylvatica*) were conducted to assess the sensitivity of the simulation results to the choice of tracked species.

6.B.2 Application scenario A2

Application scenario A2 was used in previous studies to investigate the influence of interannual bioclimate variability on the northwards migration of *O. carpinifolia* (Nabel et al., 2012, 2013; see Chapters 2 and 3). Bioclimate influences were derived from CRU data (1901-2000 – Mitchell et al., 2003) followed by an SRESA1B scenario simulation calculated with CLM (2001-2100 – Lautenschlager et al., 2009 which was downscaled to $30''$ with WorldClim data (Hijmans et al., 2005) and projected to 1km^2 with FIMEX-0.28 (Klein, 2012). In addition to the monthly climate data, static data for the simulation area on slope, aspect and water holding capacity was used (see supplementary material to Nabel et al. (2013) for more details; see Appendix 3.B).

A2 simulations were conducted for 1600 years (1400-3000) and in addition to *O. carpinifolia* a 20 other species were simulated: *A. alba*, *L. decidua*, *P. abies*, *P. cembra*, *P. sylvestris*, *Taxus baccata*, *A. platanoides*, *A. pseudoplatanus*, *A. incana*, *B. pendula*, *C. betulus*, *C. sativa*, *F. sylvatica*, *F. excelsior*, *P. tremula*, *Q. petraea*, *Q. pubescens*, *S. aucuparia*, *T. cordata*, *T. platyphyllos* and *U. scabra*.

As opposed to all other species, saplings of *O. carpinifolia* were restricted to the southern part of the transect up to the 65^{th} transect km north in the initialisation phase (1400-1800) of the A2 simulations. From the simulation year 1800 on the northwards migration of *O. carpinifolia* was simulated. For the A2 simulations discussed in the main text the optimistic end of the range of plausible species parameters for *O. carpinifolia* (see Nabel et al., 2012; see Chapter 2) was used because the migration through the transect was not restricted for this parameter set in a previous simulation study (Nabel et al., 2013; see Chapter 3). In addition to this parameter set from the optimistic end, a predominantly moderate parameter set was simulated to assess the sensitivity of deviations in the simulation results on the parameter set of the migrating species (see Section 6.C.3.2). This second parameter set used moderate values for all parameters other than the required sum of daily mean temperatures above $5.5\,^{\circ}\text{C}$ because this parameter was critical for a successful migration in a previous simulation (Nabel et al., 2013; see Chapter 3).

6.B.3 Extrapolation of the bioclimate time series

To extrapolate the available bioclimate time series to cover the entire simulated time spans a stochastic method was used. Nabel et al. (submitted) (see Chapter 4) recommended that a method used to extrapolate time series

for spatially explicit simulations should account for the spatial correlation of climatic fluctuations in the extrapolated data. Therefore, the simple method of drawing complete bioclimate maps from a set of base years used in Nabel et al. (submitted) was also used in this study. For extrapolation of past simulation years the first 30 years of the input data for each of the two application scenarios (A1: 1961-1990 and A2: 1901-1930) were used to derive a set of detrended base years (see supplementary material to Nabel et al. (2013) (see Chapter 3) for more information on the detrending). For extrapolations of future simulation years the last 30 years (2071-2100 for both application scenarios) were used to derive a second set of detrended base years.

In the pre-structuring of the simulation area, required for two-layer simulations with TreeMig-2L, the bioclimate information is transferred from the cell level to the bioclimate types. This does not affect the applicability of the extrapolation method: The only difference to simulations on one layer is that in each year a bioclimate map for all bioclimate types is drawn instead of a bioclimate map for all single cells.

Appendix 6.C Additional results and sensitivity tests

6.C.1 Pre-structuring of the simulation areas

The number of cells associated with the bioclimate types is influenced by the number of supporting periods, the number of bioclimate bins and the heterogeneity of the simulation area. Bioclimate types representing bins with frequent occurrences in the simulation area will end up with more cells than bioclimate types representing rare bioclimatic conditions. The distribution of cells to bioclimate types for the two application scenarios (A1 and A2) and the three sets of bioclimate bins (E1-E3 – see Table 6.2, main text) reflect this (see Fig. 6.C.1, Fig. 6.C.2 and Fig. 6.C.3).

In the pre-structuring of the simulation area, each bioclimate type receives a unique ID (see Section 6.A.2). This ID is theoretically arbitrary, however, the underlying algorithm in TreeMig-2L assigns the IDs in a specific order. When searching for similarities among cells, one supporting period after the other is processed and the three bioclimate variables are considered in the order: (1) sum of daily mean temperatures above $5.5\,^{\circ}\mathrm{C}$ ($\mathrm{DDsum}_{>5.5\,^{\circ}\mathrm{C}}$), (2) minimum winter temperature, and (3) drought index; each increasing from the smallest to the largest occurring value. Thus, the IDs of the bioclimate types are monotonous increasing with the $\mathrm{DDsum}_{>5.5\,^{\circ}\mathrm{C}}$ of the first supporting period and allow some insights into the distribution of IDs for the $\mathrm{DDsum}_{>5.5\,^{\circ}\mathrm{C}}$ in the simulation area (Fig. 6.C.1 and Fig. 6.C.4). For example, the tendency for bioclimate types with many associated cells to have IDs in the middle of the ID-ranges, i.e. $\mathrm{DDsum}_{>5.5\,^{\circ}\mathrm{C}}$ values in the moderate range of the simulation area.

A finer division by means of smaller bioclimate bins in the pre-structuring of the simulation area tends to lead to a smaller number of cells associated with the bioclimate types (Fig. 6.C.1) and to smaller deviations between the averaged bioclimate and the bioclimate of the single associated cells (Fig. 6.C.2 and Fig. 6.C.3). This is also supported by the differences among the bioclimate variables. For all sets of bioclimate bins the $\mathrm{DDsum}_{>5.5\,^{\circ}\mathrm{C}}$ was divided into more bins (see Table 6.2, main text) leading to smaller maximum differences between $\mathrm{DDsum}_{>5.5\,^{\circ}\mathrm{C}}$ time series of bioclimate types and their associated cells than for the other variables (Fig. 6.C.2 and Fig. 6.C.3).

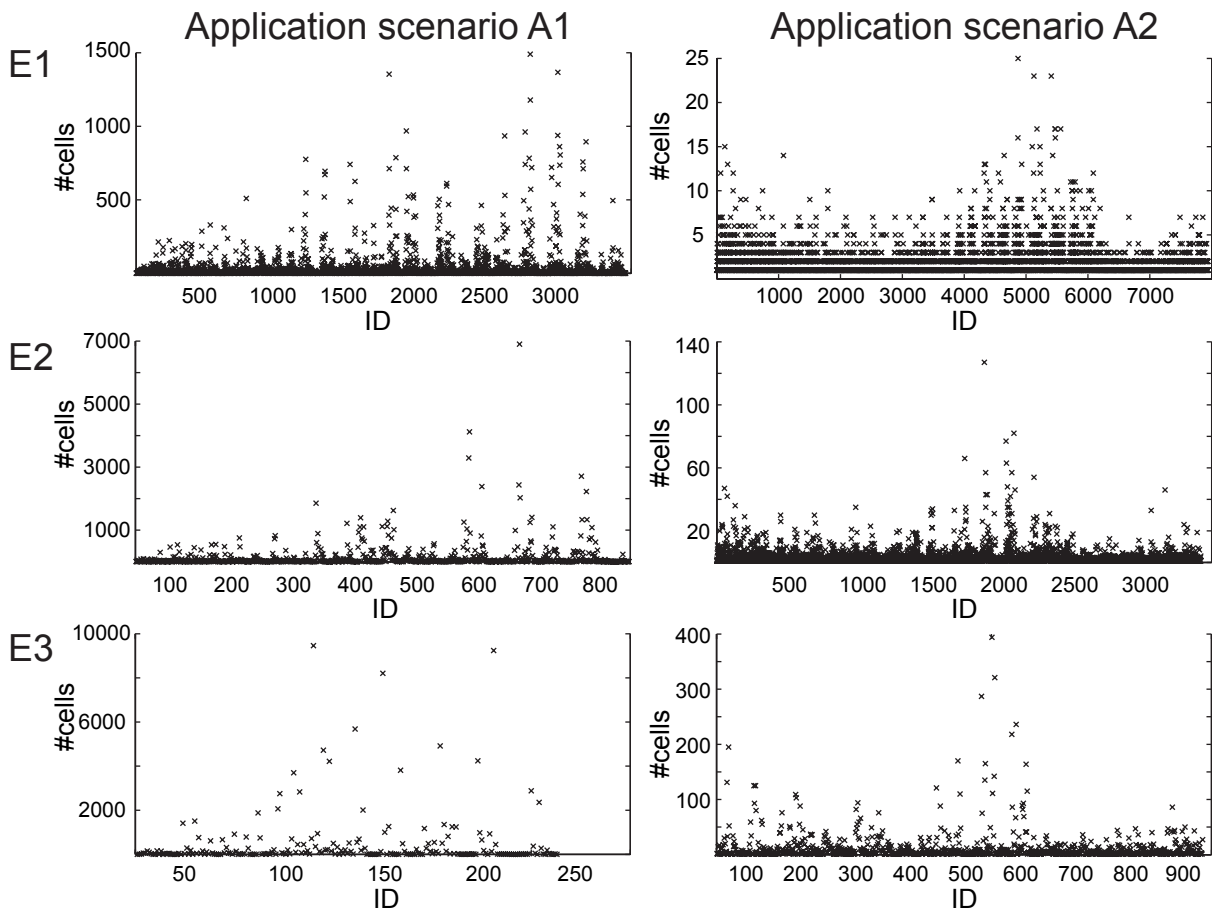

Figure 6.C.1 : Number of cells associated with bioclimate types derived with the three sets of bioclimate bins (E1-E3 – Table 6.2, main text) for the two simulation areas of application scenario A1 and A2. The number of cells per bioclimate type varies strongly among the three sets and the simulation areas (note the different scales).

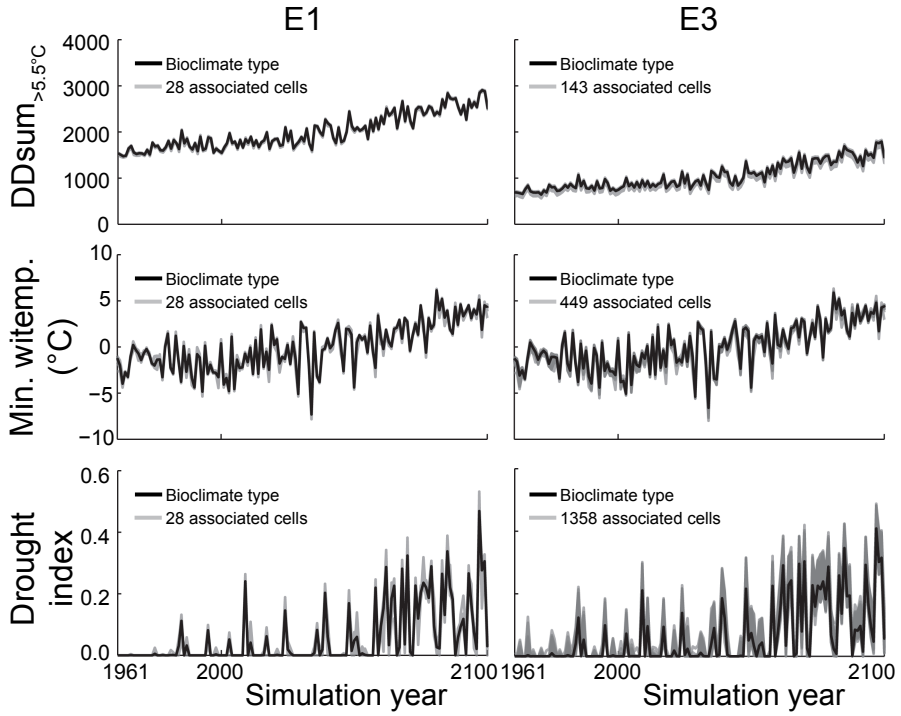

Figure 6.C.2 : Average bioclimate for the bioclimate types (black lines) and for their associated cells (grey half-transparent lines). Depicted are the bioclimate types which averages deviate the most from one of their associated cells for pre-structurings of the simulation area of application scenario A1 with the fine (E1) and the coarse (E3) bioclimate bins (Table 6.2, main text) for each of TreeMig's bioclimate drivers (DDsum$_{>5.5\,^{\circ}\mathrm{C}}$: Sum of daily mean temperatures above $5.5\,^{\circ}\mathrm{C}$; Min. witemp.: Minimum winter temperature; and the drought index).

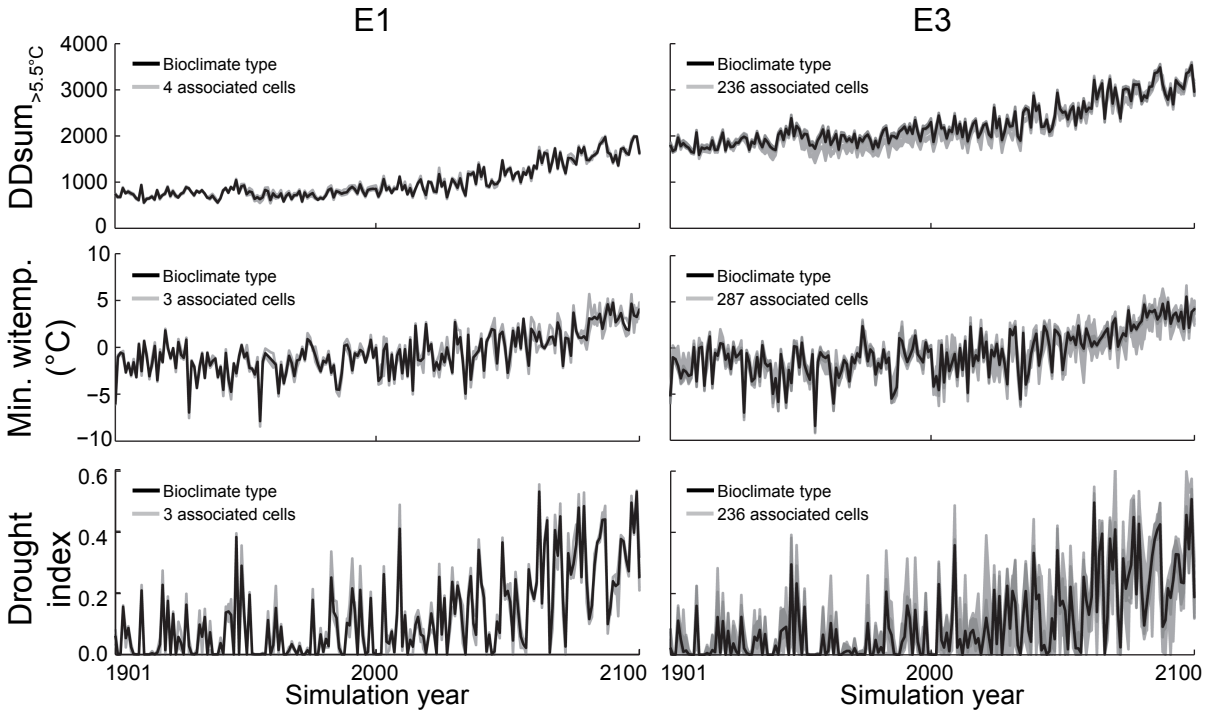

Figure 6.C.3 : Average bioclimate for the bioclimate types (black lines) and for their associated cells (grey half-transparent lines). Depicted are the bioclimate types which averages deviate the most from one of their associated cells for pre-structurings of the simulation area of application scenario A2 with the finer (E1) and the coarser (E3) bioclimate bins (Table 6.2, main text) for each of TreeMig's bioclimate drivers ($DDsum_{>5.5\,°C}$: Sum of daily mean temperatures above $5.5\,°C$; Min. witemp.: Minimum winter temperature; and the drought index).

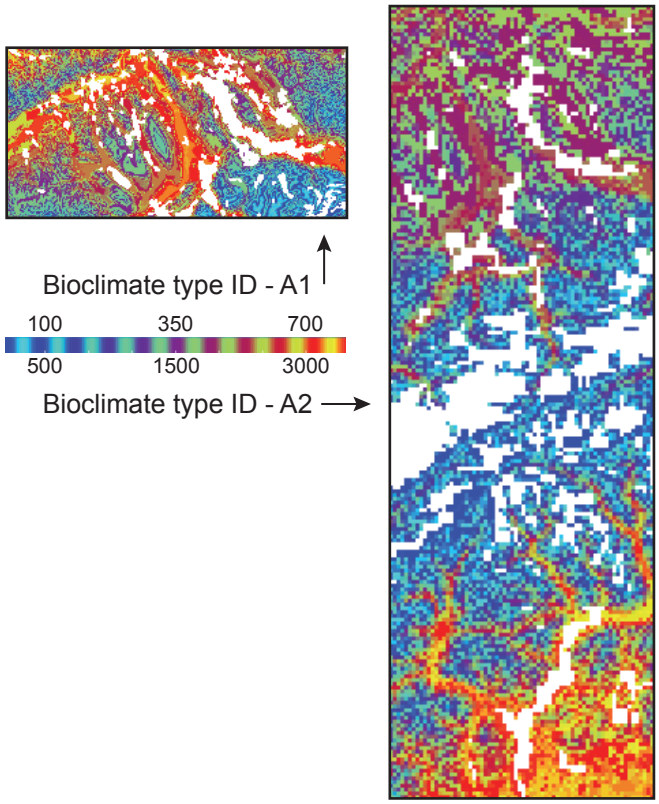

Figure 6.C.4 : Distribution of the IDs of the bioclimate types in space for the two application scenarios A1 and A2. Depicted are bioclimate type IDs for the moderate set of bioclimate bins (E2 – see Table 6.2, main text). Although the IDs of the bioclimate types are theoretically arbitrary they allow some insights into the distribution of IDs for the $\mathrm{DDsum}_{>5.5\,^{\circ}\mathrm{C}}$, due to the algorithm used to derive the bioclimate types (see text of Section 6.C.1). For both simulation areas close IDs (i.e. IDs with close $\mathrm{DDsum}_{>5.5\,^{\circ}\mathrm{C}}$ values) visibly cluster in space, following elevations in the transect area (see Fig. 6.2, main text). ID-maps were created with ncview (Pierce, 2012).

6.C.2 Additional results

To assess the relevance of deviations from one in the different similarity coefficients (SCs), results from 1L-ORG runs with different pseudo-random number streams (PRNSs) used to extrapolate the bioclimate driver were compared among each other. Since these runs only differ in the stochastically extrapolated bioclimate (before 1961 for A1, before 1901 for A2, and after 2100 for both application scenarios – see Section 6.B.3) deviation from one in their SCs (Table 6.C.1 and Fig. 6.C.5) are due to the interannual variability in the bioclimate driver.

Table 6.C.1 : The similarity coefficient (SC) was used to compare different output variables among 1L-ORG for runs applying different pseudo-random number streams (PRNSs) to extrapolate the bioclimate driver. These SCs thus show the influence of the interannual bioclimate variability on the similarity among simulations with otherwise similar conditions. SC means and standard deviations stem from comparisons among five runs with different PRNSs (ten comparisons) for A1 and 20 runs (190 comparisons) for A2.

	Avg. SC (σ)		
	SC_{sum}	SC_{spec}	SC_{OC}
A1	0.95 (0.02)	0.87 (0.04)	–
A2	0.92 (0.03)	0.86 (0.03)	0.79 (0.05)

Inter-comparisons of 1L-ORG runs led to SC_{spec} (Fig. 6.C.5a) and SC_{sum} (not shown) values close to one until 2100 for the homogeneous simulation area of application scenario A1. For the more heterogeneous sim-

ulation area of application scenario A2 there were small deviations from one in the SCs (Fig. 6.C.5b and c), which vanished during the time span simulated with a deterministic bioclimate driver (1901-2100). Directly after 2100 the SCs rapidly decreased and quickly stabilised on a lower level for both application scenarios. The lower levels in the SCs after 2100 were mainly due to the larger drought index values and the higher interannual variability in the drought index (see e.g. Fig. 6.C.2 and Fig. 6.C.3) which entail larger fluctuations in the simulated species' abundances.

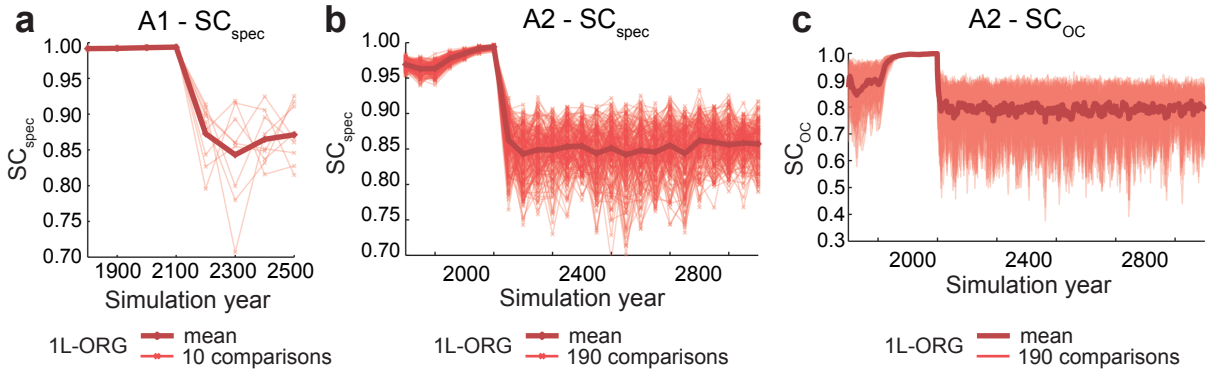

Figure 6.C.5 : Temporal development of the SC_{spec} for application scenario A1 and A2 and the SC_{OC} for application scenario A2 from comparisons of 1L-ORG runs applying different pseudo-random number streams to extrapolate the bioclimate driver. SC_{spec} values were calculated every 100 years for A1 and every 50 years for A2 simulations; SC_{spec} was calculated for every simulation year. SC_{spec} for A1 stems from comparisons among five runs (ten comparisons); SCs for A2 stem from comparisons among 20 runs (190 comparisons). Single runs and their means are printed half-transparent and bold, respectively.

For both application scenarios, and the three different kinds of conducted simulation settings (2L, 1L-PB and 2L-NDA), the development over time of SC_{spec} (Fig. 6.C.6 and Fig. 6.C.7) and SC_{sum} (not shown) were comparable among simulations conducted with bioclimate types resulting for all three sets of bioclimate bins (E1-E3) and most simulation settings: the SCs decreased in the transient phase of climate change (from around 2000 on) and stabilised after a few centuries. Comparable to the 1L-ORG simulations (Fig. 6.C.5) the SCs stabilised on a lower level than before the transient phase, which is again mainly due to the larger drought index values. Deviations resulting from simulations with the original drought indices and the averaged drought indices have a stronger impact for larger than for smaller drought indices.

Trajectories for the SC_{OC} measured for application scenario A2 with 2L-NDA simulations (Fig. 6.C.8) differ from the other trajectories. The 2L-NDA simulations were conducted without dynamic associations. Because no splits were conducted *Ostrya carpinifolia* quickly covered the whole simulation area after the spin-up since seeds germinated in any of the cells associated with one element contributed to the average number of germinated seeds in that element. In 1L-ORG simulations, 1L-PB simulations and in the 2L simulations with dynamic associations, in contrast, *O. carpinifolia* was initially absent in the northern parts of the transect and only slowly migrated through the transect (Fig. 6.C.9). Therefore, the SC_{OC} is much smaller for 2L-NDA simulations than for 2L simulations (maximum differences in the SC of more than 0.3 – Fig. 6.C.8). Because 2L-NDA simulations were conducted without dynamic associations they mainly reflect the changes in the bioclimate over time. In the application scenario A2, the bioclimate driver was deterministic from 1901-2100 (see Section 6.B) and a changing climate following the SRESA1B scenario was simulated. After 2000 the temperatures in the southern part of the transect got more and more favourable for *O. carpinifolia* leading to an increase in the biomass of *O. carpinifolia* by the year 2025 for simulations with all simulation settings (Fig. 6.C.9). Because the SC is calculated as the ratio of differences compared to similarities over all cells of a simulation area (see Eq. 1, main text) an increase of the abundances in the south for all simulation settings and stable abundances in the north led to a rapid increase in the SC_{OC} for 2L-NDA runs (Fig. 6.C.8, Fig. 6.C.9). However, after only some decades the bioclimate in the north of the transect also got warm enough to allow for an increase in the biomass of *O. carpinifolia* in the 2L-NDA simulations (Fig. 6.C.9). This led to a sharp decrease in the SC_{OC} because now the

difference in biomass amounts of *O. carpinifolia* in the north of the transect compared to 1L-ORG simulations increased (Fig. 6.C.8). After 2100 the SC_{OC} stayed on a stable level for some centuries and started to slowly increase again by the time *O. carpinifolia* started to spread on the northern side of the Alps in simulations with the other simulation settings (Fig. 6.C.8, Fig. 6.C.9).

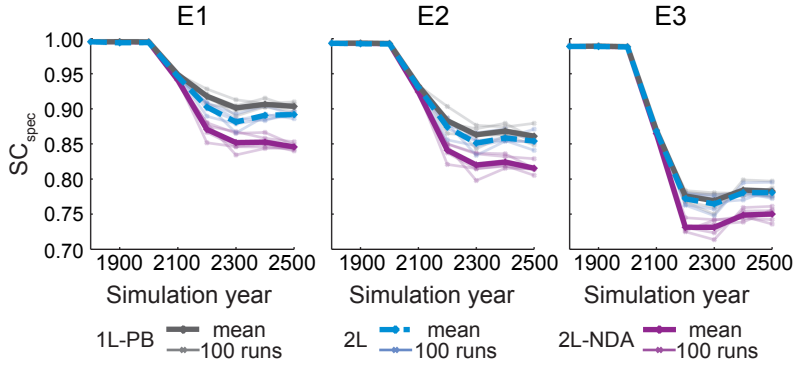

Figure 6.C.6 : Temporal development of the SC_{spec} for application scenario A1 from comparisons of 1L-ORG runs to runs with bioclimate types derived with all three sets of bioclimate bins (E1-E3 – Table 6.2, main text). SC_{spec} values were calculated every 100 years for two-layer runs with and without dynamic associations (2L and 2L-NDA, respectively) and runs on one layer but with the bioclimate of the associated bioclimate types (1L-PB). For each setting five repetitions were compared, which were simulated with different pseudo-random number streams used to extrapolate the bioclimate driver before 1961 and after 2100. Single runs and their means are printed half-transparent and bold, respectively.

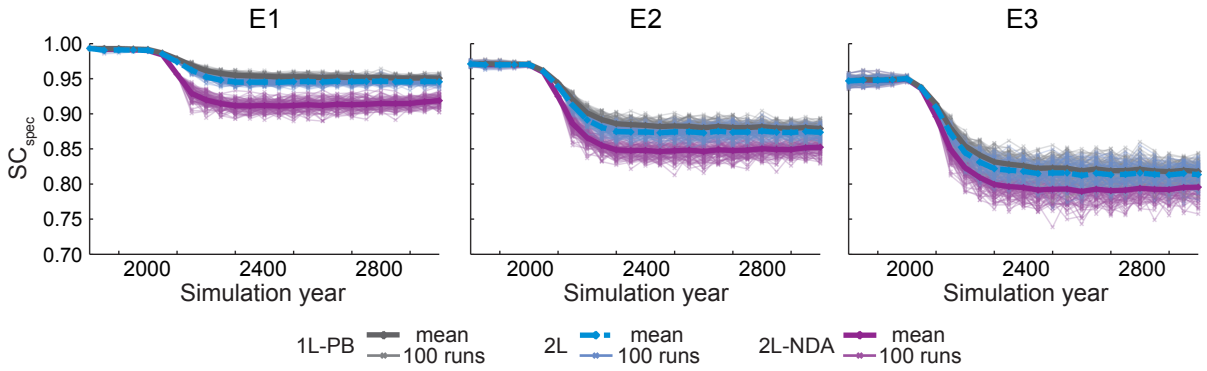

Figure 6.C.7 : Temporal development of the SC_{spec} for application scenario A2 from comparisons of 1L-ORG runs to runs with bioclimate types derived with all three sets of bioclimate bins (E1-E3 – Table 6.2, main text). SC_{spec} values were calculated every 50 years for two-layer runs with and without dynamic associations (2L and 2L-NDA, respectively) and runs on one layer but with the bioclimate of the associated bioclimate types (1L-PB). For each setting 100 repetitions were compared, which were simulated with different pseudo-random number streams used to extrapolate the bioclimate driver before 1901 and after 2100. Single runs and their means are printed half-transparent and bold, respectively.

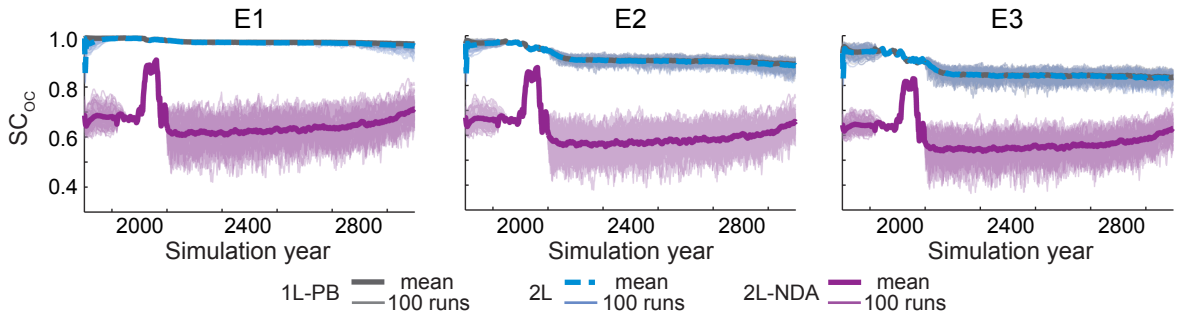

Figure 6.C.8 : Temporal development of the SC_{OC} comparing simulations of application scenario A2. Depicted SC_{OC} values stem from comparisons of 1L-ORG runs to runs with bioclimate types derived with all three sets of bioclimate bins (E1-E3 – Table 6.2, main text). Simulations were conducted with two-layers with and without dynamic associations (2L and 2L-NDA, respectively) and with one layer but with the bioclimate of the associated bioclimate types (1L-PB). For each setting 100 repetitions were compared, which were simulated with different pseudo-random number streams used to extrapolate the bioclimate driver before 1901 and after 2100. Single runs and their means are printed half-transparent and bold, respectively.

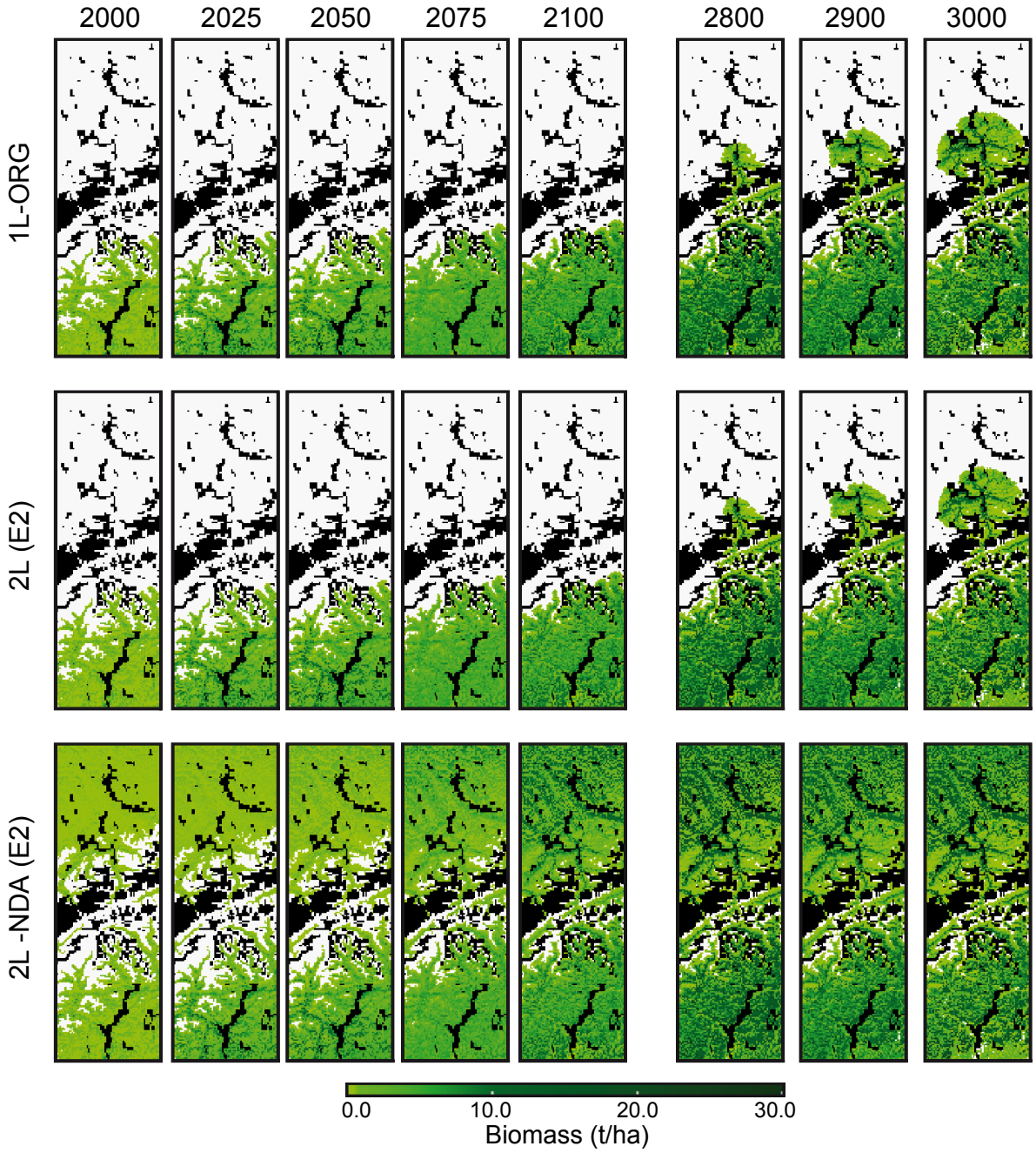

Figure 6.C.9 : Maps of the biomass of *Ostrya carpinifolia* for different simulation years resulting in one-layer simulations with the original bioclimate driver (1L-ORG) and simulations with bioclimate types derived with the moderate set of bioclimate bins (E2 – Table 6.2, main text) and simulated with and without dynamic associations between cells on the two-dimensional layer and elements on the non-spatial layer (2L and 2L-NDA, respectively). Differences in the spatial spread of *O. carpinifolia* between 1L-ORG and 2L simulations on one side and 2L-NDA simulations on the other side demonstrate the problem of simulations with a general availability of seeds for all species – as assumed in many dynamic vegetation models (see e.g. Snell et al., submitted; see Appendix A) – and underline the importance to simulate migration explicitly. Maps of the biomass of *O. carpinifolia* were created with Paraview (Ahrens et al., 2005).

6.C.3 Sensitivity tests

In addition to the simulations discussed in the main text, several sensitivity tests were conducted with different splitting and merging thresholds and a different merging interval.

6.C.3.1 Sensitivity tests for application scenario A1

For application scenario A1, each combination of the variants listed in Table 6.C.2 was simulated with bioclimate types derived with all three sets of bioclimate bins (E1-E3 – Table 6.2, main text) and with five different pseudo-random number streams used to extrapolate the bioclimate driver, i.e. 360 simulations were conducted.

Table 6.C.2 : Simulated variants of tracked species, splitting and merging thresholds and merging intervals.

Tracked species	**2**: *P.s.*[1] and *Q.p.*[2]	**4***: The two and *O.c.*[3] and *L.d*[4]	**6**: The four and *P.a.*[5] and *F.s.*[6]
Splitting thresholds[a]	**1**: 0.05	**2***: 0.005 and 0.5	
Merging accuracy	**c***: Coarse merging thresholds[b]	**f**: Fine merging thresholds[c]	
Merging interval	**decade**	**century***	

[1] *P. silvestris* [2] *Q. pubescens* [3] *O. carpinifolia* [4] *L. decidua* [5] *P. abies* [6] *F. sylvatica*

* Combination of variants used in the experiments in the main text.

[a] germinated seeds per patch area

[b] Similarity thresholds of 50.0, 25.0, 20.0, 15.0, 10.0, 7.5, 5.0, 2.5 individuals per patch for the lowest eight height classes, respectively and 1.0 for all other height classes.

[c] Similarity thresholds of 5.0 individuals per patch area for the first seven height classes and 1.0 individuals for all other height classes.

The different variants led to dramatic differences in the number of elements on the non-spatial layer over the simulated time span. The extremes of these combinations spanned a range of peak ratios of number of elements compared to number of cells in the simulation area from below 2% up to around 70% (Fig. 6.C.10). Despite the dramatic differences in the number of elements on the non-spatial layer over time, maximum differences in CPU time reductions were only around 12% (Fig. 6.C.11) with larger differences among simulations with different number of tracked species when merging every century. The set of bioclimate bins (E1-E3 – Table 6.2, main text) used to derive the applied bioclimate types had even lesser effects on the CPU time reductions than the number of tracked species combined with the merging interval. The level of the SC_{spec}, in contrast, was mainly determined by the applied bioclimate types. In summary, simulations with application scenario A1 showed that the only notable increases in CPU time reductions were achieved by reducing the number of tracked species or by shortening the merging interval from centuries to decades, which in turn had small influenced the SC_{spec}. However, when merging with the finer set of merging thresholds the effect on the SC_{spec} was comparably very low ($\leq$ 0.02 differences in the SC).

6.C.3.2 Sensitivity tests for application scenario A2

For application scenario A2, two different sensitivity tests were conducted: Firstly, the influence of a different parameter set for the migrating species on the accuracy of TreeMig-2L simulations was tested and secondly – as also done for application scenario A1 – tests on the influence of splitting and merging thresholds and merging intervals were conducted.

Simulating migration with another species parameter set In addition to the parameter set used in the main text, a less optimistic parameter set was simulated (see Section 6.B.2) to assess the sensitivity of deviations in the simulation results on the parameter set of the migrating species. As in the main text, northernmost occurrences of *O. carpinifolia* and its spread in the last simulation year were compared between 2L simulations with bioclimate types derived with all three sets of bioclimate bins (E1-E3 – Table 6.2, main text) and 1L-ORG simulations (Fig. 6.C.12). Whilst the distribution of the northernmost occurrences in the last simulation year resulting from two-layer simulations with E1-E3 were comparable to simulations with the optimistic parameter

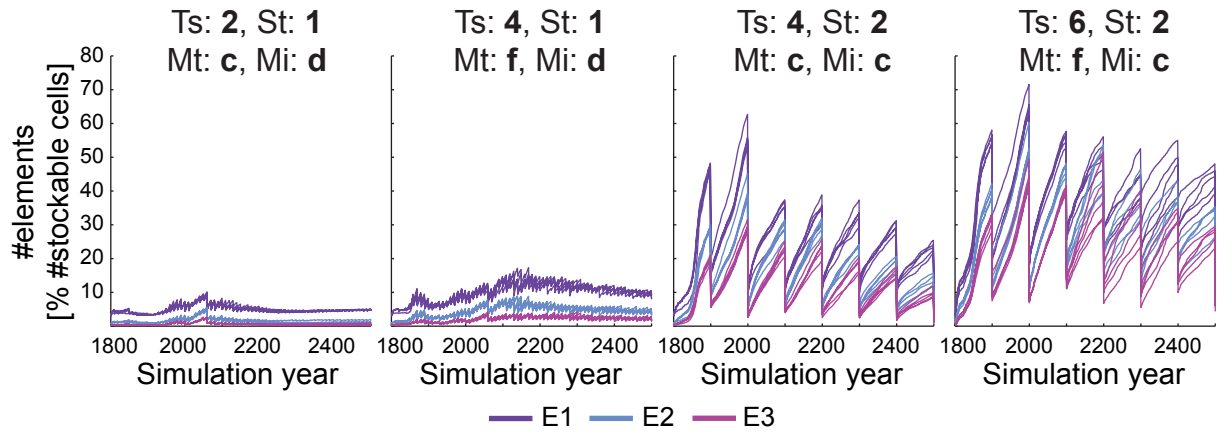

Figure 6.C.10 : Temporal development of the elements on the non-spatial layer relative to the number of cells in the simulation area. Depicted are simulations with different combinations of tracked species (Ts), splitting (St) and merging accuracy (Ma) and merging intervals (Mi) with bioclimate types derived with all three sets of bioclimate bins (E1-E3 – Table 6.2, main text). Shown are the extreme combinations (Table 6.C.2): tracking absence and presence (St: 1) of two species (Ts: 2) and merging every decade (Mi: d) with coarse merging thresholds (Ma: c) on the left, and tracking six species (Ts: 6) with two splitting thresholds (St: 2) and merging every century (Mi: c) with finer merging thresholds (Ma: f) on the right, as well as two moderate combinations, of which one is the combination shown in the main text, namely tracking four species (Ts: 4) with two splitting thresholds (St: 2) and merging every century (Mi: c) with coarse merging thresholds (Ma: c). CPU times and SC_{spec} values of these and other combinations are shown in Fig. 6.C.11.

set (Fig. 6.7, main text), the distribution resulting from simulations with E3 – the coarsest set of bins – for the moderate parameter set for *O. carpinifolia* clearly stick out (Fig. 6.C.12a), showing a strong tendency for a faster crossing of the bottlenecks caused by the coarser averaging of the bioclimate driver. Biomass distributions are again comparable over broad parts of the simulation area, however, migration paths appear to be slightly different for each of the simulated settings, at least for the depicted run (Fig. 6.C.12b).

Sensitivity on splitting and merging thresholds and merging intervals For application scenario A2, the same splitting and merging threshold and the same merging intervals as for application scenario A1 (Table 6.C.2) were simulated. In addition, simulations were conducted with a larger set of splitting thresholds (Six thresholds: 0.0005, 0.005, 0.05, 0.5, 5.0 and 50.0 germinated seeds per patch area). A2 simulations were conducted for each combination of variants with bioclimate types derived with all three sets of bioclimate bins (E1-E3 – Table 6.2, main text) and with 20 different pseudo-random number streams used to extrapolate the bioclimate driver, i.e. 720 simulations were conducted. Besides the large differences among simulations with bioclimate types derived with the different bioclimate bins, changes in other settings for application scenario A2 showed only tiny differences in the resulting mean CPU time reductions (maximum differences smaller than 3%) and the resulting mean SC_{spec} values (max differences smaller than 0.01 – Fig. 6.C.13). The same was observed for most settings for mean SC_{OC} values (Fig. 6.C.14), however, merging intervals of a decade in combination with the coarse merging thresholds led to stronger decreases in the mean SC_{OC} (maximum differences of about 0.08).

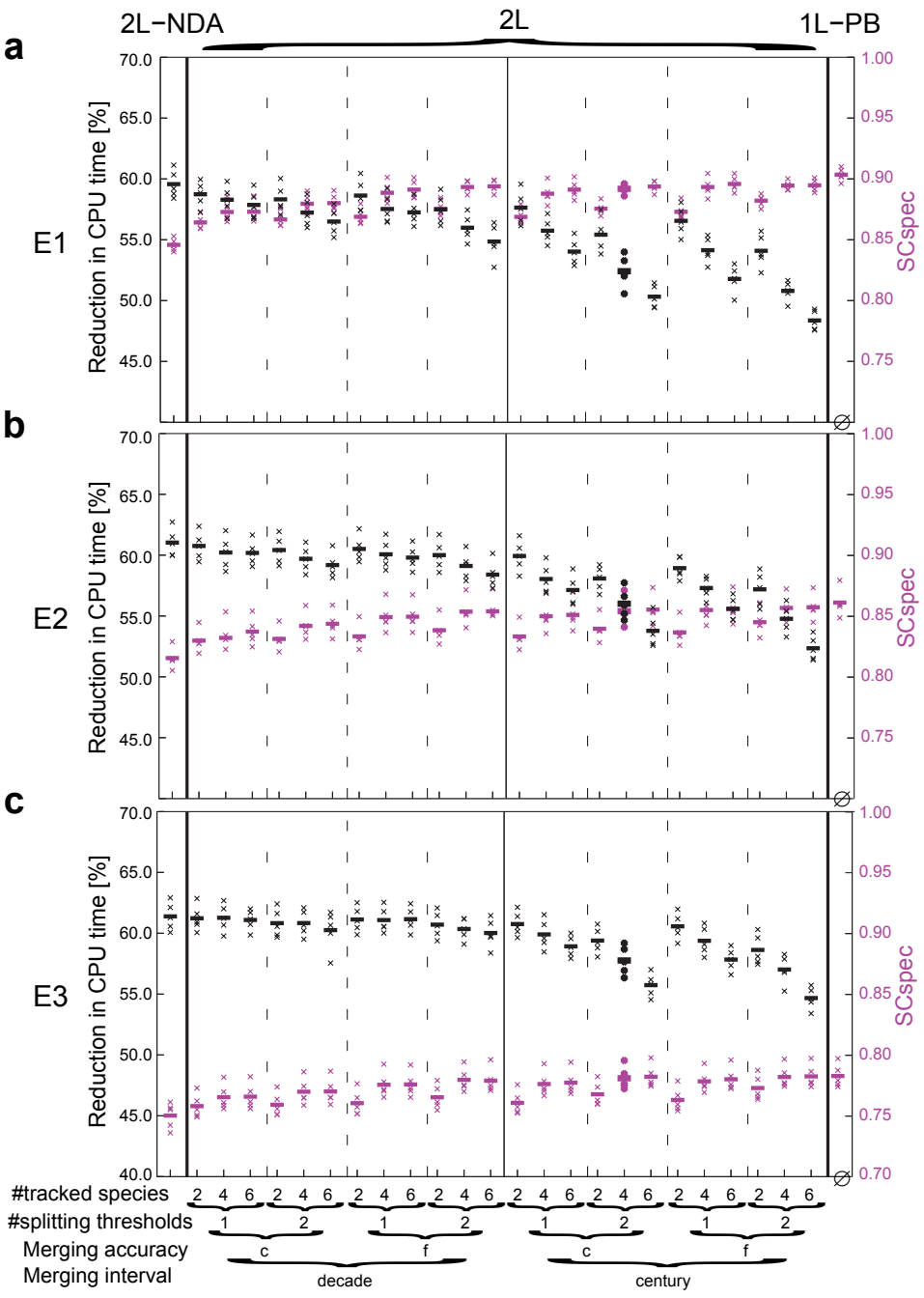

Figure 6.C.11 : CPU time reductions and SC_{spec} values resulting from simulations with different splitting and merging settings (numbers and letters on the x-axis are according to Table 6.C.2) and bioclimate types derived with each of the three sets of bioclimate bins (E1-E3). Additionally, CPU time reductions and SC_{spec} values resulting from two-layer simulations without dynamic associations (2L-NDA) and one-layer simulations with the bioclimate driver from the bioclimate types (1L-PB) are depicted. 1L-PB simulations did not led to reductions in CPU times (indicated by the empty set sign). Each simulation setting was repeated in five runs with different pseudo-random number streams used to extrapolate the bioclimate driver. The CPU times for single runs and the resulting SC_{spec} values in the last simulation year are depicted as crosses, the mean of the five runs for each setting as a dash. The combination shown in the main text is depicted with a thicker stroke.

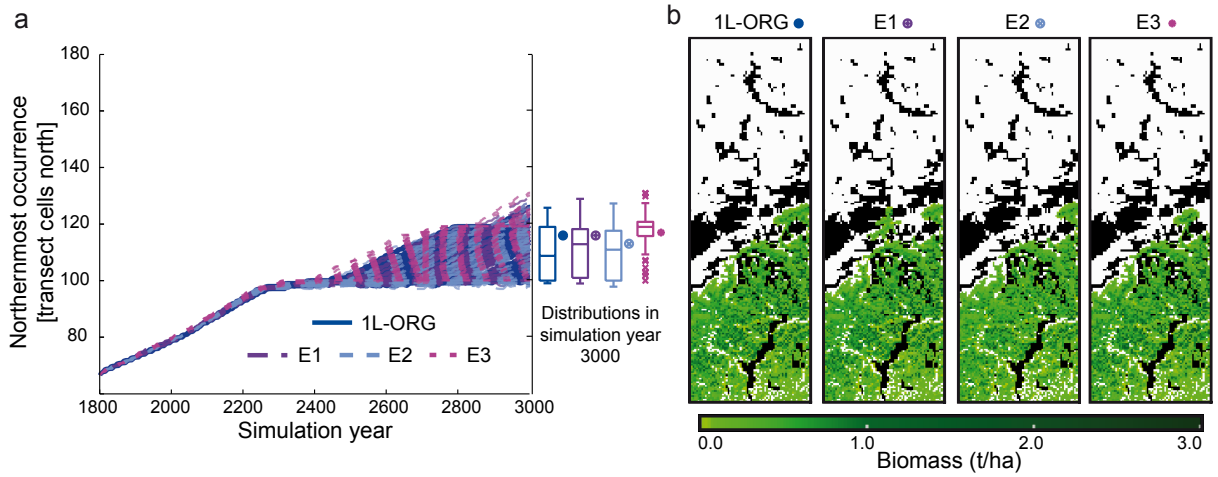

Figure 6.C.12 : Accuracy of the simulation of migration with TreeMig-2L for a less optimistic parameter set for *Ostrya carpinifolia* than simulated in the main text (see Fig. 6.7, main text). (Panel a) The temporal development of the simulated northwards migration of *O. carpinifolia* (depicted as the northernmost occurrence over time; smoothed over ten year intervals) resulting from 2L simulations with bioclimate types derived with the three sets of bioclimate bins (E1-E3 – Table 6.2, main text) resemble the results from the 1L-ORG simulations. Distributions of the northernmost occurrences in the last simulation year (box-plots on the right side of panel a), calculated from 100 repetitions with different pseudo-random number streams (PRNSs) used to extrapolate the bioclimate driver, are quite similar in mean and standard deviations for most settings. However, the distribution resulting from simulations with E3 – the coarsest set of bins – clearly sticks out indicating a strong tendency for a faster crossing of the bottleneck situation. (Panel b) Maps of the spatial spread of *O. carpinifolia* resulting from runs with the same PRNS as depicted in Fig. 6.7, main text. Again, broad parts of the simulation area are comparable, reflected in their SC_{OC} values: E1: 0.96 E2: 0.89 E3: 0.80. However, migration paths appear to be slightly different for each of the simulated settings for the depicted run. The northernmost occurrences in the last simulation year of the four runs depicted in panel b are marked with differently coloured symbols on the right side of panel a. Maps of the biomass of *O. carpinifolia* were created with Paraview (Ahrens et al., 2005).

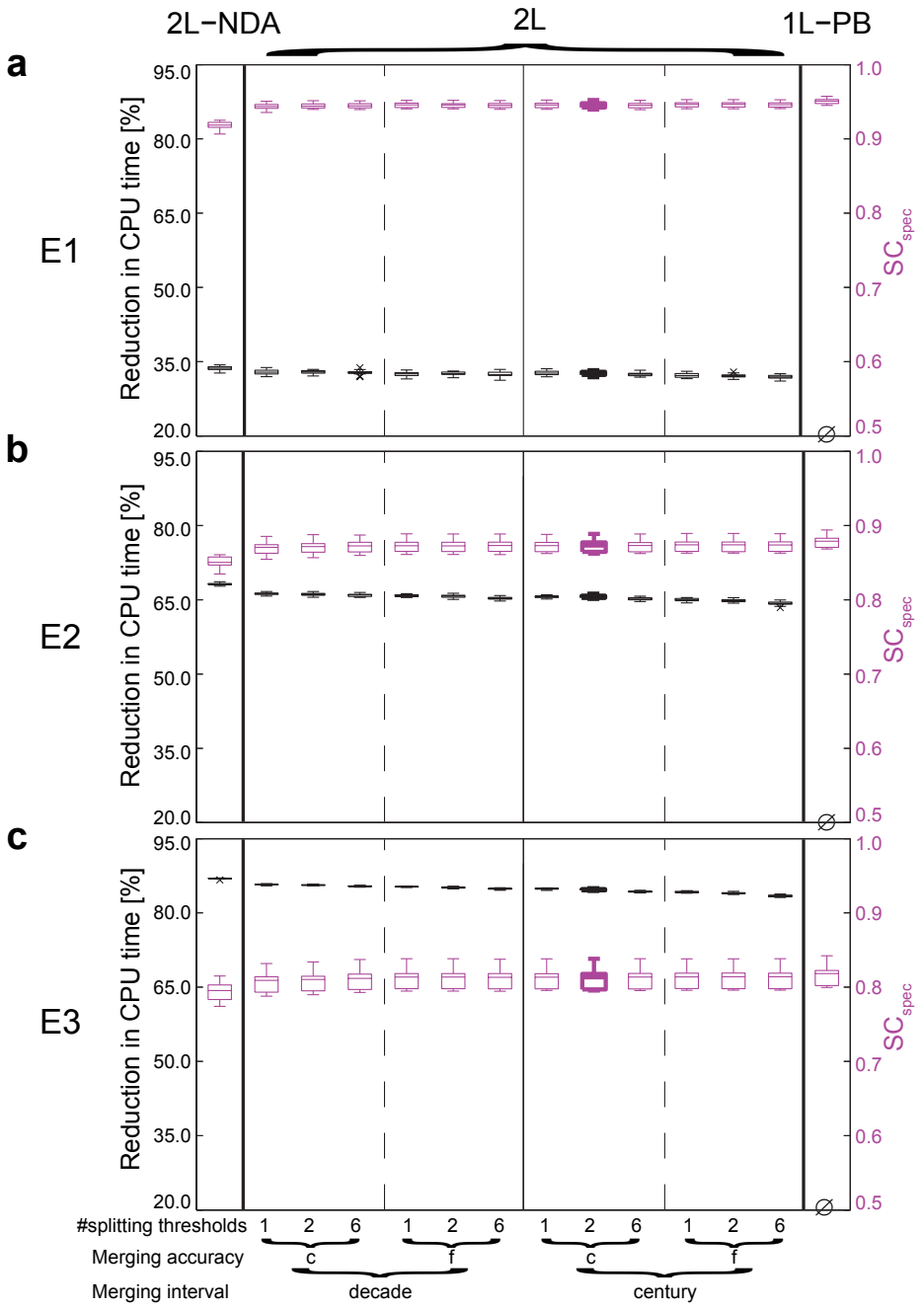

Figure 6.C.13 : CPU time reductions and SC_{spec} values resulting from simulations with different splitting and merging settings (numbers and letters on the x-axis are according to Table 6.C.2; for '6' splitting thresholds see text to Section 6.C.3.2) and bioclimate types derived with each of the three sets of bioclimate bins (E1-E3). Additionally, CPU time reductions and SC_{spec} values resulting from two-layer simulations without dynamic associations (2L-NDA) and one-layer simulations with the bioclimate driver from the bioclimate types (1L-PB) are depicted. 1L-PB simulations did not led to reductions in CPU- times (indicated by the empty set sign). Each simulation setting was repeated in 20 runs with different pseudo-random number streams used to extrapolate the bioclimate driver. The combination shown in the main text is depicted with a thicker stroke.

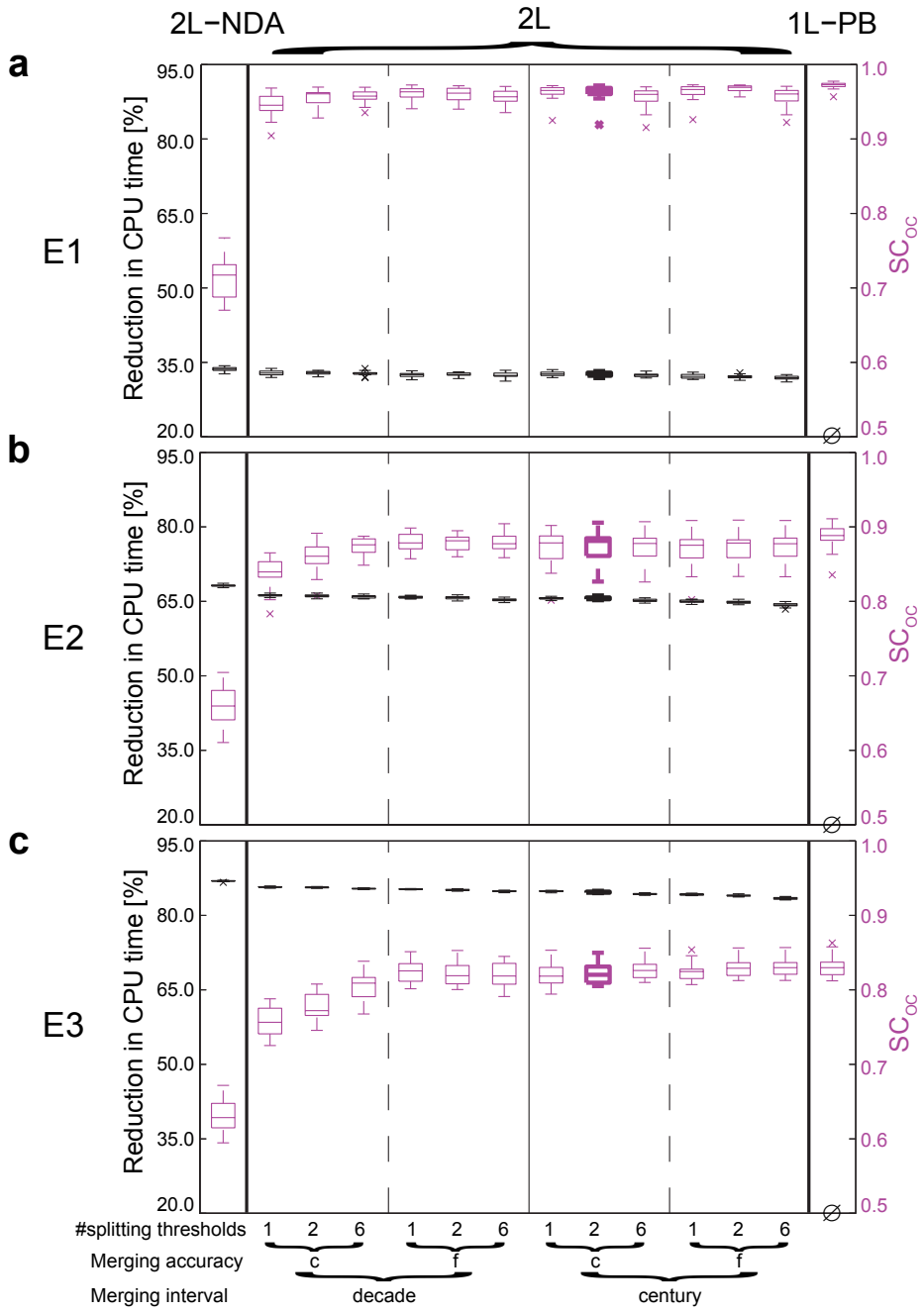

Figure 6.C.14 : CPU time reductions and SC_{OC} values resulting from simulations with different splitting and merging settings (numbers and letters on the x-axis are according to Table 6.C.2; for '6' splitting thresholds see text to Section 6.C.3.2) and bioclimate types derived with each of the three sets of bioclimate bins (E1-E3). Additionally, CPU time reductions and SC_{OC} values resulting from two-layer simulations without dynamic associations (2L-NDA) and one-layer simulations with the bioclimate driver from the bioclimate types (1L-PB) are depicted. 1L-PB simulations did not led to reductions in CPU times (indicated by the empty set sign). Each simulation setting was repeated in 20 runs with different pseudo-random number streams used to extrapolate the bioclimate driver. The combination shown in the main text is depicted with a thicker stroke.

References

Ahrens, J., Geveci, B., Law, C., 2005. ParaView: An End-User Tool for Large-Data Visualization, in: Visualization Handbook. Butterworth-Heinemann.

Bugmann, H., 1994. On the Ecology of Mountainous Forests in a Changing Climate: A Simulation Study. Ph.D. thesis. Swiss Federal Institute of Technology Zurich.

Bugmann, H., Cramer, W., 1998. Improving the behaviour of forest gap models along drought gradients. Forest Ecology and Management 103, 247–263.

Frei, E., Vökt, U., R., F., Brunner, H., Schai, F., 1980. Bodeneignungskarte der Schweiz auf Grund der Bodeneigenschaften ausgewählter physiographischer Landschaftselemente. Bundesämter für Raumplanung, Landwirtschaft und Forstwesen. Bern.

Hijmans, R.J., Cameron, S.E., Parra, J.L., Jones, P.G., Jarvis, A., 2005. Very high resolution interpolated climate surfaces for global land areas. International Journal of Climatology 25, 1965–1978.

Kjellström, E., Bärring, L., Gollvik, S., Hansson, U., Jones, C., Samuelsson, P., Rummukainen, M., Ullerstig, A., U., W., Wyser, K., 2005. A 140-year simulation of European climate with the new version of the Rossby Centre regional atmospheric climate model (RCA3). SMHI Reports Meteorology and Climatology No. 108, SMHI, SE-60176, Norrköping, Sweden, 54 pp.

Klein, H., 2012. FIMEX-0.28. https://wiki.met.no/fimex/start. Last access date: 09.01.12.

Lautenschlager, M., Keuler, K., Wunram, C., Keup-Thiel, E., Schubert, M., Will, A., Rockel, B., Boehm, U., 2009. Climate Simulation with CLM, Scenario A1B run no.1, Data Stream 3: European region MPI-M/MaD. World Data Center for Climate. http://dx.doi.org/10.1594/WDCC/CLM_A1B_1_D3.

Lischke, H., Löffler, T.J., Fischlin, A., 1998. Aggregation of Individual Trees and Patches in Forest Succession Models: Capturing Variability with Height Structured, Random, Spatial Distributions. Theoretical Population Biology 54, 213–226.

Lischke, H., Zimmermann, N.E., Bolliger, J., Rickebusch, S., Löffler, T.J., 2006. TreeMig: A forest-landscape model for simulating spatio-temporal patterns from stand to landscape scale. Ecological Modelling 199, 409–420.

Löffler, T.J., Lischke, H., 2001. Incorporation and influence of variability in an aggregated forest model. Natural Resource Modeling 14, 103–137.

Mitchell, T., Carter, T., Jones, P., Hulme, M., New, M., 2003. A comprehensive set of climate scenarios for Europe and the globe. Tyndall centre Working paper 55.

Nabel, J.E.M.S., Kirchner, J.W., Zurbriggen, N., Kienast, F., Lischke, H., submitted. Extrapolation methods for climate time series revisited – spatial correlations in climatic fluctuations influence simulated tree species abundance and migration.

Nabel, J.E.M.S., Lischke, H., 2013. Upscaling of spatially explicit and linked time and space discrete models studying vegetation dynamics under climate change. In: Environmental Informatics and Industrial Environmental Protection: Concepts, Methods and Tools.

Nabel, J.E.M.S., Zurbriggen, N., Lischke, H., 2012. Impact of species parameter uncertainty in simulations of tree species migration with a spatially linked dynamic model. In: R. Seppelt, A.A. Voinov, S. Lange, D. Bankamp (Eds.) (2012): International Environmental Modelling and Software Society (iEMSs) 2012. International Congress on Environmental Modelling and Software. Managing Resources of a Limited Planet: Pathways and Visions under Uncertainty, Sixth Biennial Meeting, Leipzig, Germany, 909–916.

Nabel, J.E.M.S., Zurbriggen, N., Lischke, H., 2013. Interannual climate variability and population density thresholds can have a substantial impact on simulated tree species' migration. Ecological Modelling 257, 88–100.

Nakicenovic, N., Alcamo, J., Davis, G., de Vries, B., Fenhann, J., Gaffin, S., Gregory, K., Grübler, A., Jung, T.Y., Kram, T., La Rovere, E.L., Michaelis, L., Mori, S., Morita, T., Pepper, W., Pitcher, H., Price, L., Riahi, K., Roehrl, A., Rogner, H.H., Sankovski, A., Schlesinger, M., Shukla, P., Smith, S., Swart, R., van Rooijen, S., Victor, N., Dadi, Z., 2000. IPCC Special Report on Emissions Scenarios. Cambridge University Press.

Pierce, D., 2012. Ncview-1.93g. http://meteora.ucsd.edu/~pierce/ncview_home_page.html. Last access date: 14.07.12.

Rickebusch, S., Lischke, H., Bugmann, H., Guisan, A., Zimmermann, N.E., 2007. Understanding the low-temperature limitations to forest growth through calibration of a forest dynamics model with tree-ring data. Forest Ecology and Management 246, 251–263.

Snell, R.S., Huth, A., Nabel, J.E.M.S., Bocedi, G., Travis, J.M.J., Gravel, D., Bugmann, H., Gutiérrez, A.G., Hickler, T., Higgins, S.I., Scherstjanoi, M., Reineking, B., Zurbriggen, N., Lischke, H., submitted. Using individual based forest models to simulate species range shifts.

Thornton, P.E., Running, S.W., White, M.A., 1997. Generating surfaces of daily meteorological variables over large regions of complex terrain. Journal of Hydrology 190, 214–251.

Appendix A

Using dynamic vegetation models to simulate plant range shifts

Ecography, accepted

R.S. Snell[a], A. Huth[b], J.E.M.S. Nabel[c,d], G. Bocedi[e], J.M.J. Travis[e], D. Gravel[f], H. Bugmann[a], A.G. Gutiérrez[a,g], T. Hickler[h,i,j], S.I. Higgins[k], M. Scherstjanoi[c], B. Reineking[l,m], N. Zurbriggen[c], H. Lischke[c]

[a]*Forest Ecology, Institute of Terrestrial Ecosystems, Department of Environmental Systems Science, ETH Zürich, 8092 Zürich, Switzerland.*
[b]*Department of Ecological Modeling, Helmholtz Centre for Environmental Research (UFZ), 04319 Leipzig, Germany.*
[c]*Dynamic Macroecology, Landscape Dynamics, Swiss Federal Institute for Forest, Snow and Landscape Research WSL, Zürcherstr. 111, 8903 Birmensdorf, Switzerland*
[d]*Department of Environmental Systems Science, Swiss Federal Institute of Technology ETH, Universitätstrasse 16, 8092 Zürich, Switzerland*
[e]*Institute of Biological and Environmental Sciences, University of Aberdeen, Zoology Building, Tillydrone Avenue, Aberdeen. AB242TZ. UK.*
[f]*Département de biologie, chimie et géographie, Université du Québec à Rimouski, 300 Allée des Ursulines, Rimouski, Canada, G5L 3A1*
[g]*Instituto de Conservación Biodiversidad y Territorio, Facultad de Ciencias Forestales y Recursos Naturales, Universidad Austral de Chile, Casilla 567, Valdivia, Chile.*
[h]*Biodiversity and Climate Research Centre (BiK-F), Senckenberganlage 25, 60325 Frankfurt am Main, Germany.*
[i]*Goethe University, Department of Physical Geography, Altenhöferallee 1, 60438 Frankfurt am Main, Germany.*
[j]*Senckenberg Gesellschaft für Naturforschung, Senckenberganlage 25, 60325 Frankfurt am Main, Germany.*
[k]*Botany Department, University of Otago, PO Box 56, Dunedin 9054, New Zealand.*
[l]*Irstea, UR EMGR Ecosystèmes Montagnards, 2 rue de la Papeterie-BP 76, 38402 St-Martin-d'Hères, France*
[m]*Biogeographical Modelling, Bayreuth Center of Ecology and Environmental Research BayCEER, University of Bayreuth, Universitätsstr. 30, 95447 Bayreuth, Germany*

Abstract

Dynamic vegetation models (DVMs) follow a process-based approach to simulate plant population demography, and have been used to address questions about disturbances, plant succession, community composition, and provisioning of ecosystem services under climate change scenarios. Despite their potential, they have seldom been used for studying species range dynamics explicitly. In this perspective paper, we make the case that DVMs should be used to this end and can improve our understanding of the factors that influence species range expansions and contractions. We review the benefits of using process-based, dynamic models, emphasizing how DVMs can be applied specifically to questions about species range dynamics. Subsequently, we provide a critical evaluation of some of the limitations and trade-offs associated with DVMs, and we use those to guide our discussions about future model development. This includes a discussion on which processes are lacking, specifically a mechanistic representation of dispersal, inclusion of the seedling stage, trait variability, and a dynamic representation of reproduction. We also discuss upscaling techniques that offer promising solutions for being able to run these models efficiently over large spatial extents. Our aim is to provide directions for future research efforts and to illustrate the value of the DVM approach.

Introduction

Understanding and predicting the regional and global distribution of plants is fundamental due to their role in ecosystem functioning (Lavorel and Garnier 2002), carbon storage and release (McGuire et al. 2001), and feedbacks to the global climate system (Sitch et al. 2008). There is still an open discussion about how the current distribution of plants will be impacted by climate change. Global vegetation models already consider shifts in global biome distributions; these models are however based on the simplified assumption that plants will be able to track rapid climate change (Sitch et al. 2008). This would require some plant species to move over 1 km $year^{-1}$ (Loarie et al. 2009), which is particularly unlikely for plants with long generation times, low reproductive rates, or limited dispersal abilities.

This is not to say plants will not migrate at all; range shifts have already been recorded for some plant species in response to on-going climate change (e.g. Walther et al. 2005, Jump et al. 2012). However not all plants are shifting their ranges in the way we might have expected: range contractions (Zhu et al. 2012), shifts in the opposite direction (Crimmins et al. 2011), or significant time lags (Bertrand et al. 2011) are just some examples. Range dynamics are transient in space and time, and a variety of factors influence if, when and how species will shift their ranges. Predicting future range shifts requires a better understanding of the processes that influence current distributions, range expansions and contractions.

Species distribution models (SDM) use correlative statistics to relate environmental variables to observed species presence or absence (Guisan and Thuiller 2005). These relationships are then used to project how a species potential habitat niche might shift under different environmental conditions. Although SDMs are the most commonly used tools for evaluating current and future species ranges (Dormann et al. 2012), their limitations and assumptions are also widely acknowledged (e.g. Hampe 2004, Heikkinen et al. 2006, Thuiller et al. 2008). SDMs do not explicitly represent the processes that determine the boundaries of the species distribution such as dispersal, demography and biotic

interactions (e.g. Thuiller et al. 2013). SDMs also assume that species distributions are in equilibrium with the environment, even though range shifts will almost always involve scenarios where species are in disequilibrium with the current climate (Svenning and Sandel 2013). These assumptions cause uncertainty in their ability to predict future range shifts. Therefore, a process-based approach is necessary for understanding the transition phase and how the boundaries of ranges are determined.

Within the SDM field of research, the solution has been to include some processes into existing SDMs (i.e. the hybrid or fitted process-based models), such as dispersal (e.g. Engler et al. 2012) and demography (papers in this issue; Dullinger et al. 2012). In this perspective paper, we would like to promote an alternative way forward; improving and using dynamic, process-based, vegetation models to advance our understanding and ability to simulate how processes and interactions influence plant species ranges and their shifts. We aim to do so by: (1) emphasizing why a process-based approach would be beneficial for simulations of species range shifts, (2) evaluating key processes to include and/or improve so as to better simulate range dynamics, and (3) discussing the limitations and methodological challenges associated with using DVMs. We highlight different upscaling approaches using examples, and address the issues of parameterization and model validation. Although DVMs come with their own restrictions, they provide an alternative to SDMs and thus enrich the toolbox for understanding climate change impacts on vegetation.

Dynamic vegetation models (DVMs)

We define a dynamic vegetation model (DVM) as a model that includes processes based on ecological and physiological knowledge of the factors influencing individual plant demography. In particular, the following three points are constitutive for a DVM. First, DVMs simulate more than one species or plant functional type at the same time. Therefore, a fundamental property of DVMs is their explicit treatment of interspecific competition. Second, DVMs simulate the dynamic changes through time in the occurrence, abundance, and productivity of plant species (or functional types). These changes reflect how individual plant performance is influenced by environmental conditions, biotic interactions (mostly resource competition, but some models also include herbivory), and disturbances. Third, plant population dynamics and demographic rates are not prescribed but are instead emergent properties of these models. DVMs simulate the processes and interactions shaping plant demography; including reproduction, growth, recruitment and mortality.

Using a dynamic model with multiple interacting processes has several advantages for studying plant range shifts. First, species presence or absence at a particular site is a direct consequence of interactions with lower-level processes and higher-level constraints such as the physiological response to the environment, dispersal limitations, biotic interactions, and even historical contingencies if management is taken into account (e.g. Schumacher and Bugmann 2006). Including multiple processes and their interactions is important to capture non-linear and non-additive relationships (Wu and David 2002). Second, a process-based approach is flexible to the development of novel interactions under new environmental conditions. For example, species respond to climate independently of each other (i.e. species migrate, not communities; Huntley 1991) which could lead to non-analog communities with unknown behavior in the future (Williams and Jackson 2007). Third, the dynamic nature of DVMs allows us to address questions about when and how range shifts will occur. DVMs can account for long-term, transient ecological processes like succession (e.g. Hickler et

al. 2012, Bodin et al. 2013), as well as lags caused by dispersal limitation (Normand et al. 2011) and biotic interactions (Svenning et al. 2014). Finally, it is likely that different processes are important at the leading versus trailing edge of a migrating species (Thuiller et al. 2008). For long lived organisms such as trees, consideration of longevity, plasticity and tolerance can be particularly important for understanding local extinction rates at trailing edges, which in turn influence the advancement of other species.

Box 1. Brief summary of the different types of Dynamic Vegetation Models (DVMs) mentioned in the text.

Dynamic Global Vegetation Models (DGVMs) simulate biogeochemical cycles, vegetation distribution, structure and the ecological processes and disturbances that determine the balance between different plant types, such as establishment, competition, growth and mortality (e.g. Cramer et al., 2001). DGVMs include feedbacks between the atmosphere and land surface, and are often coupled with General Circulation Models to simulate the global climate. DGVMs typically do not simulate individual species, but group similar species into plant functional types (PFTs). DGVMs were designed to predict global or continental distributions of biomes, carbon pools and fluxes.

Hybrid DGVMs combine the generalized ecophysiological process representations of DGVMs with the detailed patch-scale population dynamics of forest gap models (e.g. Sato et al. 2007, Scheiter and Higgins 2009). This structure allows these models to simulate vertical structure and competition for light within a grid cell, as well as more realistic representations of mortality, gap formation and succession. Hybrid models are often applied over smaller areas at a finer resolution compared to DGVMs, which means the PFTs can be parameterized to better represent regional vegetation or individual species (e.g. Hickler et al. 2012).

Forest gap models simulate forest dynamics at the stand scale (typically, several hectares) by considering tree population dynamics on multiple patches. They include individual-based calculations of tree growth, competition for light, space and water, regeneration, and mortality as functions of the abiotic environment (climate, soil). The death of a large tree creates a gap in the canopy, which causes increased growth and recruitment in understory trees and results in forest succession (Bugmann 2001). Forest structure is derived by averaging the properties simulated at several patches, usually representing spatial scales >10 ha. Spatially explicit forest gap models include additional spatial interactions and processes such as seed dispersal, spread of disturbances or competition from neighboring grid cells (e.g. FORMIND, Köhler and Huth 2007; review in Bugmann 2001).

Forest landscape models often apply upscaled versions of forest gap models over a grid-based landscape (typically, several 100 to 10'000 ha) by selecting a range of methods and processes to upscale. TreeMig, for example, uses a height structured description of tree populations and includes seed production and dispersal (Lischke et al. 2006). LandClim is an example of a spatially explicit, stochastic landscape model; it simulates processes at the patch scale (i.e. growth and mortality) on annual time steps, whereas landscape-scale processes (i.e. disturbances, harvesting, and seed dispersal) are simulated in decadal time steps (Schumacher and Bugmann 2006).

Despite their potential, only a few studies have used DVMs to study range shifts explicitly. Scheller and Mladenoff (2008) used LANDIS-II to illustrate that the future northward migration of tree species in northern Wisconsin may strongly be limited by interspecific competition and landscape fragmentation. TreeMig simulated species range shifts along transects through Siberia and the Alps under future climate change (Epstein et al. 2007, Nabel et al. 2013) and for parts of Switzerland under Holocene conditions (Lischke et al. 2006). LPJ-GUESS simulated vegetation range shifts for Sweden (Koca et al. 2006) and Europe (Hickler et al. 2012), however these simulations assumed unlimited seed dispersal.

While increasing complexity can be an advantage, it may be an important reason why DVMs are not used as frequently to study range shifts. Complex models are difficult to parameterize and approach the limits of current computational resources. The addition of processes and parameters makes it hard to evaluate error propagation, to understand the different sources of uncertainty, and their relative importance. Including processes also requires a good understanding of the underlying mechanisms, which is not always available. Finally, DVMs were not necessarily designed to study range dynamics explicitly and thus may be limited in their extent or comprehensiveness, or lacking important processes such as seed dispersal, which can have strong consequences for simulating range dynamics. We address some of these limitations below.

We use a sample of DVMs covering all four categories (see Box 1, Table 1) to illustrate the variation in the models available, and point to the gaps and processes that are typically present or missing from DVMs. We refer to Bugmann (2001), Lischke (2001), Scheller and Mladenoff (2007), and Quillet et al. (2010) for a more comprehensive review of DVMs.

Important elements for simulating range dynamics

All DVMs include formulations of the main ecological processes determining plant population dynamics, specifically reproduction, establishment, growth and mortality (Table 2). Each of these processes is influenced by the environment, plant physiology, competition, community structure, and subject to trait variability and selection (Figure 1). The representation of these processes however differs greatly among models. Some of these processes, such as reproduction and establishment, are currently included as very simple formulations. Additionally important processes, such as seed dispersal and trait variability, are only included in a few DVMs (Table 2). We have chosen to focus on these four processes since we believe they could be better represented in DVMs, and would be particularly beneficial for the future application of DVMs to simulate species' range dynamics.

Reproduction

Plant reproductive effort is known to vary as a function of age and size (Thomas 2011) and environmental conditions (e.g. Ladeau and Clark 2006, Bykova et al. 2012). The onset of reproduction, or maturation age, can also be influenced by abiotic factors (Sakai et al. 2003). As variations in plant reproduction affect migration rates (Clark et al. 2001) and species distributions (Bykova et al. 2012), it is important to include these relationships in DVMs.

All DVMs include some representation of reproduction, but the implementation varies strongly between models (Table 2). In general, PFT or species-specific parameters describe seed or propagule production and the onset of reproduction (Tables 1 and 2). For example in TreeMig and FORMIND, the onset and amount of seed production is determined by tree height and species (Lischke et al. 2006, Köhler and Huth 2007). Alternatively, in LPJ-GUESS and aDGVM propagule production is, at least partly, a function of assimilated carbon or net primary productivity. In both cases, larger or more productive plants produce more seeds than smaller plants. As growth is determined by environmental conditions, reproduction is only indirectly influenced by external factors. It would be relatively simple to replace the existing reproduction parameters with functions that more directly relate seed production to plant characteristics such as age, and environmental factors such as temperature and precipitation, provided the required empirical data are available. For example, a dynamic carbon allocation approach has already been adopted in aDGVM (Scheiter and Higgins 2009) for partitioning among roots, stems and leaves depending upon environmental conditions, and could be adapted to include reproduction.

Using dynamic calculations for reproductive rates would allow DVMs to simulate some additional effects of global change on plant range dynamics. When grown under elevated CO_2, trees may reach reproductive maturity at smaller sizes, younger ages and allocate more to reproduction (Ladeau and Clark 2006). If future climate change and increased CO_2 modify life history strategies, we may expect to see faster migration rates (i.e. younger maturation age and higher fecundity) although potentially at the cost of shorter life spans (Sakai et al. 2003, Bugmann and Bigler 2011).

Interannual variability in reproduction may have important consequences for the dynamics of range expansions (Mustin et al. 2013). A direct link between reproduction and climate would also allow DVMs to simulate masting in a more mechanistic way (as opposed to a simple mast frequency based on average occurrence intervals). In nature, the occurrence of a masting event is related to large scale climatic cues, such as high summer temperatures during ENSO events (Koenig and Knops 2005). Increasing temperature is expected to result in more frequent mast events (Schauber et al. 2002) whereas decreasing precipitation will likely reduce mast frequency (Perez-Ramos et al. 2010). If reproductive effort was directly linked to plant performance under varying climate, DVMs could be used to investigate hypotheses about the influence of climate change on mast frequency and resulting effects on species range shifts.

Dispersal

The dispersal characteristics of a plant species are a key determinant of how likely it is to track climate change (Bullock et al. 2012) and any predictive model of transient range dynamics at large scales should include this process. DVMs have typically assumed that the colonization of new sites is not limited by dispersal; seeds of all species (or functional types) arrive every year in every simulated grid cell if the environmental conditions allow establishment. This assumption is justifiable when projecting potential equilibrium vegetation under alternative climate scenarios, or when simulating successional dynamics at a local scale where dispersal limitation is unlikely. The few DVMs that explicitly include seed dispersal use a fixed species/PFT-specific dispersal kernel (Table 2). However, the distribution of the distances travelled by seeds can be sensitive to wind conditions (e.g. Stephenson et al. 2007) or to the behavior and composition of animal dispersal agents (e.g. Morales et al. 2013). Importantly, this variability can have a non-linear effect on population spread rates (Bullock

et al. 2012). There is an urgent need to integrate emerging approaches for modeling both wind and animal dispersal of seeds into DVMs to better simulate transient range dynamics.

Mechanistic models are now available for simulating wind dispersal (Kuparinen 2006, Nathan et al. 2011). For local scale simulations, fine scale resolution models that explicitly simulate air flow and turbulence (e.g. Thompson and Katul 2013) might be useful for capturing seed dispersal and range dynamics along altitudinal gradients. For larger spatial extents, models such as WALD (Katul et al. 2005) could provide new possibilities. WALD requires minimal parameters that are relatively straightforward to collect (e.g. seed release height and seed terminal velocity), is computationally efficient and retains links to key mechanisms involved in seed transport by wind. WALD has also been shown to perform well in capturing rare, long-distance dispersal events (Katul et al. 2005) that are most important for range shifts (Clark et al. 2001).

Significant progress has recently been made in modelling seed dispersal by animals (Nathan et al. 2008, Bullock et al. 2011). At a relatively small spatial extent, the realized dispersal kernel could emerge from the DVM based on simulated interactions between seed properties, animal characteristics (e.g. gut retention time, fur adhesion time), distribution and the spatial structure of the environment. The explicit consideration of animal seed dispersal could significantly alter migration rates if there is a spatial mismatch between the plant and the disperser. The coupling with DVMs could be achieved using a hierarchical approach, where dispersal kernels would be generated using a mechanistic model for the specific landscape characteristics of the local grid cell.

One important consideration will be the thematic resolution of plants (i.e. species or PFTs) and knowledge about their seed dispersal vectors. Simulating the range dynamics at a species level would require a model to describe the specific vector that is known to be the most important dispersal agent for each species, as well as simultaneously requiring a distribution model for the specific dispersing agents. However, for DVMs that use a PFT resolution, it may be more appropriate to use 'seed dispersal types' (Vittoz and Engler 2007), where each dispersal type uses a more generic dispersal pattern (e.g. movement rules or landscape-dependent kernel).

It will be relatively straightforward, albeit computationally expensive, to incorporate such mechanistic dispersal modules. The advantage is that DVMs will readily incorporate the effect of climate (Bullock et al. 2012, Travis et al. 2013) and landscape contingencies (e.g. Carlo et al. 2013) on seed dispersal, rather than simply assuming a fixed distribution kernel.

Establishment

Plant establishment in new areas is a crucial step for range expansion (Germino et al. 2002, Körner 2012). Seedlings are small (commonly < 15 cm high), and thus respond to environmental variability at a much smaller scale, exhibit different environmental sensitivities and react faster to environmental stress than older trees (Barbeito et al. 2012). Factors specifically important for seedling success are microclimate and microtopography (Scherrer and Körner 2010), facilitation and competition by ground vegetation (Germino et al. 2002, Venn et al. 2009), herbivory (Myster 2009), and nutrients (Zurbriggen et al. 2013). Due to the large number of seedlings and the large degree of stochasticity in this stage, DVMs usually simulate establishment as the transition of a young tree above a threshold size, such as minimum tree diameter in FORMIND (e.g. stem diameter of 10 cm; Köhler and Huth 2007) or minimum tree height in TreeMig (e.g. height above 1.37 m; Lischke et al. 2006). This implies that the seedling stage is not explicitly included, and most DVMs would require an additional size or

age class to distinguish seedlings from older trees (see Wehrli et al. 2007, Zurbriggen et al. 2013). As seedlings may have different environmental constraints, the transition from the seedling to later stages should be represented more explicitly in DVMs.

For example, a refined submodel for regeneration that included herbivory and shading was found to improve simulated species composition and successional dynamics in a forest gap model (Wehrli et al. 2007). Thus, submodels that focus on the establishment phase and simulate seedlings as individuals (e.g. Peringer and Rosenthal 2011) could be used as part of a stochastic, multi-scale approach. Seedlings would be simulated at a fine scale and adult trees at coarser spatial and temporal resolutions. Alternatively, it may be more efficient to use these complex individual-based models to upscale the processes and their influencing factors (see upscaling section below). Although the establishment phase is a crucial step in range shifts, the large variability in this stage can make it difficult to establish clear relationships between environmental factors and establishment success (e.g. Meiners et al. 2000). More experimental studies and novel parameterization techniques will improve our ability to model plant establishment.

Trait variability

Individual plants can show large variability in traits, both within and between populations. Theoretical evidence suggests that ignoring intra-specific variability may cause substantial errors in projections of species range dynamics (e.g. Atkins and Travis 2010, Bocedi et al. 2013). Local adaptation, phenotypic plasticity and blocking effects by maladapted individuals (Borges 2009) could influence the rate of species range expansions, contractions and local extinctions. Traditionally, DVMs have not explicitly treated variability, plasticity or heritability of traits: species (or PFTs) have one set of parameters that is applied to every individual. However, some traits in these models vary in response to climatic conditions, such as the leaf to fine root ratio, leaf nitrogen content and leaf area to sapwood cross-sectional area ratio (Sitch et al. 2003, Hickler et al. 2006), and the aDGVM2 model even allows each individual to have a potentially unique set of traits (Scheiter et al. 2013). Due to the likely importance of trait variability for range dynamics, we propose several approaches that could be used to incorporate intra-specific (or intra-PFT) variability in DVMs.

The first approach is the simplest, and would require minimal or no modifications of the existing DVMs. Each species (or PFT) would be composed of a finite set of environment types, each of which is locally adapted to different environmental conditions. For example, rather than simulating broadleaf evergreen trees as a single PFT where each individual or cohort has the exact same parameters, broadleaf evergreen trees would be simulated as ten PFTs. Each simulated individual would be assigned randomly to one of these ten types that, for example, would range from cool- to warm-adapted, with temperature-adapted base respiration rates (e.g. Lavigne and Ryan 1997). Heritability could be coarsely captured by having the offspring retain the identical environmental type as their parent. This assumption could be relaxed to accommodate a situation where heritability is less than 100% by allowing an individual's phenotype to deviate to one of the neighbouring environmental types with a given probability.

A second method would take a quantitative genetics approach. This method assumes that many alleles contribute to variability in local adaptation, but does not explicitly simulate alleles or loci. Each individual or cohort would hold a single quantitative trait value determining the conditions to which it is optimally adapted. Continuous variability in local adaptation to one or more environmental

conditions would be allowed, such as a temperature optima and drought tolerance. In the simplest case, offspring would have the same 'environmental condition values' as their parent with some degree of randomness (e.g. values would be drawn from a normal distribution with a mean equal to that of its parent).

A third approach takes advantage of the individual-based structure of some DVMs and allows each individual to adopt a potentially unique combination of trait values. For example, plants in aDGVM2 are defined by traits that specify the influence of the environment on rates of plant growth, respiration, carbon assimilation and allocation (Scheiter et al. 2013). Individuals with a poor combination of traits die, and those with a better combination survive and reproduce. Tradeoffs between traits prevent the emergence of an individual adapted to all conditions. Inheritance of traits is managed by a genetic optimization algorithm which allows mutation and recombination to define the combination of traits in seeds, while at the same time restricting gene flow to within suites of individuals. The assemblages of plant communities that emerge are adapted to a site's biotic and abiotic conditions (Scheiter et al. 2013).

A fourth method – the most complex, although potentially the most biologically realistic – takes an allelic modeling approach (e.g. Schiffers et al. 2013). In this case, a finite number of loci contribute to the degree of local adaptation to particular conditions. A sophisticated genetic architecture (e.g. linkage, epistasis, pleiotropy) underpinning the traits can be incorporated. This fourth option would allow DVMs to generate reliable estimates for the rate of local adaptation. Unfortunately, the information needed to parameterize models to include this degree of ecological genetic realism is not yet available.

In general, parameterizing models that incorporate local adaptation will be a major challenge. However, we anticipate that considerable progress could be made over the next decade using the first three methods. For example, for the first two methods, data from reciprocal transplant or warming experiments can provide the information needed to define population dependent plasticity of physiological traits (e.g. Gunderson et al. 2000, Ishizuka and Goto 2012), while species distribution maps or experiments can indicate the range of climatic tolerances for each species. There is also potential for inverse modeling approaches (e.g. Hartig et al. 2012) to infer the characteristics of local adaptation. One further challenge when incorporating local adaptation will be in determining the starting conditions for our scenarios. Thus careful thought will be required about the assumptions we make regarding initialization (e.g. in determining the nature of a spin-up).

Important processes that require more information

Above we discussed four processes that we believe need to be improved in DVMs to better simulate species' range dynamics. However, other limiting processes and factors may be of high importance for simulating changes in species' ranges. Tree mortality, for example, is a key process particularly for populations at the trailing edge of species distributions (Jump et al. 2009). Although progress has been made over the past 15 years in the statistical modeling of tree mortality (e.g. Wyckoff and Clark 2002, Bigler and Bugmann 2004, Wunder et al. 2008), the existing models do not lend themselves for integration into DVMs because their structure and parameter values appear to vary in both time and space (Macalady and Bugmann 2014). In addition, the mechanisms underlying global change-induced tree mortality remain hotly debated (cf. McDowell et al. 2013). Thus, more empirical and theoretical work needs to be done before mortality processes can be represented in DVMs in a meaningful way.

Another example is how rising atmospheric CO_2 levels could affect competition among plants by promoting changes in growth (Dawes et al. 2011) or water-use efficiency in trailing edges (Peñuelas et al. 2008), with strong consequences for range dynamics. In fields such as this, more synthesis work is required that must be based on a solid theoretical basis (e.g. Bugmann and Bigler 2011), as additional short-term experiments are unlikely to provide conclusive answers.

Further examples include global warming impacts on seed development, germination and establishment (e.g. Milbau et al. 2009), understanding frost tolerance of different plant tissues (e.g. Charrier et al. 2013), how changes in growing season length, growing degree-days and chilling temperature will affect plant phenology (e.g. Zhao et al. 2013), and the importance of soil processes (e.g. Lenka and Lal 2012). Overall, models are a reflection of what we know, and they never will be better than the underlying data and our knowledge about ecological processes. Developing a solid theoretical understanding of the processes briefly reviewed above will allow us to incorporate them into DVMs and improve our ability to predict species range dynamics.

Methodological challenges and how to cope with them

While it is possible to improve existing processes and add more, this can lead to increasingly complex models that are difficult to parameterize. Furthermore, a common requirement for simulating species range shifts is to increase simulated spatial extents, which also increases the computational requirements. As the computational demand can be reduced only partly with technical methods (e.g. parallelization, optimizing the code), we need to consider scaling solutions (Lischke et al. 2007). These are more than a methodological technique, however. They also help to understand how local scale processes effectively influence larger scale community organization.

For our purposes, *scaling* refers to all methods that change the spatial, temporal or thematic resolution of a model (thematic resolution refers to the description of state variables). *Upscaling* refers to the derivation of models that operate at coarser resolution (Figure 2), often with simplified model formulations while retaining the essential information and dynamics of the original model. Upscaling approaches are complicated by the nonlinearity of processes, interactions, feedbacks and heterogeneity, and range from pure or approximated analytical derivations of aggregated model formulae to heuristic assumptions, or the creation of an entirely new model (reviewed in Lischke et al. 2007). In most situations, analytical derivations are not feasible for vegetation models due to the complexity of resource competition. Therefore upscaling is often conducted heuristically, with subsequent tests of the upscaled model against simulations using the original model (Acevedo et al. 1995).

Sophisticated upscaling approaches have the potential for extending the applicability of DVMs but have only started to be applied in this field. Below we discuss some approaches to DVM upscaling, within the scope of improving predictions of range dynamics. Broadly, we divide the approaches into those that decrease spatial resolution versus those that maintain spatial resolution but change thematic or temporal resolution. We end the section by discussing ways to improve model parameterization and evaluate simulation results.

Approach 1: Decreasing spatial resolution

There is a strong trade-off between the spatial resolution of DVMs and the spatial extent of the study region (Table 1). DVMs that use a fine grid cell resolution typically operate over a smaller spatial extent (e.g. resolution of 20 m, spatial extent of 500 km^2), whereas those that simulate larger areas also have coarser grid cell resolution (e.g. 50 km, spatial extent global). However increasing grid cell resolution is a non-trivial task. DVMs that use coarser resolutions typically simulate a small patch of land (< 1 ha) every 50 km, and assume this small area is representative of the entire grid cell. One of the most important issues is how to handle the loss of information in larger cells, namely within cell heterogeneity of processes and variables, and the impact of their spatial location within the cell on spreading rates.

Within-cell heterogeneity

As cells become coarser, we lose information about fine scale landscape heterogeneity. Naive upscaling of the landscape, such as applying the same model to drivers averaged over coarser cells, can lead to strong systematic biases and impact simulated migration rates by reducing overall dispersal mortality (arrival in unsuitable habitat) and inflating spread rates (Bocedi et al. 2012). If the frequency distribution of a driver (e.g. temperature) within a grid cell is known, the entire model can be run for discrete classes of the driver and then averaged with the frequency distributions (Löffler and Lischke 2001). When there is heterogeneity of the state variables of the model, such as heterogeneity created by population shifts, more sophisticated upscaling methods may be required (e.g. scale transition theory; Melbourne and Chesson 2006).

Within-cell spread

When grid cell resolution is large (> 10 km), as is the case for most DGVMs (Cramer et al. 2001), the fact that the location of individuals within a grid cell is unknown may become problematic. If we assume them to be located in the centre of the cell, seeds are unlikely to disperse outside the grid cell. If we assume them to be homogeneously spread over the cell (e.g. as in TreeMig and LPJ-GUESS), new individuals that arrive would immediately travel the distance across the entire grid cell. Such discretization errors have made it almost impossible, thus far, to represent seed dispersal in coarse-scale model applications in a mechanistic way. Two approaches have recently been applied in DVMs to represent within cell spread:

Using within-cell patch architecture – Each grid cell in LPJ-GUESS contains a number of replicated patches (the size of a patch is usually 1000 m2, Figure 3a), and each patch contains multiple cohorts for each PFT. This within-cell patch architecture was used to simulate dispersal through a grid cell (Snell 2014). New PFTs arrive in a grid cell (cell to cell movement was determined by seed dispersal kernels), and establish in just one patch. Since patches do not have defined locations within the cell, a random spatial distribution of patches was assumed (Figure 3a) and the plant was considered to have crossed the cell when a certain proportion of patches had been occupied. The rate of this within-cell filling is a classic issue for epidemiology when describing the spread of disease in a population (Berger 1981), and is often solved using a logistic growth function. Following this approach, LPJ-DISP uses a logistic curve to calculate the number of patches who had the potential to receive seeds from a neighbouring patch given a certain percentage of patch occupancy in the grid cell (Figure 3b). Establishment success within each patch was still dependent on seed production, available space and

competition for light. Using this approach, LPJ-DISP was able to realistically simulate plant migration across a test landscape (Figure 3c; Snell 2014).

Using a meta-modelling approach – DVMs with fine resolution in time and space can be used to simulate plant migration over a small spatial extent using a wide range of initial conditions. Simulation results on the time to cross the grid cell can then be synthesized using statistical functions of migration rates given those initial conditions and local environment. TreeMig has already been used for this purpose; simulated migration rates were related to number of species, drought stress and degree day (Meier et al. 2012) and then used in a species distribution model. Note that a statistical model obtained this way would be restricted by the range of input variables, so caution should be taken when attempting extrapolation to new situations. Although this method requires a considerable amount of computing effort to generate the data, it is a promising upscaling approach.

Approach 2: Simplify state variables and reduce temporal resolution

Maintaining a fine spatial resolution implies that some processes or state variables need to be simplified so as to reduce computational expenses and allow for an increase of the simulated spatial extent. We suggest three potential avenues for doing so.

"One for many" approach

In DVMs, it is common to stratify state variables into more or less homogenous groups, and to simulate only representative units. This strategy is already employed in forest gap models with the cohort approach, where growth is calculated for one individual of the cohort and all individuals in the same cohort are identical (Bugmann 2001). Using PFTs instead of species is another common method used to simplify thematic resolution (e.g. Köhler et al. 2000, Sato et al. 2007). The same idea can be applied to landscapes by simulating only representative cells. Grid cells with similar environmental drivers and species compositions often entail repetitive calculations in grid-based DVMs. To reduce this redundancy, a dynamic two-layer classification (D2C) concept was proposed (Nabel and Lischke 2013). With the D2C concept, the majority of modelled processes are simulated in specific representative cells that constitute a new coarser layer. Only those processes that can lead to cell-specific changes, such as seed dispersal and establishment, are simulated on the original grid. The main challenges of this concept are the organizational overhead required for the assignment and tracking of representative cells. The main benefit is the conservation of detailed small-scale dynamics for simulations with a larger extent.

Simplifying vegetation heterogeneity and stochasticity

Many vegetation models rely on stochastic descriptions of demographic processes and disturbances to create spatial and temporal variability in ecosystems. However, stochastic processes require many replicates to estimate the mean and variance, and ensure adequate scaling properties (Melbourne and Chesson 2006). Several approaches have been developed to avoid these replicates while retaining information about their variability.

Aggregation of vegetation heterogeneity by using distributions – In forest gap models, vertical forest structure is described by cohorts of different heights and stand heterogeneity is maintained by simulating multiple patches at different development stages. Patch-to-patch variability of these properties is essential for shade-intolerant species to persist (Gravel et al. 2010). In TreeMig, the

vertical structure was simplified by using height-structured population dynamics. The variability between patches within a grid cell was also simplified, by assuming that all trees within each height class are randomly distributed over the stand. This results in dynamically changing probability distributions of light conditions within the stand, which in turn influence the process rates, and the dynamics (Lischke et al. 1998). This aggregation of individuals strongly reduced the simulation time to just 5% of the original time, which opened the way for a spatially explicit implementation. Such upscaling methods may however introduce errors, such as unrealistically fast height growth and accelerated spread.

Upscaling stochastic disturbances – Forest gap models are strongly driven by stochastic stand-replacing disturbances, which require many replicates and increases simulation time. To reduce the simulation effort for disturbances, the GAPPARD upscaling method was developed (Scherstjanoi et al. 2013). GAPPARD uses the output of a single patch simulation with no disturbances from bare ground to determine the succession of patch states after a disturbance. Then, together with the probability distribution of the times since disturbance (on the basis of the disturbance frequency), the expectation value of the disturbed forest's state is calculated at each point in time. To account for temporal changes in model forcing (e.g., as a result of climate change), GAPPARD performs a series of non-disturbed simulations under different environmental conditions and interpolates between the results. Applying GAPPARD to LPJ-GUESS allowed the model to simulate future climate change impacts at a 1 km resolution for all of Switzerland forests (Scherstjanoi 2013), in 10% of the time compared to LPJ-GUESS with 100 replicate patches yielding similar results. In its current form, GAPPARD is not suitable for simulating dispersal but it could be used for detecting regions of interest in a computationally efficient way before detailed range shift simulations.

Aggregation of temporal resolution

Increasing the length of the (discrete) time step can help speed up models. The effect of temporally variable drivers can be aggregated by long-term expected values for process rates based on the distribution of the variables (Lischke et al. 1997). However, when the timing of the drivers interacts with the model states, such as phenology, a multi-scale approach is preferable. Multi-scale temporal simulations calculate different processes at different time scales, and are already used in most DVMs (Table 1). For example, LPJ-GUESS and FORMIND calculate photosynthesis and water balance on a daily time step, but calculate growth and reproduction on an annual time scale. For simulating range dynamics, each of the processes reviewed above (i.e. reproduction, dispersal, establishment, and trait variability) could be a candidate for temporal upscaling, but more research would be needed. For example, the expensive simulation of wind dispersal (hourly or daily time steps) could be replaced by an upscaled description of migration (annual time steps). A detailed upscaling study would be needed to test if the dynamics at the fine temporal resolution could be adequately captured within a longer time step. It is also important to note that the relevance of temporal aggregation increases with the length of the study period. Paleo-applications, which simulate vegetation shifts after the last glacial maximum (e.g. Henne et al. 2011) are particularly good candidates for temporal upscaling, as time scales are long and uncertainty about the interannual variability in climatic reconstructions large (Simonis et al. 2012).

The link to reality: Parameterization and validation

DVMs are built from knowledge of the underlying ecological and physiological processes. However, the models are only as good as the data used to feed them. Data are required for model parameterization, external data sets describing environmental conditions, and independent observational data on vegetation to evaluate the simulation results.

The traditional way to parameterize DVMs uses results from field measurements and from the literature to evaluate parameter values for a species or vegetation type. However, parameters based on a specific site or for particular regions can lead to weak model performance if applied outside the area for which they were initially intended (Badeck et al. 2001) because factors not explicitly covered by the model may be masked by parameter values. In addition, within-species plasticity or differences between populations can be similar to or larger than differences between species (e.g. Lavigne and Ryan 1997). Such variations need to be accounted for as they could impact simulated migration rates (Nabel et al. 2012).

If we want to use DVMs to simulate species range dynamics, new approaches should be incorporated in parameter calibration to better reflect parameter values across the whole species range. Bayesian methods for model fitting (Purves et al. 2008, Hartig et al. 2012) provide a framework to estimate parameter values or probability distributions of parameter values. They allow the inclusion of field data of different types in the estimation process (van Oijen et al. 2005, Hartig et al. 2012) which increases the quantity of data that can be used for such purposes. In addition to Bayesian methods, further approaches of inverse modelling are available to identify parameter values for which no information or not enough direct information is available. For example, demographic rate parameters in forest gap models can be tuned so that the simulated mature forest corresponds in its biomass, tree density and species composition to real forests (Groeneveld et al. 2009).

Model parameterization will also benefit from the establishment and expansion of large vegetation databases. One example is the TRY database that includes information on life history and physiological attributes of plants (Kattge et al. 2011). Forest inventories are also becoming more available on internet platforms (e.g. USDA forest inventory, French NFF, Smithsonian Institute, Swiss NFI) offering new possibilities to estimate important plant attributes (e.g. Purves et al. 2008) and testing model predictions (e.g. Hurtt et al. 2010). These databases can also be used to re-evaluate the parameters currently being used in DVMs.

A different approach to parameterization is that adopted by aDGVM2 (Scheiter et al. 2013). Here the model focuses on parameterizing general biophysical processes, such as how transpiration rate is influenced by leaf size and each plant has a trait that evolves within the model that defines its leaf size. Ultimately this approach reduces the dimensionality of the parameterization process, since the parameterization process does not define the traits of individuals, but defines the biophysical laws that influence the performance of these trait-states.

Evaluating simulation results is an on-going challenge for modellers, but necessary to determine how well the processes and species have been represented. The first step of a model evaluation is to compare observed vegetation distribution to simulated distribution using modern climate. A combination of plot-based forest inventories, species distribution maps, potential natural vegetation maps, and remotely sensed data could be used to do so. Human impacts on the landscape and disequilibria between climate and distributions (Normand et al. 2011) present a special challenge.

Table 1. Additional details about the models used as examples in the text. An 'x' means the processes is included (in parentheses, if only in a rather limited way), and a blank means the process is not included. Cell sizes and spatial extent refer to applications so far, which are mostly flexible and depend on the availability of environmental input data. Subscripts: [1]Sitch et al. (2003), [2]Scheiter and Higgins (2009), [3]Snell (2014), [4]Scherstjanoi et al. (2013), [5]Lischke et al. (2006), [6]Schumacher and Bugmann (2006), [7]Köhler and Huth (1998)

	Dynamic Vegetation Model							
	DGVM	**Hybrid DGVM**				**Forest landscape model**		**Forest gap model**
	LPJ-DGVM[1]	aDGVM2[2]	LPJ-GUESS[1]	LPJ-DISP[3]	LPJ-Gappard[4]	TreeMig[5]	LandClim[6]	FORMIND[7]
Reproduction	x	x	x	x	x	x	x	x
Dispersal				x		x	x	x
Establishment	x	x	x	x	x	x	x	x
Reaching maturation (determined by)		age		age		tree height	age	stem diameter
Trait variability	(x)	x	(x)					
Grid cell resolution	~55 – 300 km	1ha stand on a 37 km grid	30 m – 200 km	18 km	1 km	25m – 1km	25 m	20 m
Extent	Global	Africa	Forest stand to Global	Eastern North America 32,400 km^2	Switzerland 70,000km^2	Switzerland 70,000km^2	500 km^2	500 km^2
Temporal scale	day to year	day to year	day to year	day to year	day to year	year	year to decade	day to year
Number of species or PFTs	9 PFTs	4 PFTs but variability within those types	16 species and PFTs	10 species and PFTs	15 species	30 species	30 alpine species, 4 New Zealand species	up to 400 species (grouped in 5-15 PFTs)

Table 2. General descriptions of how each process is typically represented in different model types (see Box 1). For every model type, there will be exceptions however the aim of this table is to identify the common trends.

		Dynamic Vegetation Model Type		
Processes	**DGVM**	**Hybrid DGVM**	**Forest landscape model**	**Forest gap model**
Reproduction	Percentage of carbon allocated to seeds.		Parameter based on size and/or species.	Parameter based on size and/or species.
Dispersal	Perfect dispersal. +	Perfect dispersal for most, otherwise a fixed species (or PFT) dispersal kernel.	Fixed species (or PFT) dispersal kernel.	Fixed species (or PFT) dispersal kernel. *
Establishment	Climatically suitable PFTs establish uniformly as small trees.	Climatically suitable PFTs establish as small trees, abundance depending on environmental conditions at forest floor and (in some cases) in proportion to adult density.	*Landclim* - Parameter based on species and landcover type, influenced by climate, soil, and light. *TreeMig* - Filters for germination and seedling survival, young tree growth and survival with species specific parameters.	Species specific parameters for actual evapotranspiration, light and degree-day sum determine the species which could establish. Establishment is then a stochastic process from that pool, limited by a maximum number of small trees per area.
Individual tree growth	Plant physiology approach: Carbon uptake based on photosynthesis, respiration, and allometric scaling (dynamic partitioning for aDGVM).		Species specific growth rate, influenced by light, growing degree days and drought.	Species specific growth rate, influenced by light, growing degree days and drought. Some gap models take a plant physiology approach and simulate growth as an emergent outcome (e.g. FORMIND, similar to DGVMs).
Competition	Competition for light, water, nutrients and space **			
Disturbances	Fire	Small gaps created by single tree death and large gaps by stand-replacing disturbances		
		Fire, herbivory	Fire, wind, herbivory, management	Fire, wind*, landslides*, management

+ Perfect dispersal is the assumption that seeds can arrive at any suitable location regardless of absolute distance or barriers.
*Only in spatially explicit forest gap models. ** For every DVM type, there are some models which include nutrient competition and some which do not.

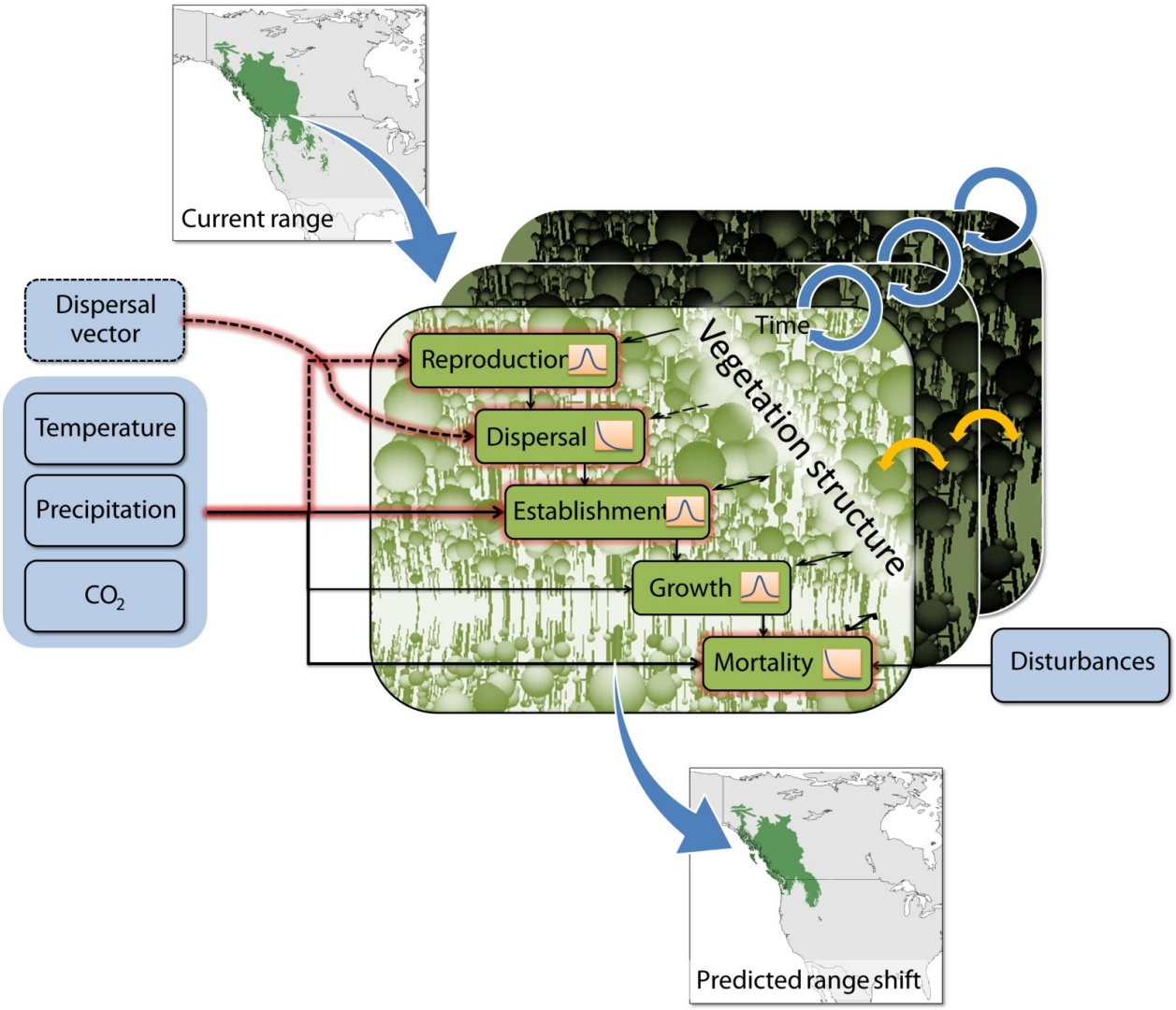

Figure 1. The interaction between processes in dynamic vegetation models (DVMs) and how they could be used for studying species range shifts. Each grid cell within the species range (represented by the large box) interacts with the neighbouring cells (yellow arrows). For each grid cell, a variety of processes are simulated (represented by the small green boxes). Blue boxes represent input, and the transfer of information is shown with arrows. Solid lines show the processes/links which are typically included in the DVMs, and dotted lines indicate the processes/links which should be added. Highlighted in red, are the processes which are discussed in more detail in the text. The frequency distributions inside each box indicate trait variability. The image of forest structure is from FORMIND (Köhler and Huth 1998), the upper map uses distribution data from Little (1971) and was generated in R (http://CRAN.R-project.org/package=maps).

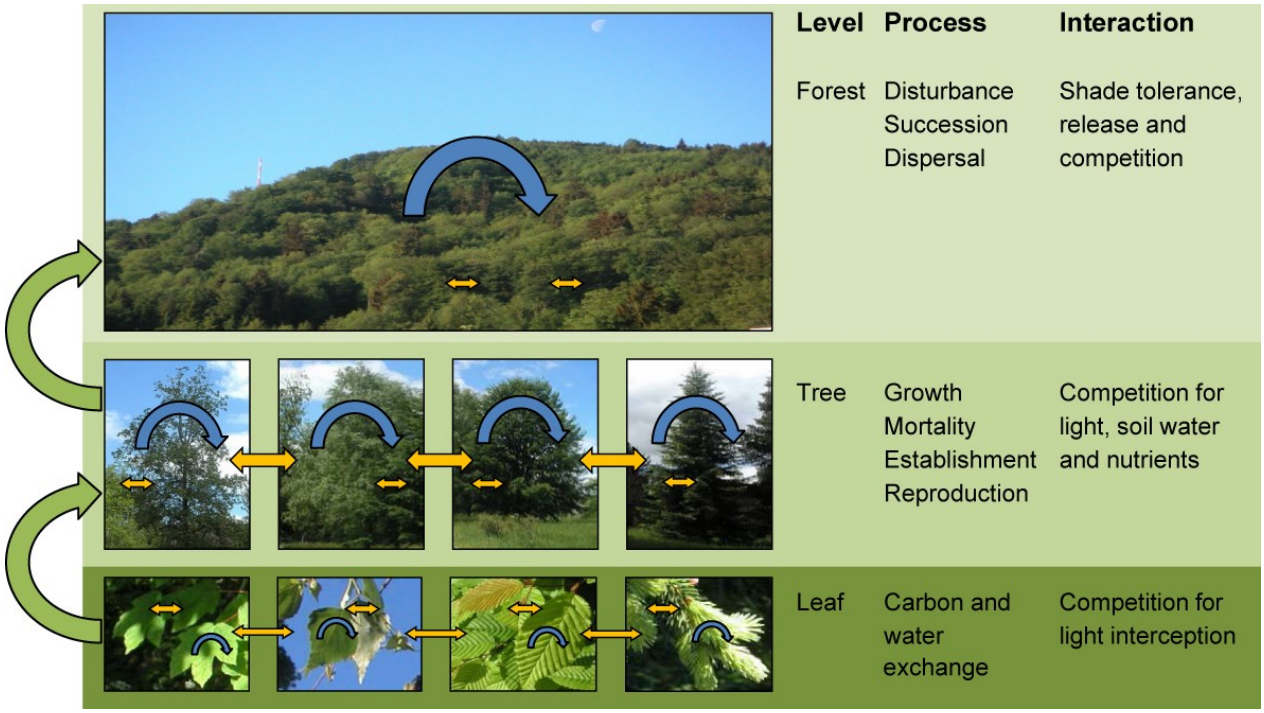

Figure 2. Principle of model upscaling. The rows illustrate the different thematic and spatial scales in a forest. Entities (e.g. leaves or trees) differ among each other and in their spatial position, creating heterogeneity. Blue arrows indicate the dynamics within a level, i.e. temporal changes influenced by the same and other entities. These relationships can lead to feedbacks and are often nonlinear. Yellow arrows show interactions between entities. Higher levels can feed back ("constrain") to lower levels. Green arrows indicate the model upscaling. Upscaling means to derive formulations for the upper level variables, processes and interactions given the lower scale interactions, processes and variables. For example, the formulation of the upper level variables can be the average or sum of the lower level state variables. Photos are courtesy of H. Lischke.

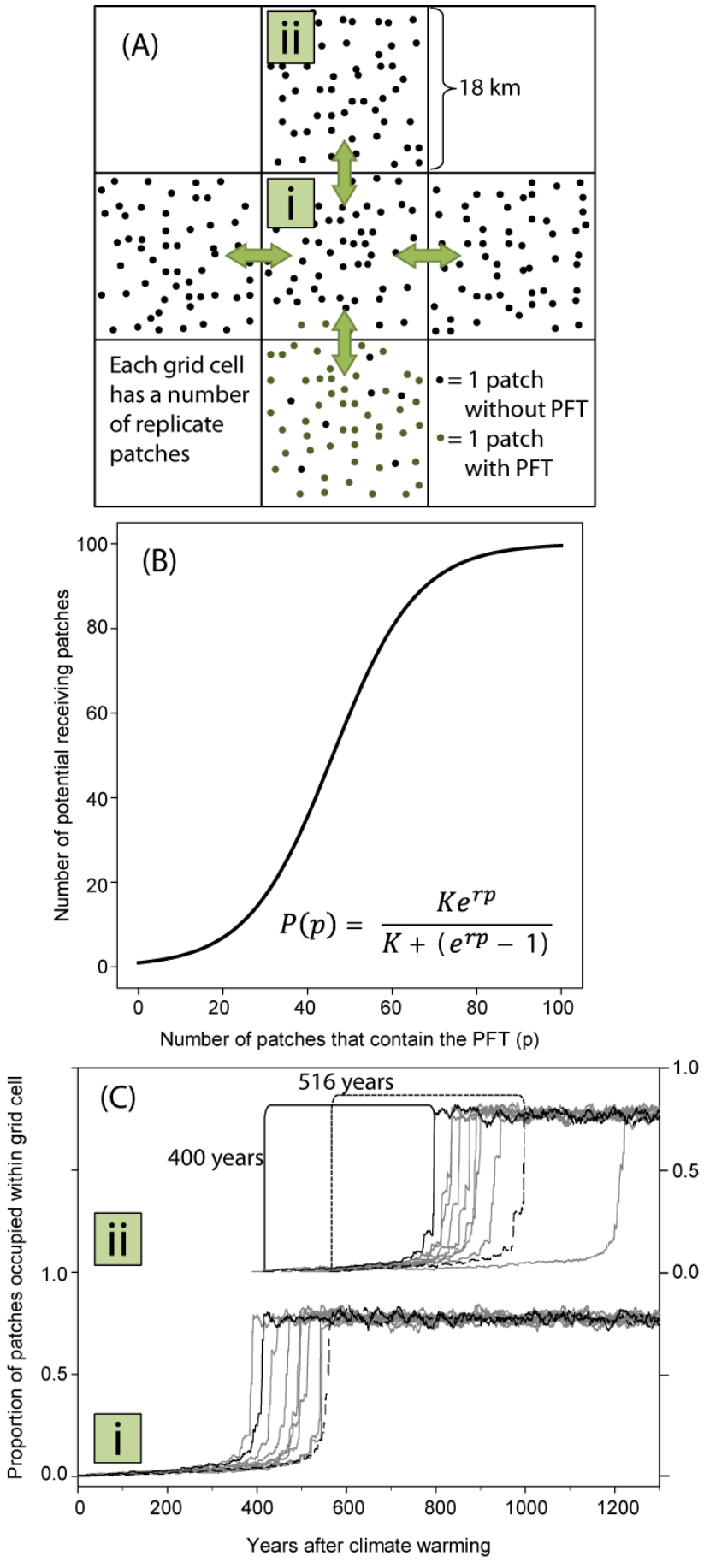

Figure 3. Simulating dispersal within large grid cells in LPJ-DISP (Snell 2014). (A) A sample 3 x 3 'landscape' of grid cells, each grid cell has a number of replicate patches within. (B) Within cell spread rate (or filling) is determined by logistic curve. It is used to calculate the probability of dispersal between patches, where P is the population of available patches for receiving seeds (i.e. have at least one neighbouring patch that contains the PFT) when there are p patches that contain reproducing adults for that PFT. The carrying capacity, K, is the total number of patches in one grid cell, and r is the spread rate. (C) A sample of 10 simulations, the same 2 grid cells are shown (these would be located in position **i** and **ii** in (A)). Each line represents one simulation, the black lines show two of the 10 simulations. In the solid black scenario, it takes 400 years to cross the one cell (migration rate 45 m/year). In the dashed black scenario, it takes 516 years to cross the same cell (migration rate 35 m/year). The average migration rate is 41 m/year. The difference between the simulations is caused by stochastic processes and disturbances.

References

Acevedo, M. F. et al. 1995. Transition and gap models of forest dynamics. - Ecol. Appl. 5: 1040-1055.

Atkins, K. E. and Travis, J. M. J. 2010. Local adaptation and the evolution of species' ranges under climate change. - J. Theor. Biol. 266: 449-457.

Badeck, F. W. et al. 2001. Tree species composition in European pristine forests: Comparison of stand data to model predictions. - Climatic Change 51: 307-347.

Barbeito, I. et al. 2012. Factors driving mortality and growth at treeline: a 30-year experiment of 92 000 conifers. - Ecology 93: 389-401.

Berger, R. D. 1981. Comparison of the Gompertz and logistic equations to describe plant-disease progress. - Phytopathology 71: 716-719.

Bertrand, R. et al. 2011. Changes in plant community composition lag behind climate warming in lowland forests. - Nature 479: 517-520.

Bigler, C. and Bugmann, H. 2004. Predicting the time of tree death using dendrochronological data. - Ecol. Appl. 14: 902-914.

Bocedi, G. et al. 2012. Projecting species' range expansion dynamics: sources of systematic biases when scaling up patterns and processes. - Methods Ecol. Evol. 3: 1008-1018.

Bocedi, G. et al. 2013. Effects of local adaptation and inter-specific interactions on species' responses to climate change. - Annals New York Academy Science in press.

Bodin, J. et al. 2013. Shifts of forest species along an elevational gradient in Southeast France: climate change or stand maturation? - J. Veg. Sci. 24: 269-283.

Borges, R. M. 2009. Phenotypic plasticity and longevity in plants and animals: cause and effect? - J. Biosci. 34: 605-611.

Bugmann, H. 2001. A review of forest gap models. - Clim. Change 51: 259-305.

Bugmann, H. and Bigler, C. 2011. Will the CO2 fertilization effect in forests be offset by reduced tree longevity? - Oecologia 165: 533-544.

Bullock, J. M. et al. 2011. Process-based functions for seed retention on animals: a test of improved descriptions of dispersal using multiple data sets. - Oikos 120: 1201-1208.

Bullock, J. M. et al. 2012. Modelling spread of British wind-dispersed plants under future wind speeds in a changing climate. - J. Ecol. 100: 104-115.

Bykova, O. et al. 2012. Temperature dependence of the reproduction niche and its relevance for plant species distributions. - J. Biogeogr. 39: 2191-2200.

Carlo, T. A. et al. 2013. Where do seeds go when they go far? Distance and directionality of avian seed dispersal in heterogeneous landscapes. - Ecology 94: 301-307.

Charrier, G. et al. 2013. Evaluation of the impact of frost resistances on potential altitudinal limit of trees. - Tree Physiol. 33: 891-902.

Clark, J. S. et al. 2001. Invasion by extremes: Population spread with variation in dispersal and reproduction. - American Naturalist 157: 537-554.

Cramer, W. et al. 2001. Global response of terrestrial ecosystem structure and function to CO2 and climate change: results from six dynamic global vegetation models. Global Change Biology 7: 357-373.

Crimmins, S. M. et al. 2011. Changes in climatic water balance drive downhill shifts in plant species' optimum elevations. - Science 331: 324-327.

Dawes, M. A. et al. 2011. Species-specific tree growth responses to 9 years of CO2 enrichment at the alpine treeline. - J. Ecol. 99: 383-394.

Dormann, C. F. et al. 2012. Correlation and process in species distribution models: bridging a dichotomy. - J. Biogeogr. 39: 2119-2131.

Dullinger, S. et al. 2012. Extinction debt of high-mountain plants under twenty-first-century climate change. Nature Climate Change 2: 619-622.

Engler, R. et al. 2012. The MIGCLIM R package - seamless integration of dispersal constraints into projections of species distribution models. - Ecography 35: 872-878.

Epstein, H. E. et al. 2007. Simulating future changes in Arctic and subarctic vegetation. - Comput Sci Eng 9: 12-23.

Germino, M. J. et al. 2002. Conifer seedling distribution and survival in an alpine-treeline ecotone. - Plant Ecol 162: 157-168.

Gravel, D. et al. 2010. Shade tolerance, canopy gaps and mechanisims of coexistence of forest trees. - Oikos 119: 475-484.

Groeneveld, J. et al. 2009. The impact of fragmentation and density regulation on forest succession in the Atlantic rain forest. - Ecol. Model. 220: 2450-2459.

Guisan, A. and Thuiller, W. 2005. Predicting species distribution: offering more than simple habitat models. - Ecology Letters 8: 993-1009.

Gunderson, C. A. et al. 2000. Acclimation of photosynthesis and respiration to simulated climatic warming in northern and southern populations of Acer saccharum: laboratory and field evidence. - Tree Physiol. 20: 87-96.

Hampe, A. 2004. Bioclimatic envelope models: what they detect and what they hide. - Global Ecology and Biogeography 13: 469-471.

Hartig, F. et al. 2012. Connecting dynamic vegetation models to data - an inverse perspective. - J. Biogeogr. 39: 2240-2252.

Heikkinen, R. K. et al. 2006. Methods and undertainties in bioclimatic envelope modelling under climate change. - Progress in Physical Geography 30: 751-777.

Heiri, C. et al. 2009. Forty years of natural dynamics in Swiss beech forests: structure, composition, and the influence of former management. - Ecol. Appl. 19: 1920-1934.

Henne, P. D. et al. 2011. Did soil development limit spruce (Picea abies) expansion in the Central Alps during the Holocene? Testing a palaeobotanical hypothesis with a dynamic landscape model. - J. Biogeogr. 38: 933-949.

Hickler, T. et al. 2006. Implementing plant hydraulic architecture within the LPJ Dynamic Global Vegetation Model. - Global Ecology and Biogeography 15: 567-577.

Hickler, T. et al. 2012. Projecting the future distribution of European potential natural vegetation zones with a generalized, tree species-based dynamic vegetation model. - Global Ecol Biogeogr 21: 50-63.

Huntley, B. 1991. How plants respond to climate change - migration rates, individualism and the consequences for plant-communities. - Annals of Botany 67: 15-22.

Hurtt, G. C. et al. 2010. Linking models and data on vegetation structure. - J. Geophys. Res.-Biogeosci. 115:

Ishizuka, W. and Goto, S. 2012. Modeling intraspecific adaptation of Abies sachalinensis to local altitude and responses to global warming, based on a 36-year reciprocal transplant experiment. - Evol. Appl. 5: 229-244.

Jump, A. S. et al. 2009. The altitude-for-latitude disparity in the range retractions of woody species. - Trends Ecol. Evol. 24: 694-701.

Jump, A. S. et al. 2012. Rapid altitudinal migration of mountain plants in Taiwan and its implications for high altitude biodiversity. - Ecography 35: 204-210.

Kattge, J. et al. 2011. TRY - a global database of plant traits. - Glob. Change Biol. 17: 2905-2935.

Katul, G. G. et al. 2005. Mechanistic analytical models for long-distance seed dispersal by wind. - Am. Nat. 166: 368-381.

Keenan, T. et al. 2011. Predicting the future of forests in the Mediterranean under climate change, with niche- and process-based models: CO2 matters! - Glob. Change Biol. 17: 565-579.

Kissling, W. D. et al. 2012. Towards novel approaches to modelling biotic interactions in multispecies assemblages at large spatial extents. - J. Biogeogr. 39: 2163-2178.

Koca, D. et al. 2006. Modelling regional climate change effects on potential natural ecosystems in Sweden. - Climatic Change 78: 381-406.

Koenig, W. D. and Knops, J. M. H. 2005. The mystery of masting in trees. - American Scientist 93: 340-347.

Köhler, P. and Huth, A. 1998. The effects of tree species grouping in tropical rainforest modelling: Simulations with the individual-based model FORMIND. - Ecol. Model. 109: 301-321.

Köhler, P. et al. 2000. Concepts for the aggregation of tropical tree species into functional types and the application to Sabah's lowland rain forests. - J. Trop. Ecol. 16: 591-602.

Köhler, P. and Huth, A. 2007. Impacts of recruitment limitation and canopy disturbance on tropical tree species richness. - Ecol. Model. 203: 511-517.

Körner, C. 2012. Alpine treelines. Functional ecology of the global high elevation tree limits. . - In: Springer Basel.

Kuparinen, A. 2006. Mechanistic models for wind dispersal. - Trends Plant Sci. 11: 296-301.

Ladeau, S. L. and Clark, J. S. 2006. Elevated CO2 and tree fecundity: the role of tree size, interannual variability, and population heterogeneity. - Global Change Biology 12: 822-833.

Lavigne, M. B. and Ryan, M. G. 1997. Growth and maintenance respiration rates of aspen, black spruce and jack pine stems at northern and southern BOREAS sites. - Tree Physiol. 17: 543-551.

Lavorel, S. and Garnier, E. 2002. Predicting changes in community composition and ecosystem functioning from plant traits: revisiting the Holy Grail. - Funct. Ecol. 16: 545-556.

Lenka, N. K. and Lal, R. 2012. Soil-related constraints to the Carbon Dioxide fertilization effect. - Crit. Rev. Plant Sci. 31: 342-357.

Linder, H. P. et al. 2012. Biotic modifiers, environmental modulation and species distribution models. - J. Biogeogr. 39: 2179-2190.

Lischke, H. et al. 1997. Calculating temperature dependence over long time periods: Derivation of methods. - Ecol. Model. 98: 105-122.

Lischke, H. et al. 1998. Aggregation of individual trees and patches in forest succession models - Capturing variability with height structured random dispersions. - Theoretical Population Biology 54: 213-226.

Lischke, H. 2001. New developments in forest modeling: convergence between applied and theoretical approaches. - Natural Resource Modeling 14: 71-102.

Lischke, H. et al. 2006. TreeMig: A forest-landscape model for simulating spatio-temporal patterns from stand to landscape scale. - Ecol. Model. 199: 409-420.

Lischke, H. et al. 2007. Model Up-scaling in Landscape Research. - In: F. Kienast et al. (eds), A changing world: challenges for landscape research. Kluwer, pp. 259-282.

Loarie, S. R. et al. 2009. The velocity of climate change. - Nature 462: 1052-U111.

Löffler, T. J. and Lischke, H. 2001. Incorporation and influence of variability in an aggregated forest model. - Natural Resource Modeling 14: 103-137.

Macalady, A. K. and Bugmann, H. 2014. Growth-mortality relationships in Pinus edulis reveal shifting mortality thresholds and climate sensitivity across warmer and cooler droughts. PLOS One. - Plos One in press.

McDowell, N. G. et al. 2013. Improving our knowledge of drought-induced forest mortality through experiments, observations, and modeling. - New Phytol. 200: 289-293.

McGuire, A. D. et al. 2001. Carbon balance of the terrestrial biosphere in the twentieth century: Analyses of CO2, climate and land use effects with four process-based ecosystem models. - Glob. Biogeochem. Cycle 15: 183-206.

Meier, E. S. et al. 2012. Climate, competition and connectivity affect future migration and ranges of European trees. - Global Ecol Biogeogr 21: 164-178.

Meiners, S. J. et al. 2000. Tree seedling establishment under insect herbivory: edge effects and interannual variation. - Plant Ecol 151: 161-170.

Melbourne, B. A. and Chesson, P. 2006. The scale transition: Scaling up population dynamics with field data. - Ecology 87: 1478-1488.

Milbau, A. et al. 2009. Effects of a warmer climate on seed germination in the subarctic. - Ann. Bot. 104: 287-296.

Morales, J. M. et al. 2013. Frugivore behavioural details matter for seed dispersal: A multi-species model for cantabrian thrushes and trees. - Plos One 8.

Mustin, K. et al. 2013. Red noise increases extinction risk during climate change. - Divers. Distrib. online early. DOI: 10.1111/ddi.12038:

Myster, R. W. 2009. Tree seedling survivorship, growth, and allocation in the Cross Timbers ecotone of Oklahoma, USA. - Plant Ecol 205: 193-199.

Nabel, J. E. M. S. et al. 2012. Impact of species parameter uncertainty in simulations of tree species migration with a spatially linked dynamic model. - In: R. Seppelt et al. (eds), International Congress on Environmental Modelling and Software: Managing Resources of a Limited Planet, Sixth Biennial Meeting International Environmental Modelling and Software Society (iEMSs).

Nabel, J. E. M. S. and Lischke, H. 2013. Upscaling of spatially explicit and linked time and space discrete models studying vegetation dynamics under climate change. - In: B. Page et al. (eds), 27th International Conference on Informatics for Environmental Protection. Shaker Verlag, pp. 842-850.

Nabel, J. E. M. S. et al. 2013. Interannual climate variability and population density thresholds can have a substantial impact on simulated tree species' migration. - Ecol. Model. 257: 88-100.

Nathan, R. et al. 2008. Mechanisms of long-distance seed dispersal. - Trends Ecol. Evol. 23: 638-647.

Nathan, R. et al. 2011. Mechanistic models of seed dispersal by wind. - Theor. Ecol. 4: 113-132.

Normand, S. et al. 2011. Postglacial migration supplements climate in determining plant species ranges in Europe. - Proc. R. Soc. Lond. Ser. B-Biol. Sci. 278: 3644-3653.

Peñuelas, J. et al. 2008. Twentieth century changes of tree-ring delta C-13 at the southern range-edge of Fagus sylvatica: increasing water-use efficiency does not avoid the growth decline induced by warming at low altitudes. - Glob. Change Biol. 14: 1076-1088.

Perez-Ramos, I. M. et al. 2010. Mast seeding under increasing drought: results from a long-term data set and from a rainfall exclusion experiment. - Ecology 91: 3057-3068.

Peringer, A. and Rosenthal, G. 2011. Establishment patterns in a secondary tree line ecotone. - Ecol. Model. 222: 3120-3131.

Purves, D. W. et al. 2008. Predicting and understanding forest dynamics using a simple tractable model. - Proc. Natl. Acad. Sci. U. S. A. 105: 17018-17022.

Quillet, A. et al. 2010. Toward dynamic global vegetation models for simulating vegetation-climate interactions and feedbacks: recent developments, limitations, and future challenges. - Environ. Rev. 18: 333-353.

Sakai, A. et al. 2003. Altitudinal variation in lifetime growth trajectory and reproductive schedule of a sub-alpine conifer, Abies mariesii. - Evol. Ecol. Res. 5: 671-689.

Sato, H. et al. 2007. SEIB-DGVM: A new dynamic global vegetation model using a spatially explicit individual-based approach. - Ecological Modelling 200: 279-307.

Schauber, E. M. et al. 2002. Masting by eighteen New Zealand plant species: The role of temperature as a synchronizing cue. - Ecology 83: 1214-1225.

Scheiter, S. and Higgins, S. I. 2009. Impacts of climate change on the vegetation of Africa: an adaptive dynamic vegetation modelling approach. - Glob. Change Biol. 15: 2224-2246.

Scheiter, S. et al. 2013. Next-generation dynamic global vegetation models: learning from community ecology. - New Phytol. 198: 957-969.

Scheller, R. M. and Mladenoff, D. J. 2007. An ecological classification of forest landscape simulation models: tools and strategies for understanding broad-scale forested ecosystems. - Landsc. Ecol. 22: 491-505.

Scheller, R. M. and Mladenoff, D. J. 2008. Simulated effects of climate change, fragmentation, and inter-specific competition on tree species migration in northern Wisconsin, USA. - Clim. Res. 36: 191-202.

Scherrer, D. and Körner, C. 2010. Infra-red thermometry of alpine landscapes challenges climatic warming projections. - Glob. Change Biol. 16: 2602-2613.

Scherstjanoi, M. 2013. Ph.D. Thesis. Towards an efficient plant physiology-based modeling of spatial forest dynamics. - In: École Polytechnique Fédérale de Lausanne.

Scherstjanoi, M. et al. 2013. GAPPARD: A computationally efficient method of approximating gap-scale disturbance in vegetation models. - Geoscientific Model Development Discussions 6:

Schiffers, K. et al. 2013. Limited evolutionary rescue of locally adapted populations facing climate change. - Philos. Trans. R. Soc. B-Biol. Sci. 368:

Schumacher, S. and Bugmann, H. 2006. The relative importance of climatic effects, wildfires and management for future forest landscape dynamics in the Swiss Alps. - Glob. Change Biol. 12: 1435-1450.

Simonis, D. et al. 2012. Reconstruction of late Glacial and Early Holocene near surface temperature anomalies in Europe and their statistical interpretation. - Quat. Int. 274: 233-250.

Sitch, S. et al. 2003. Evaluation of ecosystem dynamics, plant geography and terrestrial carbon cycling in the LPJ dynamic global vegetation model. - Global Change Biology 9: 161-185.

Sitch, S. et al. 2008. Evaluation of the terrestrial carbon cycle, future plant geography and climate-carbon cycle feedbacks using five Dynamic Global Vegetation Models (DGVMs). - Global Change Biology 14: 2015-2039.

Snell, R. S. 2014. Simulating long distance seed dispersal in a dynamic vegetation model. - Global Ecol Biogeogr 23: 89-98.

Stephenson, C. M. et al. 2007. Testing mechanistic models of seed dispersal for the invasive Rhododendron ponticum (L.). - Perspect. Plant Ecol. Evol. Syst. 9: 15-28.

Svenning, J. C. and Sandel, B. 2013. Disequilibrium vegetation dynamics under future climate change. - Am. J. Bot. 100: 1266-1286.

Svenning, J. C. et al. 2014. The influence of interspecific interactions on species range expansion rates. - Ecography accepted.

Thomas, S. C. 2011. Age-related changes in tree growth and functional biology: the role of reproduction. - In: F. C. Meinzer et al. (eds), Size- and Age-Related Changes in Tree Structure and Function. Springer, pp. 33-64.

Thompson, S. E. and Katul, G. G. 2013. Implications of nonrandom seed abscission and global stilling for migration of wind-dispersed plant species. - Glob. Change Biol. 19: 1720-1735.

Thuiller, W. et al. 2008. Predicting global change impacts on plant species' distributions: Future challenges. - Perspectives in Plant Ecology Evolution and Systematics 9: 137-152.

Thuiller, W. et al. 2013. A road map for integrating eco-evolutionary processes into biodiversity models. - Ecol. Lett. 16: 94-105.

Travis, J. M. J. et al. 2013. Dispersal and species‘ responses to climate change. - Oikos in press:

van Oijen, M. et al. 2005. Bayesian calibration of process-based forest models: bridging the gap between models and data. - Tree Physiol. 25: 915-927.

Venn, S. E. et al. 2009. Do facilitative interactions with neighboring plants assist the growth of seedlings at high altitudes in alpine Australia? - Arct. Antarct. Alp. Res. 41: 381-387.

Vittoz, P. and Engler, R. 2007. Seed dispersal distances: a typology based on dispersal modes and plant traits. - Botanica Helvetica 117: 109-124.

Walther, G. R. et al. 2005. An ecological 'footprint' of climate change. - Proc. R. Soc. Lond. Ser. B-Biol. Sci. 272: 1427-1432.

Wehrli, A. et al. 2007. Improving the establishment submodel of a forest patch model to assess the long-term protective effect of mountain forests. - Eur. J. For. Res. 126: 131-145.

Williams, J. W. et al. 2004. Late-quaternary vegetation dynamics in North America: scaling from taxa to biomes. - Ecological Monographs 74: 309-334.

Williams, J. W. and Jackson, S. T. 2007. Novel climates, no-analog communities, and ecological surprises. - Front. Ecol. Environ. 5: 475-482.

Wu, J. G. and David, J. L. 2002. A spatially explicit hierarchical approach to modeling complex ecological systems: theory and applications. - Ecol. Model. 153: 7-26.

Wunder, J. et al. 2008. Growth-mortality relationships as indicators of life-history strategies: a comparison of nine tree species in unmanaged European forests. - Oikos 117: 815-828.

Wyckoff, P. H. and Clark, J. S. 2002. The relationship between growth and mortality for seven co-occurring tree species in the southern Appalachian Mountains. - J. Ecol. 90: 604-615.

Zhao, M. F. et al. 2013. Plant phenological modeling and its application in global climate change research: overview and future challenges. - Environ. Rev. 21: 1-14.

Zhu, K. et al. 2012. Failure to migrate: lack of tree range expansion in response to climate change. - Glob. Change Biol. 18: 1042-1052.

Zurbriggen, N. et al. 2013. Performance of germinating tree seedlings below and above treeline in the Swiss Alps. - Plant Ecol 214: 385-396.

Acknowledgements

In meinem privaten wie in meinem wissenschaftlichen Leben haben mich viele Menschen begleitet, unterstützt, gefördert und gefordert und haben damit in der ein oder anderen Weise zu der Fertigstellung dieser Doktorarbeit beigetragen. An dieser Stelle möchte ich mich bei all diesen Menschen bedanken, auch wenn ich nicht alle namentlich erwähnen kann.

I express my gratitude to the supervisors of my thesis, Heike Lischke, Felix Kienast and James Kirchner, for their insights, fruitful discussions and the careful and constructive review of the various manuscripts. The three of you taught me a lot about scientific work and this thesis would certainly not have been possible without you. I am especially thankful to Heike Lischke, who initialised my Ph.D project, which was partly funded by the Swiss National Science Foundation (SNF) Grant 315230-122434. Thank you Heike for the warm welcome, the hosting in the first month and the always open office door. I am also thankful that Felix Kienast and James Kirchner agreed to supervise my thesis. Furthermore, I thank James Kirchner for providing additional funding for my research and for the English coaching hour which I enjoyed a lot.

I am grateful to Prof. Robert Scheller for acting as external reviewer of my thesis despite the long travel distance from the US.

Furthermore, I would like to thank all the helpful people at the WSL. Besonders möchte ich mich bei Thomas Wüst bedanken für die Hilfe mit der Hera und für das zwar nicht ganz erfolreiche, aber sehr lehrreiche Experiment mit dem GRID. Ich danke Dirk Schmatz, dass er die vielen Fragen zu den unterschiedlichsten Datensätzen ertragen und immer sehr gewissenhaft beantwortet hat und Urs Gimmi dafür, dass er ein super Bürokollege war. Danke fürs Kekse, Schokolade und Kaffee teilen. Thanks go to Signe Normand for the help with the glossary and the opportunity to participate in the range shift workshops. I would also like to thank the rest of the HL E floor for distractions and also for one or the other heated discussion, e.g. about the use of nespresso capsules. Finally, I thank Ben Polter, who I seem to frequently come across, for the initial contact with the WSL.

Ich möchte mich bei Malte Meinshausen bedanken, dessen Hingabe zu seiner Arbeit mich tief beeindruckt hat und der mir gezeigt hat, dass es unterschiedliche Wege gibt, exzellente Wissenschaft zu betreiben und mich dadurch auf zukünftige Erfahrungen vorbereitet hat. In diesem Sinne möchte ich mich auch bei Herrn Prof. Andreas Fleischer bedanken, für die Anleitung bei meinen ersten unsicheren wissenschaftlichen Schritten damals in der Uni. Danke, dass Sie fortwährend versucht haben, mich darauf aufmerksam zu machen, dass wiederkehrende grundlegende Muster das Interessante sind und weniger die vielen unwichtigen Details, in welche ich mich so gerne verloren habe und immer noch verliere. Und wo ich grade von der Uni spreche möchte ich mich auch ganz doll bei Marek Walczak, dem besten Kommilitonen überhaupt, bedanken. Ohne Dich wäre das Studium der Informatik nicht denkbar gewesen.

Auch bei den vielen lieben Menschen, die ich in meiner Zeit in Zürich kennengelernt habe, möchte ich mich bedanken. Ein ganz besonderer Dank geht an meine grosse-kleine-Doktor-Halbschwester Dr. Natalie Zurbriggen für das geniale Tandem, das geteilte Leid, die Freundschaft und das Verständnis und für die hervorragende Betreuung, auch über die Zeit Deiner eigenen Diss hinaus. Danke Natalie, ohne Dich wäre das hier überhaupt nicht möglich gewesen. Ganz doll möchte ich mich auch bei Linda bedanken fürs Kümmern, Kuscheln und Umsorgen, fürs Kochen, Tratschen und die Spaziergänge und für die Möglichkeit gerade zum Ende der Diss hin doch noch das ein oder andere Mal den Schreibtisch zu verlassen. Danke auch an Martin für die beiden schönen Wanderungen die wir zusammen mit Linda gemacht haben und dass Du ertragen hast, dass ich immer nur über Arbeit rede. Dafür möchte ich mich auch bei Ellen bedanken, ich weiss es war schwer. Danke für die vielen langen und kurzen Spaziergänge, das Radfahren zur Arbeit, die Musik und das ein oder andere Bier auf Deinem Balkon. I also would like to thank my flatmate Dr. Emre Togan for bearing the permanent blockade of the living room in the last months and for his desk. Further thanks go to the people from Seed City and from the ASVZ pair acrobatics class, particularly to Tommy for teaching me forearm stand.

Many thanks and a deep bow to Dr. Claudine Chen, my personal goddess of English, for her friendship and for the endless answering of English questions and the hours of sentence engineering. Thanks also to Tristan for solving tiles when Claudine and me (I?) crashed barriers. Claudine, I still have a bad conscience that I lately only came to Skype when I had English questions, I am more than positive that this will get better now.

Und auch bei meinen Freunden aus und in Hamburg möchte ich mich bedanken, bei Melanie, Anna, Mieke, Jette, Marika, Conny und Flo, bei Marius, Sophie und Zora und ganz besonders bei Jan, Bente und Kalle, bei denen ich mich immer Willkommen und wie zu Hause gefühlt habe bei meinen leider immer weniger werdenden Besuchen. Ich freue mich bald bei Euch um die Ecke zu wohnen!

Zum Schluss, aber nicht am wenigsten möchte ich mich bei meiner Familie bedanken. Allen voran David für die unermüdliche Unterstützung, die Diskussionen, das kritische Nachfragen, die Hilfe mit Linux und Latex, aber vor allem für Deine Zuneigung und den unerschütterlichen Glauben an mich, der meine eigenes Vertrauen oft überstiegen hat. Danke für die immerwährende Bestätigung und die Erinnerungen daran, was ich schon alles geschafft habe, wenn ich mich verloren gefühlt habe, besonders am Ende meiner Diss. Ich danke Dir David. Und ich danke meiner liebsten Schwester Katha, meiner großartigen Oma und meinen geliebten Eltern, die immer für mich da waren und sind.

In Gedenken an Sarah, die für mich ein unglaublich wichtiger Mensch war
und die diese Welt viel zu jung verlassen hat.

Publications

Nabel, J.E.M.S., J.W. Kirchner, N. Zurbriggen, F. Kienast, H. Lischke (in revision). Extrapolation methods for climate time series revisited – spatial correlations in climatic fluctuations influence simulated tree species abundance and migration.

Snell, R. S., A. Huth, **J.E.M.S. Nabel**, G. Bocedi, J. M. J. Travis, D. Gravel, H. Bugmann, A. G. Gutiérrez, T. Hickler, S. .I. Higgins, M. Scherstjanoi, B. Reineking, N. Zurbriggen, H. Lischke (accepted). Using dynamic vegetation models to simulate plant range shifts.

Svenning, J.-C., D. Gravel, R. D. Holt, F. M. Schurr, W. Thuiller, T. Münkemüller, K. H. Schiffers, S. Dullinger, T. C. Edwards, Jr., T. Hickler, S. Higgins, **J.E.M.S. Nabel**, J. Pagel, S. Normand (2014). The influence of interspecific interactions on species range expansion rates. *Ecography*.

A. Voinov, R. Seppelt, R. Reis, **J.E.M.S. Nabel**, S. Shokravi (2014). Values in socio-environmental modelling: Persuasion for action or excuse for inaction. *Environmental Modelling and Software* 53: 207–212.

N. Zurbriggen, **J.E.M.S. Nabel**, M. Teich, P. Bebi, H. Lischke (in press). Explicit avalanche-forest feedback simulations improve the performance of a coupled avalanche-forest model. *Ecological Complexity*.

Nabel, J.E.M.S., N. Zurbriggen, H. Lischke (2013). Interannual variability and population density thresholds can have a substantial impact on simulated tree species' migration. *Ecological Modelling* 257: 88–100.

Nabel, J.E.M.S., H. Lischke (2013). Upscaling of spatially explicit and linked time and space discrete models studying vegetation dynamics under climate change. In: Environmental Informatics and Industrial Environmental Protection: Concepts, Methods and Tools: 842–850.

Nabel, J.E.M.S., N. Zurbriggen, H. Lischke (2012). Impact of species parameter uncertainty in simulations of tree species migration with a spatially linked dynamic model. In: R. Seppelt, A.A. Voinov, S. Lange, D. Bankamp (Eds.) (2012): International Environmental Modelling and Software Society (iEMSs) 2012, Sixth Biennial Meeting, Leipzig, Germany: 909–916.

Nabel, J.E.M.S., J. Rogelj, C. M. Chen, K. Markmann, D. J. Gutzmann and M.Meinshausen (2011). Decision support for international climate policy - the PRIMAP emission module. *Environmental Modelling and Software* 26:1419–1433.

Rogelj, J., C. Chen, **J. Nabel**, K. Macey, W. Hare, M. Schaeffer, K. Markmann, N. Höhne, K. Krogh Andersen and M. Meinshausen (2010). Analysis of the Copenhagen Accord pledges and its global climatic impact - a snapshot of dissonant ambitions. *Environmental Research Letters* 5(3): 034013.

Rogelj, J., **J. Nabel**, C. Chen, W. Hare, K. Markmann, M. Meinshausen, M. Schaeffer, K. Macey and N. Hohne (2010). Copenhagen Accord pledges are paltry. *Nature* 464(7292): 1126.

Rogelj, J., B. Hare, **J. Nabel**, K. Macey, M. Schaeffer, K. Markmann and M. Meinshausen (2009). Halfway to Copenhagen, no way to 2°C. *Nature Reports Climate Change* (0907): 81.